Alma Mater Studiorum – Università di Bologna

DOTTORATO DI RICERCA IN

CHIMICA

Ciclo XXVIII

Settore concorsuale di afferenza: **03/C2**

Settore scientifico disciplinare: **CHIM 04**

SUSTAINABLE CATALYTIC PROCESSES FOR THE VALORISATION OF LIGHT ALCOHOLS

Presentata da: Andrea Malmusi

Coordinatore dottorato:
Prof. Aldo Roda

Relatore:
Prof. Fabrizio Cavani

Esame finale anno 2016

INDEX

1. GENERAL INTRODUCTION

This PhD thesis is structured in three main chapters, a general introduction and concluding remarks.

In the introduction, main motivations for the research work are described. Moreover, the experimental methods used to carry out catalytic tests and catalysts characterization are also described.

The three central chapters deal with the research work I carried out during my PhD: (a) ethanol transformation to chemicals over vanadium-based mixed oxides, (b) methanol as an alternative to formaldehyde for the alkylation of isobutene aimed at the production of isoprene, and (c) ethanol transformation to hydrogen by partial oxidation over Pt nanoparticles. The latter research topic was carried during my stage at the Lieibniz Institute für Katalyse, Rostock (DE). Concluding remarks summarize the results obtained Bibliographic references are listed at the end of the thesis.

1.1 Brief overview on sustainable chemistry and alcohols as platform chemicals

Nowadays, the major part of the industrial production of chemicals and fuels derives from fossil sources. The main source, which provides the building blocks for further and more complex transformations, is petroleum[1, 2]. From oil, it is possible to obtain almost all of the raw materials that can be transformed to a wide range of useful intermediates and products, such as elastomers, fuels, plastics and so on. During the past century, the industrial technology was strongly focused on the transformation of these raw materials into useful chemicals. Therefore, nowadays petrochemical processes are fully optimized and widely used; however, the chemical industry is continuously facing new challenges to improve and develop more efficient technologies. Nowadays the biggest challenge regards the development of more sustainable chemical processes; "sustainability" of a chemical process means to combine topics such as work safety, human health and respect for the environment, without forgetting economical profits[1, 2].

Some guidelines for the development of more sustainable chemical processes can be found in the 12 principles of Green Chemistry[3]. Green Chemistry is a multidisciplinary topic with the scope to provide some guidelines for the development of a chemistry with reduced environmental impact. However, Green Chemistry alone is not sufficient to develop new technologies, because an economic and social evaluation is also necessary. Indeed, a "green" chemical process will be developed only if economically affordable, moreover, only if it generate profits it will also generate job and social welfare.

Therefore, in order to develop new chemical processes, we need to take into account all these principles, not only those suggested by Green Chemistry. Because of this, it is more correct to talk about Sustainable Chemistry, which includes all the aforementioned principles.

One of the most important issue in the development of more sustainable chemical processes, concerns the substitution of fossil sources with renewable raw materials[2, 4]. Renewable materials can reduce the environmental impact of a chemical process by the establishment of a closed circle. Theoretically, the waste produced from the end use of a good should become the feed to grow new (renewable) raw materials. This circle is never 100% closed, there is always a fraction of the mass that cannot be reintegrated inside the circle and finally becomes waste; anyway, a chemistry based on renewable sources often shows a lower environmental impact than a chemistry based on petroleum[2, 5]. A further step in the direction of a more sustainable chemical industry is the development of chemical processes which exploit second generation sources, such as wastes from agricultural or food

and wood related industrial activities. This would lead to the valorisation of materials that otherwise would become a waste.

These aspects have been deeply investigated during latest decades, and nowadays it is possible to identify a list of chemical products which can be obtained from renewable sources and from waste[2, 4]. These chemical products are the so-called "platform chemicals". In the case of petrochemistry, the so-called "building blocks" are represented by a small number of molecules on which all the chemical industry is based. Platform chemicals are the analogues of building blocks, but they are derived from renewable sources. from this, the bio-refinery concept is derived; it consists in all those process aimed at the transformation of renewable raw materials into platform chemicals, bio-chemicalsand bio-based fuels[6].

Once platform chemicals have been obtained, two main routes are possible: either transform them to the same intermediates also produced by conventional chemistry (drop-in chemical), or transform them to new compounds, which might replace the conventional ones. In the first case, a platform chemical is transformed to a chemical product that is already used in industry, in this way it is possible to integrate the bio-refinery with the existing production chains. In the second case, instead, it is necessary to develop new technologies[2].

Literature reports about several examples for both cases. For example, it is possible to synthesize polyethylene from ethylene, the latter being produced by bio-ethanol dehydration[2, 7], to replace polyethyleneterephthalate with polyethylenefuranoate, substituting terephthalic acid with 2,5-furandicarboxylic acid[1, 4, 8], to produce new lubricants from vegetable oils,[9, 10] and so on[1, 2].

Despite of the importance of the subject, the use of renewable sources is not the only principle on which a more sustainable chemistry might be developed. Another important principle states that, when possible, it is advisable to use non-hazardous chemicals[11], replacing them with less dangerous chemicals[12].

Bio-alcohols can meet most of these requirements. Most of them can be obtained by biomass fermentation, they are not dangerous (although a problem is their volatility and easy flammability), and they can be transformed into a wide range of products[1, 2, 4].

Because of the versatility of the OH moiety, they can be oxidized to aldehydes (ketones) or acids, or dehydrated to olefins; these can be intermediates for several other transformations.

Ethanol, for example, can be dehydrated to ethylene for the production of polyethylene, it can be transformed to C_4 molecules such as 1,3-butadiene, through the Lebedev process, or 1-butanol, through the Guerbet reaction. Moreover, ethanol can be dehydrogenated to acetaldehyde, which can be used to produce C_4 molecules, or can be oxidized to acetic acid, employed in the chemical and food industry[13, 14, 15, 16, 17, 18].

Another chemical widely employed in chemical industry is methanol. It is not possible to produce methanol by fermentation, but it can be obtained from syngas, which in turn can be produced by biomass gasification[7, 8].

The research work described in this PhD thesis deals with alcohols transformation into value-added chemicals. More specifically my work was focused on ethanol and methanol. Ethanol was investigated as a renewable source for two purposes: production of acetaldehyde by means of oxidation/dehydrogenation over Vanadium oxide-based catalysts, and production of high purity hydrogen through partial oxidation catalyzed by supported Pt nanoparticles.

Methanol was investigated as less hazardous alternative to formaldehyde in the reaction of isobutene alkylation to isoprene.

More detailed information about each one of these topics are provided at the beginning of corresponding chapters.

1.2 Common experimental methods

Some of the experimental methods employed were common to the research projects I carried out. The objective of this paragraph is to describe instruments and methods used to carry out the experiments.

The common subject of this thesis concerns heterogeneous catalysis; more specifically, the three research projects concerned gas-phase catalysis for the transformation of alcohols. In order to carry out a gas-phase catalyzed reaction, it is necessary a set-up that is basically made of two parts:

- A reactor in which it is possible to load the catalyst and through which the gaseous reagents flow, equipped with devices aimed at the control of temperature, pressure, gas flows and contact time;
- An analytical system able to qualitatively identify the products of the reaction and to evaluate the amount of each product and of unconverted reagents.

The general set-up used duirng these research projects and the analytical methods are described in the next paragraphs.

1.2.1 Catalysts characterization

In order to determine the structural and morphological properties of catalysts, we used some characterization techniques: XRD and IR spectroscopy to determine their crystallinity and structure, single-point BET method to measure the specific surface area (SSA), and SEM combined with EDX analysis to evaluate the morphology and the distribution of the elements.

XRD patterns of catalysts powders were collected with a Bragg/Brentano Philips PV 1710 operating with the Cu K_α wavelength; the signal was acquired between 5 and 80° 2θ, with an acquisition time of 1 s every 0.1° 2θ.

IR spectra were collected with a Bruker Alpha spectrometer, equipped with a diamond plate-ATR device. Spectra were registered from 4000 to 360 cm^{-1} with a resolution of 1 cm^{-1}.

The specific surface area (SSA) was measured with a Fisons Sorpty 1750.

SEM-EDX images were collected with a Zeiss EP EVO 50, equipped with an EDX probe Oxford Instruments INCA ENERGY 350. General conditions of the microscope were: EHT 20 KeV, high vacuum (10^{-6} Pa) or variable vacuum between 60 – 100 Pa. The EDX probe used a Mn K_α radiation with 133 eV of resolution.

Some specific properties of selected catalysts, such as surface acidity or the amount of coke deposited, were measured using specific equipments, which will be described in the experimental part of each section.

1.2.2 Lab-scale catalytic plant

The lab-scale plant (schematized in Figure 1) used for the catalytic tests can be divided in three parts:

- Inlet line
- Reactor
- Outlet line and on-line GC.

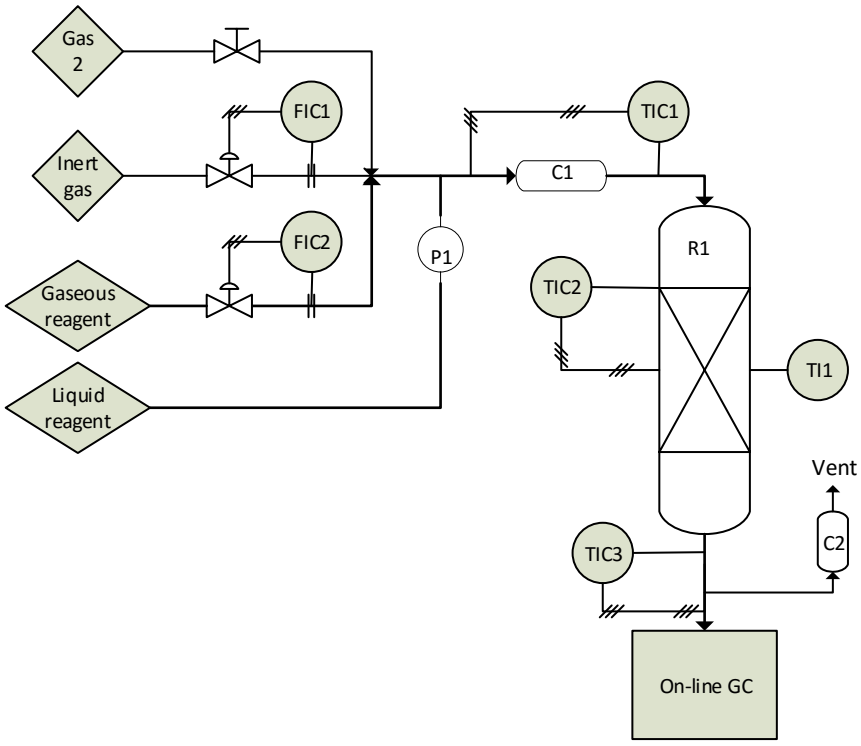

Figure 1: Scheme of the micro-plant used for lab-scale catalytic tests

The inlet line was built up with the objective to ensure vaporization and mixing of liquid reagents before the reactor. Gaseous reagent and inert gas (N_2 or He) flows were regulated by two mass flowmeters (respectively FC2 and FC1), and were mixed at a "cross" point of the inlet pipeline. It was also possible to feed an additional gas to the plant through the auxiliary line (gas 2); in this case the flow was regulated manually through a needle valve. All the gaseous flows were measured by means of a bubble flow-meter (not shown in Figure 1).

Liquid reagents were fed to the reactor by means of a syringe pump, whose needle was inserted inside the inlet pipeline through a GC-inlet septum. The inlet line was heated (TC1) at 180°C in order to ensure pre-heating of gas flows and complete vaporization of liquid reagents; mixing of gases and vapours took place in a part of the inlet line filled up with Raschig rings (C1). The heated inlet flow then passed through the catalytic bed located inside a PFR glass reactor (R1). The latter was placed inside an electrically heated oven (TC2). The temperature of the catalytic bed was measured by means of a thermocouple (TI1). Downstream the reactor, off-gases were conveyed through an electrically heated line (TC3), maintained at 220°C in order to keep all the products in the vapour phase. The off-gas flow

was then splitted into two flows. The first part was purged to the vent after a scrubbing in water (C2) aimed at the removal of high-boiling compounds, which might clog the lines. The second part was collected by the on-line GC sampling-valve and then analyzed.

In each catalytic test, with the exclusion of catalysts lifetime tests, off-gases exiting the reactor were analyzed by on-line GC three times: after 10, 45 and 80 min from the beginning of the reaction. The result of each test was then calculated by the average of these three analysis. The aim of this procedure was to check catalyst stability and to obtain a representative set of data.

At the bottom of the reactor, a sampling point was also available made of a GC-inlet septum installed in a blind end of the "cross" connection downstream the reactor.

This sampling point was used to sample the off-gas with a gas syringe in order to qualitatively analyze the products by injection in an off-line GC-MS. The instrument used was an Agilent 6890 equipped with a 30 m HP-5 MS column with an inner diameter of 0,20 mm and a stationary phase film of 0,003 mm. The GC was equipped with an Agilent 5973N Mass spectrometer. This system allowed to separate identify each product from its mass spectrum. This technique was used to qualitatively analyze the off-gases of the reaction, in order to confirm the presence of the products previously identified by means of their retention time in the GC plot (see next paragraphs).

1.2.3 Analysis of products by means of on-line GC

The GC system employed for the analysis was configured in such a way to run two parallel analysis in two columns, each one connected to a detector as shown in Figure 2.

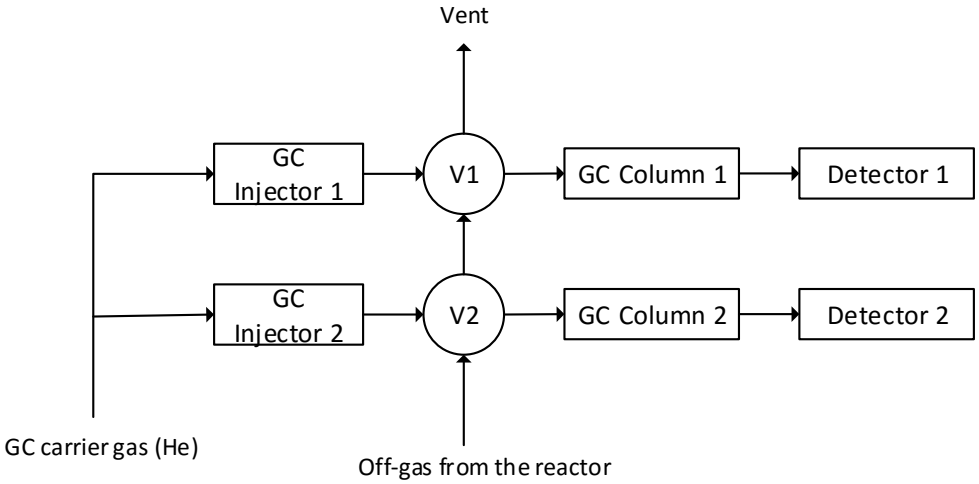

Figure 2: scheme of the GC system employed for the analysis

Products flowing out from the reactor were sampled by two valves, each one equipped with sampling loops, which ensured the sampling of precise volumes (usually 0,200 mL if the sample was analyzed with a TCD). When the analysis was started, the valves were switched

to the injection position and the compounds inside the loops were injected into the columns.

Qualitative identification of peaks was done by comparison of elution times; each peak had a typical elution time depending on the type of column used, temperature ramp and carrier flow. Once these parameters were fixed, the elution time of each compound could be considered constant within a low error range. The elution time was determined by injecting each pure compound of in the GC .

Quantitative determination was done by means of the calibration technique. This method allows to attribute a response factor to each compound, which allows to calculation the number of moles from the corresponding chromatographic peak area.

The calibration was made by injecting a known amount of each compound; the "response factor" was calculated by dividing the GC peak area by the number of moles injected. Different amounts for each compound were injected, in order to determine the response factor as the slope of the peak area vs concentration line.

1.2.4 Determination of reagents conversions and products yields

The aim of the catalytic tests is to determine the conversion of reactants and the yields to each product in function of the catalyst type and reaction conditions used, such as temperature and contact time. Once the product has been identified by its elution time, its GC peak area value is used to calculate the number of moles.

Reagent conversion, products yields and selectivity were calculated using the following formulas:

- Product conversion: $X = \frac{n_r^{in} - n_r^{out}}{n^{in}}$
- Reagent yield: $Y = \frac{n_p^{out}}{n_r^{in}} \cdot \frac{c_r}{c_p}$
- Reagent selectivity: $S = \frac{n_p^{out}}{n_r^{in} - n_r^{out}} \cdot \frac{c_r}{c_p}$

Where:

- "n" indicates the number of moles
- "c" indicates the stoichiometric coefficient
- subscript "p" indicates a product
- subscript "r" indicates a reagent
- superscript "in" indicates the parameter quantified before the reaction (instance.g., the moles of the reagent fed to the reactor)
- superscript "out" indicates the parameter quantified after the reaction (e.g., the moles of the unconverted reagent or of a product)
- Yields were referred to the limiting reagent.

The number of moles of reagents entering the reactor were quantified by sampling the gas flow in the absence of reaction, which means either at a temperature low enough to avoid any reactant conversion (usually 100-150°C), or without the catalyst.

These are the general methods and techniques used during all research projects carried out during my PhD; detailed information regarding GC lab-scale set-up configurations are provided in the next chapters.

2. ETHANOL TRANSFORMATION OVER VANADIUM-BASED MIXED OXIDES

2.1 Introduction

In recent years, the transformation of bio-ethanol into chemicals by means of oxidation has been the object of a renewed interest, because of its growing availability from bio-sourced 2nd generation raw materials at a convenient price[19, 20, 14]. Chemicals which can be produced from ethanol are all those that are nowadays produced from ethylene (the latter could also be produced from ethanol), and it is foreseen that in the future an ethanol-based platform might become competitive with the cracking-derived ethylene platform from both a sustainability and an economic standpoint.

Amongst the various catalyst types used for the gas-phase oxidation of ethanol, those based on Vanadium oxide as the key component have been widely investigated. The majority of literature works have focused on supported Vanadium oxide[21, 22, 23, 24, 25, 26, 27, 28, 29, 30, 31, 32, 33], whereas little attention has been given to mixed oxide catalysts[34, 35, 36, 37].

In the case of supported Vanadium oxide, main conclusions from literature can be summarized as follows:

1) In the case of γ-Al_2O_3-supported V_2O_5, polyvanadate domains were found to be more active than monovanadate species for ethanol oxidative dehydrogenation (ODH) to acetaldehyde, with the abstraction of an H atom from the adsorbed ethoxide being the kinetically relevant step[21].
2) With vanadia supported over TiO_2 anatase, under optimized conditions it was possible to obtain either high selectivity to acetaldehyde, at low temperature, or to acetic acid, at high temperature[23, 38]. Also in this case, the monolayer Vanadium oxide was proposed to give the greater contribution to catalytic activity, and the kinetically relevant step is H abstraction from the ethoxide[27, 39].
3) A relationship was established between the activation energy for ethanol ODH and the enthalpy of oxygen defect formation in catalysts made of V_2O_5 dispersed over different type of supports, which showed that the reducibility of V sites can be used as a reactivity descriptor[40].
4) Active catalysts in ethanol ODH to acetaldehyde (main by-products being acetic acid, acetals and CO_2) were also obtained by supporting V_2O_5 over TiO_2-SiO_2 by means of grafting[28, 41, 42] or impregnation. Yield to acetaldehyde as high as 74% was reported with the optimized catalyst composition[43].
5) Alcohols favour the spreading of bulk vanadium oxide over TiO_2, methanol being much more efficient than ethanol, due to the mobility and volatility of metal-alkoxy species[26]. Conversely, in the case of silica-supported Vanadium oxide, because of the weak interaction between the V species and the support, agglomeration of Vanadium oxide was induced by the alcohol.[24] With silica support, the oxidation of ethanol was

found to be rather insensitive on the structure of the active species, producing mostly acetaldehyde regardless of the V_2O_5 loading[25].

Amongst the various classes of V-based mixed oxides used for alcohols and polyols oxidation, Fe-V-O (hereinafter referred as FeVO) catalysts have recently received much attention,[36, 44, 45, 46, 47, 48, 49, 50] especially for the oxidation of methanol to formaldehyde, but have also been used for other reactions, such as the reduction of NO_x[51]. In brief, the main features of this catalytic system, compared to other V oxide-based catalysts, are:

1) Compared with Vanadium oxide, Fe has little effect on catalytic performance, but it stabilizes V decreasing its volatility (an effect which however is lost when the mixed oxide is deposited over a support)[46]; nevertheless, triclinic $FeVO_4$ is unstable and develops a spinel-type phase during methanol oxidation, of general composition $Fe_{3-x-y}V_x\square_yO_4$; the spinel is stable and non-volatile, and is also flexible structure, since the cations could change oxidation state so inducing the formation of cationic vacancies while retaining the same structure. The selectivity to formaldehyde was a function of the Fe/V ratio, and the best selectivity was shown at Fe/V atomic ratio equal to 14, indicating that isolated Vanadium perform better than polymeric vanadia structures[44 47]. In this sense, Fe plays the main role of diluting the V active species, decreasing the number of less selective V-O-V ensembles.
2) The incorporation of Al in $FeVO_4$ increases the stability of the triclinic structure; nevertheless the structure undergoes structural changes during reaction: $FeVO_4$ develops the spinel phase, while $AlVO_4$ remains unchanged. However, the presence of Al does not show important effects on catalytic behavior, and all samples show a selectivity to formaldehyde as high as 90% at high methanol conversion, irrespective of the Fe/Al ratio. The surface of the used catalyst does not reveal any change in composition with respect to the bulk.[45]
3) A surface layer of ca 1 nm thickness consisting of an amorphous Vanadium oxide-enriched structure develops at the outer surface of bulk $FeVO_4$, and clearly affects the catalytic performance.[50] The importance of the generation of supra-surface V^{5+} species in V-Fe-Sb-O catalysts (and in general in V mixed oxide catalysts) was also pointed out by Millet et al.[36]

On the other side, not much attention has been given to other vanadates; for example, very few papers can be found in literature on catalytic properties of Copper-Vanadium mixed oxides. These oxides were mainly investigated as catalysts for ODH of hydrocarbons[52 53 54] and methanol[55 56]. Copper is usually added to Vanadium in a mixed oxide with the aim to increase catalyst reducibility and improve the oxidizing properties of the final material. However, several different Cu-V mixed oxides can be formed; their activity in ODH seems to depend mainly on both the quantity of Cu and the oxidation states of the elements[52]. In

general, highly oxidized materials are more active but less selective in ODH because the presence of Cu leads to a strong improvement in the oxidizing power of the catalyst, which implies higher conversion but also higher selectivity to CO_x[53].

In case of methanol ODH to formaldehyde, $Cu_3(VO_4)_2$ appears to be effective in improving aldehyde yield with respect to bare V_2O_5[55], but no information is given about catalyst stability and structural modifications occurring during reaction.

In this part of thesis, results of a study on the reactivity of bulk $FeVO_4$ in the oxidation of ethanol are reported, including the reactivity study carried out in the absence of oxygen. The same experiments were also carried out with a Copper-Vanadium mixed oxide. Catalytic tests, combined with characterization of fresh and used catalysts, allowed us to develop a deep understanding on relationships between catalyst structure and catalytic performance.

2.2 Experimental

2.2.1 Catalysts preparation and characterization

An Iron-Vanadium mixed oxide (FeVO) was prepared by co-precipitation in aqueous basic environment, followed by filtration, drying and calcination. Briefly, a solution made by dissolving 23.5 g $Fe(NO_3)_3$ nonahydrate in 50 mL of distilled water was added to a solution made of 6.7 g NH_4VO_3 and 2.9 g $H_2C_2O_4$ dissolved in 50 mL of water in order to obtain a Fe/V atomic ratio equal to 1/1. Afterwards, the pH was adjusted to 6.8 by adding 25% ammonia solution; a precipitate was obtained, which was then aged for 1h, filtered, washed with 2 L of distilled water and dried at 120°C overnight. Finally, the solid was calcined at 650°C for 3 hours. The surface area after calcination was 8 m^2/g.

A Copper-Vanadium mixed oxide (CuVO) was prepared following the same procedure as for FeVO. $CuCl_2$ dihydrate was the Cu precursor. In order to obtain a Cu/V molar ratio of 3/2 (which is the molar ratio of Copper (II) Vanadate), 15.0 g of the precursor was used.

V_2O_5 99.9% and Fe_3O_4 97% (100 – 50 nm particle size), were provided by Sigma-Aldrich.

Cu and Fe oxides were prepared using the same procedure as for vanadates, but without adding the Vanadium precursor.

All catalysts before catalytic experiments were pelletized, crushed and sieved to obtain a material with particle size between 0.395 and 0.400 mm.

2.2.2 Catalytic tests

As previously described in chapter 1.2, catalytic tests were performed in a lab-scale fixed-bed glass reactor, at atmospheric pressure. Ethanol was continuously fed to the reactor by a syringe pump, which injected the liquid in a vaporization chamber connected to the reactor. The carrier gas (nitrogen) and, if needed, oxygen, were fed to the reactor by means of a Brooks 5850E mass-flow meter. Water, when used, was fed through a syringe pump.

Typical reaction conditions were as follows: time factor W/F (measured at room temperature) 0.5 g s/mL, total gas flow 60 mL/min; inet feed composition 5% ethanol in N_2. Data were taken after ca 2h reaction time, at each temperature level.

Unconverted Ethanol and reaction products were determined by on-line gas-chromatography using an Agilent 7890A GC equipped with two columns working in parallel, each one connected to a TC detector. The first column was an HP-Molesieve, used for the separation of CO, CO_2 and N_2, the second one was an HP-Plot U, used for the separation of all the other compounds. GC carrier gas was He. A blank test was conducted by feeding the reaction mixture to the empty reactor; thermal dehydration of ethanol to ethylene and water was noticed at 350°C and 400°C with ethylene yield of 1% and 5%, respectively.

2.2.3 Catalysts characterization

Catalysts were characterized before and after reaction in order to establish a correlation between catalytic properties and chemical-physical features. These determinations were carried out exploiting the techniques described in chapter 1.2.1. Moreover, Raman spectra were collected in order to evaluate coke deposition and structural modifications. Raman spectra were collected using a confocal Raman microscope. The instrument was made of a Raman spectrometer Renishaw 1000, and of an optical microscope Leica DMLM. The spectra were collected with an Ar ion laser at 514 nm; the power of the laser was modulated in order to avoid coke burning. For each sample, 4 spectra were collected by focusing the laser beam on different particles in a spectral range between 3000 and 100 cm^{-1} Raman shift, with 2 cm^{-1} resolution.

2.2.4 DRIFT-MS experiments

Some DRITF-MS experiments were carried out by feeding either ethanol or an ethanol/oxygen mixture on FeVO in order to investigate on the species adsorbed on the catalyst in different reaction conditions. Samples were pre-treated at 450°C in a He flow (10 mL min^{-1}) for 45 min, in order to remove any molecules adsorbed on the material. Then the sample was cooled down to 300°C and ethanol was fed at 0.6 mL min^{-1}, vaporized and sent to the environmental cell either using He or air as the carrier gas. Spectra were recorded continuously every minute. The following selected mass spectroscopy signals (m/z) were monitored continuously with time (and temperature): [2, 16, 25, 28, 29, 30, 31, 40, 41, 43, 44, 45, 56, 58, 59, 60, 61]. By combining the information obtained from several different m/z signals, it was possible to obtain unambiguous information on the various products formed. The IR apparatus used was a Bruker Vertex 70 with a Pike DiffusIR cell attachment. Spectra were recorded using a MCT detector after 128 scans and 2 cm^{-1} resolution. The mass spectrometer was an EcoSys-P from European Spectrometry Systems.

2.3 Results and discussion

This section reports about results obtained by catalytic and characterization tests carried out with FeVO and CuVO. Moreover, a comparison between catalytic behavior of FeVO, V_2O_5 and Iron oxide is also presented.

2.3.1 FeVO

Figure 3 shows the effect of temperature on the catalytic performance of the FeVO catalyst (surface area 8 m^2/g). The results obtained at 200°C well reproduce data reported in literature on the oxidation behaviour of this catalyst; in fact $FeVO_4$ is known to selectively transform methanol to formaldehyde in the presence of oxygen[44 46 47 50]. At 200°C acetaldehyde was produced with 97% selectivity, but with ethanol conversion of 45% only. However, at higher temperatures, acetaldehyde selectivity declined in favour of CO_x. Also the selectivity to acetic acid increased, but it was no higher than 7% at 350°C. Ethylene formation was detected at 300 and 350°C with an increasing trend, but, according to the blank experiment, part of this ethylene was due to thermal dehydration. Selectivity to C_4 compounds, 2-butenal (crotonaldehyde(and butanal (butyraldehyde), was always less than 2%. For all experiments, the C balance was over 90%.

Figure 4 compares the X-Ray diffraction patterns of the freshly calcined catalyst with those of samples downloaded after reaction at 300°C and 400°C. The pattern of the fresh catalyst correspond to that one of triclinic $FeVO_4$; the pattern of the catalyst used until 300°C was the same as that of the fresh one, while the sample used at the higher temperature showed the pattern corresponding to the spinel phase of Fe and V (either FeV_2O_4 or VFe_2O_4)[57 58 59 60 61], with broad and intense peaks at ca 30.5, 35.5, 43.5, 58 and 63 2θ degrees, similar to the pattern of magnetite Fe_3O_4 and γ-Fe_2O_3 (maghemite)[44 47]. The structural formula of $V_xFe_{3-x}O_4$ spinels ($0 \leq x \leq 2$) has been described as $(Fe_\alpha^{2+}Fe_{1-\alpha}^{3+})_A(Fe_{1-\alpha}^{2+}Fe_{1-\alpha}^{3+}V_x^{3+})_BO_4$, with α=x/2, A and B representing tetrahedral and octahedral sites, respectively[60]. Characterisation by SEM-EDX (see Figure 5) of the used catalyst (after reaction at 300°C) showed an uniform distribution of Fe, V and O, without any apparent metal oxides segregation.

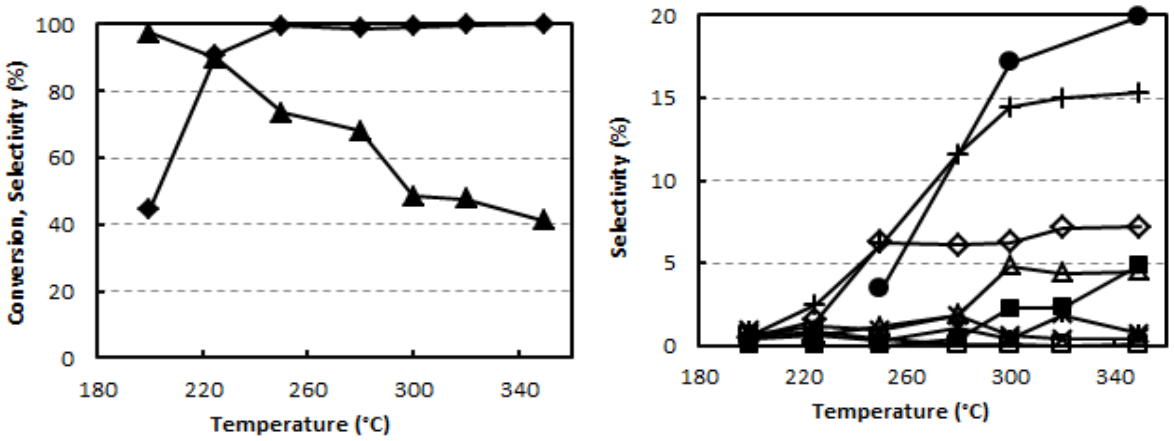

Figure 3: Effect of temperature on ethanol conversion and products selectivity with FeVO catalyst. Reaction conditions: feed 5% ethanol, 5% O_2, 90% N_2; W/F 0.5 g·s/mL. Symbols: ethanol conversion (◆), selectivity to acetaldehyde (▲), ethylene (■), crotyl alcohol (✳), butyraldehyde (✕), acetone (□), diethyl ether (△), acetic acid (◇), CO(●) and CO_2 (+). Results were taken after ca 2h of "equilibration".

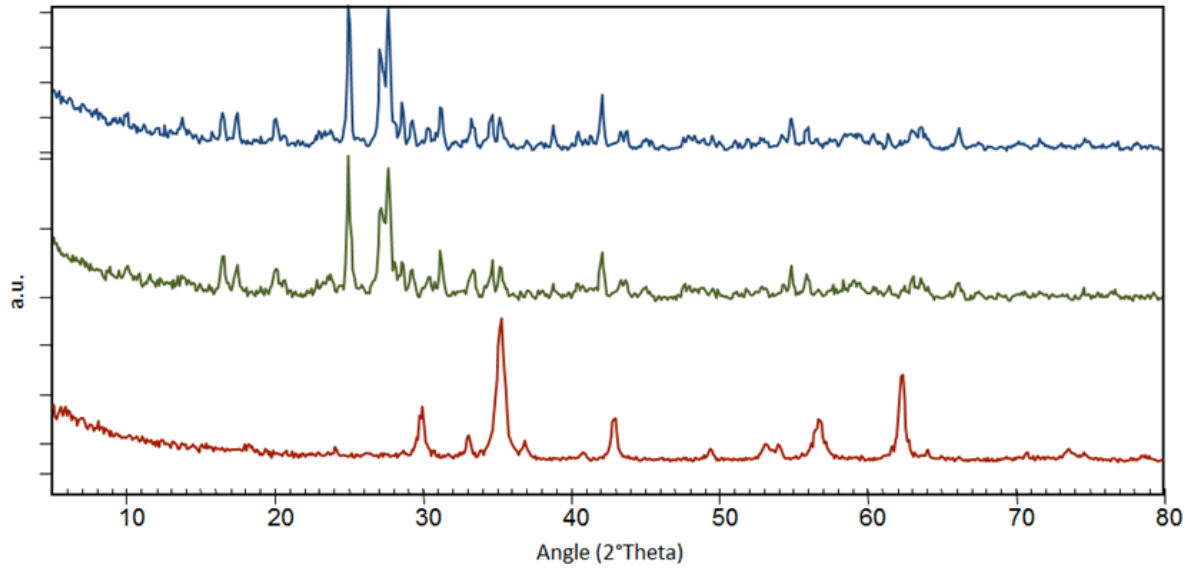

Figure 4: XRD patterns of FeVO catalyst; from top to bottom: calcined, used after reaction at 300°C and 400°C, in ethanol + O_2.

Therefore, it is evident that at the higher temperature both V and Fe underwent reduction; this was due to the fact that O_2 was the limiting reactant, and already at 300°C its conversion was close to 100%. It is surprising to see that results reported in Figure 3 did not show any discontinuity of the catalytic behaviour in function of temperature, as it might be expected because of the structural change occurring at temperatures higher than 300°C. This might be explained by taking into account that indeed the catalytic performance is affected by the first atomic layers on the surface of the FeVO catalyst, which in turn might be not so much influenced by the underlying bulk structure[36, 50]. However, at these conditions we did not notice the formation of ethane, which was instead formed under anaerobic conditions on the reduced catalyst (see below for the description of these latter experiments). This may be explained by taking into account that ethane forms by disproportionation of ethanol:

$2\ CH_3CH_2OH \rightarrow CH_3CHO + CH_3CH_3 + H_2O$

as recently reported in the literature[62]; at high temperature, under conditions leading to ethanol complete conversion, bimolecular reactions might be disfavoured, because of the low concentration of adsorbed ethanol.

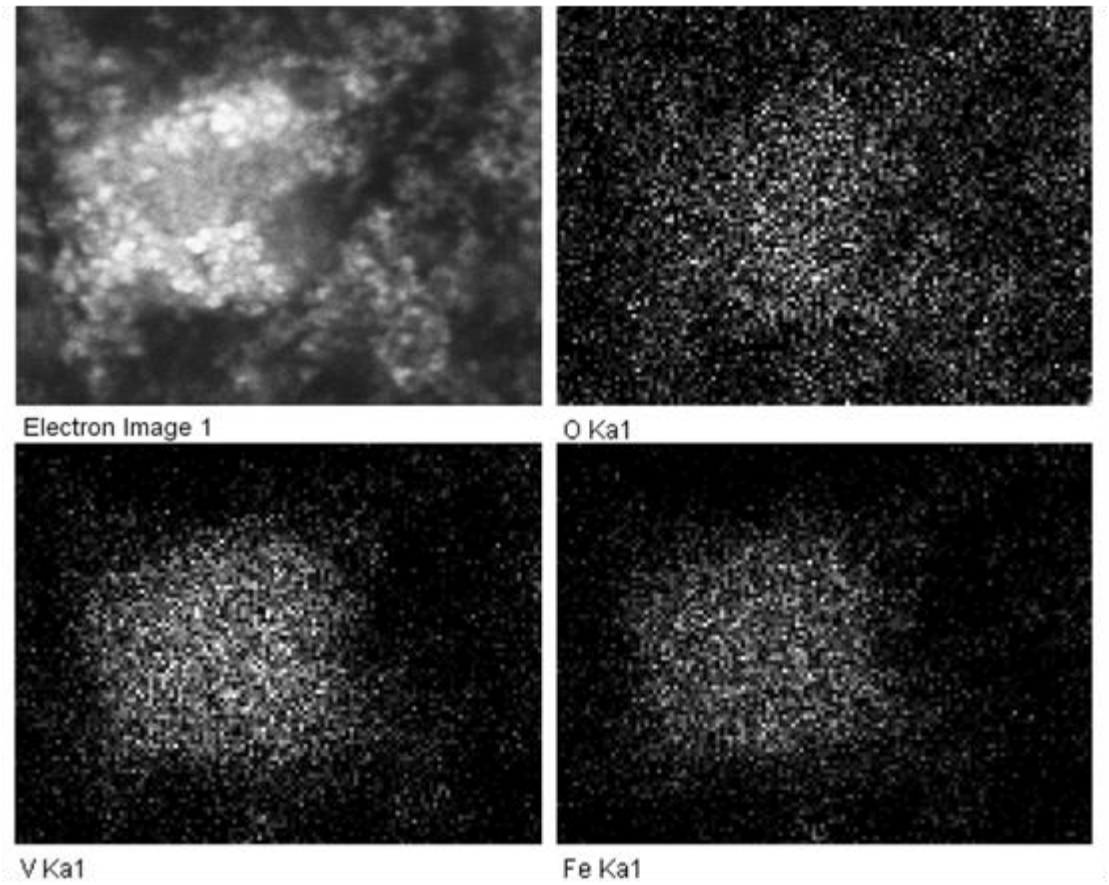

Figure 5: SEM-EDX maps of Fe, V and O in FeVO catalyst used at 300°C with ethanol and O_2. Top, left: SEM image, top right: Oxygen mapping, bottom left: Vanadium mapping, bottom right: Iron mapping.

Figure 6 compares transmission FTIR (samples diluted in KBr) and ATR (pure compounds) spectra for fresh and used catalysts. After reaction at 300 and 350°C, the IR spectrum was the same as that one of the fresh calcined sample, corresponding to $FeVO_4$. More specifically, bands at ca 965, 919, 843 and 740 cm^{-1} are attributable to the stretching of VO_4 units (Td), V^{5+}-O (Td), V^{5+}-O (Oh) and Fe^{3+}-O bonds, respectively[63], whereas for bands at ca 992, 855, 700 and 679 cm^{-1} no specific attribution is given in the literature, but are anyway typical of $FeVO_4$[50, 63, 64]. Conversely, the spectrum of the catalyst used at 400°C was completely different. Worth of note, the latter sample was black, whereas the used but still oxidised one was orange. It is also interesting to see that ATR-IR spectra were different from those recorded in the transmission mode.

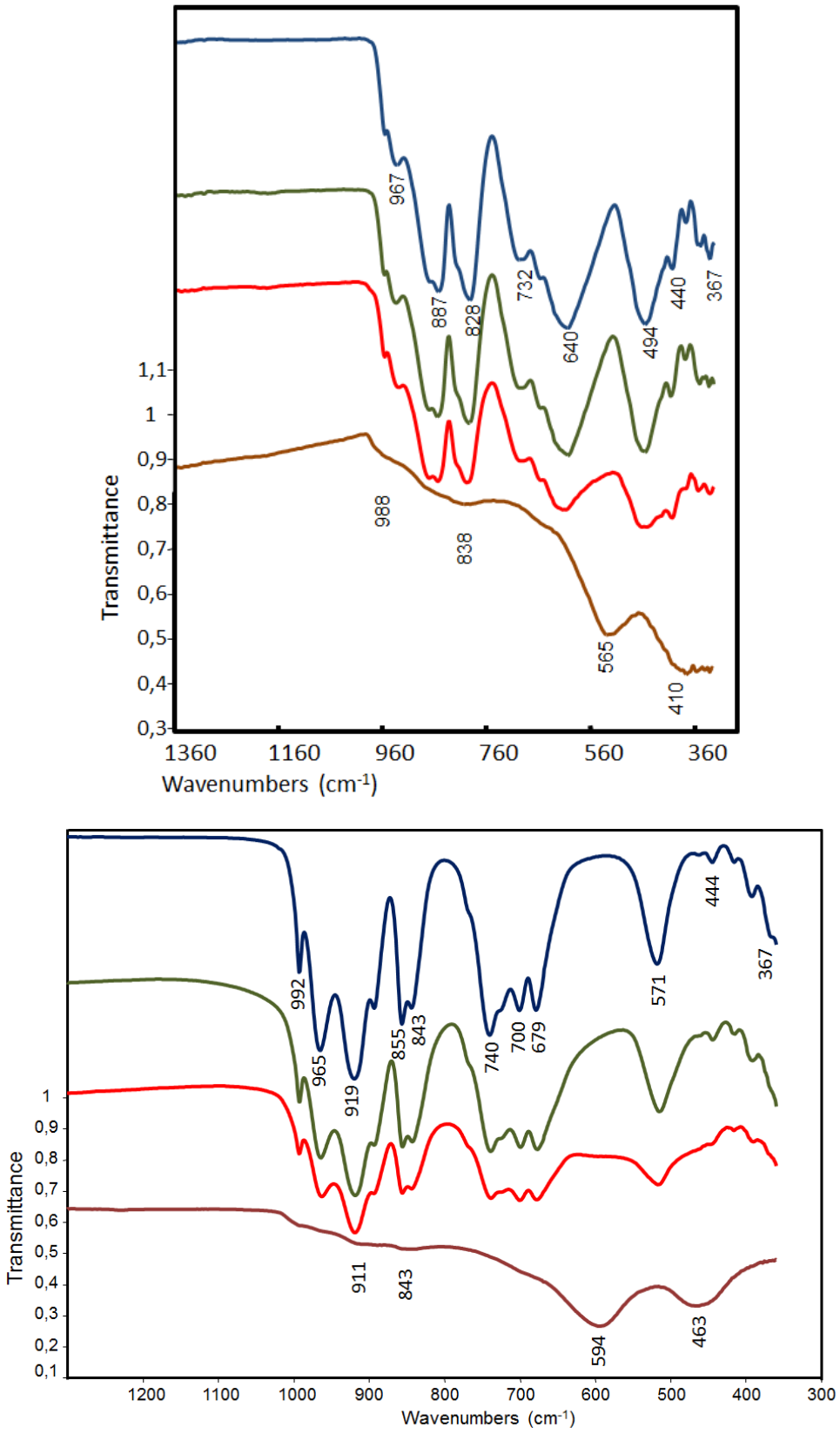

Figure 6: FTIR (top) and IR-ATR (bottom) spectra of FeVO catalyst; from top to bottom: calcined, used after reaction at 300°C, 350°C and 400°C, in ethanol + O_2.

The same conclusions are drawn from the comparison of Raman spectra (Figure 7); it is also shown that in the case of the sample used at 400°C, Raman bands attributable to coke

started to appear; again, this is attributable to the fact that oxygen was completely converted. In Raman spectra, bands at 931 and 965 are attributable to the symmetric stretching of terminal V=O, at 906, 894 and 830 cm^{-1} to the asymmetric stretching of V=O, at 767, 732 and 495 cm^{-1} to the stretching of Fe-O-V, and at 368, 321 and 451 cm^{-1} to vibrations of VO_4 unit[50, 63, 65].

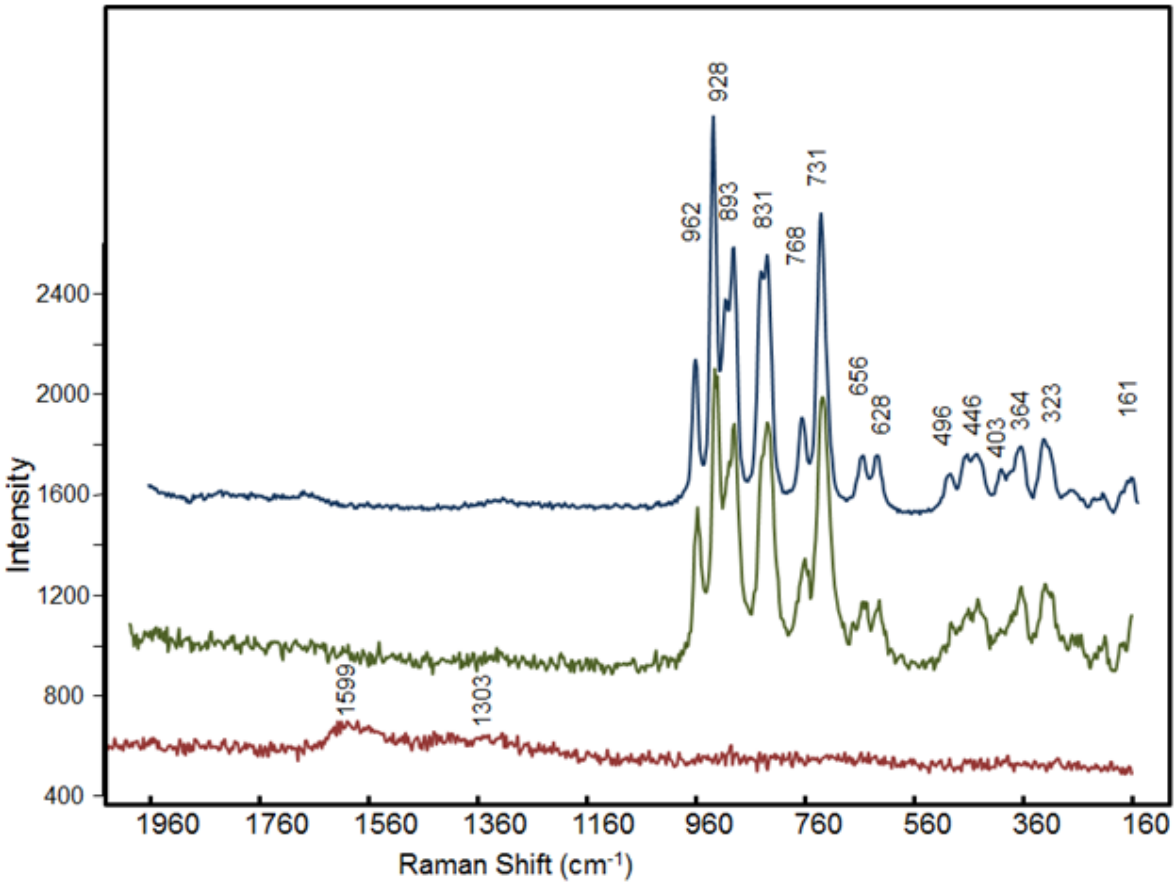

Figure 7: Raman spectra of FeVO catalyst; from top to bottom: calcined, used after reaction at 300°C and 400°C, in ethanol + O_2.

In order to better investigate the events occurring during ethanol oxidation, we undertook the study of the anaerobic oxidation of ethanol. Figure 8 (top) shows the catalytic performance at 300°C, in function of time-on-stream, with 5% ethanol in N_2. It is shown that an equilibration time was needed in order to reach the steady-state performance after ca 70 min reaction time. During this period of time, both ethanol conversion and acetaldehyde selectivity decreased; at the same time, we observed a progressive increase of selectivity to ethane; finally, selectivity to ethane and acetaldehyde were similar. The selectivity to ethylene was very low, between 0.5 and 1%; CO formation also was negligible. Moreover, a small amount of CO_2 was detected during the first 60 minutes of reaction, and then disappeared. Yield to C_4 products, derived from acetaldehyde condensation, showed a slight increase; a small amount of diethyl ether (< 0.3%) was also detected. In overall, the C

balance was close to 80% during the first 50 min reaction time, but then increased and became greater than 92%.

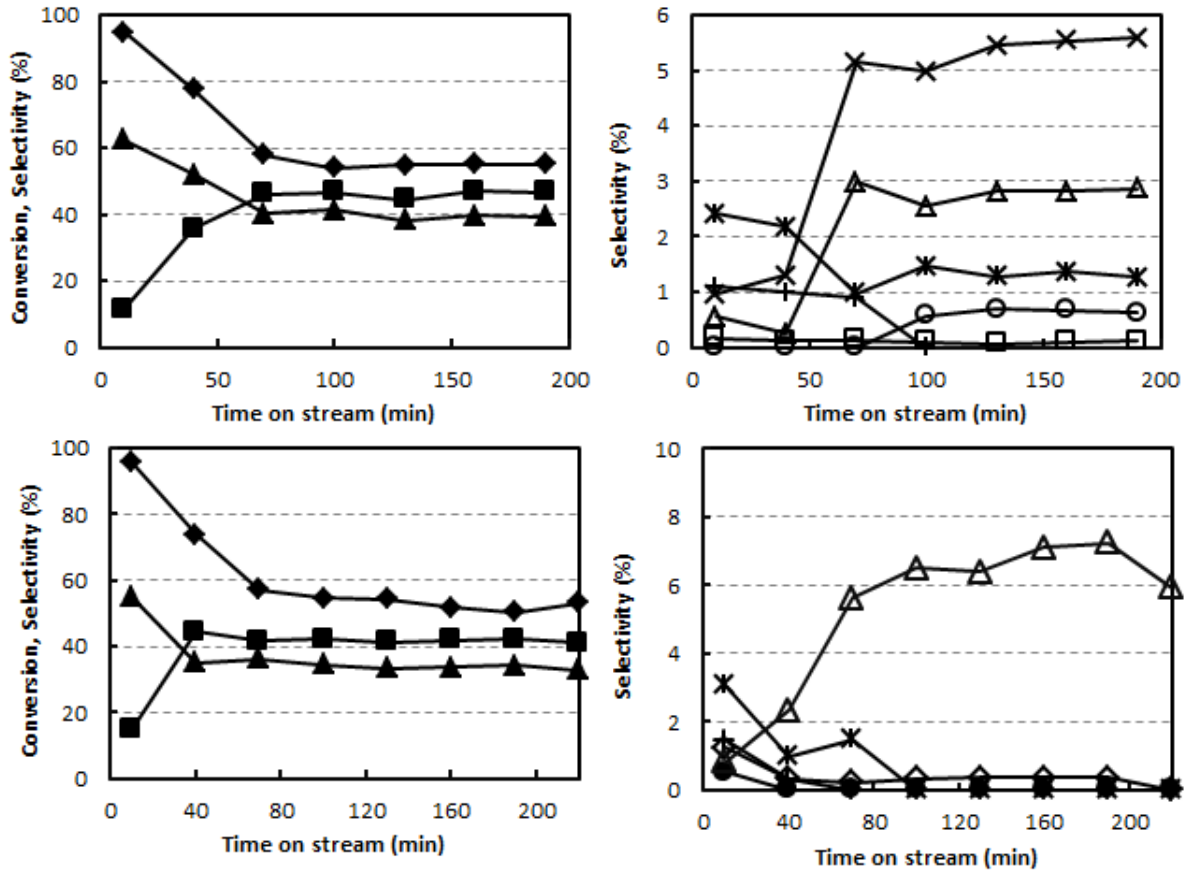

Figure 8: Effect of time-on-stream on ethanol conversion and products distribution with FeVO catalyst. Reaction conditions: T 300°C, feed 5% ethanol in N_2; W/F 0.5 g s/mL. Symbols: ethanol conversion (◆), selectivity to acetaldehyde (▲), ethane (■), crotyl alcohol (○), crotonaldehyde (✳), butyraldehyde (×), acetone (□), ethylacetate (△), and CO2 (+). CO formed in traces only. Top: fresh catalyst. Bottom: after regeneration of used catalyst, 3h at 450°C in air.

Figure 8 (bottom) shows the behaviour after regeneration of the catalyst previously used for 190 min (top figure), by calcination in air at 450°C; it is shown that the initial catalytic behaviour was completely restored after the treatment. This indicates that changes shown during the previous catalytic test were not due to irreversible structural modifications, but to catalyst reduction and carbonaceous residues accumulation. Afterwards, the same behaviour previously shown was replicated during time-on-stream, with only some differences in the distribution of minor products.

As it will be shown later, the non-steady behaviour was due to the development of the spinel phase, which in the absence of O_2 already occurred at 300°C.

As already mentioned, the formation of ethane derived from a disproportionation reaction catalysed by the reduced Vanadium oxide[62].

After the stable behaviour had been reached, experiments were carried out with variation of the reaction temperature. Results are shown in Figure 9. An almost equimolar formation of

ethane and acetaldehyde was observed; selectivity to both compounds increased for an increase of the reaction temperature. Other products formed in minor amount were butyraldehyde, crotonaldehyde, ethyl acetate and crotyl alcohol; the overall C balance was low at low temperature (ca 60%), but it improved when the temperature was increased, and became higher than 85-90% for temperatures higher than 300°C.

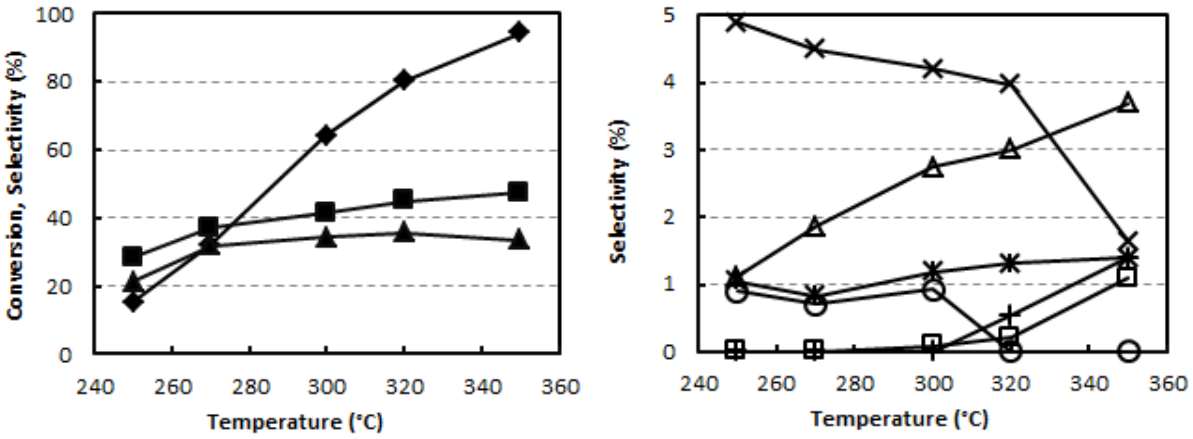

Figure 9: Effect of temperature on ethanol conversion and products distribution with FeVO catalyst. Reaction conditions: feed 5% ethanol in N_2; W/F 0.5 g s/mL. Symbols: ethanol conversion (◆), selectivity to acetaldehyde (▲), ethane (■), butyraldehyde (✕), crotyl alcohol (○), crotonaldehyde (✳), acetone (□), ethylacetate (△), and CO_2 (+). CO formed in traces only.

Figure 10 shows the XRD patterns of the catalyst used after reaction at 300 and 400°C; in both cases, the pattern shown was that typical of the spinel phase. Figure 11 displays the SEM-EDX maps of the used catalyst; also in this case, there was no evidence for phase segregation. Figure 12 and Figure 13 show the FTIR, ATR-IR and Raman spectra of used catalysts. It is confirmed that samples were reduced already after reaction at 300°C in ethanol; Raman bands attributable to coke were also evident.

In the FTIR spectrum of used catalysts, bands at ca 600 and 467 cm^{-1} correspond to those reported in the literature for the spinel compound; more specifically, the shoulder at ca 600 cm^{-1} has been attributed to the presence of non-stoichiometric oxides.[50, 57, 59, 60, 66, 67, 68, 69, 70, 71, 72, 73].

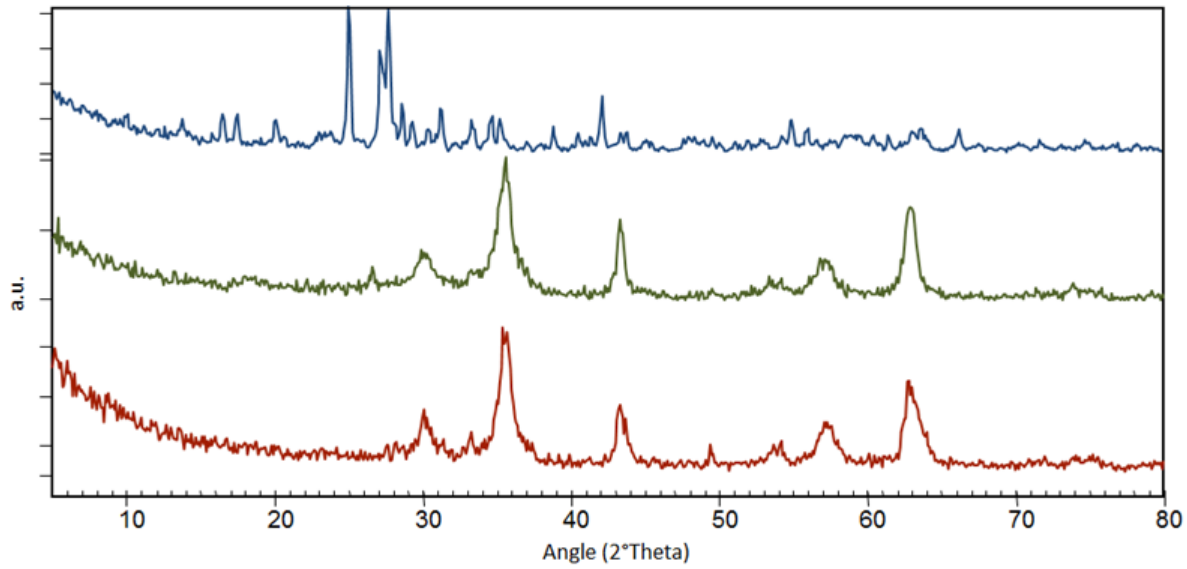

Figure 10: XRD patterns of FeVO catalyst; from top to bottom: calcined, used after reaction at 300°C and 400°C, in ethanol.

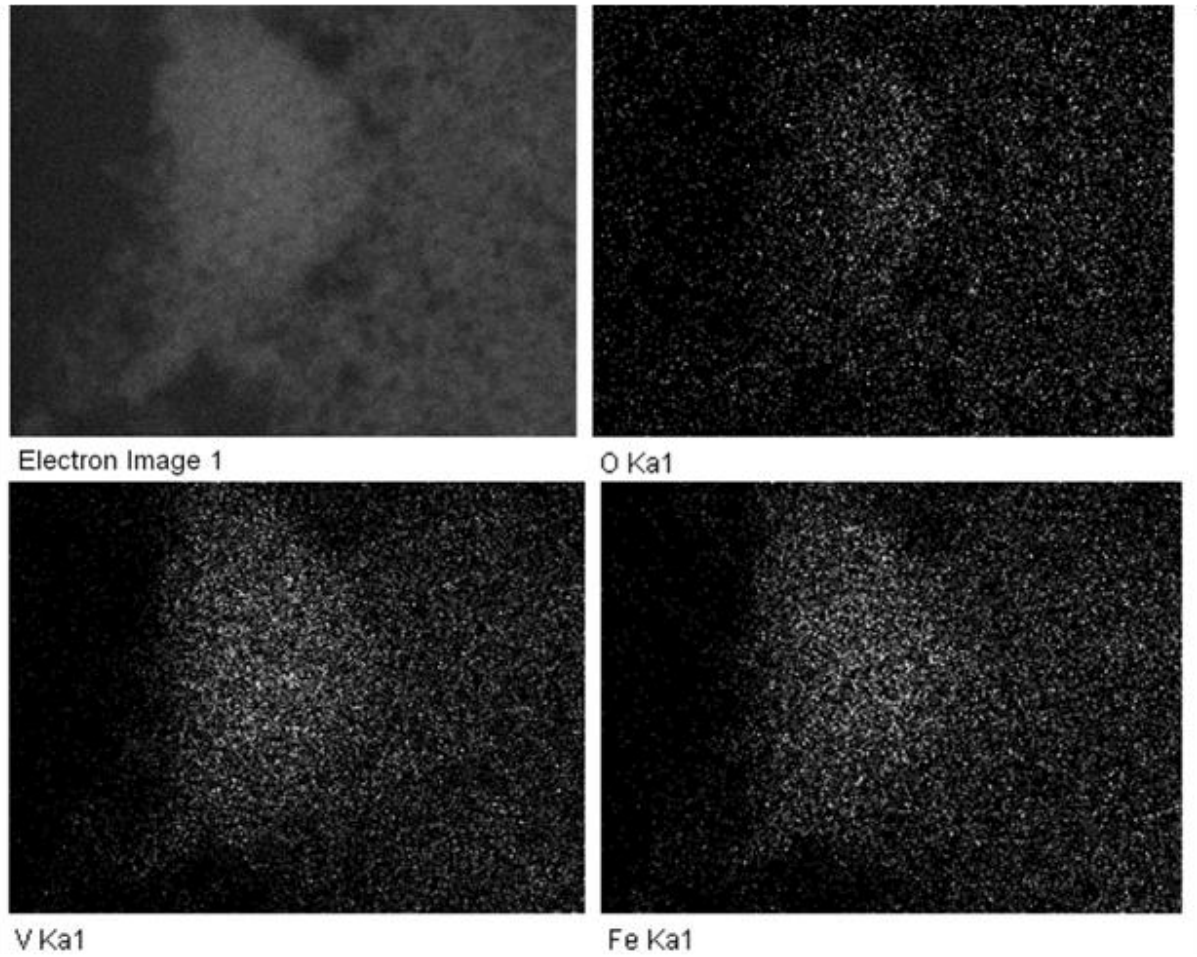

Figure 11: SEM-EDX maps of FeVO catalyst used at 300°C with ethanol. Top left: SEM image; top right: Oxygen mapping; bottom left: Vandium mapping; bottom right: Iron mapping.

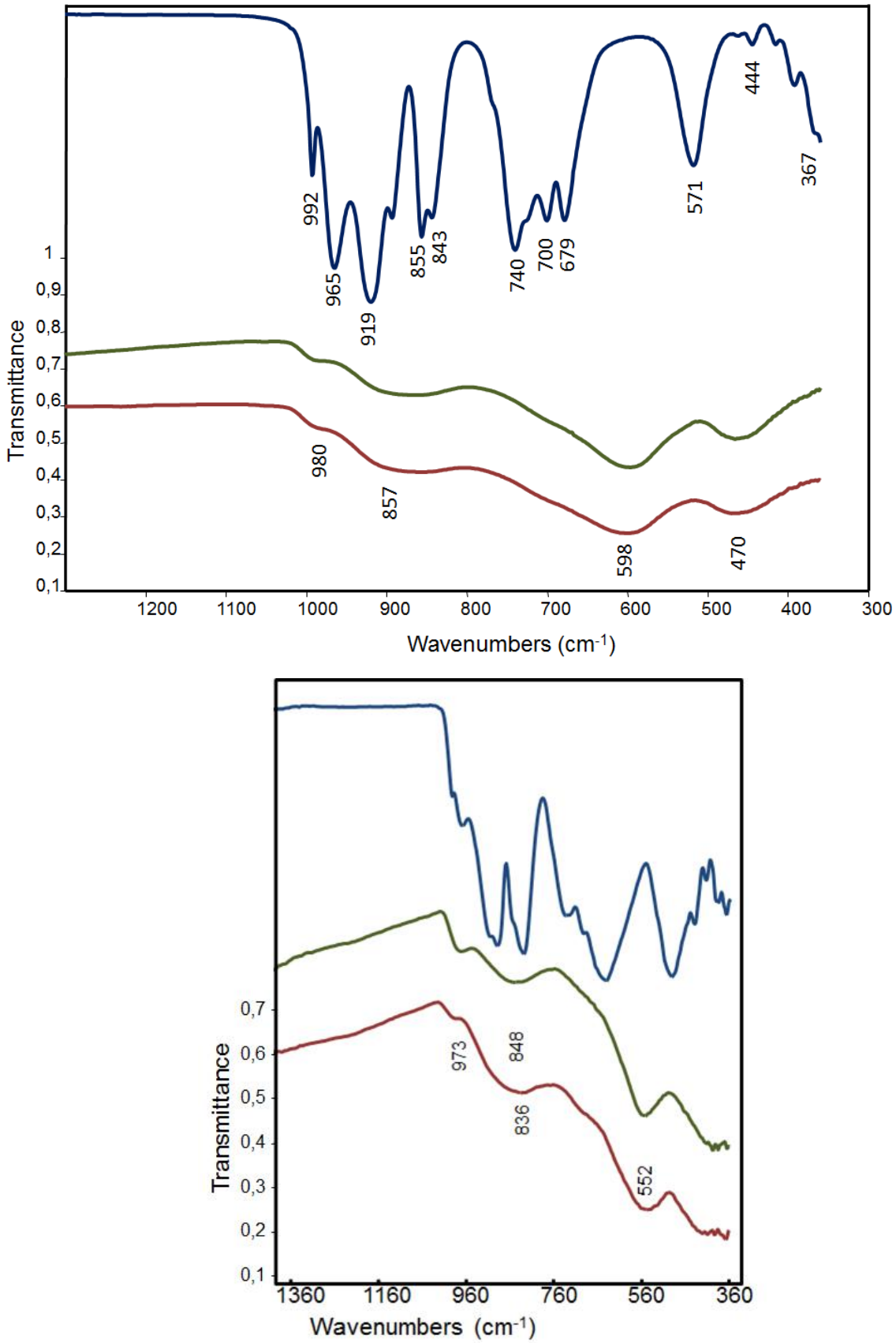

Figure 12: FTIR (top) and IR-ATR (bottom) spectra of FeVO catalyst; from top to bottom: calcined, used after reaction at 300°C and 400°C, in ethanol.

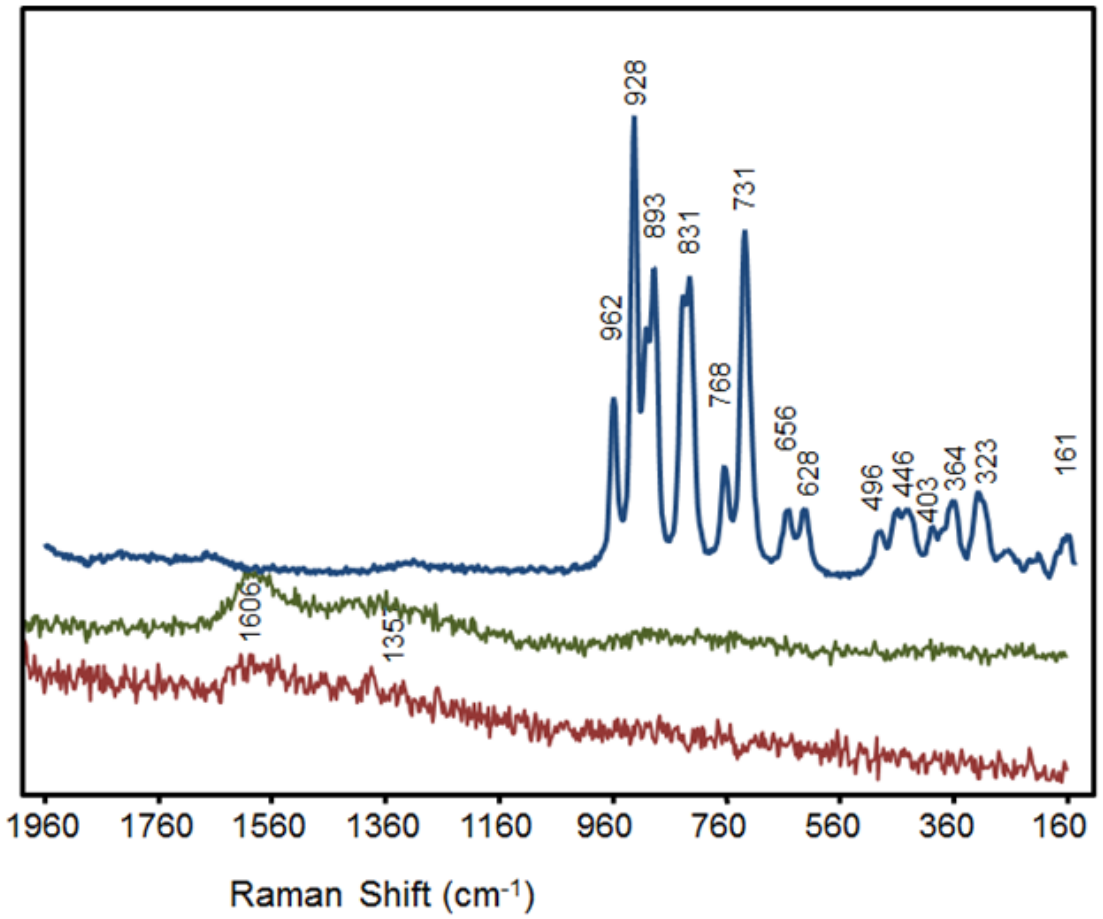

Figure 13: Raman spectra of FeVO catalyst; from top to bottom: calcined, used after reaction at 300°C and 400°C, in ethanol.

Since water is known to promote the reoxidation of Fe and Fe^{2+} to Fe^{3+},[74, 75, 76, 77] we carried out experiments by co-feeding ethanol (5%), and steam (20%). If water promotes the reoxidation of reduced Fe species, a catalytic behavior different form that one shown with ethanol only, should be observed. Results of catalytic experiments are reported in Figure 14.

The behavior in the presence of steam was different from that one observed without steam. At 240°C, the catalyst was selective to acetaldehyde, which was the prevailing product (with also 2% selectivity to diethylether, not shown in Figure, and a C balance which was about 85%). This indicates that water was able to keep the catalyst oxidised at this temperature. However, when the temperature was raised, the selectivity to acetaldehyde declined, and that to ethane increased, until the two compounds formed with similar selectivity at 300°C, as expected from the stoichiometry for ethanol disproportionation. This means that at above 250°C the catalyst underwent reduction, and that steam could not reoxidise it; in fact, steam-reoxidation of reduced Fe oxide is thermodynamically disfavoured at high temperature.[78] A further increase of temperature led to a decline of acetaldehyde selectivity, with formation of acetone and CO_2 as major by-products; these two latter

compounds formed with equal selectivity, suggesting that they were co-produced in the same reaction, as outlined in the scheme below:

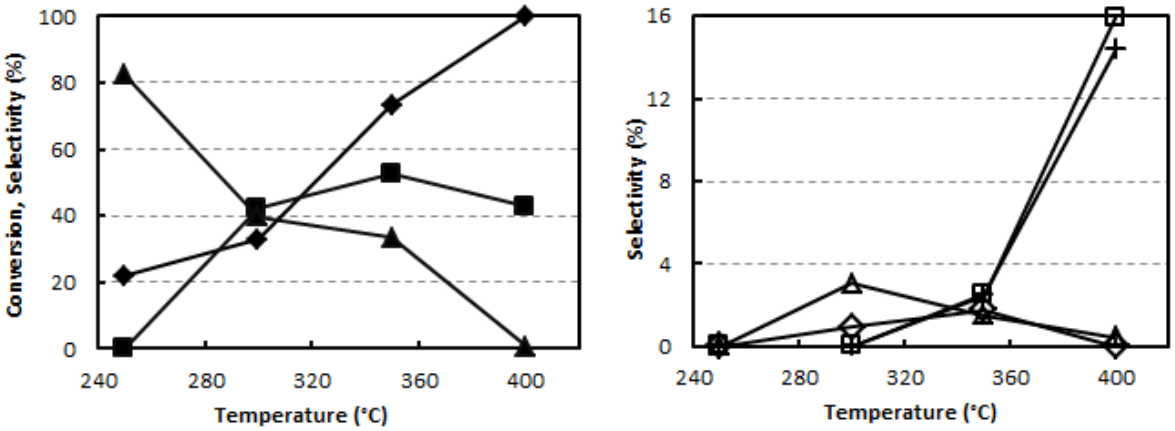

Figure 14: Effect of temperature on ethanol conversion and products distribution with FeVO catalyst. Reaction conditions: feed 5% ethanol, 20% H_2O in N_2; W/F 0.5 g s/mL. Symbols: ethanol conversion (◆), selectivity to acetaldehyde (▲), ethane (■), acetone (□), ethylacetate (△), acetic acid (◇) and CO_2 (+). CO formed in traces.

$CH_3CHO + CH_3CH_2OH \rightarrow CH_3\text{-}CH{=}CH\text{-}CH_2OH + H_2O$

$CH_3\text{-}CH{=}CH\text{-}CH_2OH \rightarrow CH_3\text{-}CH{=}CH\text{-}CHO + H_2$

$CH_3\text{-}CH{=}CH\text{-}CHO + H_2O \rightarrow CH_3\text{-}CH(OH)\text{-}CH_2\text{-}CHO$

$CH_3\text{-}CH(OH)\text{-}CH_2\text{-}CHO \rightarrow CH_3\text{-}CH(O)\text{-}CH_2\text{-}CH_2OH$

$CH_3\text{-}CH(O)\text{-}CH_2\text{-}CH_2OH \rightarrow CH_3\text{-}C(O)\text{-}CH_3 + H_2CO$

$H_2CO + H_2O \rightarrow CO_2 + 2\ H_2$

The formation of crotyl alcohol may occur by direct reaction between acetaldehyde and ethanol, as recently proposed.[79] The alcohol easily dehydrogenates to crotonaldehyde, which is then hydrated due to the presence of excess steam to produce acetaldol (hydration may occur more easily on the unsaturated aldehyde). The isomerisation of 3-hydroxybutanal leads to 4-hydroxy-2-butanone, which finally gives retroaldol condensation (a reaction that at high temperature is more favoured than aldol condensation) to co-produce acetone and formaldehyde. The latter finally reacts with steam to produce CO_2. At 400°C, C balance was close to 80%.

Characterisation of catalysts used after reaction with ethanol and steam is shown in Figure 15 and Figure 16. XRD patterns and spectra were similar to those recorded with ethanol only; the $FeVO_4$ was reduced to the spinel phase already after operation at 300°C. In the presence of steam however, the formation of carbonaceous residua was considerably decreased compared to ethanol only.

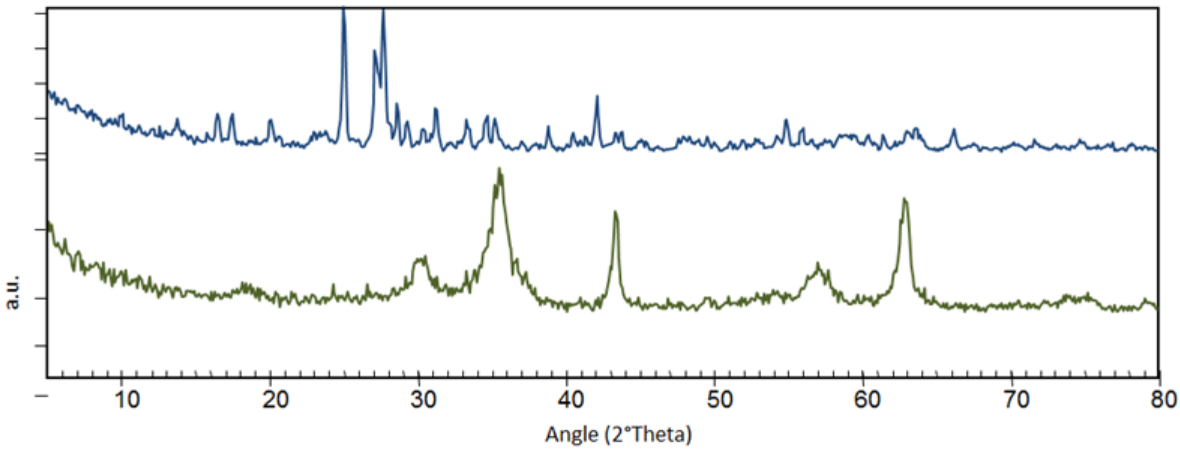

Figure 15: XRD patterns of fresh calcined catalyst (top), and after reaction at 300°C (bottom) in ethanol + H_2O.

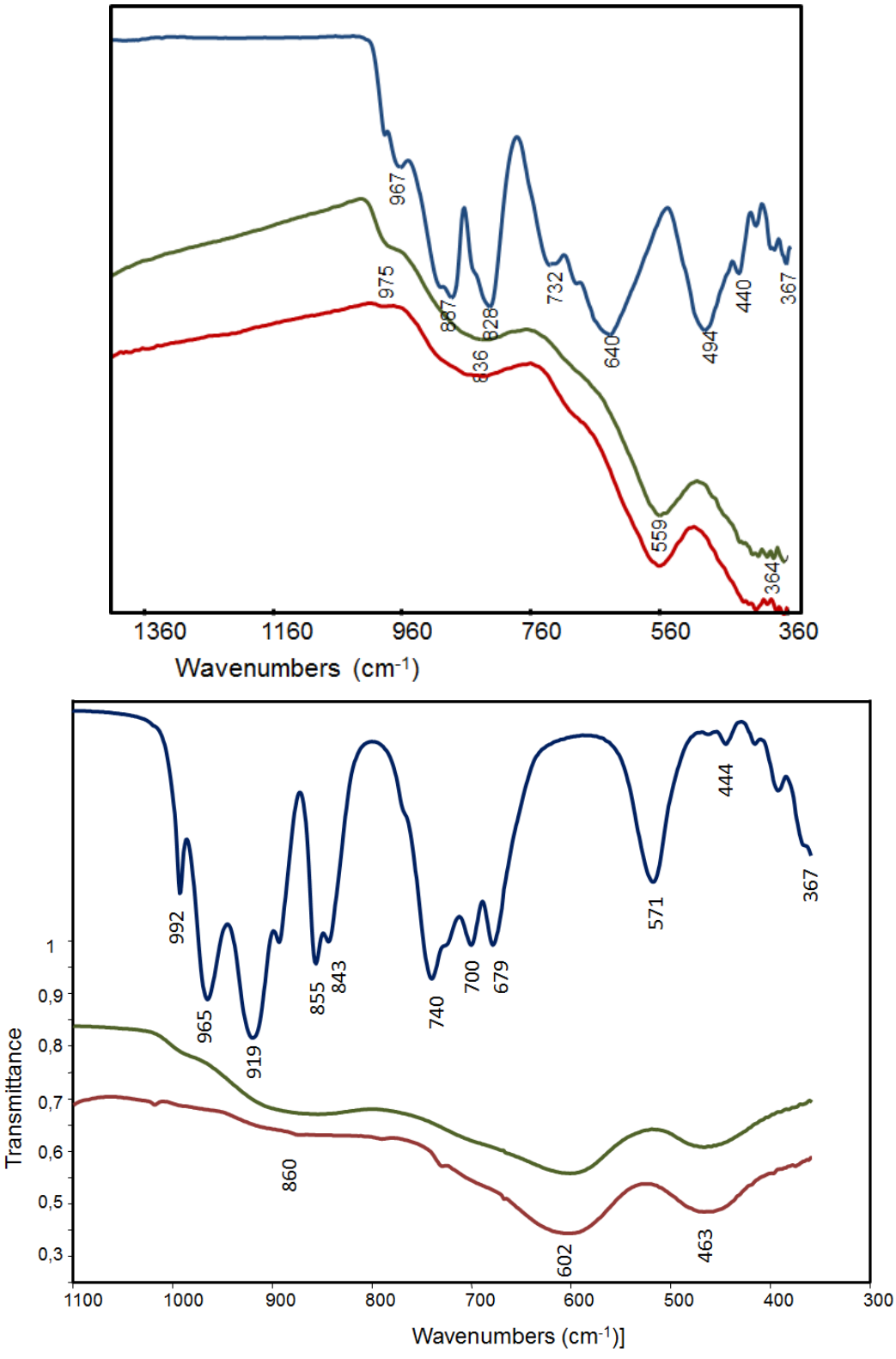

Figure 16: FTIR (top) and IR-ATR (bottom) spectra of fresh calcined catalyst (top), after reaction at 300°C (middle) and 400°C (bottom) in ethanol + H_2O.

In the co-presence of O_2 and H_2O, results were very similar to those obtained with O_2 only (Figure 17). Conversely, a great difference was obviously shown compared to experiments carried out with co-fed steam only. However, characterisation of used samples (Figure 18

and Figure 19) showed that in this case the catalyst still appeared to be oxidised even after reaction at 400°C; in fact, the used sample still was orange.

Results of experiments carried out with variation of either the W/F ratio (with ethanol + O_2 and with ethanol only), or ethanol partial pressure, are shown in Figure 20, Figure 21 and Figure 22, respectively.

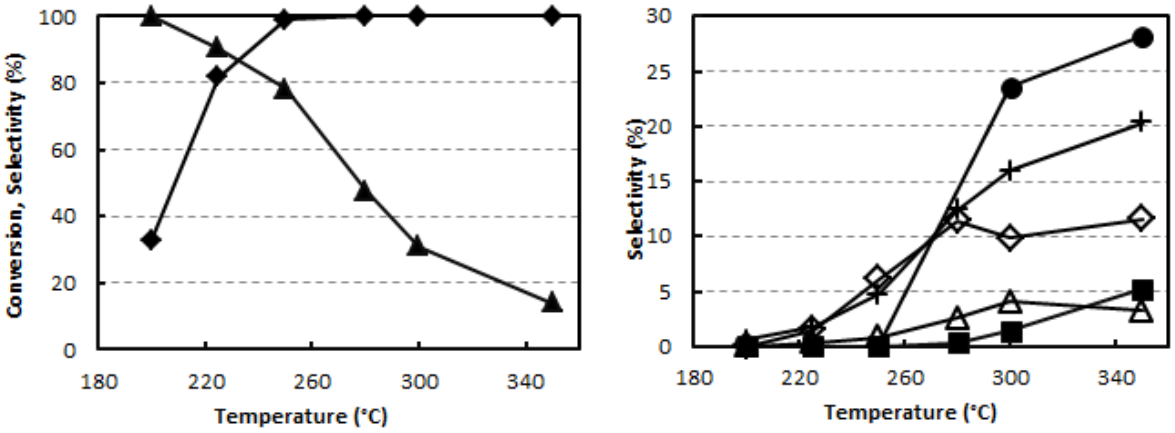

Figure 17: Effect of temperature on ethanol conversion and products selectivity with FeVO catalyst. Reaction conditions: feed 5% ethanol, 5% O_2, 20% H_2O, rest N_2; W/F 0.5 g s/mL. Symbols: ethanol conversion (◆), selectivity to acetaldehyde (▲), ethane (■), diethylether (△), acetic acid (◇), CO (●) and CO_2 (+).

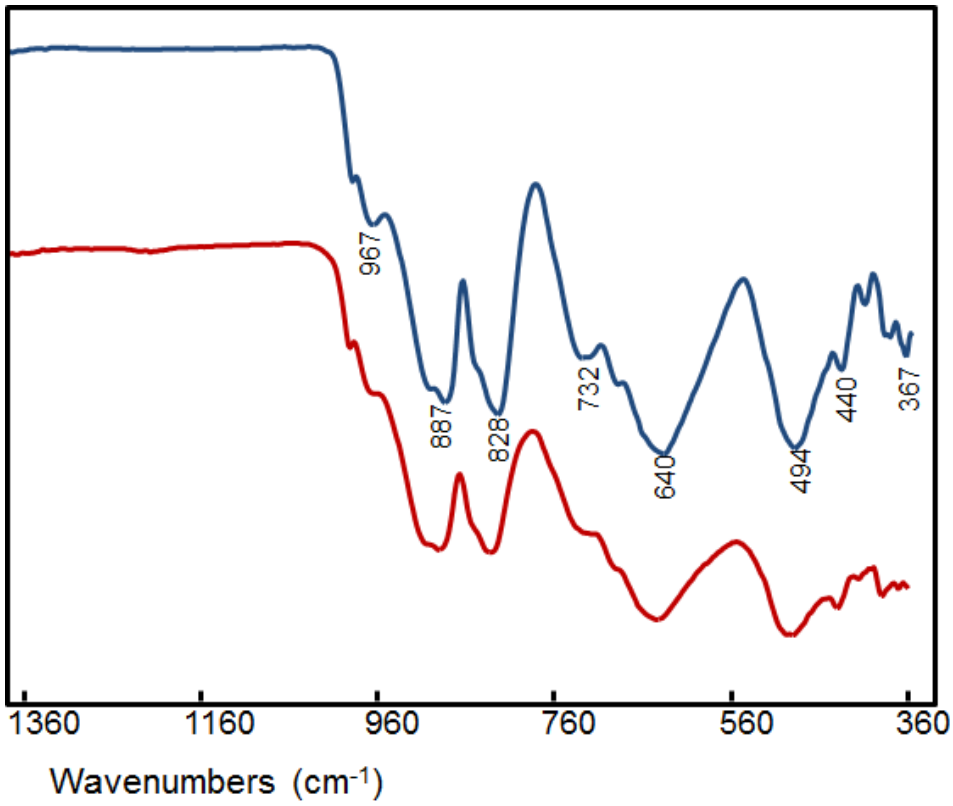

Figure 18: IR-ATR spectra of fresh calcined catalyst (top), and after reaction at 400°C (bottom), in ethanol + H_2O + O_2.

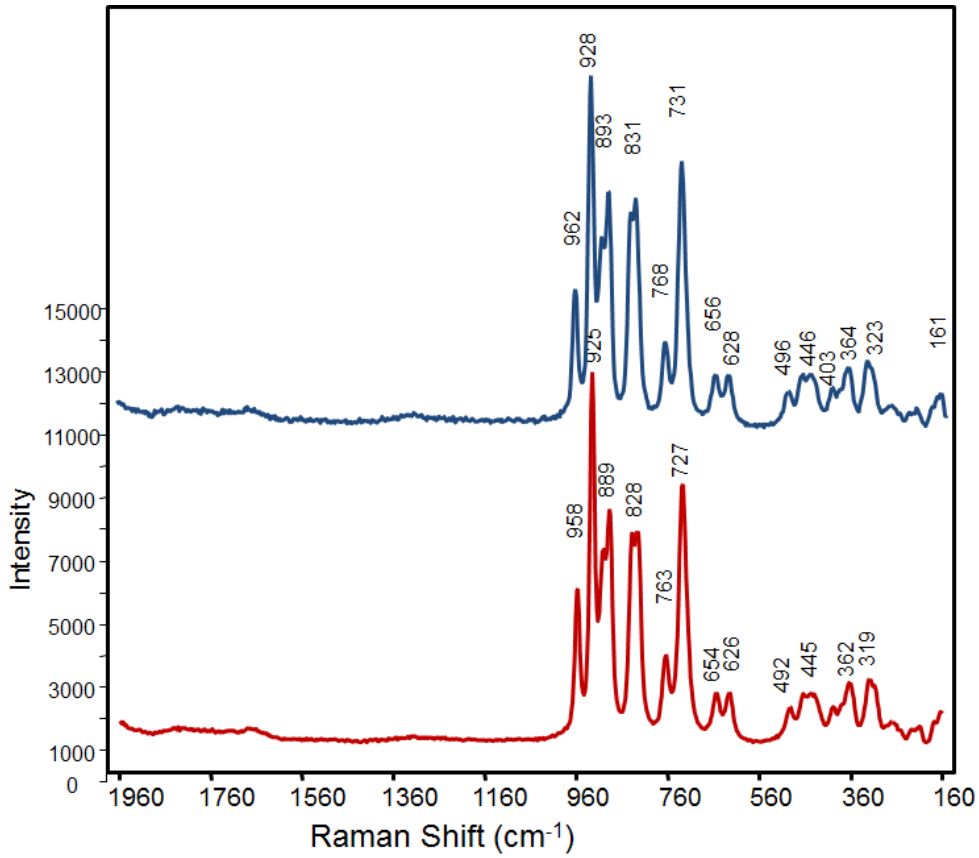

Figure 19: Raman spectra of fresh calcined catalyst (top), and after reaction at 400°C (bottom) in ethanol + H_2O + O_2.

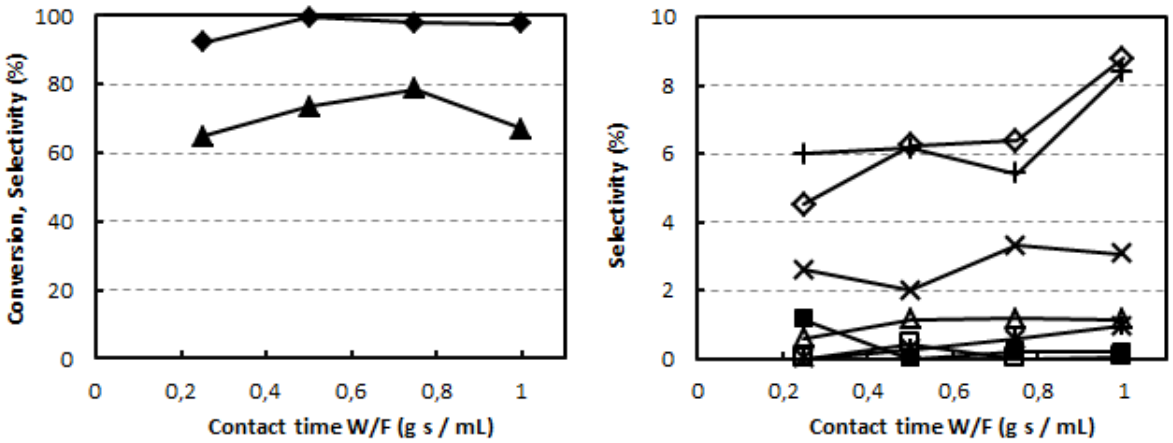

Figure 20: Effect of W/F ratio on ethanol conversion and products distribution with FeVO catalyst. Reaction conditions: feed 5% ethanol, 5% O_2, in N_2; T 300°C. Symbols: ethanol conversion (◆), selectivity to acetaldehyde (▲), butyraldehyde (✕), crotonaldehyde (✳), acetone (□), ethylacetate (△), acetic acid (◇), ethylene (■) and CO_2 (+).

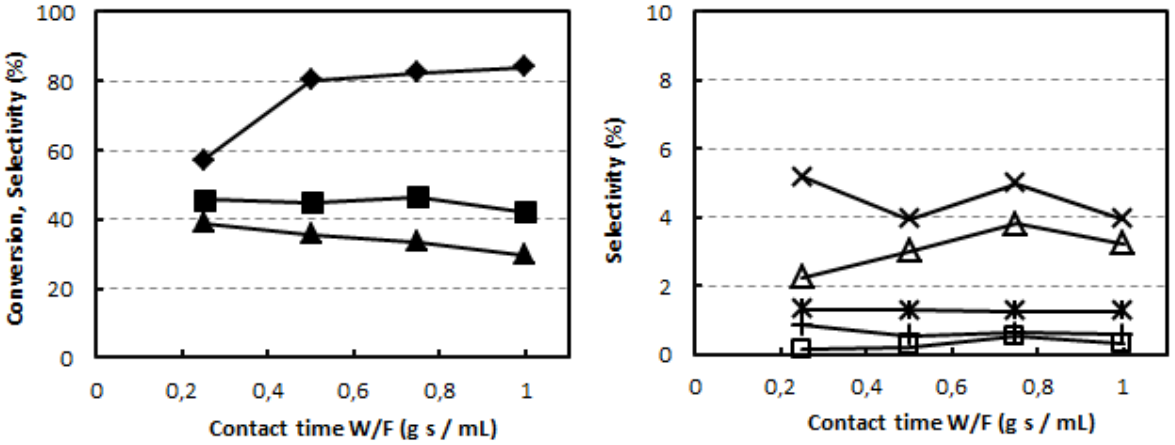

Figure 21: Effect of W/F ratio on ethanol conversion and products distribution with FeVO catalyst. Reaction conditions: feed 5% ethanol, in N_2; T 300°C. Symbols: ethanol conversion (◆), selectivity to acetaldehyde (▲), ethane (■), butyraldehyde (×), crotonaldehyde (✳), acetone (□), ethylacetate (△), and CO_2 (+).

In the presence of O_2, an increase of selectivity to acetaldehyde was shown between 0.25 and 0.75 g s/mL W/F ratio; this increase was due to improved values of C balance (from 81 to 96%). The decline of acetaldehyde selectivity shown at W/F 1 g s/mL was due to the higher formation of both acetic acid and CO_2, products formed by consecutive oxidation. With ethanol only (Figure 19), the decline of selectivity to acetaldehyde (the co-product of ethanol disproportionation), was due mainly to the greater formation of heavy compounds, as inferred from the worse values of C balance (from 95% at 0.25 g s/mL, down to 81% at 1.00 g s/mL).

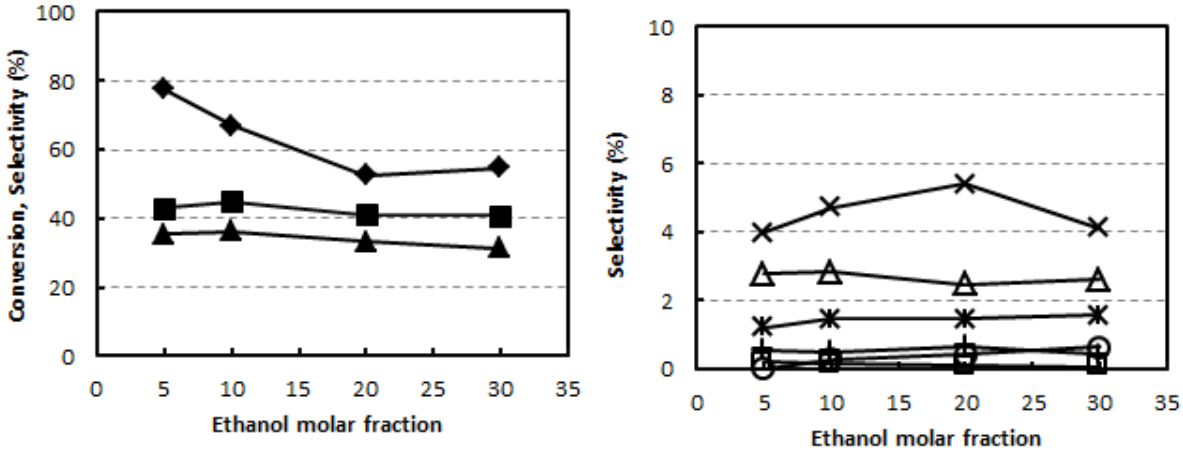

Figure 22: Effect of ethanol molar fraction on ethanol conversion and products distribution with FeVO catalyst. Reaction conditions: feed ethanol in N_2; T 320°C, W/F 0.5 g s/mL. Symbols: ethanol conversion (◆), selectivity to acetaldehyde (▲), ethane (■), butyraldehyde (×), crotonaldehyde (✳), acetone (□), ethylacetate (△), crotyl alcohol (○) and CO_2 (+).

An increase of ethanol molar fraction, for tests carried out under anaerobic conditions, led to decline of ethanol conversion, whereas the distribution of products was not much affected.

2.3.1.1 *The reactivity of V_2O_5 and Fe_3O_4*

In order to assess about the role of V and Fe in the FeVO catalyst, we carried out the reactivity experiments with V_2O_5, Fe_2O_3 and Fe_3O_4. Figure 23 summarizes the catalytic performance of V_2O_5; the results were recorded during the equilibration of the catalyst, in the presence of 5% ethanol, at 300°C. Main products were acetaldehyde and ethane, formed by disproportionation; minor amounts of C_4 compounds (mainly ethylacetate and crotonaldehyde), and CO_x were also formed.

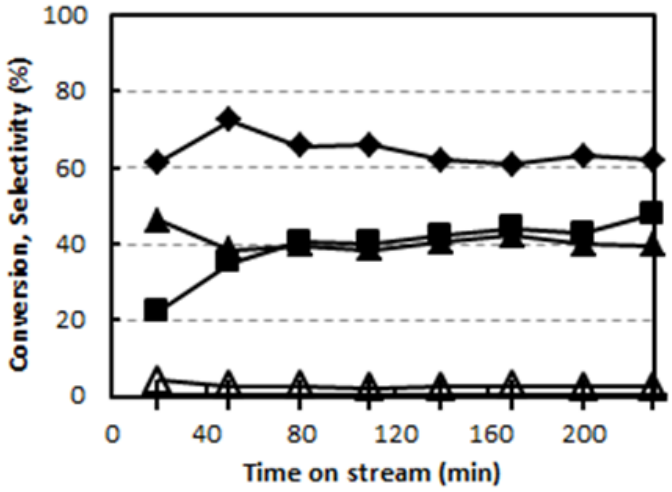

Figure 23: Effect of time-on-stream on ethanol conversion and products distribution with V_2O_5 catalyst. Reaction conditions: T 300°C, feed 5% ethanol in N_2; W/F 0.5 g s/mL. Symbols: ethanol conversion (◆), selectivity to acetaldehyde (▲), ethane (■), C4 (crotonaldehyde and ethylacetate) (△), and CO_x (+).

Conversion of ethanol underwent only minor changes, an event which suggests that the reduction of V^{5+} was much quicker than for the FeVO catalyst; selectivity to acetaldehyde also was not much affected, whereas that to ethane increased and finally became the same as that of acetaldehyde. Carbon balance was close to 75% at the beginning of the experiment, but finally was higher than 90%. In overall, compared to the FeVO catalyst (Figure 6), V_2O_5 gave a higher selectivity to acetaldehyde and a lower selectivity to C_4 compounds, which reflects the contribution deriving from Fe sites in FeVO.

The effect of temperature is summarised in Figure 24. Ethane and acetaldehyde formed in similar amount at 300°C, but at higher temperatures acetaldehyde selectivity declined, with an increase of selectivity to both C_4 and heavy compounds.

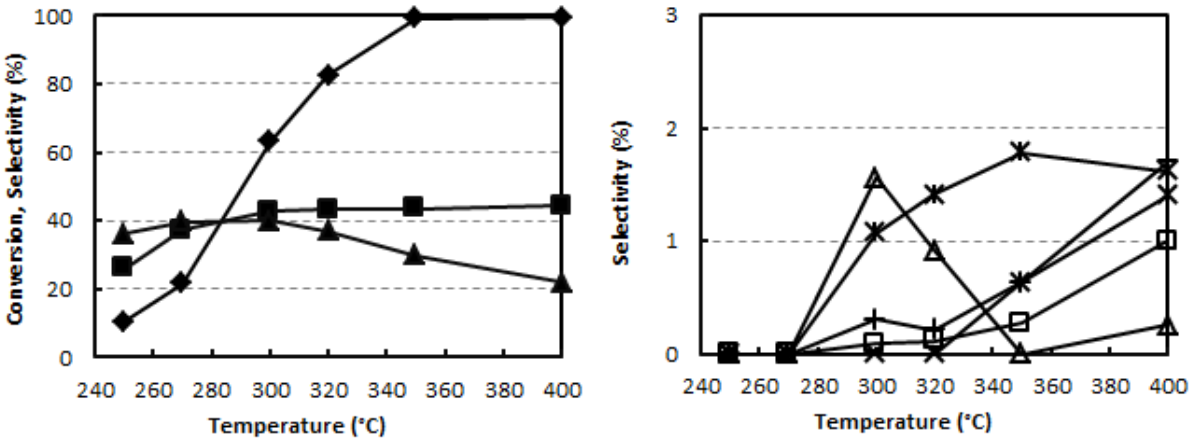

Figure 24: Effect of temperature on ethanol conversion and products distribution with V_2O_5 catalyst. Reaction conditions: feed 5% ethanol in N_2; W/F 0.5 g s/mL. Symbols: ethanol conversion (◆), selectivity to acetaldehyde (▲), ethane (■), butyraldehyde (×),crotonaldehyde (✳), acetone (□), ethylacetate (△), and CO_2 (+). Only by-products with selectivity higher than 1% are shown.

The C balance was 62% at low temperature, but increased up to 86% at 300°C, and then decreased until 74% at 400°C. Other products formed in minor amount (not shown in Figure) were CO, acetic acid and diethyleteher; major C_4 products were ethylacetate and crotonaldehyde. Again, the comparison with the FeVO catalyst (Figure 9) shows that the presence of Fe led to both a higher selectivity to C_4 compounds and a considerably lower formation of heavy compounds or carbonaceous residues (both contributed to the poor C balance with the V_2O_5 catalyst).

Figure 25 shows the effect of temperature on catalytic behaviour in the presence of ethanol and O_2. In this case, major differences were observed compared to FeVO (Figure 3): the amount of C_4 compounds was very low (no crotonaldehyde and butyraldehyde were formed; ethylacetate formed with 1% selectivity only at 250°C); on the other hand, CO and acetic acid formed with greater selectivity, whereas the selectivity to CO_2 was similar for the two catalysts; also the selectivity to ethylene was greater with V_2O_5. C balance was higher than 90% until 320°C, then decreased approaching 80% at 400°C. Similar results were obtained with steam co-feeding (Figure 26).

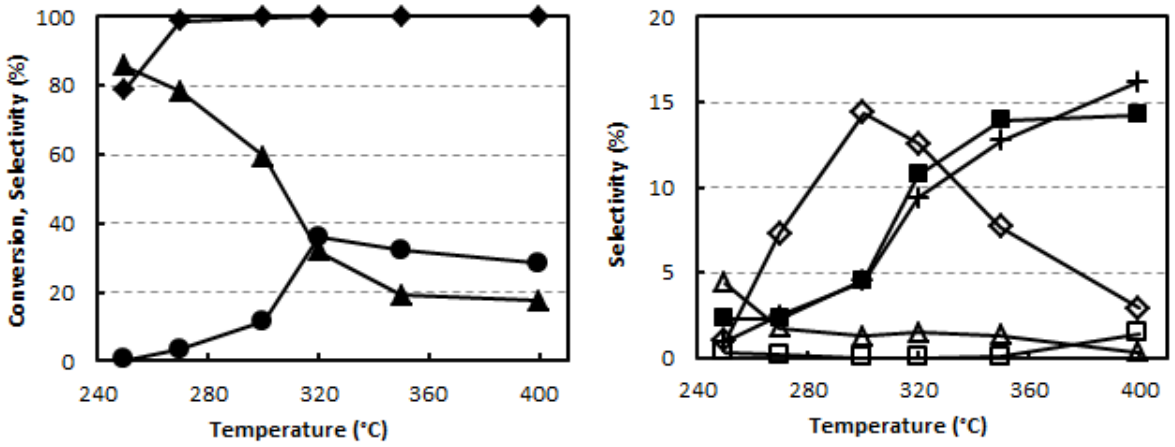

Figure 25: Effect of temperature on ethanol conversion and products selectivity with V_2O_5 catalyst. Reaction conditions: feed 5% ethanol, 5% O_2, 90% N_2; W/F 0.5 g s/mL. Symbols: ethanol conversion (◆), selectivity to acetaldehyde (▲), ethylene (■), acetone (□), diethylether (△), acetic acid (◇), CO (●) and CO_2 (+).

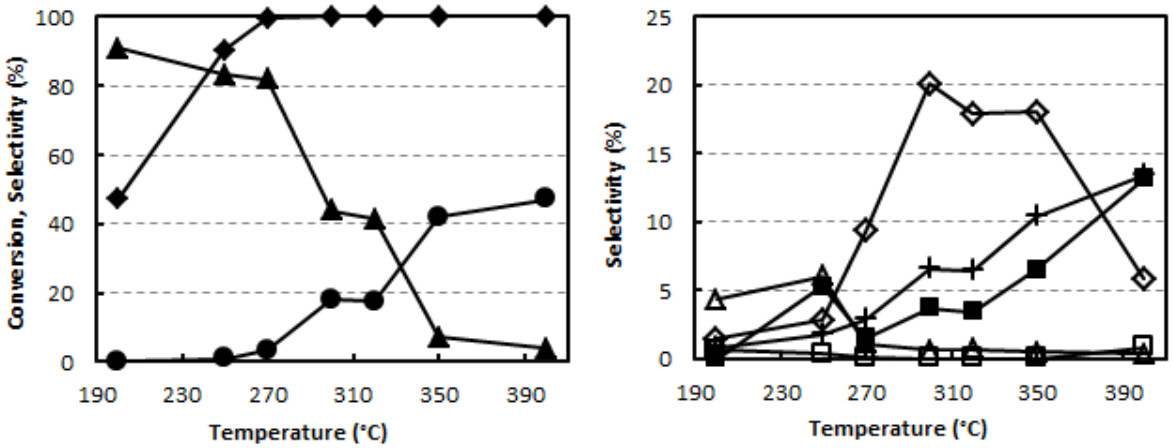

Figure 26: Effect of temperature on ethanol conversion and products selectivity with V_2O_5 catalyst. Reaction conditions: feed 5% ethanol, 5% O_2, 20% H_2O, rest N_2; W/F 0.5 g s/mL. Symbols: ethanol conversion (◆), selectivity to acetaldehyde (▲), ethylene (■), acetone (□), diethylether (△), acetic acid (◇), CO (●) and CO_2 (+).

Concluding, the reactivity of V_2O_5 showed some differences compared to that one of the FeVO catalyst: a smaller selectivity to C_4 compounds, and a greater selectivity to CO and acetic acid.

The characterization of used Vanadium oxide by means of FTIR spectroscopy allowed us conclude that the catalyst underwent deep reduction, especially during reaction in the absence of O_2.

At 400°C, synthesized Fe_2O_3 gave 29% ethanol conversion in an experiment carried out by feeding ethanol (5% in N_2), with formation of acetaldehyde as the main product (ca 60% selectivity), with minor formation of ethylene, crotyl alcohol, butenes and acetone. More interesting was the reactivity of commercial Fe_3O_4 (from Sigma Aldrich, 500 nm crystal size), displayed in figures below. With ethanol only (Figure 27), main products were acetone at low temperature, ethylacetate and acetaldehyde at intermediate temperature, and ethylene, acetone and CO_2 at high temperature. CO formed with selectivity of 2% at 400°C; other C_4 compounds were absent; C balance was between 50 and 65%.

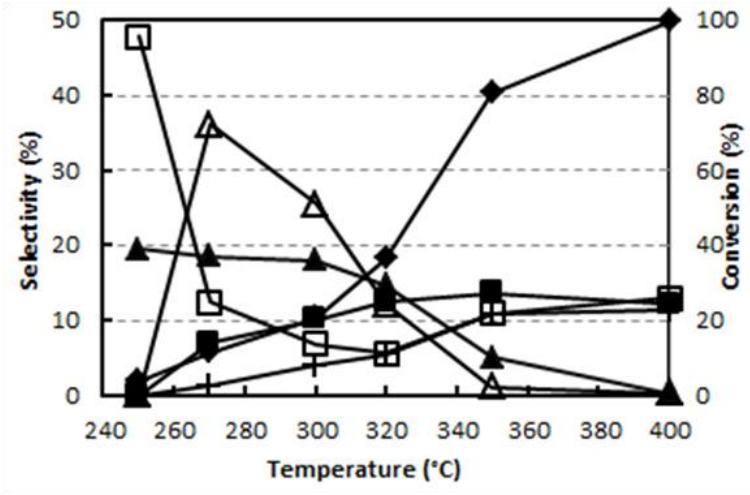

Figure 27: Effect of temperature on ethanol conversion and products selectivity with Fe_3O_4 catalyst. Reaction conditions: feed 5% ethanol, rest N_2; W/F 0.5 g s/mL. Symbols: ethanol conversion (◆), selectivity to acetaldehyde (▲), ethylene (■), acetone (□), ethylacetate (△), and CO_2 (+).

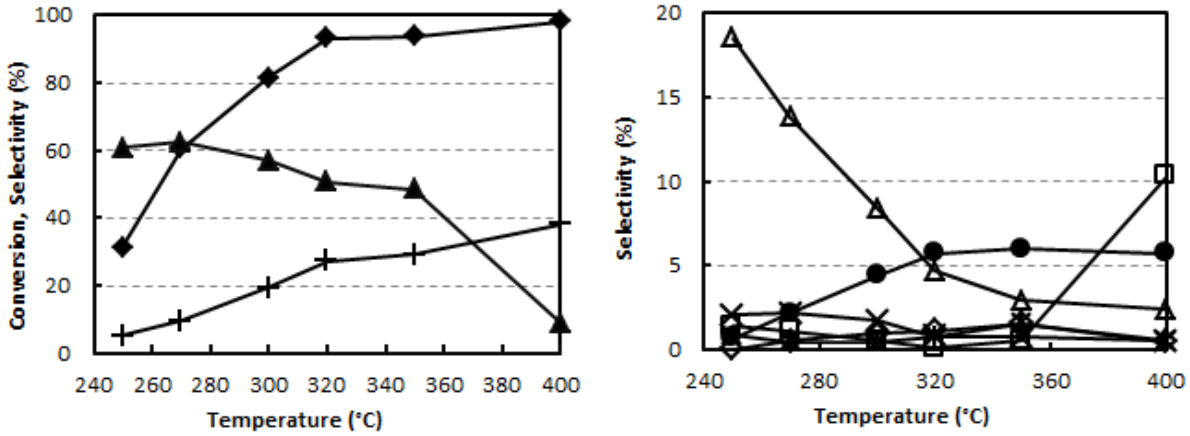

Figure 28: Effect of temperature on ethanol conversion and products selectivity with Fe_3O_4 catalyst. Reaction conditions: feed 5% ethanol, 5% O_2, rest N_2; W/F 0.5 g s/mL. Symbols: ethanol conversion (◆), selectivity to acetaldehyde (▲), ethylene (■), acetone (□), acetic acid (◇), diethylether (△), crotonaldehyde (✳), ethylacetate (×), CO (●), and CO_2 (+).

In the presence of O_2 (Figure 28), major differences with respect to tests without oxygen were the much greater formation of acetaldehyde and of CO_2; diethylether also formed with high selectivity, whereas the formation of ethylene was negligible. A similar behavior was shown with both co-fed O_2 and H_2O (Figure 29).

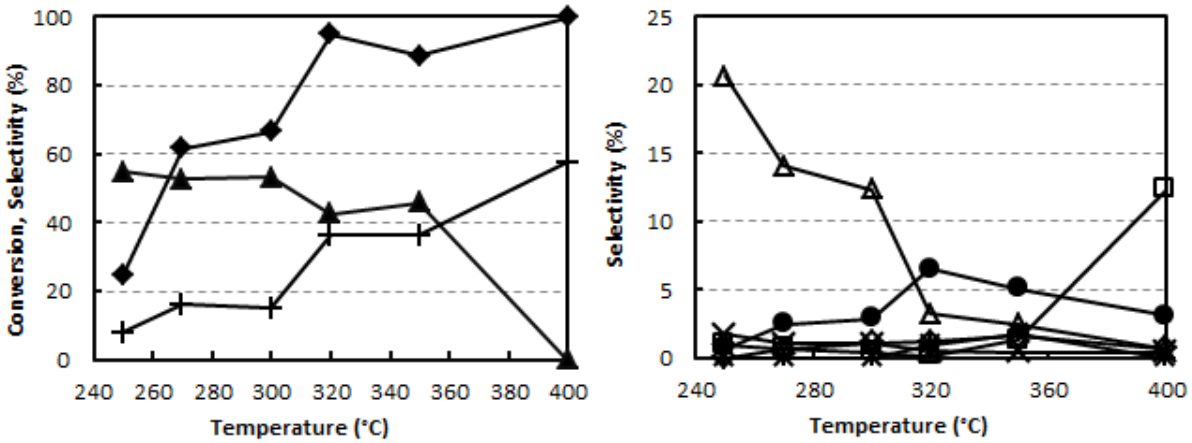

Figure 29: Effect of temperature on ethanol conversion and products selectivity with Fe_3O_4 catalyst. Reaction conditions: feed 5% ethanol, 5% O_2, 20% H2O, rest N_2; W/F 0.5 g s/mL. Symbols: ethanol conversion (◆), selectivity to acetaldehyde (▲), ethylene (■), acetone (□), acetic acid (◇), diethylether (△), crotonaldehyde (✳), ethylacetate (✕), CO (●), and CO_2 (+).

2.3.1.2 In-Situ DRIFT-MS ethanol adsorption

Figure 30 shows the spectra of the FeVO catalyst during the adsorption of ethanol at 300°C. In this case, the spectrum of the catalyst (shown in the bottom) was not subtracted because it was changing with time. Even after only 5 minutes, some bands due to the adsorbed ethanol were observed (2982 cm^{-1}), as well as those for adsorbed acetaldehyde at 1760 cm^{-1} (bands not present in the catalyst spectrum).

After 60 minutes of adsorption, the disappearing of the low frequency bands (862, 1015 cm^{-1}) confirm that the catalyst was undergoing structural modifications. However, the intensity of the band at 3265 cm^{-1} (attributed to an OH stretching) increased.

Mass spectrometer signals (m/z) versus time-on-stream well reproduced the results of catalytic experiments (Figure 31). In fact, both ethane and ethanol signals increased (which means a decrease in ethanol conversion and a reduction of the catalyst, which catalysed ethanol disproportionation). The intensity of the acetaldehyde signal slightly decreased probable because on the reduced catalyst there was a minor contribution of the oxidative dehydrogenation and acetaldehyde formed by ethanol disproportionation.

As regards water signal trend, it decreased during time, and this decrease appeared to be parallel to the ethane signal increase. This means that during the first hour, water was produced probably from ethanol oxidative dehydrogenation to acetaldehyde and further oxidation to CO_2 (the latter has been detected in trace level both in DRIFT/MS and in reactivity experiments). Then, after the stabilization time, water came from ethanol disproportionation.

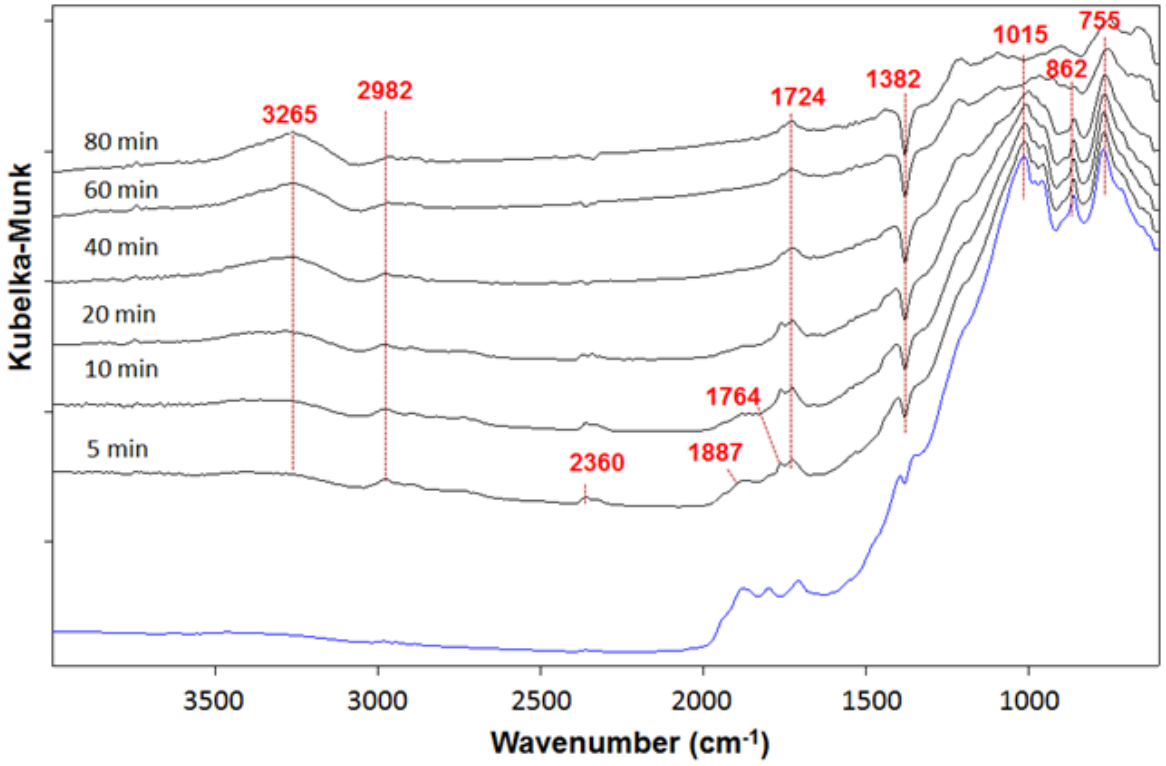

Figure 30: In situ DRIFT spectra of FeVO catalyst during ethanol adsorption at 300°C (anaerobic conditions).

Another DRIFTS-MS experiment (Figure 32) was conducted feeding continuously air and ethanol and periodically registering spectra. Results indicate that the structure of the catalyst was stable throughout the experiment, which means that no reduction occurred in these conditions. Moreover, the spectra did not reveal any OH band formation, indicating the absence of new OH groups that were present instead when the sample was reduced with ethanol. This is in agreement with what reported by Ueda et al., who also investigated on ethanol transformations on reduced vanadium oxides[31]. Actually they proposed that ethanol disproportionation to acetaldehyde and ethane should pass through the adsorption of molecular ethanol on the surface of V_2O_3. Then ethanol rearranges to the products. This can explain why no OH band was observed when the catalyst was still oxidized or when it was oxidized because of the presence of oxygen.

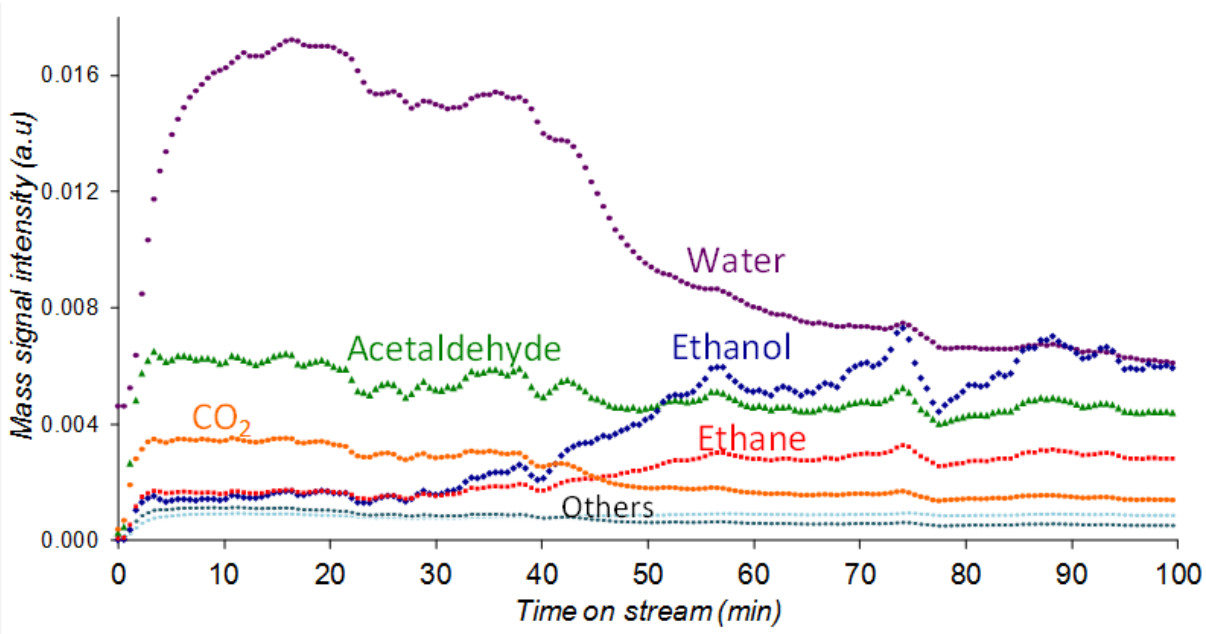

Figure 31: Mass signals intensity versus time-on-stream registered during ethanol continuous feeding at 300°C with FeVO catalyst.

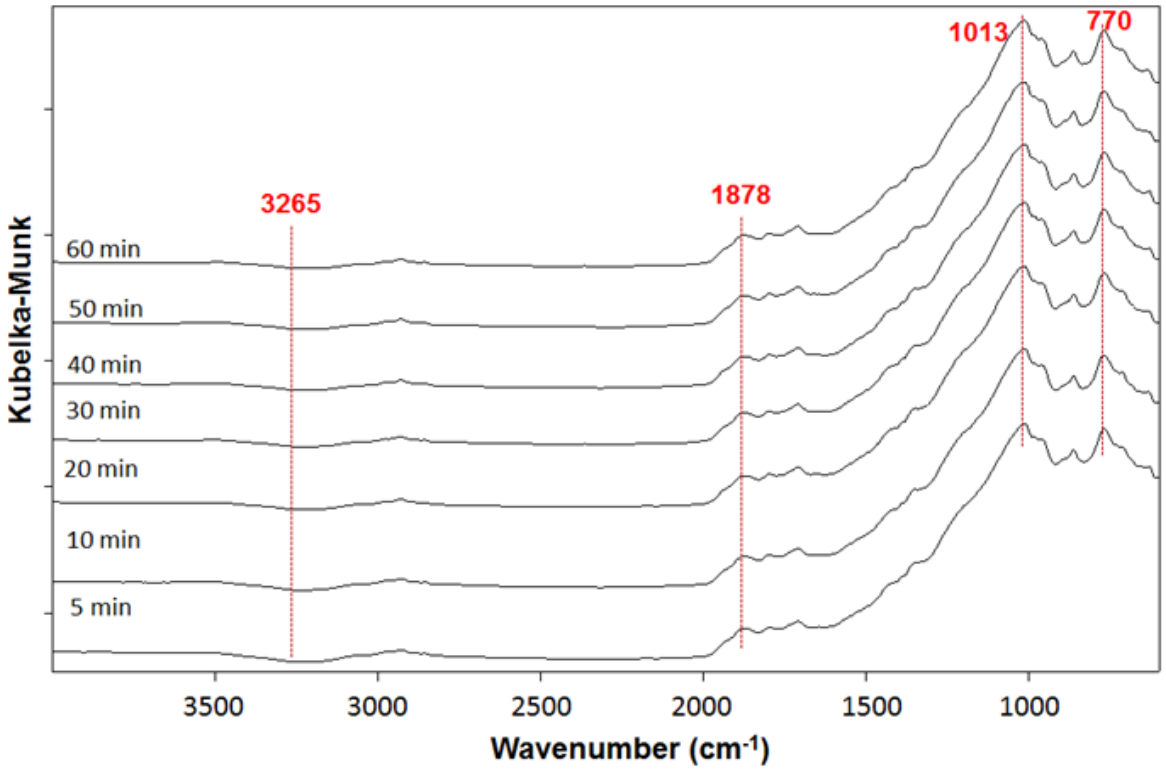

Figure 32: In situ DRIFT spectra of FeVO catalyst during ethanol adsorption at 300°C (aerobic conditions).

Experiments were also performed with bare V_2O_5 (Figure 33). In the absence of O_2, the catalyst was reduced after only 30 minutes, as evidenced by the disappearance of the characteristic V=O overtones bands for V_2O_5 (two bands at 1971 and 2020 cm^{-1}). This reduction time was shorter than that required for FeVO under the same conditions. In fact,

the reactivity experiments revealed that V_2O_5 start to form ethane (which is produced by disproportionation on the reduced catalyst) earlier than FeVO. Also with this catalyst the band attributable to the generation of new OH groups (at ca 3200cm^{-1}) developed during the reduction, as it was for FeVO also.

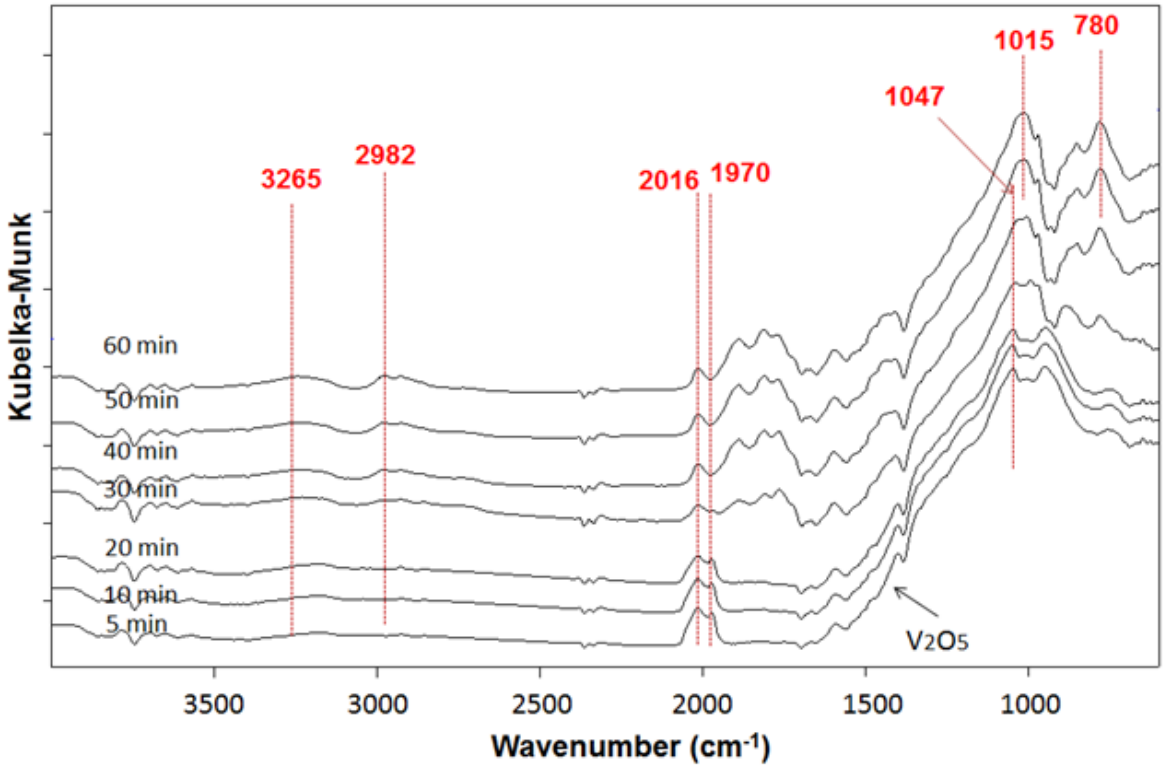

Figure 33: In situ DRIFT spectra of V_2O_5 catalyst during ethanol adsorption at 300°C (anaerobic conditions).

2.3.1.3 Summary on FeVO catalyst

FeVO proved to be an active catalyst for the oxidation of ethanol with good selectivity to acetaldehyde. Under anaerobic conditions, its progressive reduction caused the change of the reaction mechanism; the reduced catalyst, made of spinel Fe-V-O, catalysed the disproportionation of ethanol to acetaldehyde and ethane, with minor formation of C_4 compounds.

Under anaerobic conditions, the FeVO catalyst showed similar behavior compared to V_2O_5; differences however concerned the reducibility of V^{5+}, which was slower with FeVO, the minor formation of C_4 components (which formed on the Fe sites from the intermediately formed acetaldehyde) and the worse C balance observed with Vanadium oxide. Similar differences were observed in the presence of O_2; in this latter case, moreover, Vanadium oxide was more selective to CO and acetic acid than FeVO. Conversely, the mixed catalyst showed a remarkably different behavior compared to magnetite.

In overall, the data obtained support the hypothesis that the surface reactivity of the Fe-V-O system is much closer to that of V oxide than to magnetite; however, the reactivity of V^{5+} is

clearly affected by the presence of neighbouring Fe cations, which influence its properties, and play a direct role in acetaldehyde transformation into C_4 compounds.

2.3.2 CuVO

Figure 34 shows results of catalytic tests carried out with the CuVO catalyst (surface area 2 m^2/g), by feeding 5% ethanol and 5% oxygen at W/F 0.5 g·s/mL and different temperatures. Because of technical reasons it was possible to determine CO selectivity only at 250, 300 and 400°C. Carbon balance, calculated only for the experimental points at which CO yield was determined, was never less than 90%.

As expected from literature data[55], CuVO was very active in the dehydrogenation of ethanol to acetaldehyde; in fact, the reaction was carried out with 97% selectivity at 250°C. However, at higher temperatures, despite of an increase of ethanol conversion, acetaldehyde selectivity decreased, mainly in favour of CO_x. Ethylene selectivity increased with temperature also, mainly because of thermal dehydration of ethanol, as determined in blank experiments. Acetic acid selectivity first increased, but then decreased when the temperature was raised, in favour of CO_x. We also detected diethyl ether, derived from ethanol etherification, butyraldehyde and crotonaldehyde, each one with selectivity never higher than 2%.

Figure 35 compares XRD patterns of fresh CuVO and of the same catalyst after reaction with ethanol and oxygen, at 300 and 400°C. The pattern of fresh catalyst showed reflections with low intensity, which suggest a poor crystallinity of the structure. Anyway, it was possible to identify two crystalline phases. The main reflection at 28.6, together with those at 21, 22, 29, 31, 32 34 and 35 °2θ, can be assigned to $Cu_3(VO_4)_2$. Reflections at 18.7, 24.7 and 28.7 °2θ can be assigned to $Cu_2V_2O_7$. Others were unrecognized, because of both their weak intensity and the complexity of the pattern. Anyway, it is possible to say that the resulting material was not made of a single compound, but it was a mixture of different Cu-V mixed oxides. The XRD pattern registered for the used catalyst at 300 and 400°C showed the formation of crystalline compounds different from those present in the fresh catalyst, which indicates that the catalyst transformed during reaction.

At 300°C, the XRD pattern of the used catalyst was difficult to interpret, because of both pattern complexity and poor cristallinity. Major reflections at 31, 33, 34, 38, 40 and 63 °2Θ indicate the presence of $CuVO_3$, whereas remaining signals could not be identified.

At 400°C the formation of metallic copper was evident, as shown by the narrow and more intense reflections at 43, 50 and 74 °2θ. Those registered at 31, 33 and 34 °2θ suggest the formation of $CuVO_3$, whereas those at 37 and 28 °2θ indicate the possible formation of Cu oxides, whereas others reflections were not identified. SEM-EDX images, obtained with the

catalyst downloaded after reaction at 300°C, show an homogenous distribution of Cu, O and V, without any apparent metal oxides segregation.

Figure 37 shows FT-IR spectra of CuVO, both fresh and used after reaction with ethanol and oxygen at 300 and 400°C. Because of the scarce literature in this field, it was not possible to make a complete assignment of IR bands, but it was anyway possible to make an hypothesis about the nature of the compounds. The spectrum of fresh CuVO showed bands attributable to different compounds; a broad and intense signal at 775-743 cm^{-1} is related to the V-O stretching mode. This band is split probably because of the presence of different V species and their interaction with Cu. Bands at 883 cm^{-1} and 460 cm^{-1} are related to vibration modes of vanadate ion (VO_4^{3-})[80, 81, 82], which confirm the presence of $Cu_3(VO_4)_2$, also detected by means of XRD. Bands at 907, 883 and the shoulder between 743 and 672 cm^{-1} can be assigned to $Cu_2V_2O_7$[81, 83]; other bands are not attributable to any known compound.

Spectra of catalysts after use at 300 and 400°C were different, indicating a modification of the catalysts, which already occurred during reaction at 300°C. In these two cases, because of the broadness of signals, the complexity of material and lack of literature data, it was not possible to gain useful information from IR spectra. Anyway, it is possible to see that the spectrum registered after reaction at 300°C was more similar to that one after reaction at 400°C than to the fresh catalyst. This means that the catalyst started to change in the reaction environment already at 300°C.

Figure 38 shows Raman spectra of fresh CuVO, and of CuVO after reaction with ethanol and oxygen at 300 and 400°C. Spectra were collected several times, focusing the laser beam on different particles, which resulted in different spectra. Figure 38 shows all the different types of spectra registered, although not all of them were attributable to a specific compound, because the poor cristallinity of the material affected the quality of Raman spectra. Despite this, it is possible to hypothesize that the strong band centred at around 900 cm^{-1} belongs to a V-O stretching mode, shifted at lower wavenumber with respect to bare V_2O_5 because of the presence of Cu, which weakened V-O bond and caused it to vibrate at lower energies[84].

Raman spectra of fresh CuVO, in agreement with XRD analysis, shows the presence of different compounds. The top spectrum in Figure 38-A shows the typical bands of $CuVO_3$[85]. The other two spectra in the same figure show bands of different Cu-V mixed oxides; bands at 847 and 750 cm^{-1} belong to $Cu_3(VO_4)_2$[86], whereas those at around 800 and 330 cm^{-1} are attributable to $Cu_2V_2O_7$; other bands were not identified. Anyway, the formation of a mixed Cu-V oxide is confirmed by the absence of bands attributable to Cu or V oxides [137, 87].

Raman spectrum of CuVO after reaction at 300°C with ethanol and oxygen showed a weakened V-O stretching signal at about 900 cm^{-1}, probably related to $CuVO_3$, which presence was identified also by XRD. Bands at 853 and 809 cm^{-1} can indicate the presence of some more oxidized Cu-V mixed oxide.

Finally, the catalyst used after reaction with ethanol and oxygen at 400°C, showed again the same bands related to V-O stretching in Cu-V mixed oxides, but also bands attributable to coke (at 1595 and 1415 cm^{-1}).

To summarize: CuVO in presence of both ethanol and oxygen behaved as a good oxidehydrogenation (ODH) catalyst, especially at low temperatures. In fact, already at 300°C part of the ethanol was oxidised to CO_x. The catalyst underwent structural modifications, depending on reaction temperature. Despite the presence of oxygen, which was anyway in defect with respect to the reaction stoichiometry, CuVO started to be reduced to cCu(I)-V mixed oxides at 300°C. At 400°C, the extent of reduction was greater, in fact at this temperature it was possible to detect the formation of metallic Copper also. Moreover, at 400°C coke deposits accumulated over the catalyst surface.

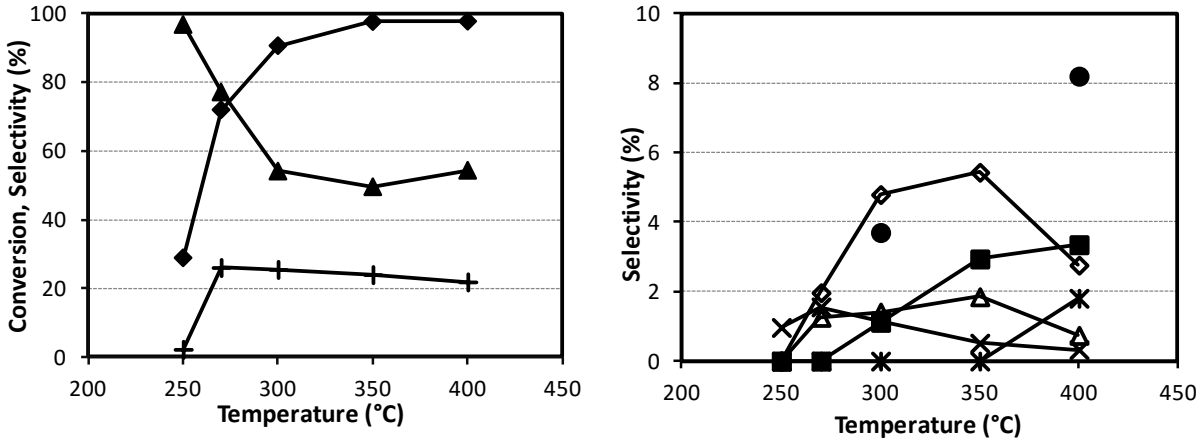

Figure 34: Effect of temperature on ethanol conversion and products selectivity with CuVO catalyst. Reaction conditions: feed 5% ethanol, 5% O_2, 90% N_2; W/F 0.5 g·s/mL. Symbols: ethanol conversion (◆), selectivity to acetaldehyde (▲), ethylene (■), crotonaldehyde (✳), butyraldehyde (✕), diethyl ether (△), acetic acid (◇), CO (●) and CO_2 (+). Results were taken after ca 2h of "equilibration".

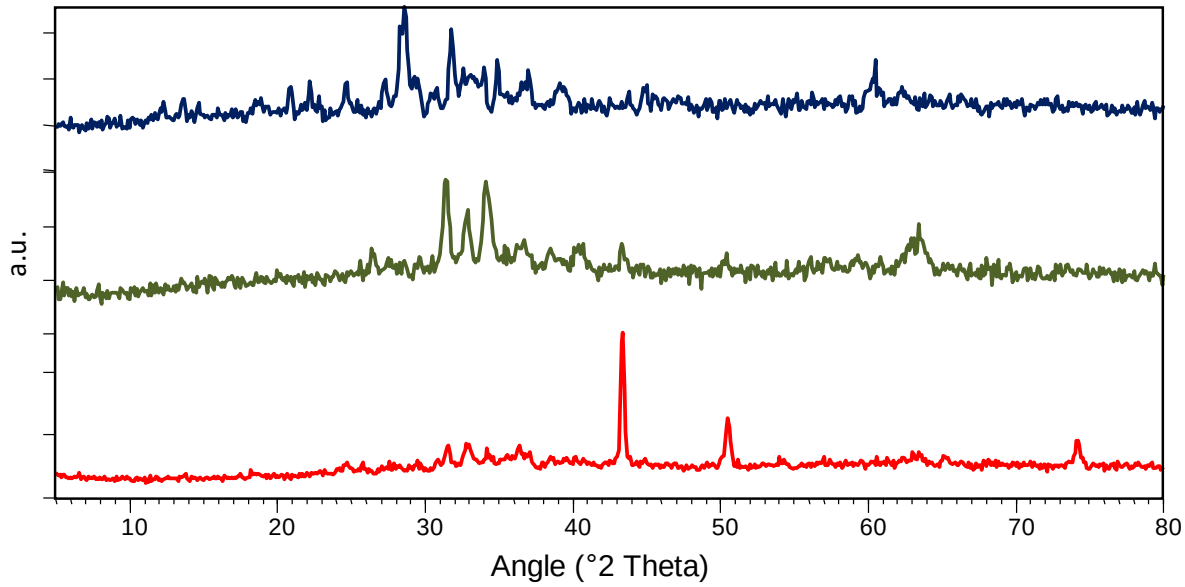

Figure 35: XRD patterns of CuVO catalyst; from top to bottom: calcined, and after reaction at 300°C and 400°C, in ethanol + O_2.

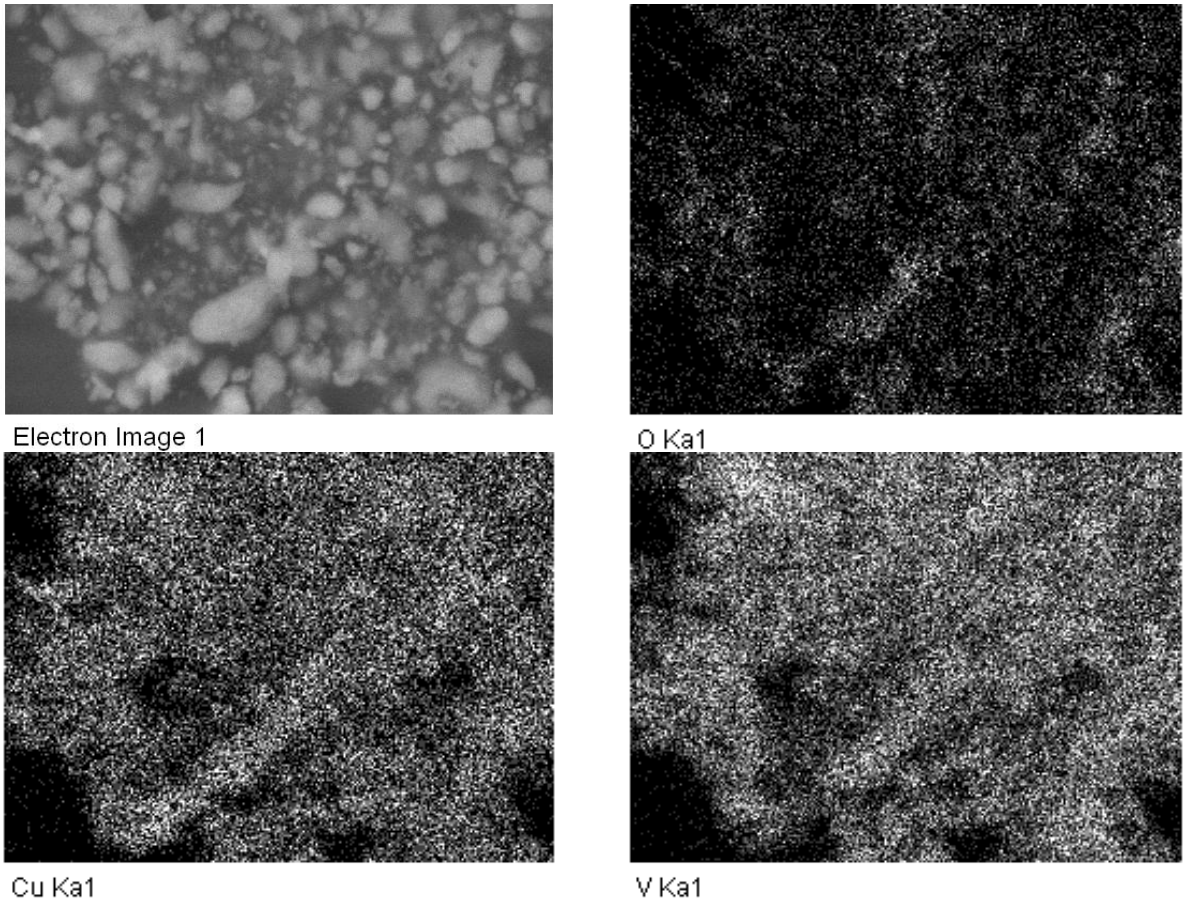

Figure 36: SEM-EDX maps of Fe, V and O in FeVO catalyst used at 300°C with ethanol and O_2. Top, left: SEM image, top right: Oxygen mapping, bottom right: Vanadium mapping, bottom left: Copper mapping

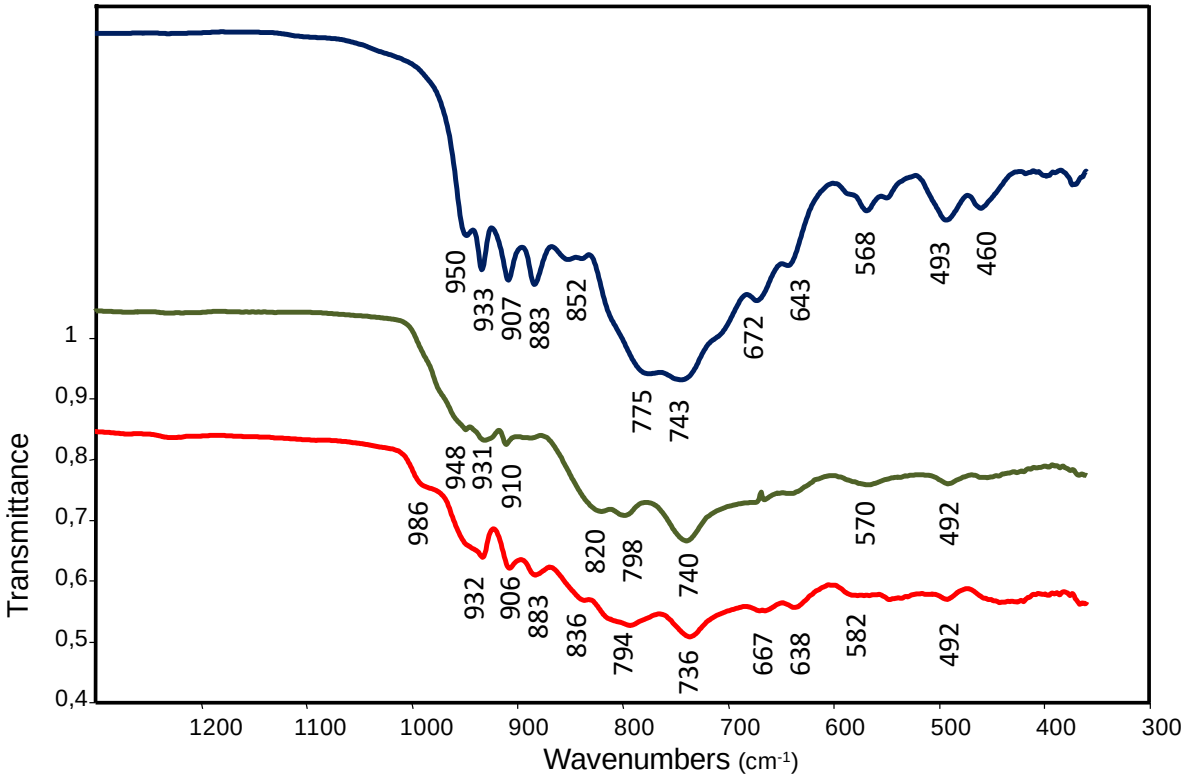

Figure 37: FT-IR spectra of CuVO catalyst. From top to bottom: fresh catalyst, and after reaction at 300°C and 400°C, in ethanol + O_2.

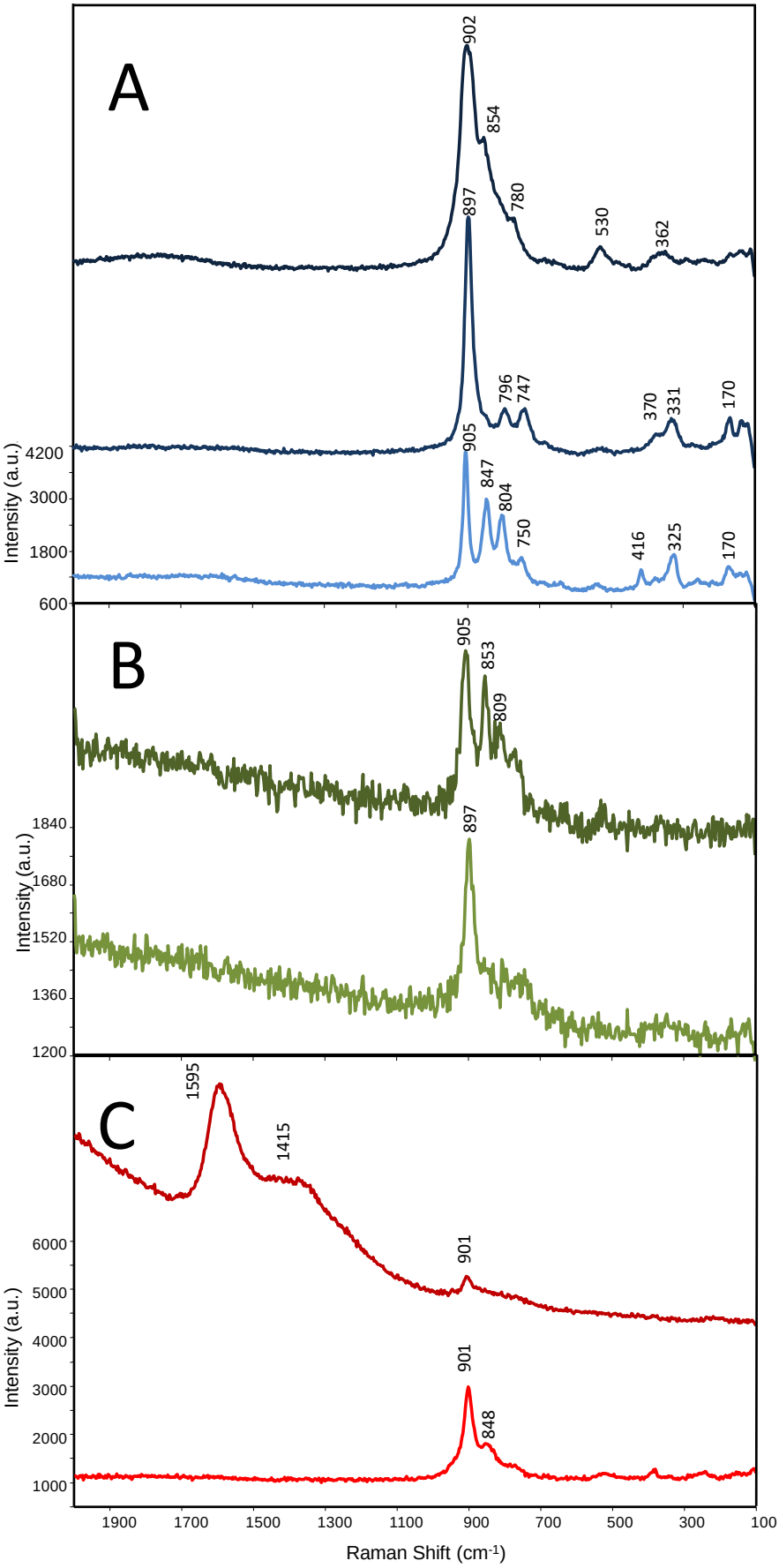

Figure 38: Raman spectra registered on different spots of CuVO fresh (A), and after reaction at 300°C (B) and 400°C (C), in ethanol + O_2.

In order to investigate on catalytic properties of CuVO, we carried out some experiments of ethanol transformation in anaerobic conditions.

Figure 39 (top) shows ethanol conversion and products selectivity in function of time-on-stream, with 5% ethanol in N_2 at 300°C. An equilibration time of ca 120 min was needed in order to reach a steady performance of the catalyst. During this period, both acetaldehyde selectivity and ethanol conversion decreased, whereas ethane selectivity increased. As described for FeVO, ethane can form from ethanol disproportionation[48]. As inferred from characterization results, the non-steady state behaviour was due to the development of some reduced phases.

When the steady state was reached, acetaldehyde selectivity still was higher than ethane selectivity, even if during the equilibration time the former decreased and the latter increased. Ethylene was detected in low amount (selectivity always < 1%), and the same was for CO. CO_2 and acetic acid formed on the fresh catalyst, but their selectivity rapidly decreased down to values close to zero.

C_4 products, which derive from acetaldehyde condensation (including ethylacetate[88, 89]), showed a slight increase with time-on-stream. Carbon balance was always higher than 90%.

Figure 39 (bottom) shows catalyst behaviour in the same conditions, but after 250 min time-on-stream (top figure) and regeneration in air at 450°C for 3h. The catalytic behaviour typical of the fresh catalyst was only partially recovered by the regeneration treatment, in fact initial acetaldehyde selectivity was lower than that shown by fresh catalyst. Moreover, initial selectivity to CO_2 and acetic acid were also lower. This means that the catalyst probably underwent some irreversible structural modification during the first reaction period, and the regeneration treatment was not able to restore the chemical-physical characteristics of the fresh calcined sample (see characterization results). Probably these structural modifications can also explain the lower selectivity to C_4 and the absence of butyraldehyde for the regenerated catalyst.

Figure 40 shows the effect of temperature with 5% ethanol in nitrogen feedstock, with CuVO; experiments were carried after the steady state had been reached.

The two main products were acetaldehyde and ethane; at temperatures lower than 300°C acetaldehyde formed with higher selectivity, but then its selectivity decreased with the increase of temperature. Conversely, an opposite behaviour was shown by ethane. As a result, acetaldehyde and ethane showed similar yields at temperatures higher than 350°C. Other products formed in minor amounts were ethylacetate, acetic acid, butyraldehyde, crotonaldehyde, acetone and CO_2. Carbon balance was always higher than 90%, except at 350 and 400°C, when it decreased, probably because of heavy compounds formation and coke deposition.

Figure 40 shows the XRD pattern of the catalyst after reaction at 300 and 400°C; in both cases, the presence of only metallic Copper was detected.

SEM-EDX maps clearly indicates the presence of segregated metallic Copper, mainly on the borders of the particles. EDX semi-quantitative analysis indicates that bright zones in the SEM image were made mainly of metallic Copper (>60% m/m), while other zones were made of mixed oxides in which the Cu/V/O atomic ratio was close to 1/1/5. Since a Cu-V mixed oxide with this atomic ratio does not exist, the formation of a mixed oxide together with segregated oxides of Cu and V can be hypothesized, with an average composition corresponding to that one found experimentally by means of EDX.

Therefore, the non-complete recovery of catalytic properties after regeneration can be due to the presence of segregated metal oxides, which could not be converted back to the original mixed compounds.

Figure 43 shows FT-IR spectra of CuVO, both fresh and after reaction with ethanol at 300 and 400°C. Spectra of spent catalysts confirm the formation of a compound different from that one present in the fresh catalyst; moreover the same compounds seem to be present after reaction at 300 and 400°C. As in previous cases, also these spectra show bands attributable to different compounds. Signals at 981, 618 and 524 are related to vibration modes of V_2O_3[90], while other bands could not be attributed to any specific compound. Anyway, it is possible to say that they were probably due to the presence of one or more reduced V-Cu mixed oxides. In fact, by comparison with literature[82, 83, 84, 85, 86, 90], it was not possible to identify any peak corresponding to mixed oxides in which both Cu and V are present in their higher oxidation state. Moreover, it is possible to exclude segregation of Cu oxides, in fact corresponding bands were absent[81].

The spent catalyst (Figure 44-B) showed two different Raman spectra. One was characterised by a weak band related to V-O stretching, red-shifted because of the presence of Cu. Another spectrum, registered by focusing the laser beam on a different spot of the catalyst, showed bands around 1600 and 1400 cm^{-1} which indicate coke deposition.

To sum up, as in case of FeVO, also CuVO needed an equilibration in order to reach a stable behaviour. Contact with ethanol at high temperatures led to oxides reduction, in fact the spent catalyst showed segregation of metallic Cu, V_2O_3, and other unidentified reduced compounds. This phase segregation made the regeneration of the catalyst an inefficient step.

Acetaldehyde and ethane were not formed in similar amounts, as from the stoichiometry of ethanol disproportionation, but acetaldehyde formed in a higher amount. This can be explained by taking into account that ethanol disproportionation still occurred on the reduced catalyst, but the formation of metallic Cu enhanced ethanol dehydrogenation to acetaldehyde.

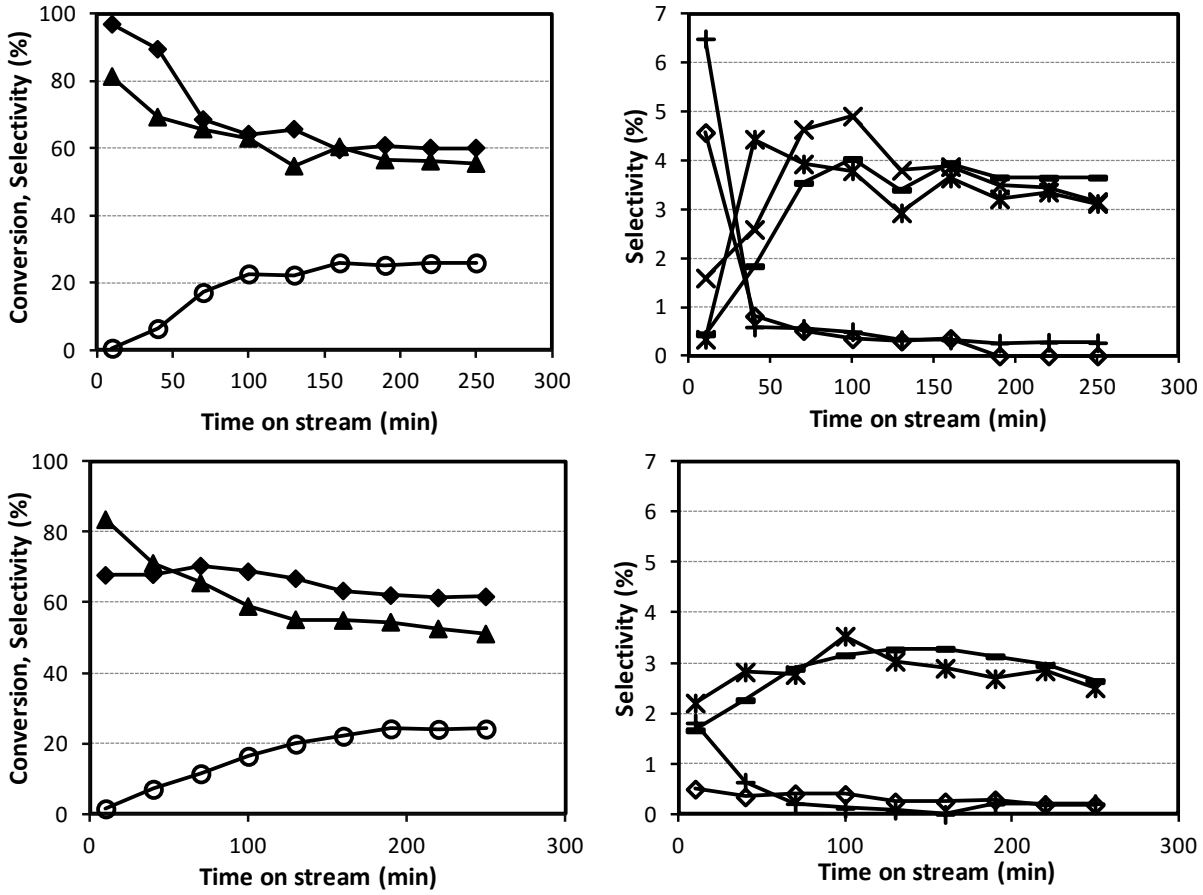

Figure 39: Effect of time-on-stream on ethanol conversion and products distribution with CuVO catalyst. Reaction conditions: T 300°C, feed 5% ethanol in N_2; W/F 0.5 g s/mL. Symbols: Ethanol conversion (◆), selectivity to: acetaldehyde (▲), crotonaldehyde (✳), butyraldehyde (✕), acetic acid (◇), CO_2 (+) ethane (O), ethylacetate (—). Ethylene formed with selectivity lower than 1%. Top: fresh catalyst. Bottom: after regeneration of used catalyst, 3h at 450°C in air.

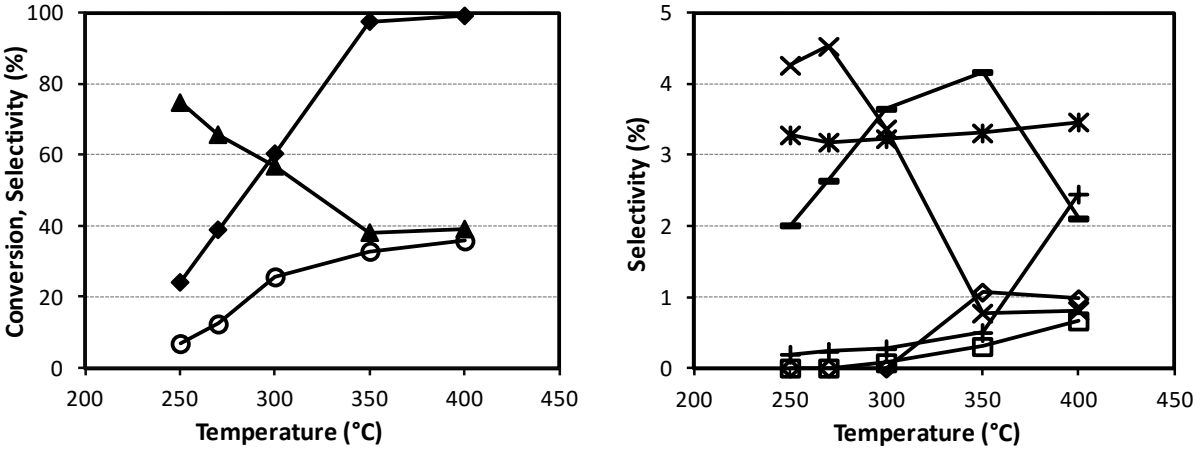

Figure 40: Effect of temperature on ethanol conversion and products distribution with CuVO catalyst. Reaction conditions: feed 5% ethanol in N_2; W/F 0.5 g s/mL. Symbols: Ethanol conversion (◆), selectivity to: acetaldehyde (▲), crotonaldehyde (✳), butyraldehyde (✕), acetic acid (◇), CO_2 (+), ethane (O), ethylacetate (—), acetone (□). Ethylene formed with selectivity lower than 1%.

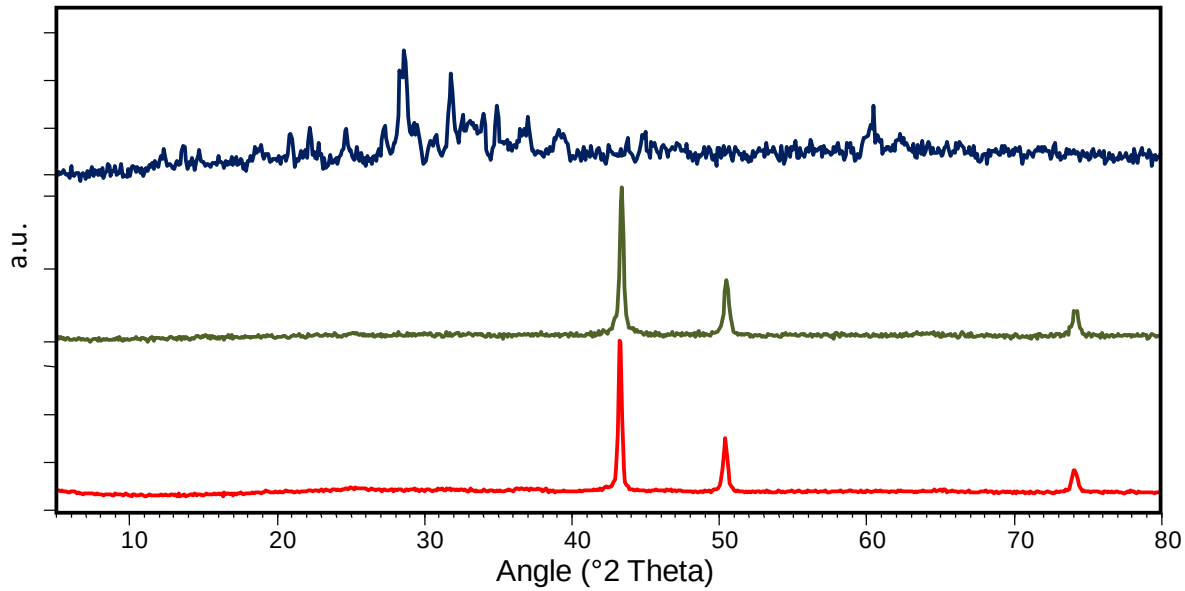

Figure 41: XRD patterns of CuVO catalyst; from top to bottom: calcined, after reaction at 300°C and 400°C, in ethanol.

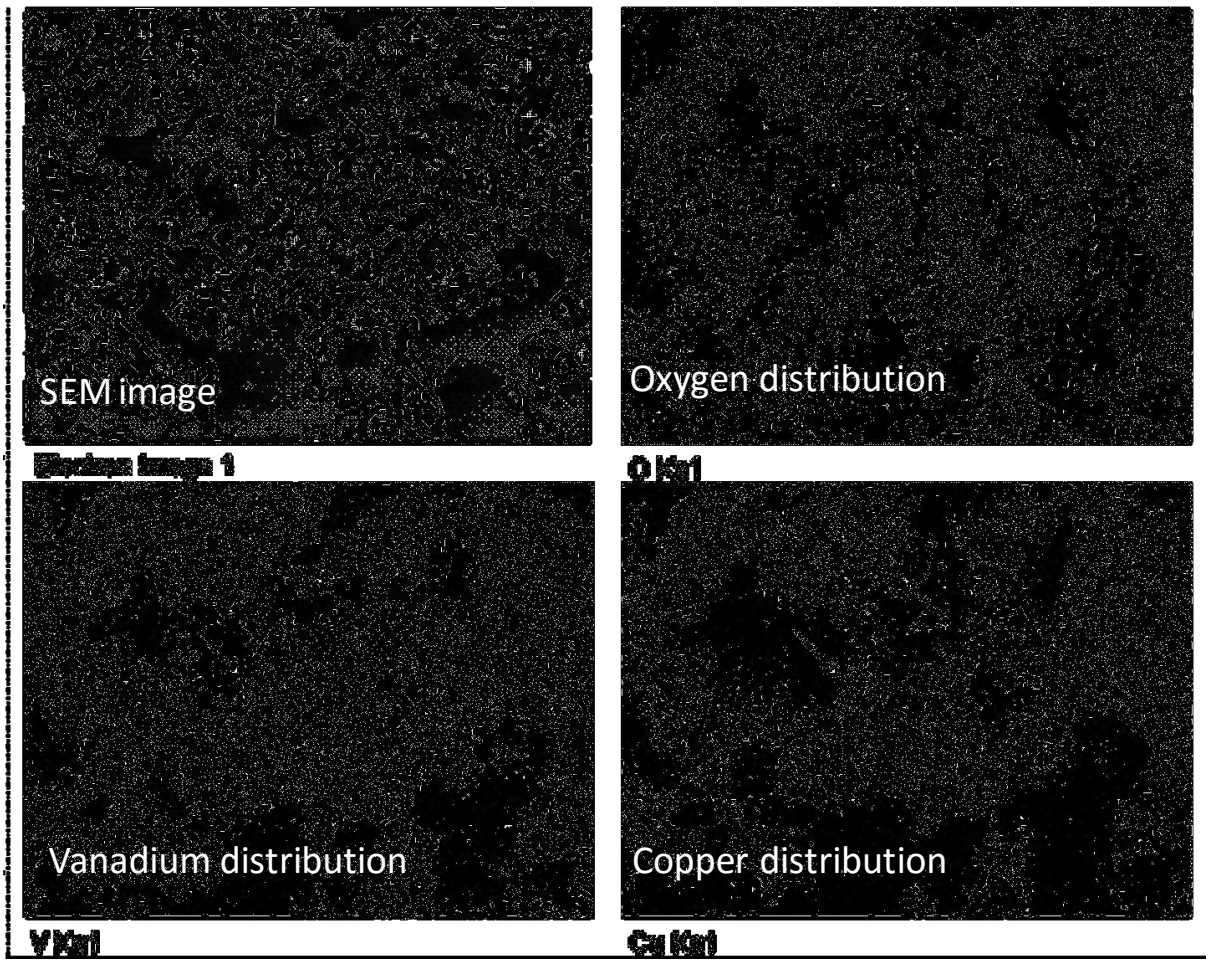

Figure 42: SEM-EDX maps of Cu, V and O in CuVO catalyst used at 300°C with ethanol. Top, left: SEM image, top right: Oxygen mapping, bottom left: Vanadium mapping, bottom right: Copper mapping. White arrows indicate some zones in which metallic copper appear to be segregated.

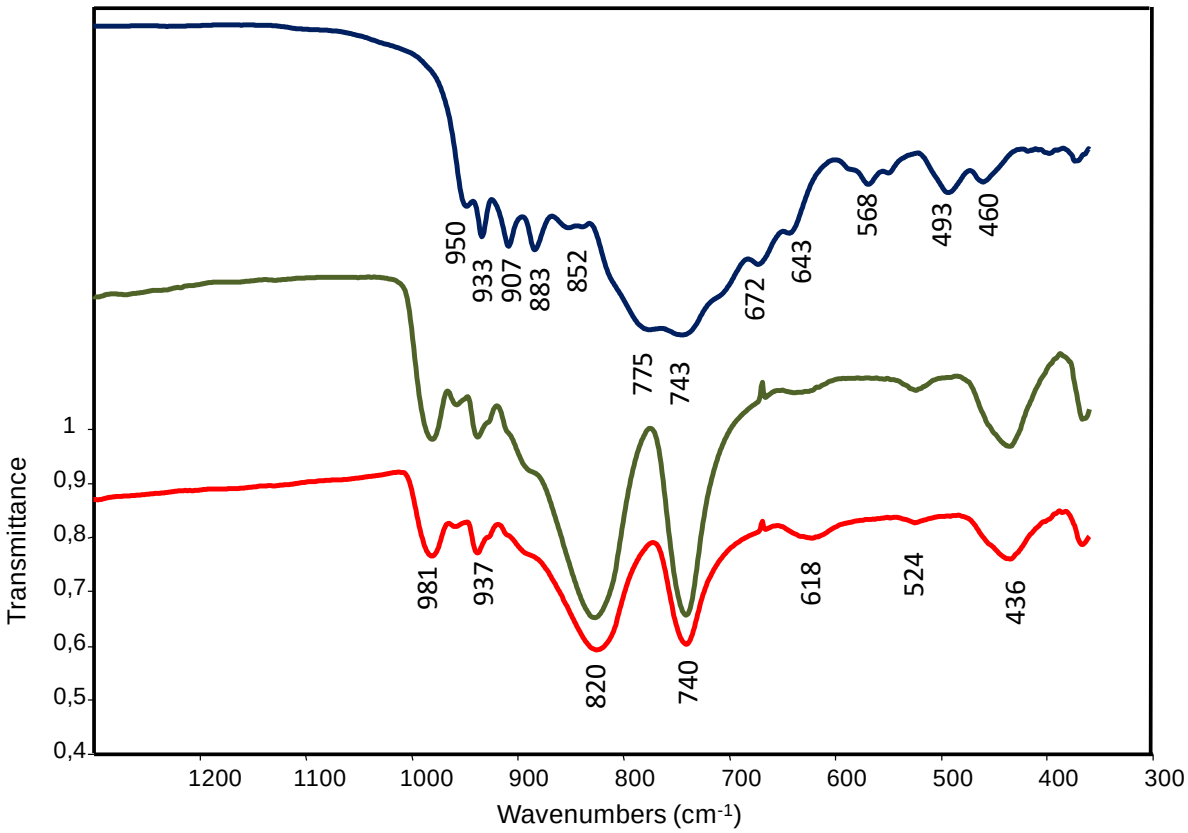

Figure 43: FT-IR spectra of CuVO catalyst. From top to bottom: fresh catalyst, after reaction at 300 and 400°C, in ethanol.

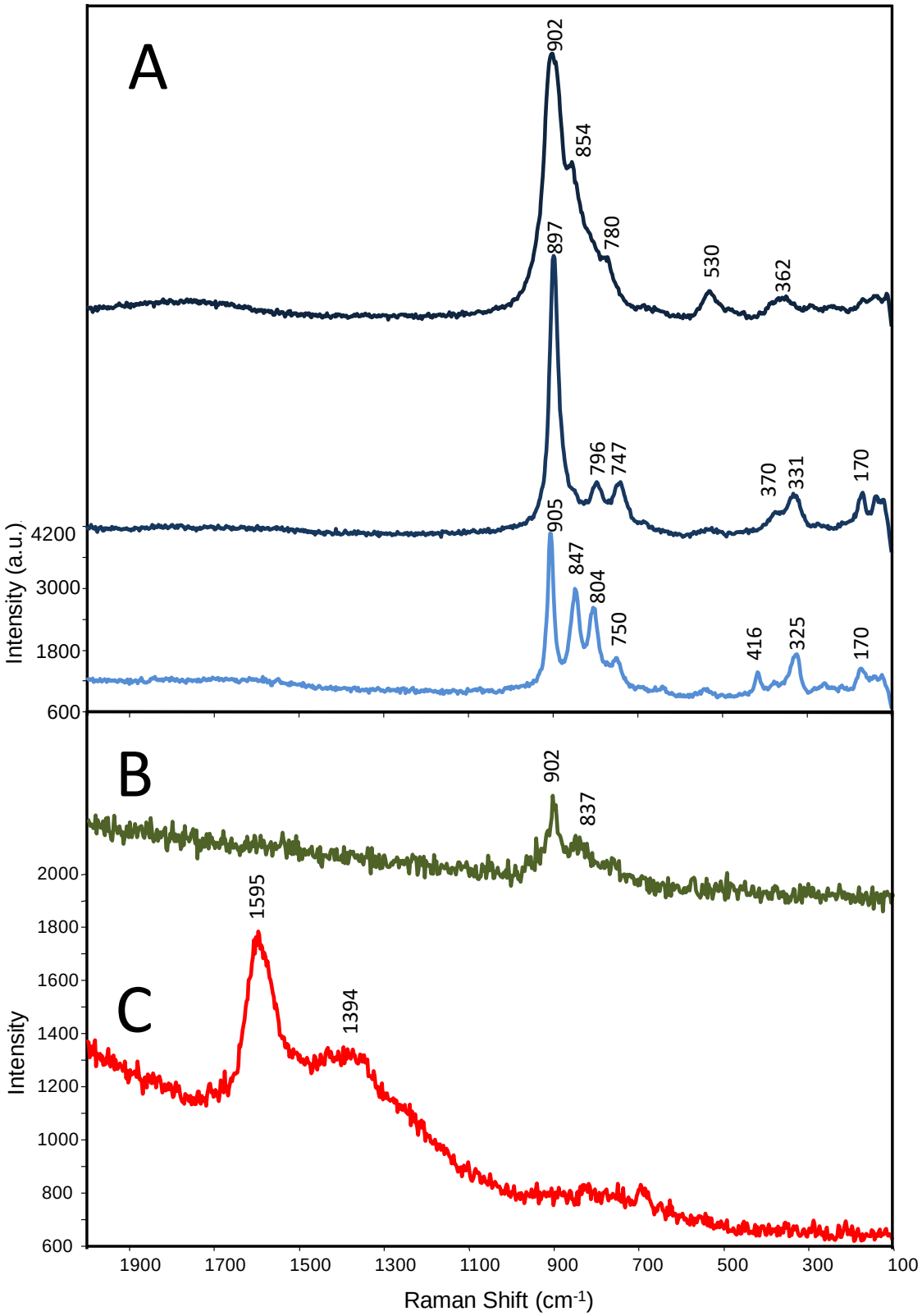

Figure 44: Raman spectra registered on different spots of CuVO fresh (A), after reaction at 300°C (B) and 400°C (C), in ethanol.

In order to have a full comparison of reactivity behavior for FeVO and CuVO, we carried out experiments by co-feeding 20% water; results are shown in Figure 45. CuVO behaviour in presence of water showed some differences compared to tests with ethanol only.

Acetaldehyde selectivity was higher at all temperatures, and ethane selectivity was lower; before 300°C ethane formation was negligible. This indicates that at low temperature water was able to keep CuVO in a more oxidized state, more selective to acetaldehyde. Amongst "minor products", the same compounds previously found without steam were also obtained with steam, the only difference was a remarkably higher yield of acetic acid. The latter was probably due to the presence of water. In these conditions, acetaldehyde can be transformed to its hydrated form and the latter can undergo dehydrogenation to acetic acid according to the following reaction:

$CH_3CHO + H_2O \rightarrow CH_3CH(OH)_2 \rightarrow CH_3COOH + H_2$

The dehydrogenation step is catalyzed by metallic Copper.

Characterization of spent CuVO, after reaction with ethanol and water at 300 and 400°C, highlighted some differences compared to the catalyst used in the same conditions, but without water.

For example, in the case of the XRD pattern of CuVO after reaction at 400°C (Figure 46), besides reflections attributable to Cu, those at 33, 37, 63 °2θ indicate the presence of $CuVO_3$, while those at 25, 32, 36, 63 °2θ suggest the presence of V_2O_3. Other reflections could not be attributed.

As in the previous case, SEM images (Figure 47) showed segregation of metallic Copper.

Raman spectra (Figure 49) were unclear because of band weakness. Anyway, it is possible to see that water was able to prevent coke formation.

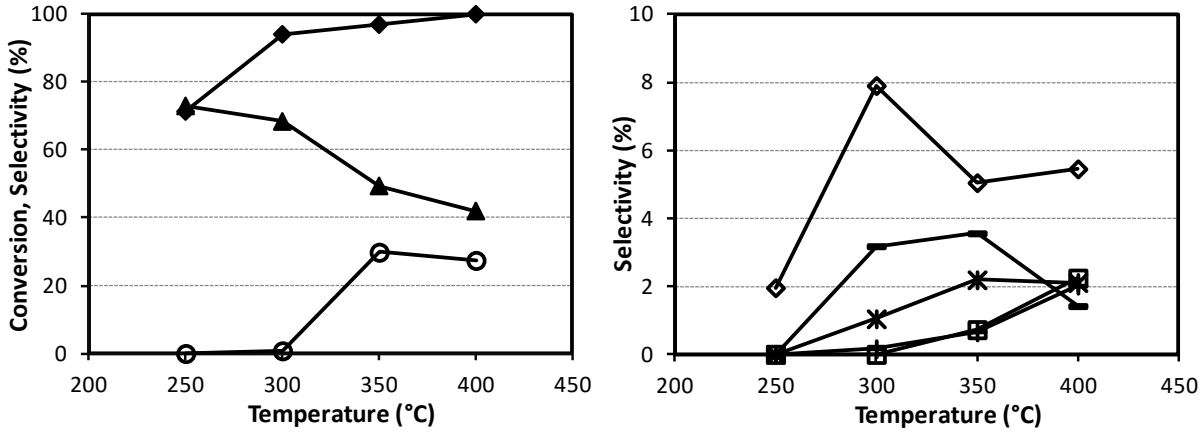

Figure 45: Effect of temperature on ethanol conversion and products distribution with CuVO catalyst. Reaction conditions: feed 5% ethanol, 20% water in N_2; W/F 0.5 g s/mL. Symbols: Ethanol conversion (◆), selectivity to: acetaldehyde (◢), crotonaldehyde (✳), acetic acid (◇), CO_2 (+), ethane (O), ethylacetate (—), acetone (□). Ethylene formed with selectivity lower than 1%.

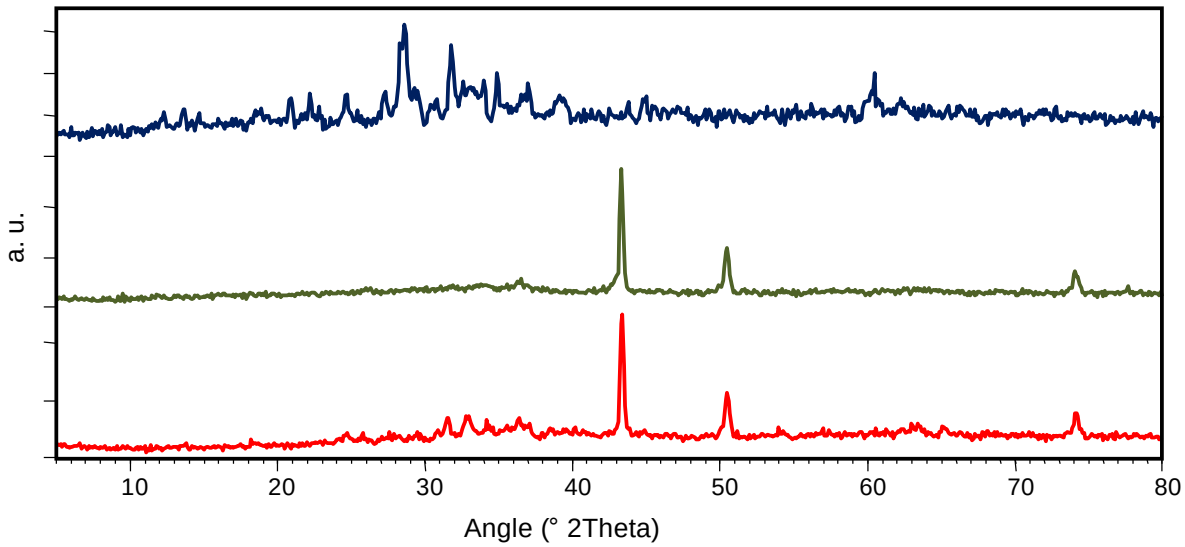

Figure 46: XRD patterns of CuVO catalyst; from top to bottom: calcined, after reaction at 300°C and 400°C, in ethanol + H_2O.

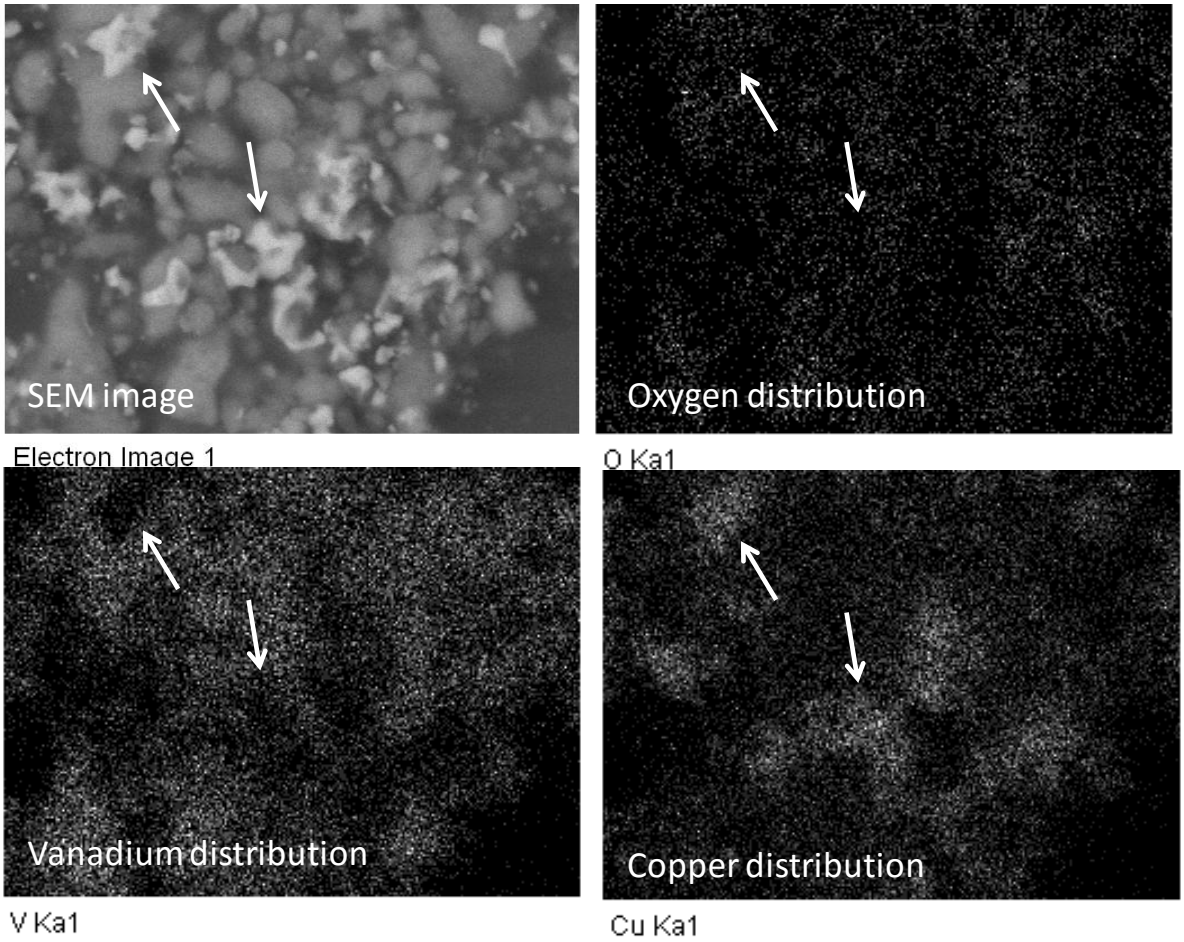

Figure 47: SEM-EDX maps of Cu, V and O in CuVO catalyst used at 300°C with ethanol and water. Top, left: SEM image, top right: Oxygen mapping, bottom left: Vanadium mapping, bottom right: Copper mapping. White arrows indicate some zones in which metallic Cu segregated.

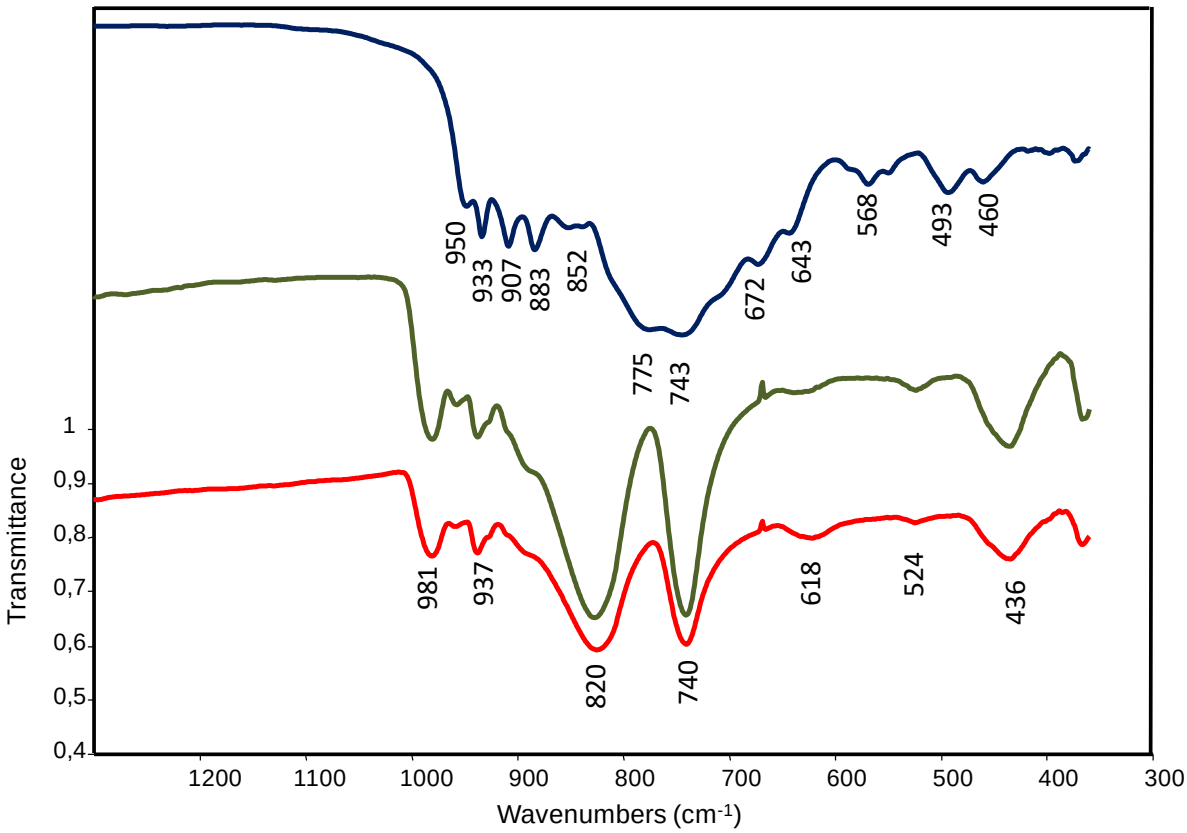

Figure 48: FT-IR spectra of CuVO catalyst. From top to bottom: fresh catalyst, after reaction at 300 and 400°C, in ethanol + H_2O.

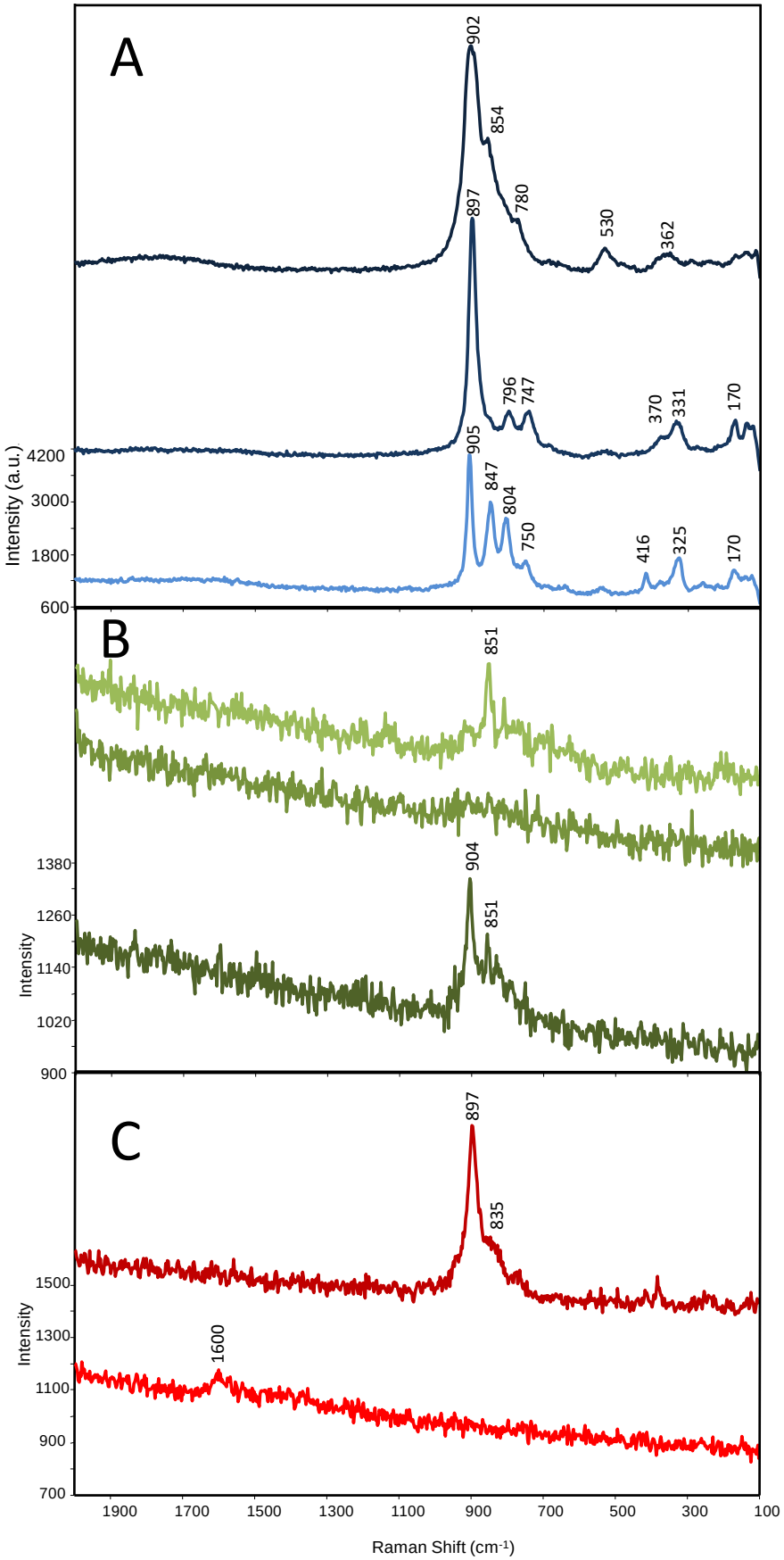

Figure 49: Raman spectra registered on different spots of CuVO fresh (A), after reaction at 300°C (B) and 400°C (C), in ethanol + H_2O.

Figure 50 shows results obtained by co-feeding 5% O_2 and 20% water with 5% ethanol on CuVO, at W/F 0.5 g·s/mL in function of temperature.

Results were similar to those obtained by feeding O_2 and ethanol, but on the other side we detected remarkable differences compared to the experiments with co-feed of steam only.

The XRD pattern of CuVO after reaction with O_2 and water at 400°C (Figure 51) showed the formation of metallic copper. Because of the weakness of the other reflections, it was not possible to provide an unequivocal identification of the other phases. Anyway, some reflections can be attributed to specific compounds: Cu_2O (36° 2θ), $CuVO_3$ (32, 36 °2θ), V_2O_3 (33, 36, 54 ° 2θ) and $CuO{\cdot}3H_2O$ (34° 2θ). IR spectra showed the presence of the same bands as for the catalyst used by feeding ethanol only. Raman spectra displayed bands attributable to Cu-V mixed oxides, with no coke formation.

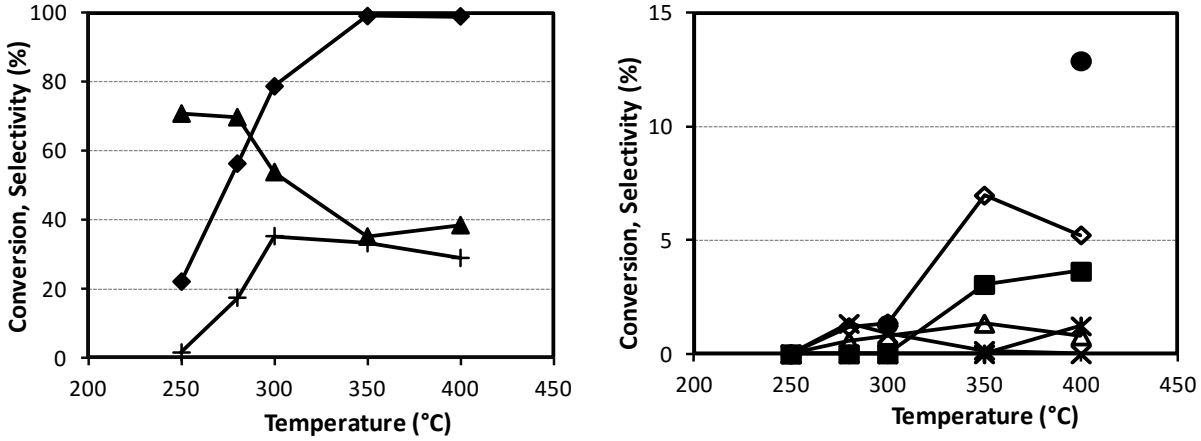

Figure 50: Effect of temperature on ethanol conversion and products distribution with CuVO catalyst. Reaction conditions: feed 5% ethanol, 20% water, 5% O_2 in N_2; W/F 0.5 g s/mL. Symbols: Ethanol conversion(◆), selectivity to: acetaldehyde (◢), crotonaldehyde (✳), acetic acid (◇), CO_2 (+), diethylether (△), ethylene (■), CO (●).

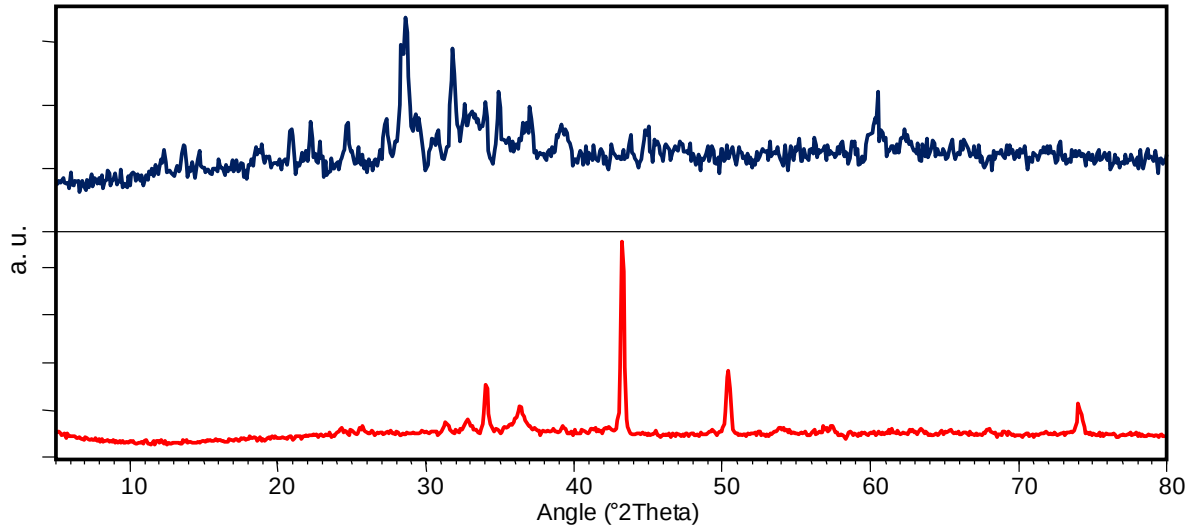

Figure 51: XRD patterns of CuVO catalyst; from top to bottom: calcined, and after reaction 400°C, in ethanol + H_2O + O_2.

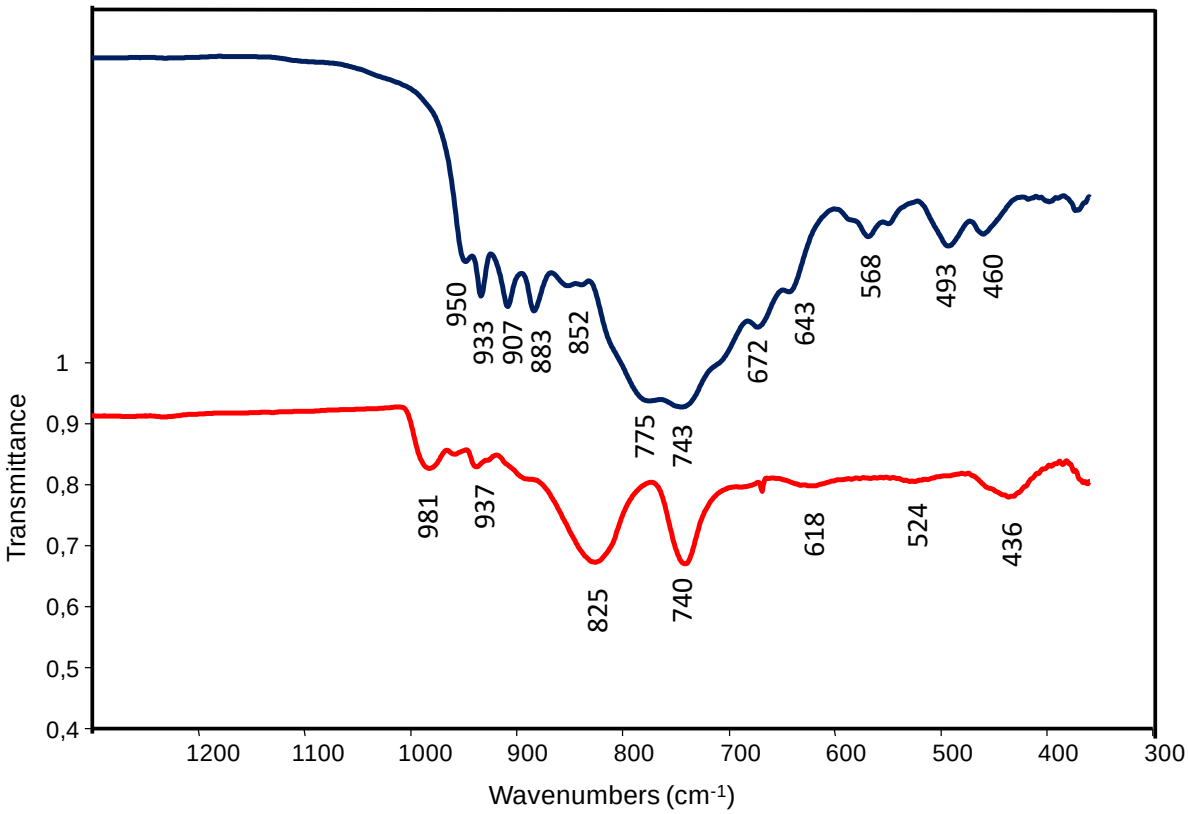

Figure 52: FT-IR spectra of CuVO catalyst. From top to bottom: fresh catalyst and after reaction at 400°C, in ethanol + H_2O + O_2.

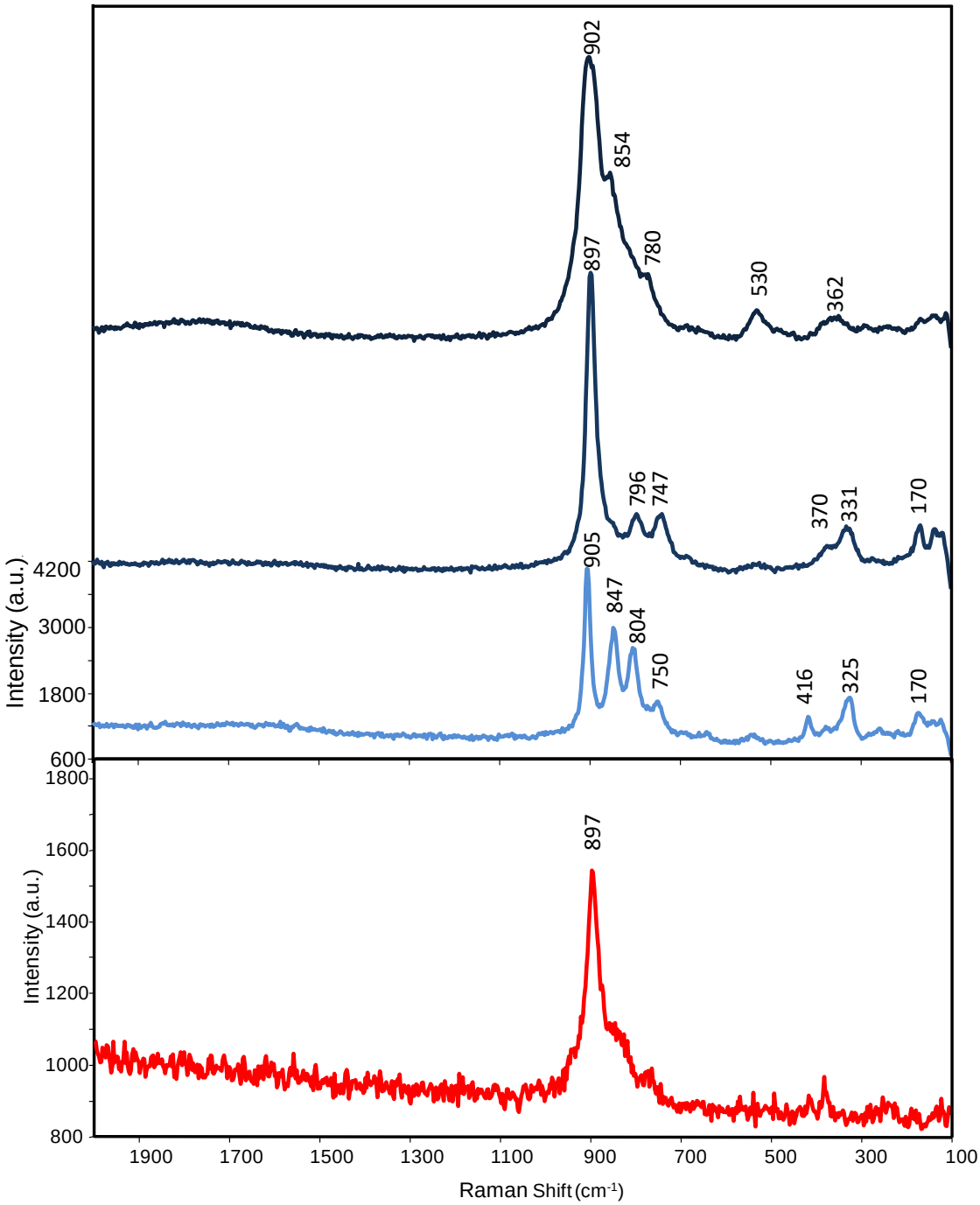

Figure 53: Raman spectra registered on different spots of CuVO, fresh, after reaction at 400°C in ethanol + H_2O + O_2..

2.3.2.1 The reactivity of CuO and V_2O_5

In order to better understand CuVO catalytic behaviour, we carried out catalytic tests with CuO and V_2O_5 (results with V_2O_5 are detailed in the previous chapter, but are reported again for a better comparison) Figure 54 shows the catalytic behaviour of CuO in the presence of ethanol and oxygen at W/F 0.5 g·s/mL, in function of temperature. Main products were acetaldehyde, CO_x and acetic acid. C_4 products deriving from acetaldehyde condensation formed with 2-3% selectivity at all temperatures. Carbon balance was always higher than

90%. CuO was selective to acetaldehyde, but it decreased with the increase of temperature. This was mainly due to consecutive oxidation to acetic acid, which seemed to occur at a greater extent starting from 350°C. Part of ethanol was burnt to CO_x.

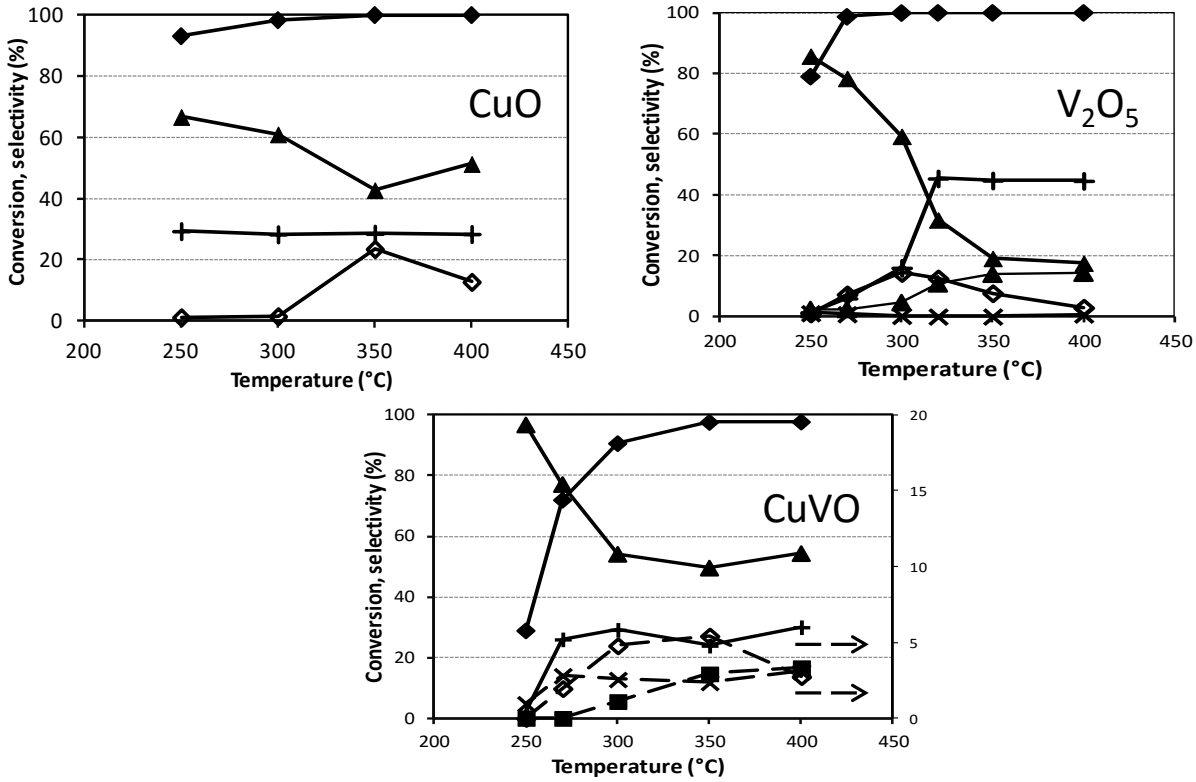

Figure 54: Effect of temperature on ethanol conversion and products distribution with CuO (top, right), V_2O_5 (top, left) and CuVO (bottom). Dashed lines are referred to secondary Y axis. Reaction conditions: feed 5% ethanol, 5% O_2 in N_2; W/F 0.5 g s/mL. Symbols: Ethanol conversion (◆), selectivity to: acetaldehyde (◢), ethylene (■), C_4 (×), acetone (□), acetic acid (◇), COx (+), ethane (O).

Figure 55 displays the catalytic behaviour of CuO in the presence of ethanol, without oxygen, at W/F 0.5 g·s/mL and different temperatures; results were taken after the steady state had been attained. The main product was acetaldehyde; CO_x were detected at all temperatures with a selectivity < 1%, C_4 products deriving from acetaldehyde condensation formed with 2-3% selectivity. A small quantity of ethylene also formed, which increased at 400°C.

CuO behaviour was similar at 300 and 350°C, but it showed a strong decrease of ethanol conversion at 400°C. This indicates that CuO deactivated fast at this temperature (data were taken after 2h).

At 300 and 350°C acetaldehyde selectivity was much higher than in the presence of O_2, because total oxidation was avoided; in fact, CO_x selectivity was no higher than 1%.

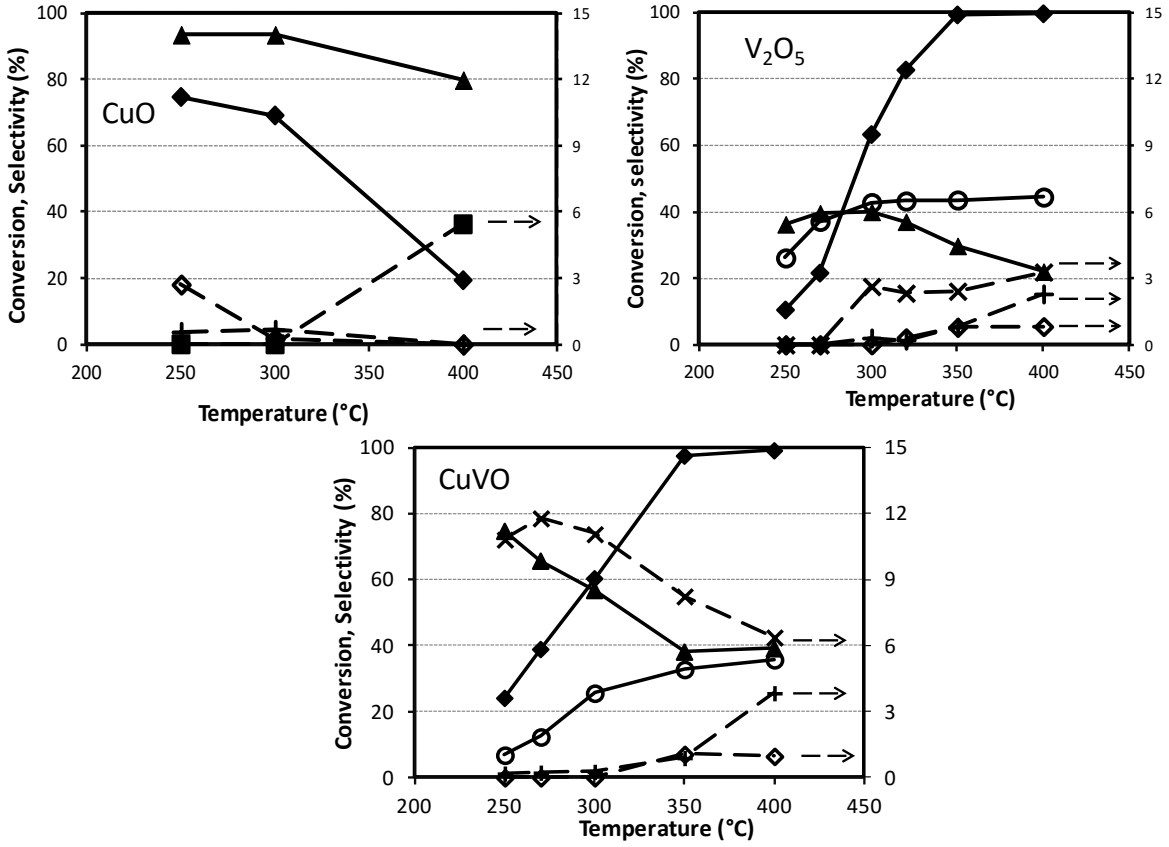

Figure 55: Effect of temperature on ethanol conversion and products distribution with CuO (top, right), V_2O_5 (top, left) and CuVO (bottom). Dashed lines are referred to secondary Y axis. Reaction conditions: feed 5% ethanol in N_2; W/F 0.5 g s/mL. Symbols: Ethanol conversion(◆), selectivity to: acetaldehyde (▲), ethylene (■), C_4 (✕), acetone (□), acetic acid (◇), COx (+), ethane (O).

These results can be compared with those obtained with CuVO and V_2O_5. In all cases, the main product was acetaldehyde, but CO_x were produced in high quantities when O_2 is present. Ethane was not formed with CuO, but it was present when the reaction was catalyzed by CuVO or V_2O_5 (in their reduced form).

CuVO a behavior was very similar to that of V_2O_5, although with some differences. Until 300°C, in the presence of oxygen, CuVO behaved likewise V_2O_5. After this temperature, V_2O_5 showed a decrease of acetaldehyde selectivity in favour of CO_x, whereas with CuVO this occurred at a lower extent. For temperatures higher than 350°C, comparing acetaldehyde and CO_x selectivity, CuVO behaved more similarly to CuO than to V_2O_5. This can be explained by taking into account characterization results. Even in the presence of oxygen, CuVO underwent reduction with segregation of metallic Cu, and this occurred at above 300°C. Therefore, the behavior at T < 300°C was that one typically shown by Vanadium-based oxides, but when the temperature was raised, the catalytic behavior of segregated phases prevailed.

The situation was different when ethanol was fed in the absence of oxygen. In this case, until300°C, CuVO behaved similarly to CuO, with a slight influence of V oxides, which was

responsible for ethane formation. After 300 and until 400°C, CuVO behavior was similar to that one of V_2O_5, but with higher selectivity to acetaldehyde and C_4.
As explained before, this was due to the segregation of metallic Copper, which improved the rate of ethanol dehydrogenation. The increase of C_4 selectivity was related to the higher production of acetaldehyde, the intermediate for C_4 formation.

2.3.2.2 CuVO summary

CuVO was tested as catalyst for ethanol oxidation or dehydrogenation. In the presence of oxygen, it gave good selectivity to acetaldehyde, but a substantial part of ethanol was burnt to CO_x. In the absence of oxygen, the catalyst was progressively reduced until it reached a stable form. The latter was made of metallic Copper, V_2O_3 and one or more unidentified Cu-V mixed oxides. Reduced phases showed the same behaviour as V^{3+} oxide, which catalyzes ethanol disproportionation to acetaldehyde and ethane. However, acetaldehyde yield was increased due to the presence of metallic Cu, which catalyzed ethanol dehydrogenation. CuVO showed a catalytic behaviour which in some cases was more similar to V_2O_5, whereas in other cases was more similar to CuO. Howeber, in both cases the contribution of the other phase was not negligible; for instance, in the former case, products distribution was affected by the presence of Copper segregated compounds, and vice-versa.

2.4 Conclusions

FeVO and CuVO were tested as catalysts for ethanol dehydrogenation under different conditions. With both catalysts the main product was acetaldehyde. When oxygen was fed together with ethanol, selectivity to acetaldehyde was very high, but when the temperature is increased, acetaldehyde selectivity declined in favour of CO_x. When the reaction was carried out without oxygen, the behaviour of the two V-based mixed oxides was more similar to that one of V_2O_5, but with some differences due to the presence of Fe or Cu. All materials (FeVO, CuVO and V_2O_5) required an "equilibration" time in order to develop a steady perfomance. When the latter was reached, the main products were ethane and acetaldehyde. According to Ueda et al.[62], these products are formed over reduced Vanadium-based oxides as a result of ethanol dismutation. Differences between CuVO and FeVO were related to the different phases developed during catalyst reduction, before the steady state attainment. FeVO developed a Fe-V spinel-type mixed oxide, which showed a behaviour similar to that one of reduced V oxides. The main difference regards C_4 selectivity, which was higher in case of FeVO. CuVO developed a reduced Cu-V mixed oxide compound, however with also metallic Copper segregation. Catalytic activity of this latter catalyst was similar to that one of reduced V-oxides, but the presence of metallic Cu enhanced acetaldehyde selectivity.

The addition of water prevented coke formation and catalyst reduction at the lowest temperatures, but when temperature was raised, the catalysts underwent reduction anyway and modified their performance accordingly. This effect was more relevant with CuVO. Water was able to keep part of CuVO in its oxidized form even at higher temperatures.

When ethanol, water and oxygen were fed together, products distribution was similar to that one obtained with ethanol and oxygen co-feeding. Under these conditions, FeVO reduction was prevented, and the more oxidised state was maintained even at 400°C; conversely, CuVO underwent reduction anyway.

To conclude, with both catalysts the catalytic behaviour was mainly dictated by Vanadium, but it was anyway also affected by the presence of either Fe or Cu. FeVO behaved more similarly to V-oxides, because Fe and V were always present in the form of a mixed oxide. CuVO behaviour was more profoundly affected by the presence of Cu, because of the formation of segregated phases.

3. ISOPRENE PRODUCTION THROUGH DIRECT METHANOL-ISOBUTENE COUPLING (MODIFIED-PRINS REACTION)

3.1 Introduction

Isoprene is the common name of 3-methyl-1,3-butadiene; it is a colourless, volatile organic liquid with typical hydrocarbon smell. It is classified as an hazardous substance because it is highly flammable (H224), mutagenic (H341), carcinogenic (H350) and pollutant for the environment (H412)[91]. The table below indicates its principal physical properties[91].

Name	Isoprene
CAS number	78-79-5
Molecular weight	68,11 g/mol
Melting point	-146°C
Boiling point	34°C
Density	0,681 g/cm^3 (25°C)

Table 1: Some physical properties of Isoprene

The core of this part of the thesis is based on the research work aimed at the substitution of formaldehyde with methanol in the Prins reaction for the production of isoprene. First, uses and production methods of isoprene are briefly described; the key aspects of isoprene production will be elucidated highlighting the main drawbacks of actual production processes. Starting from these drawbacks, an alternative approach for the synthesis of isoprene based on a more sustainable process is proposed, with replacement of formaldehyde, an hazardous chemical, with methanol, easier to handle and less dangerous for humans and environment.

3.1.1 Uses of isoprene

Isoprene is a commodity chemical, used mainly as a monomer for rubber production, only a small part of it being used as building block for the synthesis of other chemicals like 4-methylpentanone (a solvent) or higher terpenoids of chemical and pharmaceutical interest[92].

Rubbers produced from isoprene include isoprene-rubber (IR), SIS rubber, which is a block styrene-isoprene-styrene co-polymer, and butyl-rubber (BR), which is an isoprene-isobutene co-polymer.

The biggest part of isoprene is employed for the production of poliisoprene elastomers; this polymers are prepared mainly in two form: 1,4-*cis*, in which the monomers are connected through the first and the last carbon of the chain; the double bond in the monomeric unit is in a *cis* conformation; and 1,4-*trans*, in which the repeating units are in a *trans* conformation.

Both polymers are synthesized by means of Ziegler-Natta-type catalysts, which are typically made of Al(Et_3) and a promoter; the different stereochemical conformation is given by the

promoter of the catalyst; $TiCl_4$ gives the *cis* conformation, whereas VCl_3 gives the *trans* form[93].

1,4-*cis*-poliisoprene is the synthetic equivalent of natural rubber; when properly vulcanized and additivated, it is used in the manufacture of tyres.

Butyl rubber is made by the co-polymerization of isobutene and isoprene; in this type of polymer, isoprene is just added in a sufficient amount to provide cross-linking points for the vulcanization process. Butyl rubber main characteristic is an excellent impermeability to air and gases, such as helium and hydrogen; because of this property it is mainly used for the production of inner tubes of tyres or for the inner barrier in tubeless tyres. The main drawback of BR is its high price: to lower tyres costs, BR is used just in the part in which it is essential, the other parts are mainly made of 1,4-cispoliisoprene[94] and SIS rubber.

SIS (styrene-isoprene-styrene block co-polymer) production employs around 30% of worldwide produced isoprene; this polymer is a thermoplastic elastomer, which combines both thermoplastic and elastomeric behaviour without the need for a vulcanization process. In fact, in this case, the vulcanization process is based on the presence of crystalline domains given by polystyrene blocks, which confers to the material the necessary strength to be shaped in a defined form. This type of polymers, because of their thermoplastic behaviour, can also be recycled; they are mainly used in tyres manufacturing, but also in other fields such as shoes soles, catheters and adhesives[94].

Global uses of isoprene by its end-use are illustrated in Figure 56[92].

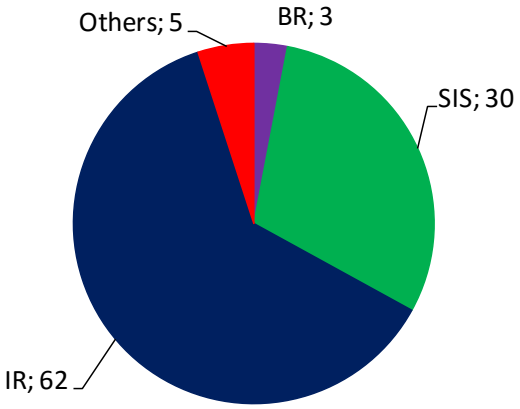

Figure 56: Principal uses of isoprene (BR: butyl rubber, SIS: styrene-isoprene-styrene co-polymer, IR: isoprene rubber), data are expressed in percentage.

3.1.2 Isoprene production

As described above, isoprene is usually employed in anionic polymerization processes, which need high purity monomers. As a consequence, production and purification processes are aimed at obtaining isoprene with high purity (≥ 99,5%)[93, 95].

Nowadays different production routes are used, but just three of them are applied at an industrial scale. They can be grouped in two classes: methods employing light refinery cuts, and methods employing reactions between other chemicals[95, 96].

In this chapter the three main industrialized routes are taken into account; in order to give a complete overview also some other relevant methods are briefly mentioned, which were used in the past or which development was stopped at the level of the pilot plant or lab-scale plant.

Nowadays industrial production of isoprene is carried out through three main processes[97]:

- Isolation and purification of isoprene from light refinery stream;
- Dehydrogenation of 2-methylbutenes and, in minor part, of 2-methylbutane;
- Prins reaction between formaldehyde and isobutene.

In order to focus the attention over the main issues regarding isoprene production, the next chapters will describe these three methods mainly from the technical point of view, while providing the basic chemistry of the technologies. A more detailed description of the Prins reaction, with a short literature overview, will be provided later in the thesis.

3.1.2.1 Isoprene production trough isolation and purification from refinery stream

The description of this process is based on the final step of purification of the C_5 refinery stream; actually it represents the more critical step in order to obtain polymerization-grade isoprene.

The greater amount of the C_5 refinery stream, from which isoprene is isolated, is a side product of ethylene production carried out by steam cracking. Because of this, the amount of isoprene and C_5 produced are related to the process conditions that maximize ethylene yield and depend upon the composition of the naphtha fraction fed to the steam cracking plant. As a general rule, the higher is the amount of heavy compounds in the naphtha fraction, the greater are C_5 and isoprene yields[98].

In any case the maximum isoprene mass yield, obtainable with this method, is between 0.5 and 0.7% of the total naphtha mass fed to the steam cracker[97].

Due to these low mass yields and according to large scale economy, which is applied to petrochemical productions, isoprene purification processes must be combined with large scale steam cracking plants in order to obtain enough C_5 fraction to allow an isoprene production adequate to ensure an economic advantage[97].

Isoprene purification is made of five basic steps, which are common to every process, but according to the approaches exploited, it is frequent to have some additional steps. These are aimed at the improvement of the purification process depending on both the composition of the feed and the side-products that can be obtained.

Such a high number of purification steps is required mainly for three reasons:

- The C_5 stream, fed to the purification plant, contains substances with similar boiling points;
- Isoprene can form azeotropes with other C_5 hydrocarbons, such as *n*-pentane;
- Azeotropes between some compounds present in the feed have a boiling point that is close to that one of isoprene.

The key point of the separation is an extractive distillation, which allows the separation of the azeotropes by the addition of a solvent, which interacts specifically with the compounds present in the mixture enhancing the difference of boiling points. The most common solvents used for this purpose are acetonitrile, N-methylpyrrolydinone or dimethylformammide; in the last case the solvent is very sensitive to water and needs anhydrous conditions [97, 99].

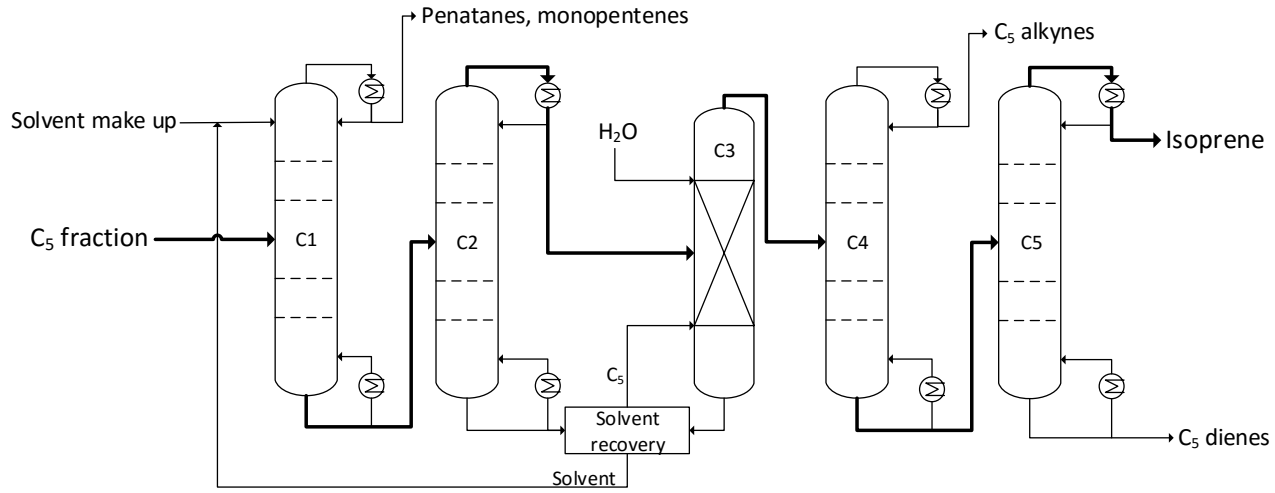

Figure 57: Simplified flow sheet of isoprene purification process.

Figure 57 shows the core steps of isoprene purification; these steps can be divided into three parts: extractive distillation, distilled fraction washing and purification of isoprene; a general description of the process is reported below[97, 99]:

1- Extractive distillation: the C_5 fraction and the solvent are fed to the first distillation column (C1). The solvent allows the separation of the fraction containing pentanes and monopentenes by increasing the boiling point of the other C_5 compounds (C_5 alkynes and dienes), which are recovered from the bottom of the first column. This fraction is then fed to the second column (C2) for the separation of the solvent from the purified C_5 stream, which is recovered from the top.

2- Distilled fraction washing: the purified C_5 stream from the extractive distillation is fed to a washing tower (C3). Here the traces of solvent are removed by contact with water. The solvent coming from the extractive distillation and from the washing tower is recovered, purified and recycled to the extractive distillation. C_5 compounds eventually adsorbed in the solvent are stripped-out and reintegrated in the process.

If dimethylformammide is used, contact with water must be avoided and this passage can be replaced by an additional distillation column that allows purification of the C_5 stream removing the remaining traces of solvent.

3- Isoprene purification: final isoprene purification occurs by means of two distillation columns (C4 and C5), in a typical industrial purification process configuration. The first column is used to remove light ends, in this case C_5 alkynes. Raw isoprene stream is than fed to the final distillation column in which it is purified by removal of other C_5 dienes. Polymerization-grade isoprene is obtained from the top of the last distillation column.

The scheme described above, as said before, is the core of the purification process; the overall process is more complex and comprises other purification steps aimed, for example, at the isolation of other compounds of interest. Moreover, some companies developed technologies that exploit the same principle of separation based on extractive distillation, but with some modifications to the scheme illustrated in Figure 57. For example, a technology developed by BASF, exploits dimethylformammide as the solvent for extractive distillation in a process configuration that allows an easier separation of linear pentadienes. In this case, instead of the washing step (C3), there is a set of two distillation columns[97]: the first column separates raw isoprene from the solvent, in which *n*-pentadienes remain solubilized. Isoprene is fed to the final set of purification columns and the mixture containing the solvent and *n*-pentanes is fed to the second column of the modified process. This column allows separation of *n*-pentadienes from the solvent. This not only allows the separation of *n*-pentadienes, but due to the fact that separation occurs in an earlier step with respect to the other processes, it is also possible to obtain technical grade cyclopentene at the bottom of the last column. The main drawback of this technique is that dimethylformammide is sensitive to water and needs an anhydrous environment.

Some common steps, besides the basic set of purification columns, are[97, 99]:

- A pre-column for the separation of lighter products, like the C_4 compounds;
- A pre-reactor for the dimerization of cyclopentadiene operating at 120°C. This allows to transform cyclopentadiene to its dimer, which is useful to avoid the formation of azeotropes that include this molecule. The dimer is than recovered from the top of the first column, then is easily separated from the other C_5 compounds in a simple distillation column and, if necessary, is brought back to the monomer form via decomposition;
- An additional step of purification of heavy compounds obtained at the bottom of C5 column.

If the recovery of side-products from the purification process is not economically advantageous, it is common to collect and burn them in order to obtain energy.

The purification processes described above are in use since several decades and are fully optimized, and there is no industrial interest for their improvement. The only possible field of improvement regards the optimization of energy efficiency, the optimisation of solvent recovery or the increase in side-products yield, such as cyclopentadiene[100, 101].

3.1.2.2 Isoprene production trough dehydrogenation processes

Isoprene yield can be improved by the dehydrogenation of some side-products obtained from isoprene purification; these processes can be carried out starting from 2-methylbutane or 2-methylbutenes[96, 97], which can be obtained from the top of the first distillation column of isoprene purification section.

The stream obtained at the end of the dehydrogenation is rich in isoprene, and is then fed to the purification process, including again extractive distillation, to obtain polymerization grade isoprene.

Both dehydrogenation processes operate in similar conditions: high temperature, to provide the heat necessary to deal with reaction endothermicity, and low reaction pressure (or reagent partial pressure), in order to shift the reaction equilibrium towards the products according to Le Chatelier principle.

2-Methylbutane dehydrogenation exploits the Houdry-Catadiene technology[95, 97]; it consists in a one-step dehydrogenation of the reactant, aimed to obtain directly the diene, as shown in Figure 58.

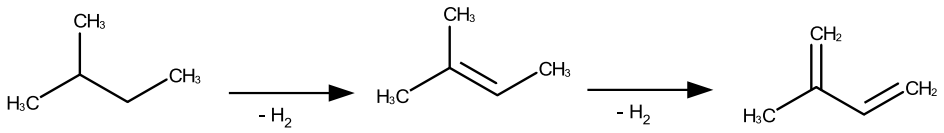

Figure 58: 2-methylbutane dehydrogenation; the intermediate can be 2-methyl-2-butene or its isomers. The Houdry-Catadiene process configuration allows to carry out the overall reaction in a single step.

This process operates at 550-650°C at about 0.14 atm pressure; Cr_2O_3 supported over Al_2O_3 is used as the catalyst[95, 102]. In this case steam cannot be used to decrease reagents and products partial pressure because water is a poison for the catalyst; therefore, vacuum is employed. These conditions allow a isoprene selectivity around 50%, with 30% 2-methylbutane per-pass conversion; reagent conversion is kept low in order to limit consecutive dehydrogenation reactions. Main by-products of the reaction are alkynes and heavy compounds due to consecutive dehydrogenation of isoprene. 2-Methylbutenes can be present due to the incomplete dehydrogenation of the reactant. The downstream purification process allows to obtain polymerization grade isoprene, however lowering the overall process yield down to 47 – 48%[102].

This process is still employed in few production sites, located mainly in Russia. Nowadays it is no longer of industrial interest and it is disappearing[103], the main reason being that 2-

methylbutane is a compound with an high octane number, widely used as an octanizer additive for gasoline; this makes it an high added-value chemical, too expensive to be employed for the production for isoprene[97]. Moreover isoprene yield is low if compared to dehydrogenation processes which start from 2-methylbutenes and the catalyst used is toxic, carcinogenic and pollutant.

Nevertheless some Russian research groups are still working on the development of a one-step dehydrogenation process. Good results were obtained with a supported Pt catalyst, which is able to carry out the one-pot dehydrogenation in a fixed bed reactor[104]. The main advantages of this system are the use of a less toxic catalyst and the low noble metal loading (0.2%)[103]; best results were obtained using a Pt/Sn catalyst; the latter shows 30-35% isoprene yield with 67% 2-methylbutanes conversion at 600°C[105]. Despite these achievement, the obtained results still are not sufficient for an industrial implementation of this technology, and the interest is shifting toward other production processes[92].

An alternative approach, mainly employed in former Soviet Union, consists in a two-step dehydrogenation of 2-methylbutane. The first step carries out the dehydrogenation of 2-methylbutane to 2-methylbutenes with a Calcium-Nickel-phosphate catalyst, the second step uses an Iron oxide-based catalyst to further dehydrogenate the intermediate to isoprene. Some research issues in this field are aimed at the investigation of coke formation mechanism and at the improvement of catalysts lifetime[106].

Anyway, mainly because of the high price of 2-methylbutane, the majority of dehydrogenation processes for isoprene production use 2-methylbutenes as feedstock. With 2-methylbutenes a class of compounds which includes 2-methyl-2-butene and all its structural isomers are referred to, in which the double bond can be in position 1 or 3.

2-methylbutenes dehydrogenation is carried out at 550-600°C and at atmospheric pressure, using water steam as diluent to lower the partial pressure of reagent and products; Fe_2O_3-K_2CO_3-Cr_2O_3 is used as the catalyst. This allows 87% isoprene yield, obtained with 40% reagent per-pass conversion. The overall process yield, considering purification steps, is around 85%[95].

Shell uses this process to dehydrogenate simultaneously *n*-butenes and 2-methylbutenes in order to obtain isoprene and butadiene using one set of reactors only[97].

All these dehydrogenation processes have to deal with the problem of catalyst deactivation, which is due to coke deposition, the latter being formed by consecutive dehydrogenation.

In order to keep catalyst activity and selectivity as high as possible, these processes usually exploit a regeneration step, which basically consists in burning coke deposits with air; this step can be also used to provide the heat for the endothermal dehydrogenation. Different reactors configuration are possible to realize this procedure. For example it is possible to use two or more parallel reactors: while the first one is used for the dehydrogenation, the others

are under purging with N_2 or under regeneration with air. It is also possible to realize a mobile bed reactor, in which the catalyst particles are suspended in the reagent flow and periodically removed and brought to the regeneration vessel. Another possibility that can be adopted for dehydrogenation processes is to co-feed water steam with the reagent; as said before, in addition to coke formation prevention, water steam decreases reagent partial pressure, shifting the reaction equilibrium toward products formation.

3.1.2.3 Isoprene production by means of the Prins reaction

Isoprene can be produced, as shown in Figure 59, by means of the acid-catalyzed Prins reaction between isobutene and formaldehyde. This reaction implies the formation of a C-C bond trough the interaction between the aldehydic carbonyl group and the electron-rich carbon atoms in the double bond.

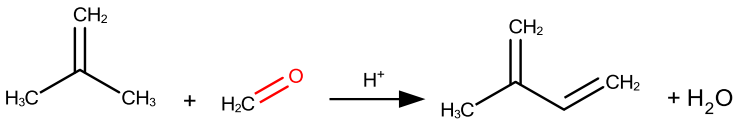

Figure 59: Prins reaction between isobutene and formaldehyde

The Prins reaction occurs in two steps: the first involves the coupling between formaldehyde and isobutene with the formation of a reaction intermediate; the second step is the decomposition of the intermediate to give isoprene.

The reaction mechanism can follow two different pathways, which differ in the type of intermediate formed; the latter can be either 4,4-dimethyl-1,3-dioxane or 2-methylbutenols. The dioxane derives from the condensation of two molecules of formaldehyde with a molecule of isobutene, 2-methylbutenols are formed when the reagents react with a one-to-one stoichiometry.

The nature of the intermediate depends mainly on the reagents ratio: the dioxane route takes place when the reaction is carried out with an excess of formaldehyde whereas 2-methylbutenes are formed in the presence of an excess of isobutene. However, the formation of either of the two intermediates does not exclusively depend on reagents ratio, but also on reaction conditions; in fact, the 2-methylbutenes route is the preferred one when the reaction is carried out over shape-selective zeolites, which cavities are narrow enough to favour smaller 2-methylbutenols instead of dioxane formation[107].

The reaction mechanism passes through the acid activation of the aldehyde. Aldehydic oxygen can be protonated with the formation of a CH_2O^+H species, which undergoes delocalization of the positive charge on the carbon atom. This carbocation can be attached by isobutene double bond with the formation of a carbocation on the tertiary carbon atom. Then the reaction can follow two different pathways, as shown in Figure 61. The first passes

through the addition of another formaldehyde molecule and formation of the dioxane which finally decomposes to isoprene, water and formaldehyde. The second route passes through the direct H^+ elimination with formation of 2-methylbutenols which finally dehydrate to isoprene.

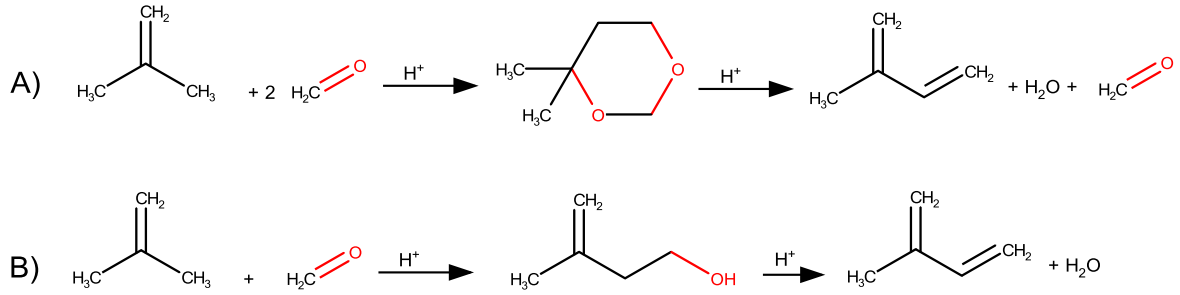

Figure 60: Different pathways to obtain Isoprene from the Prins reaction: A-through 4,4-dimethyl-1,3-dioxane, B-through 2-methylbutenols. 2-methylbutenols include the molecule shown in the figure and its isomer in which the double bond is in position 2.

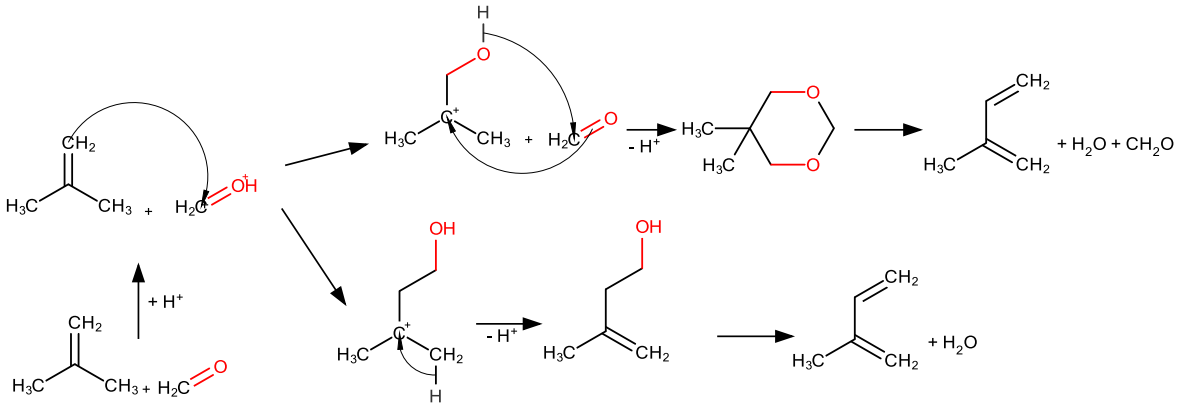

Figure 61: Possible mechanisms for isoprene formation via the Prins reaction.

Isoprene obtained in industrial processes by means of the Prins reaction employ the dioxane route (Figure 60-A).

The reaction is carried out in two different plant sections. In the first one, the dioxane is produced in the liquid phase using an homogeneous acid catalysis. In the second step, the dioxane is fed to a reactor in which it decomposes to isoprene in the presence of an acid heterogeneous catalyst.

The first step is carried out by contacting a 45-40% aqueous solution of formaldehyde with a C_4 stream containing 40-45% isobutene; 1 to 10% sulphuric acid, dissolved in the aqueous phase, is used as catalyst[97, 108]. Reaction conditions are aimed at facilitating a fast formation of 4,4-dimethyl-1,3-dioxane: 3 to 10 atm pressure is maintained with the twofold aim to favour the mass transfer between the vapour and the liquid phase, and to shift the equilibrium toward the formation of products (the reaction proceeds with a decrease of the number of moles). Because of the reaction exothermicity, it is common to have reaction

temperatures between 65 and 110°C, which is a compromise between a fast reaction and good thermodynamic yield[97, 109].

These reaction conditions give around 80% 4,4-dimethyl-1,3-dioxane yield; main side products are isobutanol, 2-methyl-1,3-butandiol, 2-methylbutenols and other products derived from the Prins reaction between formaldehyde and linear butenes presents in the C_4 stream. Actually, isobutene reacts with formaldehyde faster than *n*-butenes, so it is possible to operate at a contact time that is a compromise between product yield, reagent conversion and negligible side-reactions involving linear butenes[108].

After purification, 4,4-dimethyl-1,3-dioxane is vaporized and fed to the decomposition reactor; here it is decomposed at 250-400°C and 1 atm over an acid heterogeneous catalyst, which is usually made of supported phosphoric acid[95, 109]. High temperature is required in order to provide the heat necessary to sustain the reaction endothermicity. As schematized in Figure 60-A, 4,4-dimethyl-1,3-dioxane decomposition gives isoprene, water and formaldehyde; isobutene can be obtained as side-product from isobutanol dehydration, present as an impurity in the feeding stream. The catalyst needs to be regenerated every 2-4 hours because of fast deactivation due to consecutive reactions on formaldehyde or isoprene, which lead to heavy compounds deposition[108].

These working conditions give dioxane conversion around 50-60% with 90% isoprene selectivity; dioxane conversion is kept low in order to hinder coke formation and maximize isoprene selectivity.

The downstream purification process, consisting of distillation columns, scrubbers and extractors, is exploited to separate and recycle unconverted formaldehyde, dioxane and, finally, to obtain polymerization grade isoprene.

A typical production process is schematized in Figure 62.

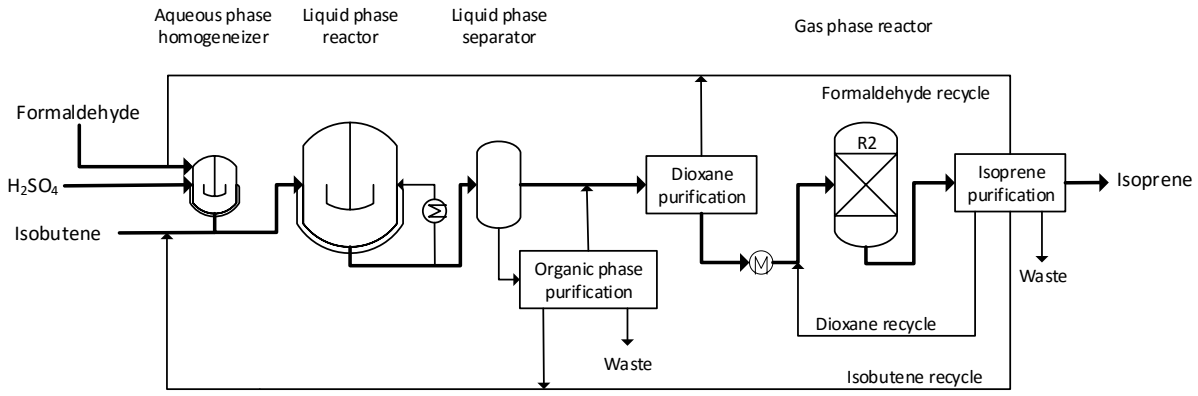

Figure 62: Simplified scheme of isoprene production process by means of the two-step Prins reaction.

The process includes three main sections:

- Synthesis and purification of 4,4-dimethyl-1,3-dioxane;
- Production of isoprene via dioxane decomposition;

- Isoprene purification.

The process is characterized by a complex set-up of separation steps involving effluents coming from both dioxane production and dioxane decomposition reactors. The purification process is not described in its details because, due to its complexity, would require a long discussion; anyway, in the next paragraph the essential information will be given in order to draw a general overview of the process.

The liquid reaction mixture resulting from dioxane production, made up of an organic and an aqueous phase, is first collected and decanted to allow phase separation. The organic phase is purified to recover and recycle isobutene to the liquid-phase reactor, wastes resulting from this step are usually burnt. The aqueous phase is first neutralized with caustic washing and then purified in a set of extraction and distillation columns. Aqueous phase purification allows the recovery of unconverted formaldehyde and purification of 4,4-dimetyl-1,3-dioxane until a purity grade sufficient for further processing is obtained[109, 97].

As described above, dioxane undergoes acid-catalyzed cleavage, which leads to a product mixture containing isoprene, formaldehyde, water, unconverted dioxane and other side-products derived from parallel and consecutive reactions, such as isobutene and heavy compounds.

Downstream purification consists in a set of, at least, eight columns comprising extraction, scrubbing and distillation units. Such a high number of columns is necessary in order to remove all the impurities from isoprene, but also to recover and recycle the formaldehyde obtained from dioxane cleavage and the isobutene obtained from isobutanol dehydration[99, 97].

The overall process isoprene yield is around 50%.

A modification of this process allow to slightly increase isoprene yield by processing also some side-products of the first step in the dioxane decomposition reactor, such as 2-methylbutenols and 2-methylbutan-1,3-diol. These alcohols can dehydrate over the acid catalyst in the decomposition unit giving isoprene and increasing its overall yield. This solution allows to decrease waste products [109], but some modification in the purification step are needed[109].

Overall, the two-step Prins process has many drawbacks, such as[109, 108, 110]:

- the process is economically, technically and energetically not much favoured;
- the high amount of different side-products requires complex purification processes;
- in some cases, side-products have no commercial value and have just to be burnt;
- isoprene yield is low;
- the first step requires sulphuric acid, which gives corrosion problems;
- formaldehyde is difficult to handle because of its toxicity and reactivity, and also may cause catalyst deactivation.

Research in this field is focused on solving these issues by the development of a one-step process and the use of a suitable acid catalyst, able to perform the Prins reaction as shown in Figure 59.

Main attempts aimed at improvind this process were done by some Japanese companies[111, 112]; they claimed the use of Bismuth supported over silica as a solid heterogeneous catalyst, able to directly convert isobutene and formaldehyde to isoprene. With such catalyst an isoprene yield of about 70% was claimed, stable over 10 hours[111].

Another purpose was to realize the one-pot synthesis by feeding the reagents to an acidic aqueous solution and simultaneously distil away the products, giving the effect of shifting the reaction equilibrium toward the products. Moreover the reaction is carried out under 15 atm pressure in order to facilitate mass transfer and avoid vaporization and spreading of the acid aqueous solution.

With this technique an isoprene yield around 70% is claimed, with 80% formaldehyde conversion. Some good results were also obtained by feeding formalin and isobutene over phosphate catalysts at atmospheric pressure; best results with these catalysts were 45-50% isoprene yield with 80-85% formaldehyde conversion, both being stable for 20 h time-on-stream[110]. It is also reported that H-Boralites can give good isoprene yield[113].

Despite the good results in terms of isoprene yield, all of these processes were not developed beyond the laboratory or pilot-plant scale; limitations may be the conditions used, far from the industrial ones, the short lifetime of the catalysts, the complex products mixture obtained and the incomplete conversion of formaldehyde.

Indeed, a new process should hold the following characteristics:

- realize the process in one step only;
- provide high isoprene yield, with low amount of side-products;
- give almost total formaldehyde conversion in order to avoid its downstream handling;
- show long catalyst lifetime.

3.1.2.4 Considerations on the three production processes

Nowadays the preferred route to isoprene is the separation and purification from C_5 stream[92], but also the other processes mentioned are still in use; a brief overview on the different production routes is given in Figure 63: Distribution of isoprene production among the three industrial production processes.

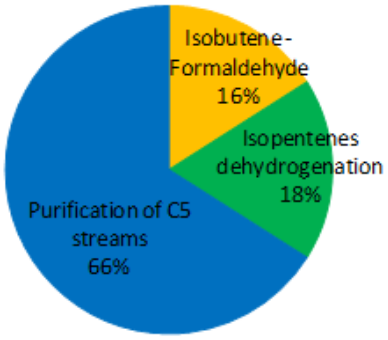

Figure 63: Distribution of isoprene production among the three industrial production processes.

The three processes have been analyzed by using literature data[92, 95, 97] in order to have an idea about their sustainability. Each process was qualitatively analyzed taking into account the following parameters:

- Consumption of raw materials;
- Nature and amount of by-products;
- Chemicals and catalysts used;
- Utilities needed to run the process (steam, cooling water, electricity)

Table 2 shows the results of this qualitative evaluation; a X is shown in the cell corresponding to the more impacting process for each parameter analyzed.

	Extractive distillation	2-methylbutenes dehydrogenation	Isobutene-formaldehyde
Raw materials	X		
By-products	X		X
Catalysts and other chemicals		X	
Utilities		X	

Table 2: qualitative evaluation of isoprene production processes (X indicates the more impacting process for each parameter)

Starting from this qualitative comparison, it is possible to highlight the strengths and drawbacks of each process; indeed, it should be necessary also to take into account other important issues, such as energy costs and local raw material availability.

As said before, the sustainability of extractive distillation depends on the side-products obtained from naphtha steam cracking; this allows to valorise a side-product by separating useful chemicals that can be commercialized, including isoprene. From this point of view, by-products do not represent a waste, but can be considered as valuable chemicals. The main drawback of this process is that it needs to be connected to very large-scale steam-cracking plants in order to obtain an isoprene productivity great enough to make it economically advantageous. Finally, it is a very complex process, that needs a large number of process units, but this is common also to the other two processes.

2-Methylbutenes dehydrogenation can be considered as an improvement of the extractive distillation: 2-methylbutenes coming from isoprene purification can be processed in order to improve isoprene yield. However, this process has not to be necessarily connected to an isoprene purification unit, it can be run also if an economically affordable source of 2-methylbutenes is available. The main drawback is the high amount of energy required to run the process; the main part of it is probably related to the dehydrogenation units, where the heat necessary to sustain the reaction has to be furnished. Another weakness of the process is the use of an harmful reagent, in fact 2-methylbutenes are dangerous low-boiling compounds that can be fatal if inhaled[114].

Finally,the isobutene-formaldehyde process, with two reaction steps and two purification steps, can be considered the more complex in terms of number pf process units and reagent recycle. However, on the other hand, it exploits relatively cheap reagents which are easier to handle, store and transport than those used, for example, in the dehydrogenation process. In fact isobutene and formaldehyde, despite some safety concerns, are not as dangerous as 2-methylbutenes. Moreover, it is less dependent on petroleum refinery stream, in fact its reagents (mainly formaldehyde) can be obtained from different sources, such as the (oxi)dehydrogenation of methanol produced from methane-derived syngas. The main drawback of the process is the use of formaldehyde, in fact it is an hazardous, toxic and carcinogenic gas with a boiling point of -19°C. Moreover it is very reactive and, if not properly stored, can spontaneously polymerize via an highly exothermic reaction, which can lead to dangerous runaway events. Because of these safety issues, formaldehyde is provided only as a solution in water (formalin), stabilized with methanol or in the form of the more stable trimer, which is not so much used in industry because it can give back formaldehyde in high concentration if overheated. To minimize hazards deriving from formaldehyde handling and transportation, it is common to find plants exploiting the Prins reaction close to a methanol oxidation/dehydrogenation unit, which provides formaldehyde for the reaction without the need of long storage time and transportation.

In conclusion, these three processes are fully developed and optimized, so it is difficult to enter this field with a new process. Nevertheless a more sustainable process is strongly desired, because of the several drawbacks above listed, which make them dangerous, difficult to carry over and often with poor economic return. Actually, despite of difficulties met for the development of a brand new process, some companies and research groups have been making efforts to improve the sustainability of isoprene production. Examples include the investigation of the one-step isobutene-formaldehyde Prins reaction, or the development of a more sustainable processes in which formaldehyde is replaced with methanol.

The next chapter will give a short overview of the alternative and innovative processes for isoprene production.

3.1.3 Alternative and innovative processes for isoprene industrial production

During the past fifty years also processes other than those described above for isoprene production were industrialized, which however were then abandoned because of different reasons.

Eni-Snamprogetti developed and industrialized a process based on acetylene-acetone coupling[108, 97], which involves three steps:

- acetone-acetylene coupling to 2-methylbutynol, carried out with liquid ammonia and catalyzed by homogeneous potassium hydroxide;
- selective hydrogenation of 2-methylbutynol to 2-methylbutenol catalyzed by palladium;
- dehydration of 2-methylbutenol to isoprene at 250 – 300°C catalyzed by Al_2O_3.

The advantage of this process was that acetylene was available at very low price because it was produced in large quantities in a facility close to the isoprene production plant. The production was stopped because of its high production costs.

Another alternative process was industrialized by Goodyear: it was based on propylene dimerization and successive cracking of the obtained C_6 to isoprene and methane[97]. It presents some advantages, such as the low quantity of side-products and a simpler purification process, but the only plant working with this process was destroyed in an accident and never rebuilt, so, nowadays, this method is no longer employed[97].

It is possible to divide research regarding innovative processes for isoprene production in two main areas:

- bio-chemical routes, which exploit enzymes or cells to produce isoprene by fermentation of different substrates;
- chemical routes, which are mainly focused on the development of catalytic processes exploiting safer, cheaper and more available raw materials.

Bio-chemical routes allow independence from fossil raw-materials by exploiting renewable sources; moreover these processes can be carried out ad mild conditions, reducing costs related to utilities required for cooling or heating. On the other side, bio-chemical routes need very precise conditions to let the microorganisms work at their maximum productivity. Moreover cells and enzymes are very expensive and may make the process too costly for an industrial application.

Despite these drawbacks, Dupont announced that they were able to produce some tyres totally based on bio-isoprene[115], but this is far from substituting an industrial production with bio-chemical routes.

Innovative chemical routes include different purposes, such as olefin metathesis and Prins-based processes with the replacement of formaldehyde with methanol.

Since this part of the thesis deals with a modified Prins reaction, few words only will be spent to briefly describe olefin metathesis, while modified Prins reaction will be more deeply described in the next paragraph.

Olefin metathesis can be carried out by reacting isobutene with 2-methylbutene, to obtain 2-methylpentene and propene; 2-methylpentene is than dehydrogenated to isoprene[116]. Another possibility is to obtain 2-methylpentene with the co-production of propene by reacting together butenes; the so-obtained 2-methylpentene is then pyrolized to obtain a stream rich in isoprene[117], which is finally purified.

However both of these processes are disadvantageous because of the two steps used and because olefins can undergo several reactions leading to a broad spectrum of by-products.

3.1.3.1 Methanol as alternative reagent for the production of isoprene with the Prins reaction

The main field of investigation for the improvement of isoprene production by chemical routes regards the optimization of Prins reaction-based processes. As said before, this process presents several drawbacks, many of which are connected to the use of formaldehyde and to the presence of two steps. Therefore, the largest part of the research is focused on the development of a single-step process and, even better, on a process which avoids the direct use of formaldehyde.

A short overview regarding the state of art on the single-step Prins process starting from formaldehyde and isobutene was presented in the previous chapter. Here the attention is focused on methods investigated that allow to avoid the use of formaldehyde, by replacing it with methanol.

The route to isoprene that involves methanol can be classified as a modified Prins reactions. In fact, as shown in Figure 64, methanol can be used as an in-situ source of formaldehyde for the Prins reaction.

The objective of this process is to generate and consume formaldehyde in-situ, so avoiding its direct use. This is possible exploiting a multifunctional catalyst able to convert methanol to formaldehyde and then to consume the latter through the Prins reaction, finally producing isoprene. In this way formaldehyde is theoretically confined on the catalytic bed, in which it is produced and then consumed.

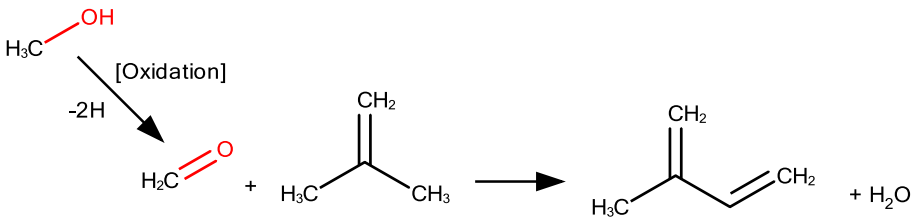

Figure 64: Isoprene production route based on methanol

The feasibility of this pathway was confirmed by Matsumoto *et al*[118]. By using a catalyst made of Ag^0 supported over SiO_2 these authors were able to obtain isoprene starting from methanol, isobutene and oxygen, which acts as the oxidant for the first step. Despite the low isoprene yield achieved (around 8% with respect to the limiting reagent), a relationship between the formation of isoprene and the presence of formaldehyde was reported, which suggests that isoprene derives from the reaction pathway shown in Figure 64.[118]

Some improvement in terms of isoprene yield was obtained by Watanabe *et al* in US patent 3621072. They describe a one-step catalytic process in which methanol (or dimethyl ether), isobutene and oxygen are fed to a catalyst based on MoO_3 supported over SiO_2; MoO_3 provides the redox sites for methanol oxidation, whereas silica, besides its function as a support, catalyzes the Prins reaction because of its acid sites[119]. Best reaction conditions were find to be at 2:1 isobutene-to-methanol ratio, oxygen concentration between 10 and 5% of the total gas phase and temperature between 250 and 300°C[119]. Still in this patent it is reported that isoprene yield can be enhanced by supporting H_3PO_4 on SiO_2 together with MoO_3. Phosphoric acid probably contributes to speed up isoprene formation by increasing catalyst acidity, which is needed for the second step. This may suggest that in this case the rate determining step is the Prins reaction, while the first step of oxidation is faster.

With these conditions the authors claimed a 38% isoprene yield based on the limiting reagent (methanol).

A modification of this process exploits methyltertbutyl ether (MTBE) as a source for both isobutene and methanol. MTBE is fed together with oxygen again over a MoO_3/SiO_2 catalyst; MTBE can decompose to methanol and isobutene because of the catalyst acidity, than the two compounds react to give isoprene[120]. This method holds the advantage of an intrinsic control of the methanol/isobutene molar ratio, which is always 1:1. However, MTBE is more expensive and its market is mainly focused on its use as an high octanizer additive for gasoline.

Despite improvements claimed, this process is far from industrialization; besides the low isoprene yield, the main drawback is the risk of formation of flammable mixtures caused by the presence of oxygen together with methanol and isobutene. This risk can become acceptable only if high isoprene yield can achieved with the use of long-life catalysts.

An alternative solution to this problem is to carry out the reaction schematized in Figure 64 using methanol dehydrogenation instead methanol oxidation. The feasibility of this route was verified by Gokhberg et al in US Patent 4147736. The patent deals with the reaction of methanol with isobutene to isoprene by using catalysts based on transition metal oxides which are typically active in alcohols dehydrogenation, such as group 6 elements, Vanadium or Chromium, supported over Al_2O_3[121]. Moreover, it was claimed that also Ta_2O_5 can be active in this reaction. Best results were obtained by contacting a mixture of isobutene and methanol at a 8:1 molar ratio with a catalyst based on MoO_3 supported over Al_2O_3 at 400°C. These conditions could lead to an isoprene yield around 16%; other products were methylbutenes with a total isomers yield around 25%[121].

Also in this case the low yields achieved made an industrial implementation unlikely, but these results highlight the possibility to develop a process for isoprene production by using methanol-isobutene coupling without the need of oxygen.

3.1.4 Aim of the work

As said before, isoprene production presents some sustainability issues. Actually, it is nowadays produced in large amount through energy-consuming and complex petrochemical routes. An alternative route exploits the Prins reaction, but this method has one main drawback in the use of formaldehyde, which is reactive, toxic and carcinogenic.

Indeed, each route to isoprene presents some critical drawbacks, which have negative effects on the sustainability of the process; the research work here presented is focused on the study of a more sustainable route to isoprene by exploiting an alternative approach for the Prins reaction.

As said in the previous chapter, it is possible to obtain isoprene in a more sustainable way by avoiding the direct use of formaldehyde. This can be obtained by feeding methanol, which can be converted into formaldehyde on the same catalytic bed in which then formaldehyde is converted to isoprene through the Prins reaction.

In overall, this method can be viewed as a two-step reaction carried out in a single passage.

The first step consists in methanol transformation to formaldehyde and the second is the reaction of formaldehyde with isobutene to give isoprene (Prins reaction).

This reaction can be called “modified-Prins reaction”, and can be carried out by co-feeding oxygen as the oxidant or by carrying out methanol dehydrogenation to formaldehyde without any oxidant. In the first case, the reaction can be called aerobic-modified-Prins reaction, in the second case it can be called anaerobic-modified-Prins reaction. These reactions are schematized in Figure 65.

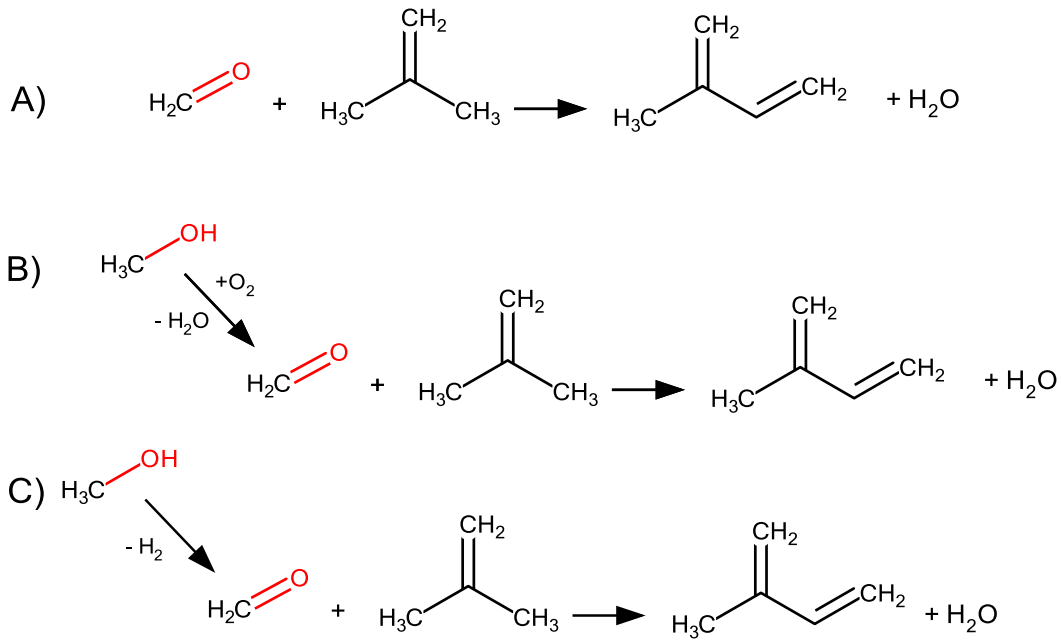

Figure 65: Prins reaction (A), aerobic-modified-Prins reaction (B) and anaerobic-modified-Prins reaction (C).

Although the feasibility of this reaction has been demonstrated, patents in this field [119] [121] [118] report low isoprene yields, which can be probably improved. Moreover, it is not possible to find any scientific paper in the literature dealing with the key aspects of this reaction and providing an overview on the possible reaction intermediates and consecutive products. So, the knowledge on the modified-Prins reaction is limited to data presented in patents, which contain very few information on the reasons for the low isoprene yield achieved or on the catalytic properties that can enhance it.

The aim of the research work presented in this thesis was to develop a catalyst able to transform methanol and isobutene to isoprene and, more importantly, to give a scientific approach to the reaction by elucidating the reaction scheme over a specific class of catalysts, in order to finally provide basic information for a further development of the modified-Pins reaction.

As shown by literature data presented in the previous chapter, the modified-Prins reaction needs a multifunctional catalyst able to transform methanol to formaldehyde, and to catalyze the Prins reaction between formaldehyde and isobutene.

Our objective was first to develop a multifunctional catalyst by using metal phosphates as the support for a metal oxide; the latter should be able to dehydrogenate methanol to formaldehyde, while the catalytic features necessary to facilitate the Prins reaction are provided by the metal phosphate[110].

However, as will be seen later on in this thesis, we discovered that despite the absence of dehydrogenation properties, Aluminium phosphate alone can catalyze isoprene formation

when methanol and isobutene are co-fed. So the core of this part of the thesis was aimed at investigating on the mechanism of the reaction.

The following chapter is divided in three parts:

- The first part deals with the investigation of the reaction scheme of methanol-isobutene coupling to isoprene over Aluminium, Lanthanum and Zirconium Phosphates.
- The second part deals with the investigation of the anaerobic-modified-Prins reaction as described in Figure 65-C, by studying the reactivity of a multifunctional catalyst made of Cu or Co oxides supported over Aluminium phosphate.
- The third part deals with the investigation on the aerobic and anaerobic-modified Prins reaction over a double catalytic bed-reactor. The first bed, made of $FeVO_4$, is able to dehydrogenate methanol to formaldehyde[137, 138], while the second bed, made of Aluminium phosphate, catalyzes the Prins reaction between formaldehyde and isobutene.

3.2 Experimental part

This part of the thesis describes procedures and techniques used to synthesize and characterize catalysts, to carry out the reaction and to calculate products yields.

3.2.1 Catalysts preparation and characterization

In this chapter methods used to synthesize catalysts and techniques for their characterization are described in detail.

Iron Vanadate was prepared and characterized as described elsewhere in the thesis; here the preparation procedure adopted for metal phosphate catalysts is described.

3.2.1.1 Preparation of metal phosphate catalysts

Aluminium, zirconium and lanthanum phosphate (respectively AlPO, ZrPO and LaPO) were prepared using a method adapted from the literature[110]. It consists in the precipitation of metal phosphates from an aqueous solution. The precipitate is then filtered, dried and calcined.

Briefly, each solution of metal cations was prepared by dissolving the precursor in water; then 300 mL of 1 M phosphoric acid solution was added under continuous stirring, the pH was then brought from acid values up to 7 with 28% aqueous NH_3 in order to promote metal phosphates precipitation. Precipitates were decanted for 3-4 hours, filtered and then washed with 2000 mL of distilled water to remove absorbed ions. Finally the white solid was dried at 120°C and calcined at 550°C for 3 hours; it was then pressed into tablets and crushed to obtain particles with size comprised between 30 and 40 mesh. This fraction was used for catalytic tests. Quantities and kind of the various cation precursors used are shown in Table 3.

	Cation precursor	weight of cation salt (g)	V of cation solution (mL)	Nominal metal to P ratio (mol/mol)
AlPO	99% $AlCl_3$	40.4	300	1/1
ZrPO	98% $ZrOCl_2 \cdot 8H_2O$	97.3	300	¾
LaPO	99,9% $La(NO_3)_3 \cdot H_2O$	103.0	300	1/1

Table 3: Quantities of cation precursors to which was added phosphate solution to obtain the corresponding phosphate.

Despite the reagents were dissolved in a precise molar ratio, the precipitation was driven by the solubility constant of the species that precipitate under those defined conditions. Once solubility constant was reached, phosphates precipitated regardless of the molar ratio used.

Nevertheless, the nominal metal-to-phosphorus ratio used was maintained close the expected stoichiometry in order to minimize waste of raw materials.

Neutral pH was necessary to both quantitatively precipitate the phosphate and to limit hydroxide formation.

3.2.1.2 Preparation of Copper and Cobalt oxides supported over AlPO

Cu and Co oxides were supported over AlPO at different nominal metal loading by means of the wetness impregnation technique.

In each case, 10 g of AlPO powder was suspended in 30 mL distilled water, then the metal oxide precursor was rapidly added (99% $CuCl_2$ in the case of Cu oxide, and 99% $CoCl_2$ in case of Co oxide). Quantities and nominal metal loadings are shown in Table 4.

Catalyst code	Weight of metal precursor (g)	Nominal metal loading (%)
5-CuO/AlPO	1.07	5
10-CuO/AlPO	2.14	10
20-CuO/AlPO	4.27	20
5-CoO/AlPO	1.11	5
20-CoO/AlPO	4.45	20

Table 4: Quantity of precursors and support used to prepare Cu and Co oxides supported over AlPO

Water was evaporated under vacuum and the wet powder was dried at 120°C and then calcined at 550°C for 3 hours. Also this catalyst was pelletized in the form of particles with size of 30 – 40 mesh before its use for catalytic tests.

3.2.1.3 Catalysts characterization

Characterization of catalysts was carried out by means of XRD, IR, SEM-EDS, and BET, as described in paragraph 1.2.1. Moreover, the phosphate acidity was measured by means of ammonia temperature programmed desorption (NH_3-TPD). A typical TPD experiment consists in three steps:

- Pre-treatment of the catalyst with a ramp of 10°C/min until 400°C, isothermal step for 30 min, in a 20 mL/min He stream;
- Cooling down to 100°C and absorption of ammonia, using a NH_3 30% in a 20 mL/min He flow, for 30 min;
- Ammonia desorption in a 20 mL/min He flow, with a temperature ramp of 10°C/min, until 500°C, and with final isotherm step for 40 min.

In between the sample holder and the TC detector a soda lime trap was placed, in order to block water and avoid signals due to water desorption.

NH_3-TPD profiles, obtained from this experiment, can provide information on the strength and the number of acid sites. The strength is measured from NH_3 desorption temperature: the higher is the temperature, the stronger are the sites. The quantity of acid sites is calculated to the area of the desorption peak. If the ammonia response factor is known, it is

possible to calculate the number of NH_3 moles desorbed, and finally express the acidity in terms of NH_3 μmoles desorbed per unit surface area or unit catalyst weight.
Catalysts 10-CuO/AlPO,20-CuO/AlPO and 20-CoOx/AlPO were also characterized by means of SEM imaging with EDX probe, in order to confirm the homogeneous deposition of the oxide on the support.

3.2.2 Catalytic tests

As previously described in chapter 1.2, catalyst granules were loaded and tested in a lab-scale micro reactor connected on-line with a GC for the analysis of the products.
The two GC columns used were:

- An Agilent HP-Plot Q, 30 m length, 0.32 mm inner diameter, 0.04 mm film thickness, used to separate and quantify CH_4 and CO_2. With this column it was also possible to separate and quantify methanol, isoprene and dimethyl ether.
- A mid-polarity stationary phase Agilent DB-628 UI, 30 m length, 0.53 inner diameter, 0.003 mm film thickness, used to separate and quantify all the products except CH_4 and CO_2.

Each column was connected to one TC detector. Helium was used as the GC carrier gas and reference and make-up gas.
Inert gas used in the lab-scale set up was N_2; however, He was used in some cases because N_2 GC peak can overlap methane and formaldehyde peaks, if the latter are present in low quantities.
A typical catalytic test was conducted by feeding methanol and isobutene at a 1-to-6 molar ratio; data were taken at different temperatures, usually 300 and 400°C. With metal phosphate catalysts, it was not possible to exceed 400°C, otherwise phosphate leaching in the form of organic phosphates led to progressive catalyst destruction. The time factor (W/F ratio) was measured by dividing the mass of the catalyst loaded in the reactor by the total gas flow fed to the reactor, measured at ambient temperature.

3.3 Results and discussion

3.3.1 Catalysts characterization

Catalysts characterization was carried out for the determination of chemical-physical properties, such as crystallinity, phase composition, SSA and metal oxide distribution in the case of supported catalysts.

Results of $FeVO_4$ characterization are reported in chapter 2.3.

3.3.1.1 Fresh catalysts characterization

IR spectra, shown in Figure 66, was used to confirm the formation of the desired phosphate. Spectra of catalysts before calcination and after calcination are shown in Figure 66. AlPO and ZrPO spectra both showed broad bands, but in case of LaPO, bands were more resolved. Therefore AlPO and ZrPO were mainly amorphous, while LaPO was more crystalline.

All spectra showed absorption bands between 980 and 1080 cm^{-1} related to P-O stretching[122] in tetrahedral PO_4^{3-}. Slight differences in the position of the P-O band vibration between calcined and non-calcined samples can be due to different hydration degrees.

Bands in the range 800-400 cm^{-1} are related to O-P-O and M-O-P vibration modes[122 128 123].

Bands centred at 1624-1634 cm^{-1} and falling in the range 3500-2900 cm^{-1} indicate the presence of water, probably adsorbed on the catalyst surface because of materials hygroscopicity. Band centred at about 1435 cm^{-1} and bands in the region 3000-2800 cm^{-1} in spectra of non-calcined samples are related to N-H vibrations. This indicates the presence of some residual ammonium ion from precursors used for catalysts synthesis. It also reveals the presence of acid sites able to bind ammonia. Anyway, the ammonium was decomposed and released into the gas phase as ammonia during calcination; in fact corresponding bands disappeared in calcined samples. The centre of phosphate absorption bands was shifted depending on a combination of factors affected by cation features, such as the covalent character of M-OP bond, the nominal charge of the cation, and the freedom of the phosphate group in the crystal lattice. Because of the complexity deriving from the combination of various effects, it is not possible to infer a simple correlation between the cation type and the position of the band. However, it is possible to obtain some information on the nature of the cation-phosphate bond. The freedom of phosphate group in the crystalline lattice and the high charge of the cation lead bonds to vibrate at lower energies (lower wavenumber). The more covalent is the bond between the cation and the phosphate group, the more the phosphate will be rigid in its position, with less freedom for vibrations and higher vibrational frequencies. The greater the cation charge, the weaker the P-O bond, and the absorption band will fall at lower wavenumbers.

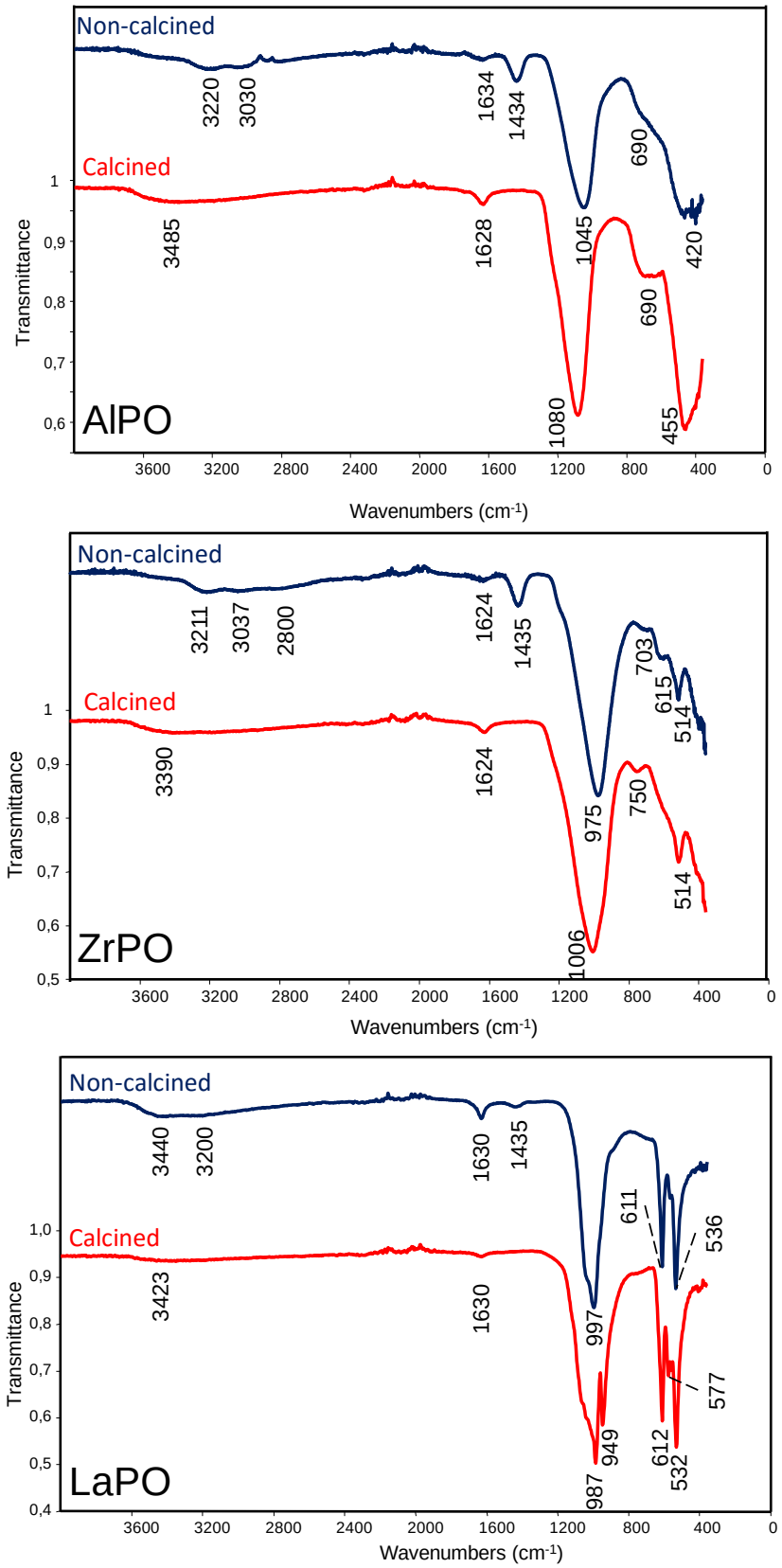

Figure 66: IR spectra of AlPO, ZrPO and LaPO. Blu lines refer to catalysts before calcination, red lines to calcined catalysts.

Taking into account these effects, it is possible to give a rough explanation of the shift of phosphate bands vibrations: AlPO shows higher absorption frequency, followed by ZrPO and LaPO.

Therefore the scale of covalency character for the metal cation-PO_4^{3-} bonds is AlPO>ZrPO>LaPO. This is in good agreement with the position of these elements in the periodic table; in fact Al features atomic orbitals at an energy level similar to P and O, which leads to an easier overlap. This can occur also in case of ZrPO by exploiting Zr d orbitals, but the effect is weaker because these orbitals are theoretically at an higher energy level. Moreover, in this case phosphate absorption band falls at lower energies because of the greater positive charge of the cation. Finally La^{3+} phosphate, as it typically occurs for Lantanides, has a strong ionic character of the bond[124].

As evident from XRD patterns in Figure 67, both AlPO and ZrPO structures appeared to be amorphous, without any crystalline domain. On the other hand, LaPO XRD pattern showed the formation of a crystalline phase, but it is not possible to exclude the presence of amorphous domains also. These spectra are in agreement with arguments inferred from the analysis of IR spectra.

LaPO XRD pattern showed the presence of $LaPO_4$, which is the expected compound, but some reflections suggested the formation of Lanthanum pyrophosphate also.

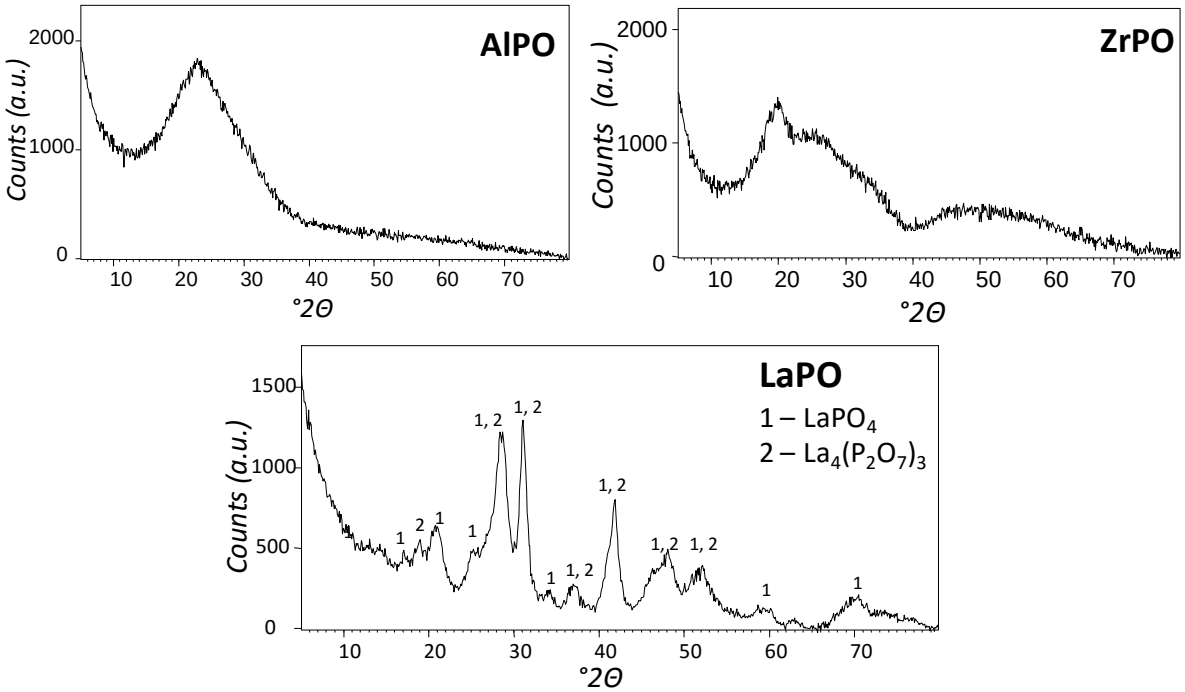

Figure 67: XRD pattern of AlPO (top left), ZrPO (top right) and LaPO (bottom).

EDX analysis carried out on different spots of the AlPO SEM image in Figure 68 gave an Al/P/O ratio always close to 1/1/4, confirming the development of $AlPO_4$,without impurities of alumina or other compounds.

On the other hand, in the case of ZrPO a 1/1.7/9 Zr/P/O atomic ratio was found, instead of the theoretical 1/1.3/5, calculated taking into account the formation of $Zr_3(PO_4)_4$. An higher amount of P than the expected one might be due to the presence of free P_2O_5, or, as reported in the literature, to the formation of zirconium phosphate that includes hydrogen atoms in the structure[125].

Concerning LaPO, we did not find the expected La/P/O atomic ratio of 1/1/4, corresponding to the formation of $LaPO_4$. EDX analysis showed an average ratio of 1/1.4/6.8. However, this might be due to the presence of both $LaPO_4$ and $La_4(P_2O_7)_3$, as also evident from the XRD pattern.

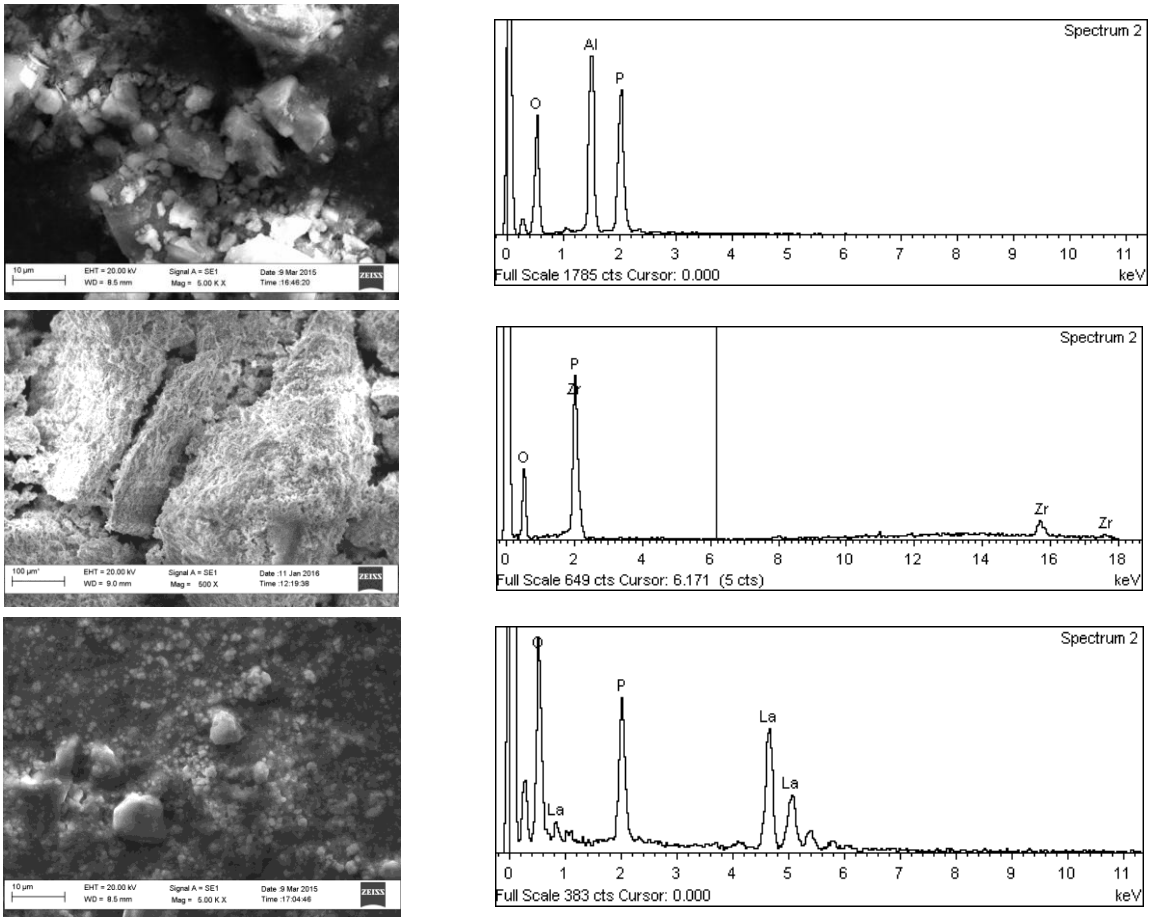

Figure 68: SEM image of AlPO (top), ZrPO (center) and LaPO (bottom) and corresponding EDX spectra.

Specific surface areas, determined by the BET technique, were 150 m^2/g for AlPO, 58 m^2/g for ZrPO and 93 m^2/g for LaPO.

The amount and strength of acid sites were determined by NH_3-TPD; ammonia desorption profiles are shown in Figure 69. Quantification of the amount of desorbed ammonia was made by integration of TPD signals; the calculated total amount of acid sites are given in Table 5.

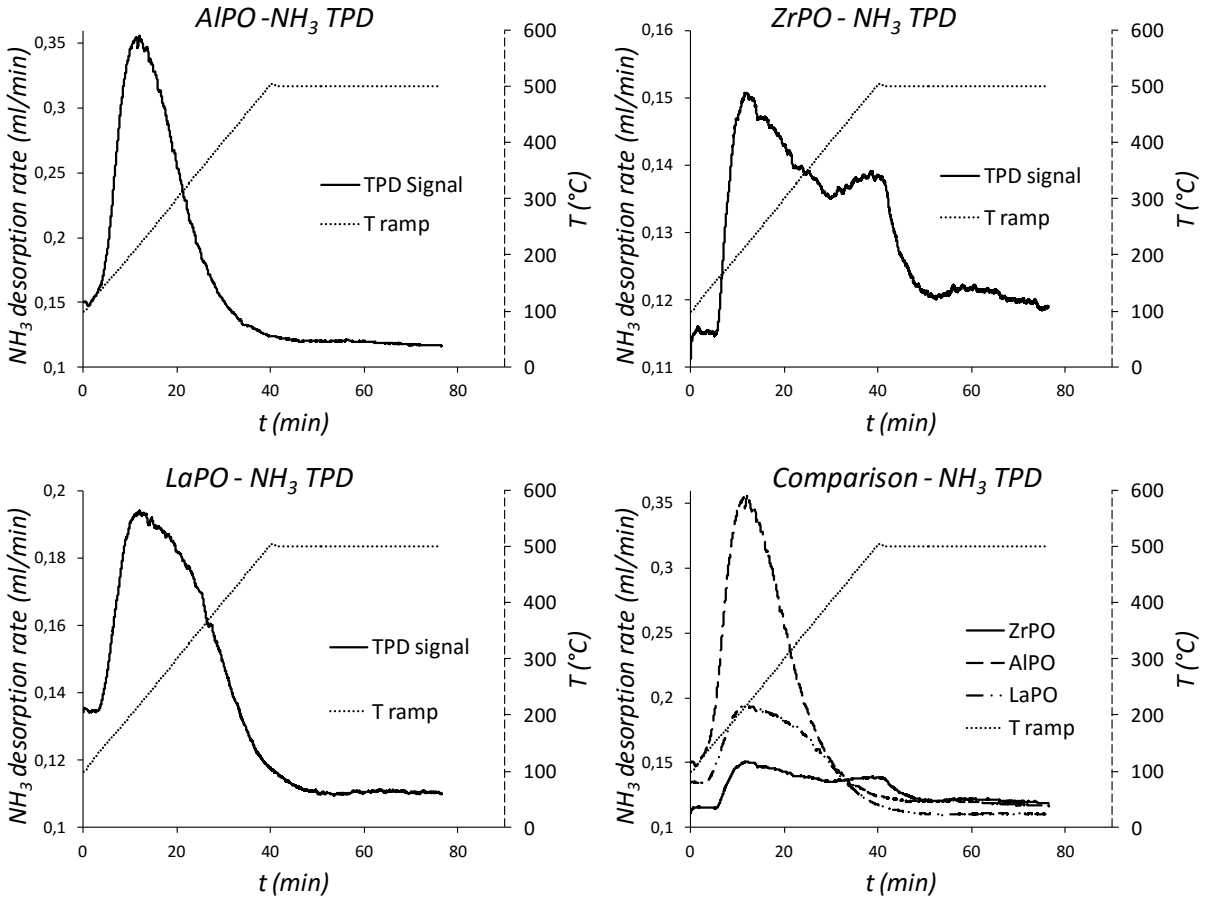

Figure 69: NH_3 TPD profiles of AlPO (top left), ZrPO (top right) and LaPO (bottom left), different scales on y principal axis are used to better show the desorption profile of each phosphate . A comparison is given in the bottom right figure.

All NH_3-TPD profile showed a peak with a maximum at around 200°C, indicating the presence of medium-strength acid sites in all samples.

The NH_3-TPD profiles of AlPO and LaPO suggest a similar strength for acid sites in the two catalysts; in fact ammonia was entirely desorbed in a narrow range of temperature. But in the case of LaPO, also stronger acid sites were present, in fact ammonia desorbed in a broader temperature range.

A different situation was shown for ZrPO. Its desorption profile displayed a broad peak indicating a continuous desorption in the range 200-500°C; this corresponds to the presence of different types of acid sites, which ranged from medium-strength to strong. However, because of this continuous profile it was not possible to precisely quantify the number of each type of acid site. A rough evaluation was done by integrating the signal area around the two maxima at 200°C and 500°C. In such a way it was possible to determine that the ratio between stronger and medium acid sites in ZrPO was equal to about 1.4.

The stronger acidity of ZrPO can be explained by taking its structure into account [125]: in fact, the structure of ZrPO likely also includes protons, which can also contribute to acidity. In the

case of AlPO and LaPO, acidity was mainly due to the presence of surface defects with formation of hydroxyl groups. .

To summarize: both AlPO and LaPO surface exhibit medium-strength acid sites with the presence of some stronger site in LaPO; ZrPO holds acid sites with strength in a range between medium-strength and strong. The amount of acid sites was higher in AlPO, while ZrPO and LaPO contained a smaller and similar amount of sites.

	AlPO	ZrPO	LaPO
SSA (m^2/g)	150	58	93
Phase	amorphous	amorphous	crystalline
Cation/P/O atomic ratio	1/1/4	1/17/9	1/1.4/6.8
Amount of acid sites	5.8 µmol/m^2	2.6 µmol/m^2	2.3 µmol/m^2
	865 µmol/g	151 µmol/g	216 µmol/g

Table 5: Summary of catalysts characterization results with NH_3-TPD.

3.3.1.2 Characterization of fresh Co and Cu oxide supported over AlPO

Some of the samples based on Cu and Co oxide supported over AlPO were characterized by means of SEM imaging. Results obtained for Cu oxide over AlPO at 10 and 20% nominal metal loading are shown in Figure 70 and Figure 71, respectively. Bright zones in the electron image (on the left) correspond to Copper-rich zones. From elements mapping of 10-CuO/AlPO, it is shown that these Cu-rich zones did not contain Al and P. This means that CuO was not deposited over the support, but it formed separate aggregates. This was true for 20-CuO/AlPO also, but in this case Copper was also spread over support surface.

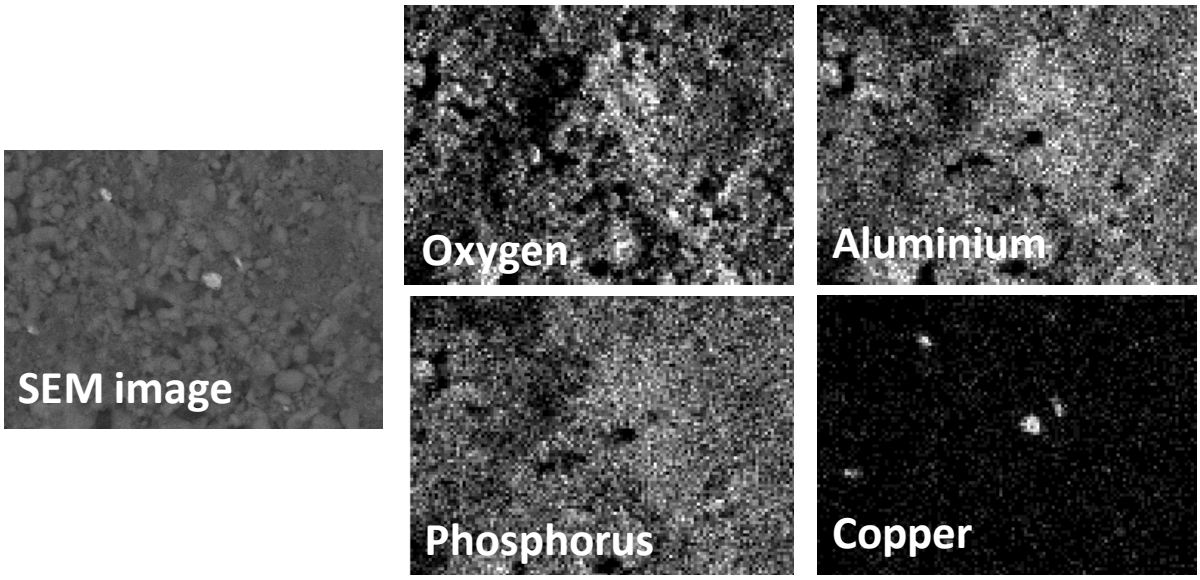

Figure 70: SEM image (left) and elements mapping for 10-CuO/AlPO catalyst.

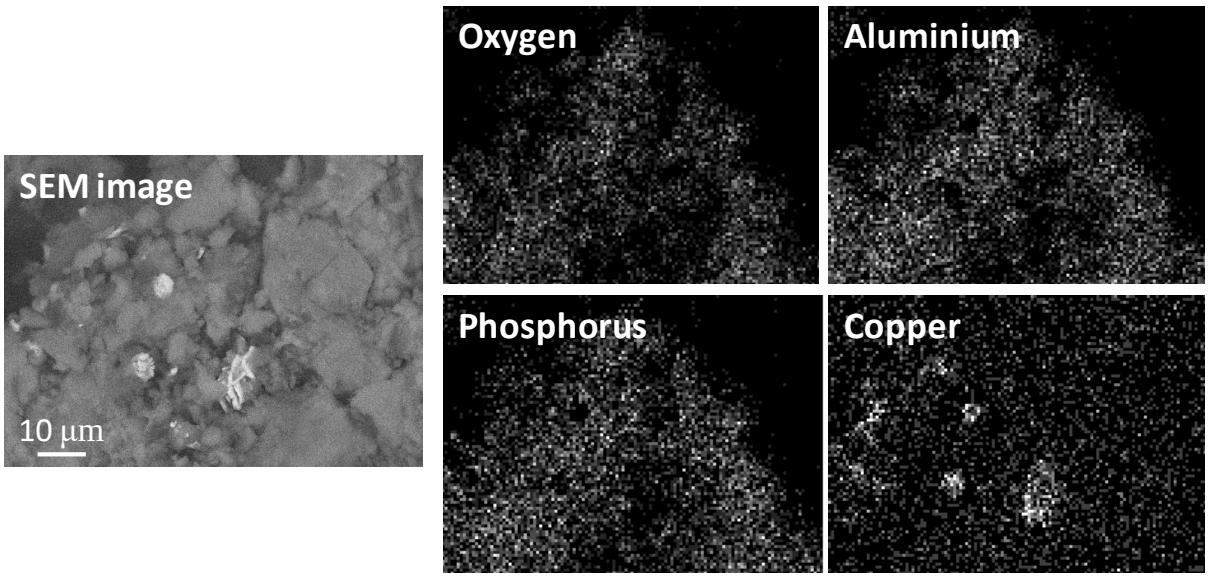

Figure 71: SEM image (left) and elements mapping for 20-CuO/AlPO catalyst.

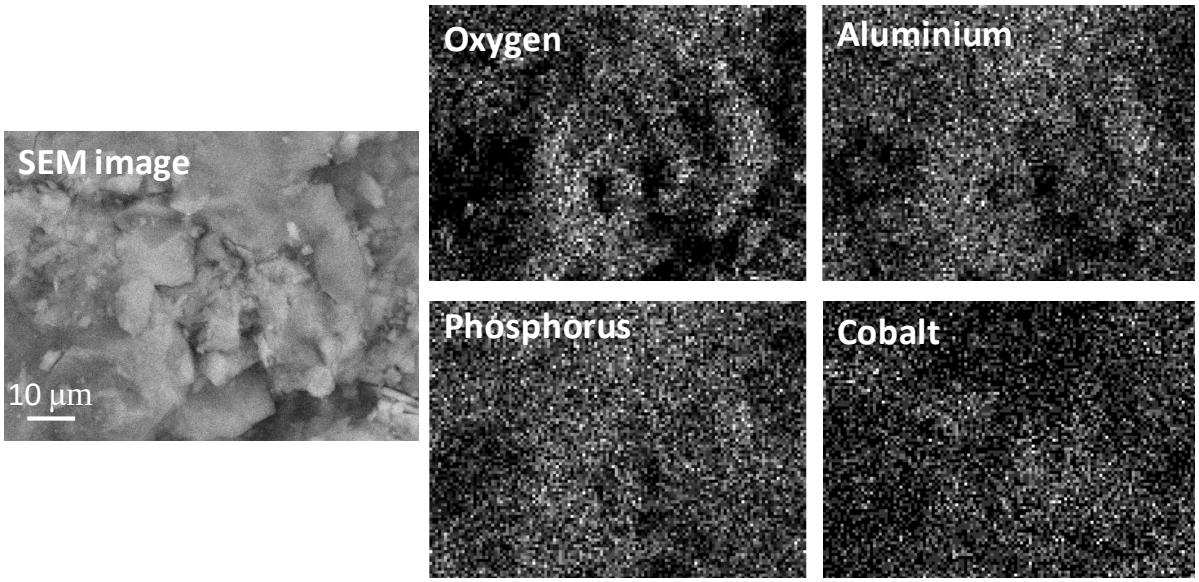

Figure 72: SEM image (left) and elements mapping of 20-CoOx/AlPO catalyst.

EDX quantitative analysis indicated a metal loading of 9% wt/wt in case of 10-CuO/AlPO and of 19% wt/wt in case of 20-CuO/AlPO.

With regards to CoO/AlPO catalysts, only the 20-CoO/AlPO sample was characterized with SEM-EDX. Also in this case, EDX analysis revealed a slight difference between the nominal and the effective Co oxide loading (19% wt/wt Co loading instead of 20%). In this case EDX mapping shows that Cobalt was well distributed on the support surface, without formation of Co-rcih aggregates.

3.3.2 Study of the reaction scheme for the anaerobic modified-Prins reaction with phosphate catalysts

As said before in the previous paragraphs, the objective of the research project was to carry out a modified-Prins reaction by contacting isobutene and methanol on a multifunctional catalyst or by carrying out the reaction in a double-bed reactor.

In both cases first dehydrogenation and then acid sites are needed. Redox sites can catalyze the transformation of methanol to formaldehyde, acid sites can facilitate the reaction of formaldehyde with isobutene.

The research work started with a screening of different classes of catalysts for the anaerobic-modified Prins reaction, with materials which theoretically possess both types of required sites; results are given in Table 6.

	T (°C)	W/F (g·s/mL)	X MeOH (%)	X i-butene (%)	Y DME (%)	Y IPE (%)
Fe_3O_4	350	0.5	92	11	0	0
CoO_x/Al_2O_3	350	0.5	87	11	53	<1
Forsterite	350	0.5	10	0	10	0
Pd^0/SAR-10	350	0.5	86	45	47	3
Hydroxyapatite	350	0.5	28	2	10	0
ZrO_2/WO_x	400	0.9	45	7	7	3
Vanadyl Pyrophosphate	300	0.9	23	<1	5	1
NbO_x/ZrO_2	400	0.5	87	2	44	<1
WVO_x	350	0.9	77	3	13	6
CuO/AlPO	300	0.9	89	4	45	9
	400		86	8	43	14

Table 6: Preliminary screening of different catalysts; best results obtained at different conditions for each catalyst are compiled. Only isoprene and dimethyl ether yields are reported, but other products, some of which unknown, were found. MeOH: methanol, i-butene: isobutene, DME: dimethyl ether, IPE: isoprene. X=conversion; Y = yield.

The catalyst that gave best isoprene yield was based on Copper oxide supported over AlPO. So, the research work started from these results; AlPO was chosen both as an acid support for the multifunctional catalysts, and as the acid bed in the double-layer catalytic bed.

We first tested the reactivity of AlPO, in order to discriminate products formed through the modified Prins reaction from those derived from other acid-catalyzed reactions.

Results are presented in Table 7.

T (°C)	X MeOH	X i-Butene	Y DME	Y IPE	Y 2-Methylbutenes
300	88	3	64	7	3
400	89	10	58	17	10

Table 7: Reagents conversions and products yields obtained by feeding 3 mol% methanol and 18 mol% isobutene over AlPO at W/F 0.9 g·s/mL..

These results surprisingly demonstrated that even with the AlPO (without Cu oxide), it is possible to obtain isoprene. This is quite unexpected because AlPO is known to be an acid catalyst, and all patent literature described in the previous chapter claim that in order to obtain isoprene from methanol and isobutene, it is necessary to combine a dehydrogenation catalyst with an acid support. But, theoretically, AlPO does not hold the dehydrogenation properties needed to carry out this transformation.

So, it was important to understand how the formation of isoprene may occur starting from methanol and isobutene with an acid catalyst.

In order to answer these questions, it is necessary to investigate on the reaction network. Therefore, we undertook a study aimed at evaluating the following aspects:

- Effect of contact time on reagents conversion and products yield distribution;
- Products distribution obtained by feeding the intermediate products;
- Product distribution obtained by feeding either methanol or isobutene only.

The study of the effect of contact time allows the identification of kinetically primary, secondary and intermediate compounds. By feeding a reaction intermediate, it is possible to understand which is the role of that compound, and which products can be formed from its transformation or decomposition. Finally, by feeding the single reagents one at a time, it is possible to infer on which compounds that reagent is transformed to.

These aspect were investigated with ZrPO and LaPO also, with the aim of understanding if this behaviour is typical of AlPO only, or if it can be considered common to other metal phosphates.

3.3.2.1 Evaluation of the reaction scheme with AlPO

In order to evaluate the reaction scheme, we carried out catalytic tests at different contact time. Detection of methane was difficult because the inert gas peak (N_2) overlapped to methane peak; the latter became visible as a shoulder on N_2 peak only when produced in sufficient amounts.

Carbon balance was always more than 90%; especially at the higher contact time, the lack in C balance was due to consecutive reactions that formed heavy compounds. The latter were detected at high elution time in the gas-chromatographic plot. Besides products, also water formed; water can be produced by different reactions, such as methanol etherification or olefins formation. The analysis of the gas-phase effluent from the reactor by means of GC-MS, allowed us to notice also the formation of 1,1-dimethylcyclopropane, albeit in small amount. This is a key intermediate of the reaction; its formation will be discussed in the next section.

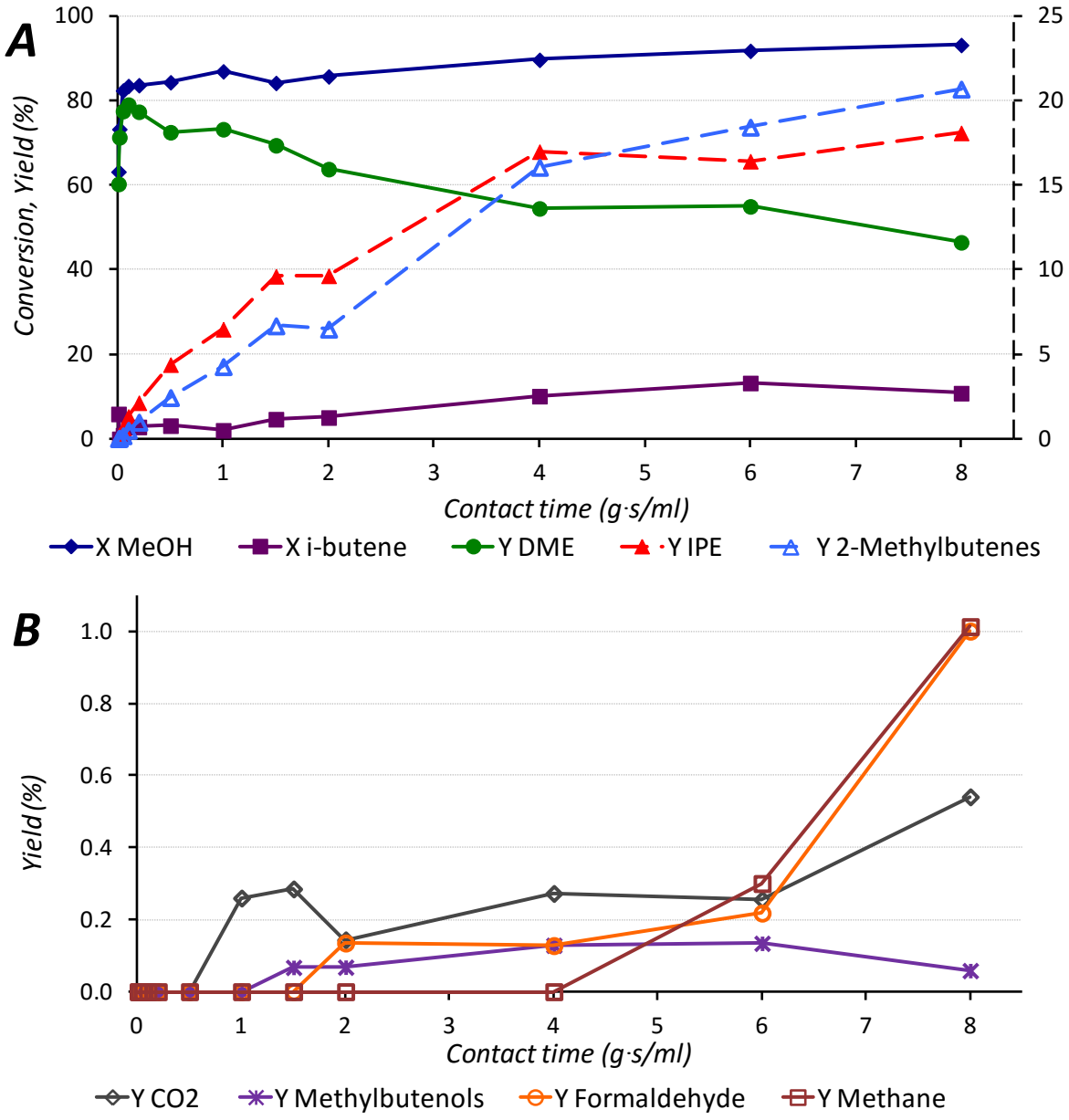

Figure 73: Reaction between 3% methanol and 18% isobutene in N_2 at 400°C with AlPO. Effect of contact time on reagents conversions and products yields. Low-yield products are plotted in graph B with a different scale. Isoprene and 2-methylbutenes yields are referred to the secondary Y axis in graph A.

Data shown in Figure 73 allowed us to conclude that:

- Methanol converted very rapidly reaching a plateau of ca 85% conversion, which started at 0.2 g·s/mL;
- The principal product was dimethyl ether (DME); it derived from the acid-catalyzed etherification of methanol. Its yield showed a profile typical of both a primary and intermediate compound: primary product its production started immediately, along with the consumption of methanol; intermediate because it showed a profile with a maximum, meaning that it started to be consumed either because it was transformed into some other consecutive compound by means of a slow reaction, or because etherification reached equilibrium, and the slow transformation methanol to

compounds other tna DME continuously shifted the equilibrium back to methanol with a corresponding decrease of DME yield.

- Besides DME, also isoprene and 2-methylbutenes showed behaviours which are typical of kinetically primary products.
- All the other products showed a yield profile which is typical of consecutive reaction products: CO_2 and methane, which can derive from C_1 decomposition (see later in the thesis), formaldehyde and 2-methylbutenols. According to reaction schemes shown in Figure 65-B and in Figure 60, the two latter products should be intermediate compounds of the Prins reaction.

However, the unexpected result was that isoprene showed a behaviour which is typical of a kinetically primary product. In fact, it should form as a consecutive compound from both formaldehyde and 2-methylbutenols, whereas it looked like as being formed before them, which is the opposite of the reaction scheme shown in Figure 65-B. Moreover, formaldehyde appeared as being a kinetically secondary (consecutive) compound with respect to 2-methylbutenols, whereas the latter should form by reaction between isobutene and formaldehyde. All these discrepancies can be explained by making the hypothesis that formaldehyde and 2-methylbutenols form through a consecutive decomposition reaction which involves isoprene, via an "inverse Prins" reaction. On the other hand, isoprene would form through a route different from that one conventionally accepted for the Prins reaction, i.e., the reaction between isobutene and formaldehyde.

Moreover, if formaldehyde were the key intermediate, isoprene should form as a kinetically secondary product and in a larger amount than 2-methylbutenes. Conversely, results showed that 2-methylbutenes and isoprene were produced in similar yields; this indicates the presence of a parallel reaction which involves methanol (and not formaldehyde) and isobutene, which leads to either isoprene or 2-methylbutenes with similar reaction rates.

In order to better understand the reaction scheme, isoprene was fed together with water to the catalytic bed, at 400°C and W/F 2.0 g·s/mL; results are shown in Table 8.

X IPE	Y i-butene	Y CH_2O	Y MeOH	Y MIPK	Y 2-Methylbutenes
39%	9%	<1%	<1%	2%	7%

Table 8: Isoprene conversion and products yield with AlPO at 400°C and 2.0 g·s/mL. MIPK: methyl-isopropyl ketone.

Isoprene could not be fed using the syringe pump, because of its high volatility; so, it was fed by bubbling the inert gas into a sealed flask containing the diolefin and maintained at -20°C. Water was fed through the syringe pump.

Results obtained in Table 8 show that indeed isoprene can undergo a consecutive reaction to form other products. There was a lack in the carbon balance close to 18%, due to heavy compounds deposition on the catalyst; in fact, the latter was black at the end of the test.

It is important to highlight that isoprene can transform into both isobutene and formaldehyde, which are the reactants from which isoprene can be obtained through the Prins reaction. This means that isoprene, in the presence of water, may give a retro-Prins reaction, which leads back to the formation of formaldehyde and isobutene. The two compounds were not produced in a 1:1 stoichiometry, because formaldehyde was rapidly converted into other compounds, due to its high reactivity, while isobutene was a much more stable compound.

Another proof of the occurrence of the retro-Prins reaction is given by the formation of methylisopropyl ketone; in fact the latter can form through rearrangement of 2-methylbuten-1-ol, which forms by isoprene hydration; indeed, the latter reaction is the first step of the retro-Prins reaction.

Concluding, the reaction of isoprene decomposition can be summarized as follows: during the first step, isoprene is hydrated to 2-methylbutenols, which then decompose to formaldehyde and isobutene or rearrange to the ketone as shown in Figure 74.

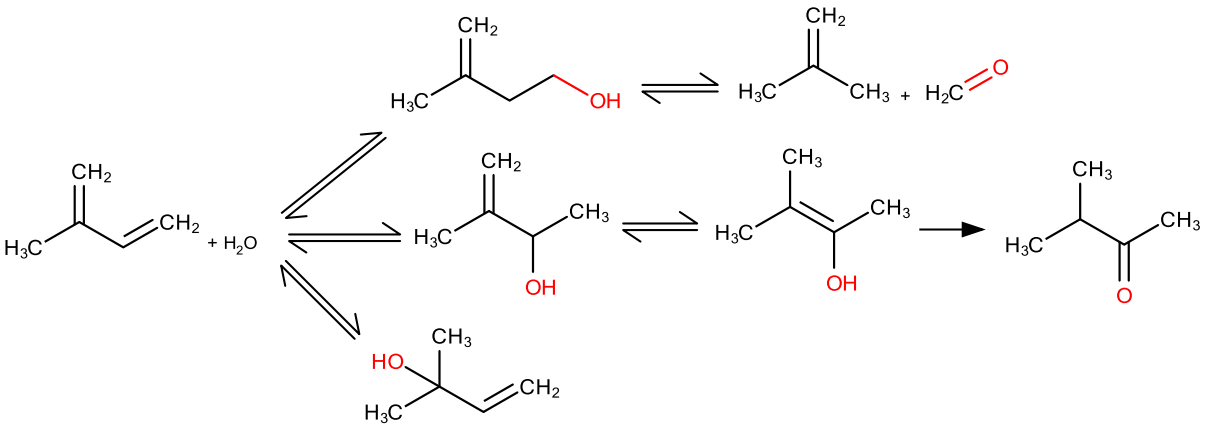

Figure 74: isoprene decomposition through hydration and retro-Prins reaction.

Results shown in Figure 73, which demonstrate that isoprene is a primary product with respect to both formaldehyde and 2-methylbutenes, can be explained by taking into account isoprene decomposition, as shown in Figure 74: first isoprene forms by reaction between isobutene and methanol, later on it is decomposed via the retro-Prins reaction.

Moreover, Table 8 shows that isoprene can also be transformed into 2-methylbutenes. This reaction needs an hydrogen transfer to saturate one of the two double bonds. Hydrogen can be furnished either from coke formation or, in case of methanol and isobutene feed, by the stoichiometry of isoprene formation, as shown in Figure 75. However, it is possible that indeed no free hydrogen was formed, and that it was exchanged directly between the two molecules by means of an intermolecular concerted mechanism.

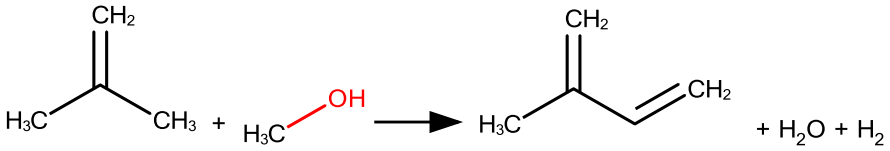

Figure 75: Balanced reaction of isoprene formation from methanol and isobutene

Finally, we investigated the role of DME in the reaction scheme. Actually DME showed a behaviour typical of and intermediate product, but from results shown in Figure 73 it is not clear if this behaviour was due to the shift of equilibrium for DME formation back to methanol at high contact time, or to a direct consecutive reaction occurring on DME itself. Elucidation on this issue was achieved by reacting together DME and isobutene at different contact times on AlPO; results are shown in Figure 76.

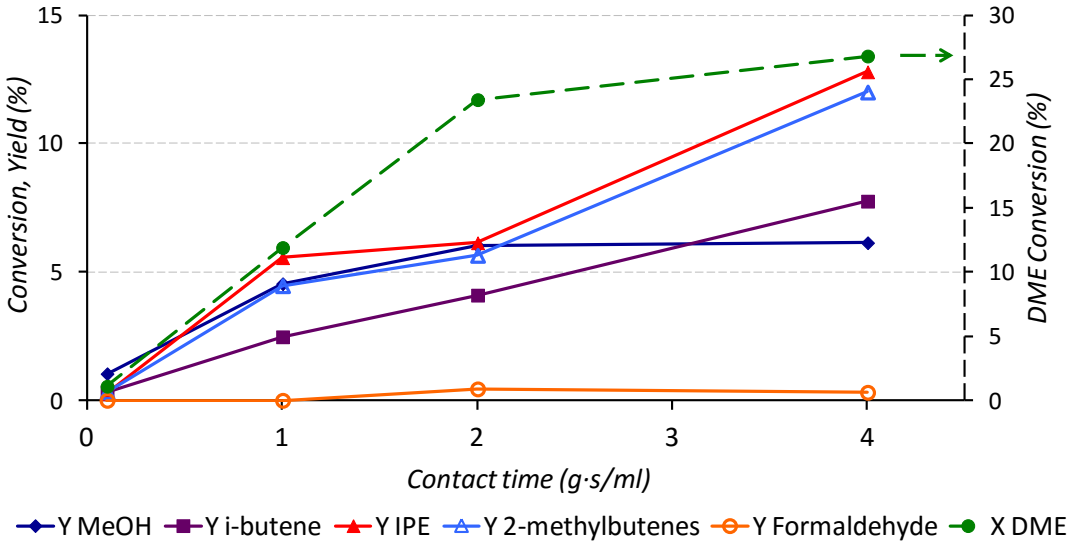

Figure 76: Reaction between 1.5% dimethyl ether and 18% isobutene at 400°C with AlPO. Effect of W/F ratio on reagents conversions and products yields; DME conversion is given in the secondary Y axis.

As it is possible to see, methanol was a kinetically primary product. One might believe that this is a proof of DME hydrolysis to methanol, thus putting a fundamental role on methanol as the reactant for isoprene formation. However, there are some evidences against this hypothesis: (a) when DME was made react with isobutene, both isoprene and 2-methylbutenes were, again, kinetically primary products. This means that DME directly reacted with isobutene to give the above mentioned products, while methanol showed a primary product behaviour because was co-produced in this reaction as exiting group. (b) hydrolysis of DME clearly requires water, which instead was not co-fed during experiments shown in Figure 23.

Moreover, it is possible to see that iso-C_5 olefins yields distribution was similar to that one obtained in the reaction between methanol and isobutene. This further supports the idea that DME is the key intermediate in the reaction, directly reacting with isobutene to give isoprene and 2-methylbutenes. Its behaviour, typical of an intermediate product in the case

of the methanol-isobutene reaction (Figure 73), it was mainly due to this direct reaction and in minor part only to DME hydrolysis to methanol.

Moreover from results shown in Figure 76 it is also possible to see that DME highly contributed to C_5 iso-olefins formation; in fact selectivity to these compounds was close to 90% at the lower contact time. On the other hand, when methanol was fed with isobutene, the principal product was DME, and iso-C_5 olefins reached only 15% maximum selectivity at 6 g·s/mL W/F. This means that both isoprene and 2-methylbutenes were mainly formed through the reaction between DME and isobutene. On the other hand, results in Figure 76 show that DME is not very reactive, in fact its conversion was low. This indicates that the rate-determining step for iso-C_5 formation from methanol and isobutene was the reaction between isobutene and DME, while methanol etherification was very fast. Finally, despite DME appeared to be the key intermediate, it is not possible to exclude that a partial contribution to iso-C_5 olefins formation derived by methanol. In fact, when methanol was fed, both isoprene and 2-methylbutenes yields were slightly higher compared to the test carried out by feeding DME and isobutene.

An overall reaction scheme, as inferred from catalytic tests described above, is given in Figure 77; as it will be seen in the next chapter, this scheme was valid for all the metal phosphates tested. In summary, even though methanol can directly react with isobutene to give isoprene and 2-methylbutenes, the largely prevailing product of methanol transformation was DME; the latter reacted with isobutene to yield both isoprene and 2-methylbutenes; this reaction, albeit slow compared to etherification, was more likely than the direct reaction of isobutene with methanol.

Isoprene can undergo different consecutive reactions, but these did not appear to be very important, because isoprene was a stable compound; however, they are important in the aim of understanding the role of each product in the reaction scheme. First, isoprene can be transformed into 2-methylbutenes, either through hydrogenation or, more likely, through direct H-transfer from another molecule. Isoprene can also undergo hydration to 2-methylbutenols; the latter can rearrange into methylisopropyl ketone or further decompose through a retro-Prins reaction to yield formaldehyde and isobutene. Formaldehyde can decompose to methane and CO_2; however, as will be shown later, the latter also might form though methanol thermal decomposition; this reaction might explain why CO_2 formed before formaldehyde in the kinetically consecutive reaction scheme.

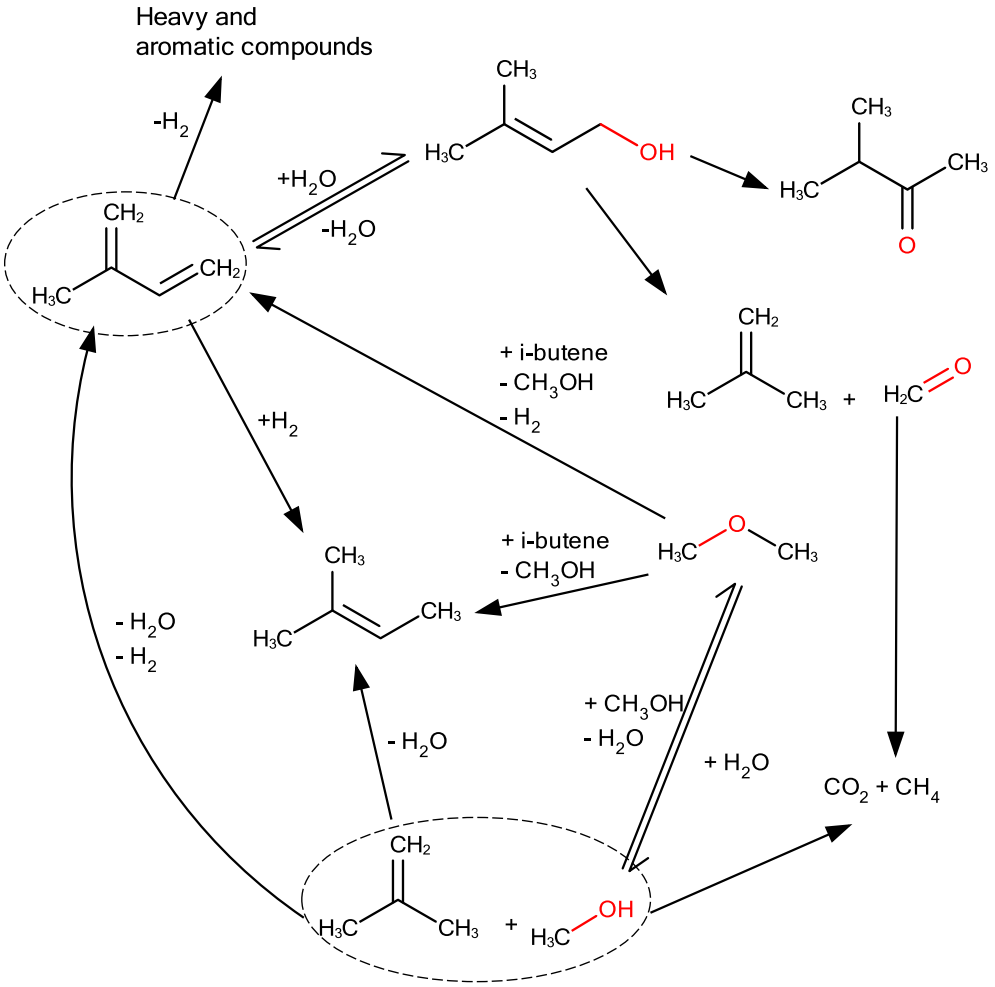

Figure 77: reaction scheme of methanol-isobutene coupling over phosphate catalysts. With regard to 2-methylbutenes and 2-methylbutenols, for each class of products only one of the three possible isomers is shown. Formation of methylisopropyl ketone occurred from 2-methyl-2-buten-3-ol.

3.3.2.2 Comparison between AlPO, ZrPO and LaPO

ZrPO and LaPO were tested under the same conditions as for AlPO, in order to determine if the mechanism described in the previous paragraph is typical of AlPO only or it can be extended to other phosphates as well. Figure 78 and Figure 79 show a comparison of the results obtained by feeding either methanol or DME, respectively, with isobutene at 400°C with ZrPO and AlPO. Figure 80 shows results obtained by feeding either methanol or DME and isobutene over LaPO at 300°C; with this latter catalyst fewer experiments were carried out.

Table 9 shows a comparison between AlPO and LaPO when isoprene was used as the reactant. Results indicate that all phosphates showed a similar behaviour. Therefore, all considerations discussed in the previous paragraph can be applied also in the case of LaPO and ZrPO.

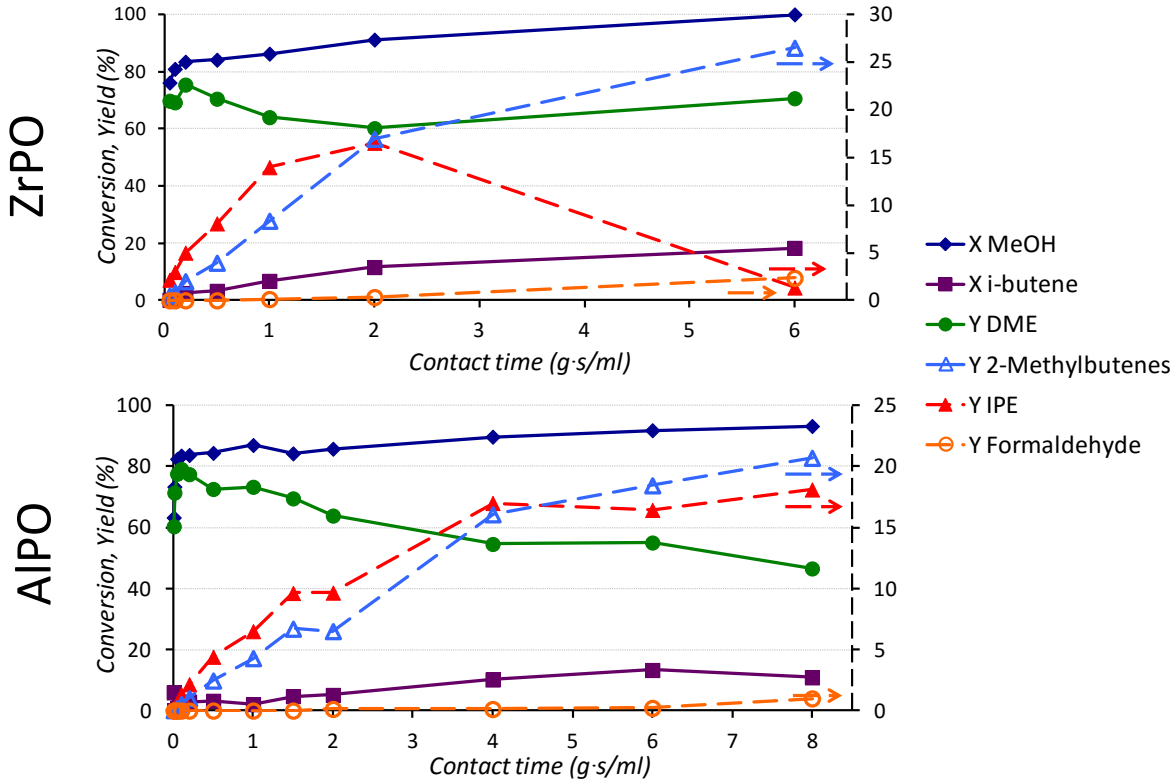

Figure 78: Reaction between 3% methanol and 18% isobutene in N_2 at 400°C with ZrPO (top), and AlPO (bottom). Effect of W/F ratio on reagents conversions and products yields. Dashed lines are referred to the secondary Y axis.

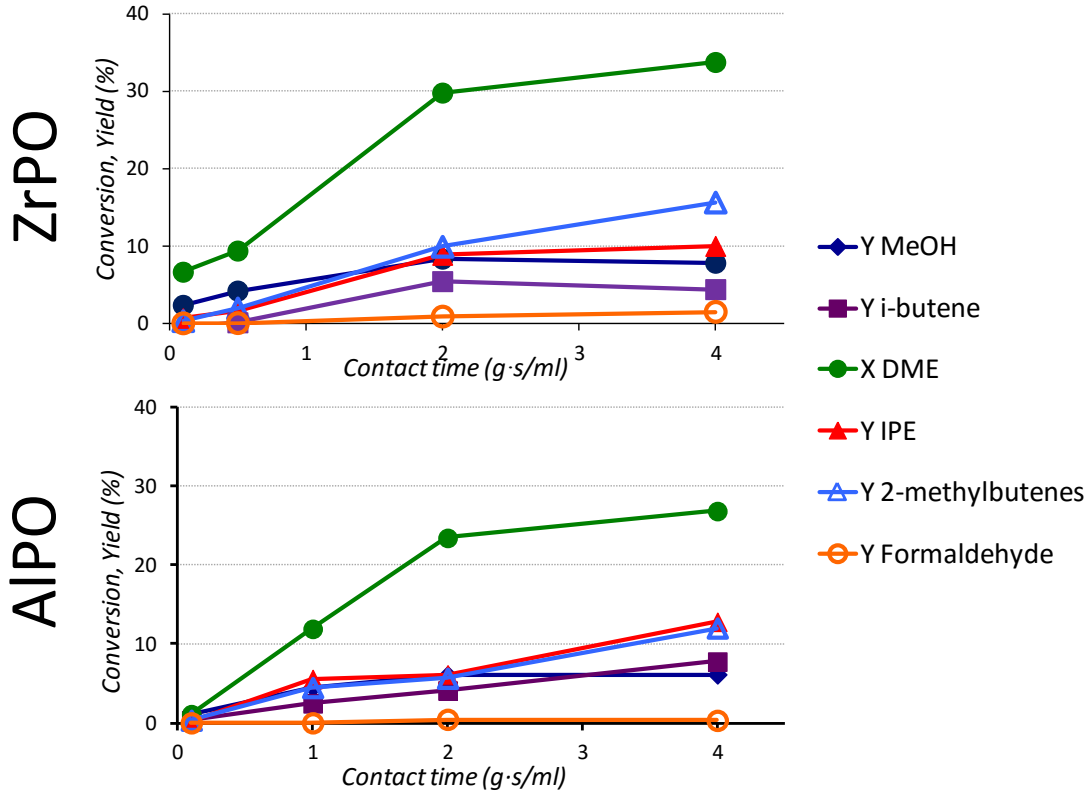

Figure 79: Reaction between 1.5% DME and 18% isobutene at 400°C with ZrPO (top), and AlPO (bottom). Effect of W/F ratio on reagents conversions and products yields on ZrPO (top) and AlPO (bottom). Dashed lines are referred to the secondary Y axis.

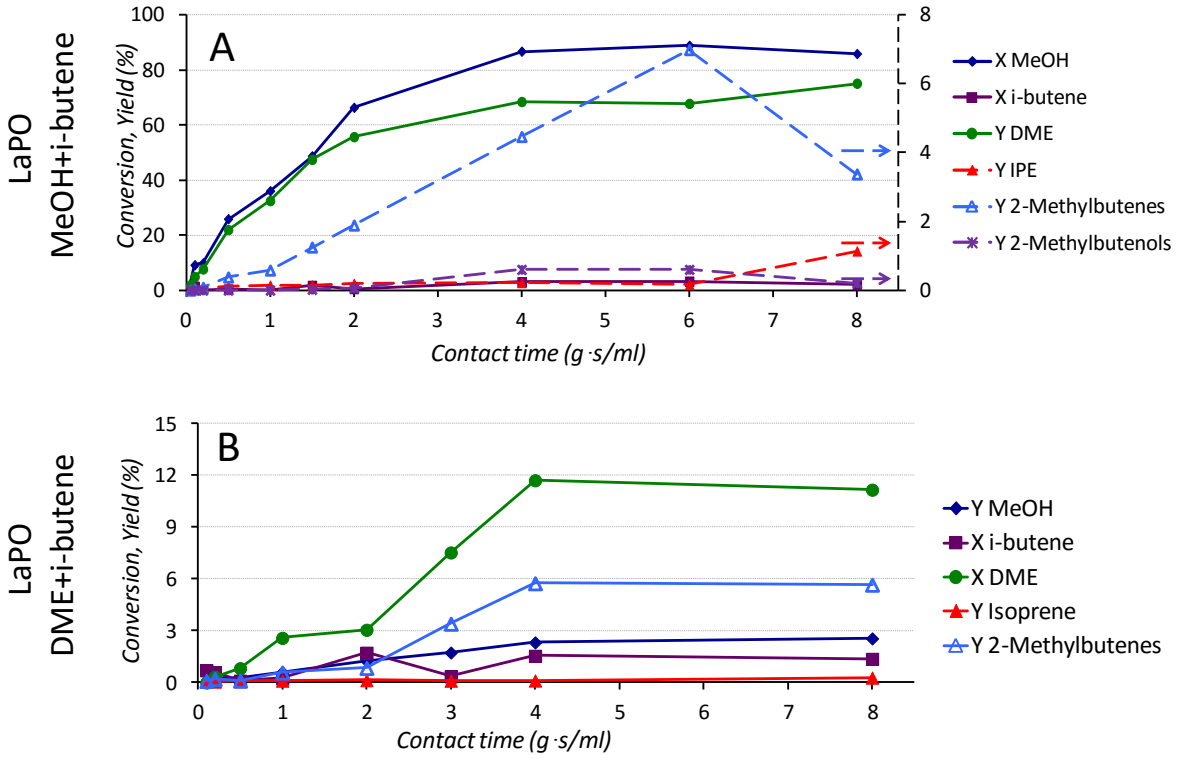

Figure 80: Reaction between 3% methanol (top) or 1.5% DME (bottom) and 18% isobutene in N_2 at 300°C with LaPO. Effect of W/F ratio on reagents conversions and products yields. Dashed lines are referred to the secondary Y axis.

	X IPE	Y i-butene	Y CH_2O	Y MeOH	Y 2-Methylbutenes
AlPO	39%	9%	<1%	<1%	7%
LaPO	53%	8%	<1%	1%	35%

Table 9: Isoprene conversion and products yield with AlPO and LaPO at 400°C and W/F 2.0 g·s/mL.

Also with ZrPO and LaPO, isoprene, 2-methylbutenes and DME were kinetically primary products, whereas 2-methylbutenols were secondary compounds. CO_2, methane and formaldehyde were detected also with ZrPO starting from W/F equal to 1.0 g·s/mL, however with yield <1%.

Again, DME played an active role in all cases; as shown in Figure 79 and Figure 80 (bottom), it reacted with isobutene to give isoprene and 2-methylbutenes, with co-production of methanol. Because of this, one might believe that similar yields of C_5 products and methanol were produced, but this was not the case, because methanol could be converted to both DME through etherification and C_5 products.

However some important differences amongst the three metal phosphates can be seen.

In the case of ZrPO, the main difference regards isoprene yield. When the reaction was carried out over AlPO, isoprene yield showed a constant increasing trend in function of contact time, and reached a plateau of 17% starting from 4 g·s/mL. In the case of ZrPO, instead, isoprene clearly showed a behaviour which is typical of intermediate compounds, in fact it reached 16% yield at W/F 2.0 g·s/mL , and then it declined down to 2% at 6.0 g·s/mL.

As described before for AlPO, isoprene can undergo different consecutive reactions; the most important were retro-Prins (via hydration) and hydrogenation (or H-transfer) to 2-methylbutenes. In this case, a slight increase of formaldehyde yield was observed, derived from the aforementioned consecutive reaction occurring on isoprene, but the more remarkable increase was observed for 2-methylbutenols yield. In fact, the latter increased from 16% at W/F 2.0 g·s/mL until 27% at 6.0 g·s/mL. This difference corresponds to the decrease of isoprene yield. This means that ZrPO was more efficient in the transformation of isoprene to 2-methylbutenes; however, this reaction required high contact time because it was a consecutive reaction. When DME was fed instead of methanol over ZrPO, a products distribution and reagent conversion similar to AlPO was shown; in this case, a slight difference in isoprene yield at W/F 4.0 g·s/mL between AlPO and ZrPO was registered, which again can be related to the above mentioned consecutive reactions. Anyway, the comparison of AlPO and ZrPO showed that these two catalysts performed similarly, and that similar results were obtained until W/F 4.0 g·s/mL.

Since the reaction scheme was the same at 300°C and 400°C (see paragraph 3.3.2.5), it is possible to compare results obtained with LaPO with results obtained with the other two phosphates.

When methanol and isobutene were fed over LaPO, isoprene yield was significantly lower, whereas 2-methylbutenes were produced with higher yields compared to the other two phosphates. Moreover DME yield was lower with LaPO, that may indicate that the latter is more rapidly converted into 2-methylbutenes. Finally, with LaPO DME was transformed into 2-methylbutenes with a yield close to that one obtained when methanol was co-fed with isobutene.

DME showed to be an intermediate in the reaction of 2-methylbutenes formation; in fact it was produced with high yields until W/F 1.0 g·s/mL, but then it was rapidly consumed, with a parallel increase in 2-methylbutenes yield.

Results shown in Table 9 might suggest that 2-methylbutenes derive mainly from isoprene; in fact a large amount of isoprene was converted to these products over LaPO. However, products distributions shown in Figure 78 and Figure 79 do not support the hypothesis that isoprene was an intermediate for 2-methylbutenes; moreover the latter were kinetically primary products, as it was isoprene. Therefore, isoprene transformation to 2-methylbutenes may occur over LaPO at a greater extent than with AlPO; however, because of isoprene low yield and low concentration at the adsorbed state, the contribution of this reaction was likely marginal, and the majority of 2-methylbutenes derived from the direct reaction between DME and isobutene.

These data confirm that DME was the key intermediate.

The reaction scheme in Figure 77 can be generalized for the three phosphates used, but some differences can be noticed.

In fact, LaPO showed to be slightly more selective to 2-methylbutenes (which are undesired products) than to isoprene, whereas the two compounds formed with similar yields with AlPO and ZrPO; with ZrPO, at high W/F, the consecutive reaction of isoprene transformation to 2-methylbutenes took place, with a strong impact on products distribution.

3.3.2.3 Insights on methanol-isobutene coupling over phosphate catalysts and mechanistic hypothesis

The mechanism of reaction between methanol (or DME) with an olefin (isobutene in this case) is generally believed to pass through the formation of formaldehyde, but data obtained with our metal phosphates catalysts, discussed in the previous paragraphs, demonstrate that this was not the case, because of the following reasons:

- Isoprene was a kinetically primary product, whereas formaldehyde was a secondary product;
- If formaldehyde were the key intermediate, we should obtain much higher yield to isoprene than to 2-methylbutenes; actually, these two products showed similar yields.

All results reported strongly suggest that isoprene and 2-methylbutenes probably shared a common intermediate or transition state, which can evolve towards different products depending on the catalyst type used.

In order to obtain more information on methanol reactivity, we carried out some tests by feeding methanol only over the three metal phosphates, while varying the W/F ratio. Since nitrogen peak can overlap some of the peaks (mainly methane) during the GC analysis, we chose to carry out these experiments using He as the ballast gas. This allowed us to avoid any interfering signal during the analysis because He was also the carrier gas in the GC. When methanol was fed to the reactor at 400°C, the main product was DME, with minor formation of other products: methane, formaldehyde, CO_2 and hydrocarbons such as ethylene and propylene. These latter products were formed in a very low amount, therefore it was difficult for us to determine their precise yield. From results shown in Figure 81, it is possible to see that methanol can undergo thermal decomposition to formaldehyde, methane and CO_2; in fact these compounds formed even in the absence of catalyst (W/F 0.0 g·s/mL). Then formaldehyde started to be consumed, probably because of catalyst acidity. These data confirm that the three catalysts were not able to dehydrogenate methanol to formaldehyde; in fact, in the latter case formaldehyde formation should increase in the presence of the catalyst, but this indeed was not the case. Worth of noting, formaldehyde was not detected at low contact time when isobutene also was fed to the reactor and in the presence of the phosphate catalyst, probably because the tiny amount of formaldehyde

produced by thermal decomposition of methanol quickly reacted to yield isoprene through the Prins reaction. However, this contribution to the overall isoprene yield was negligible, in fact "thermal" formaldehyde was produced with a yield one order of magnitude lower than that of isoprene.

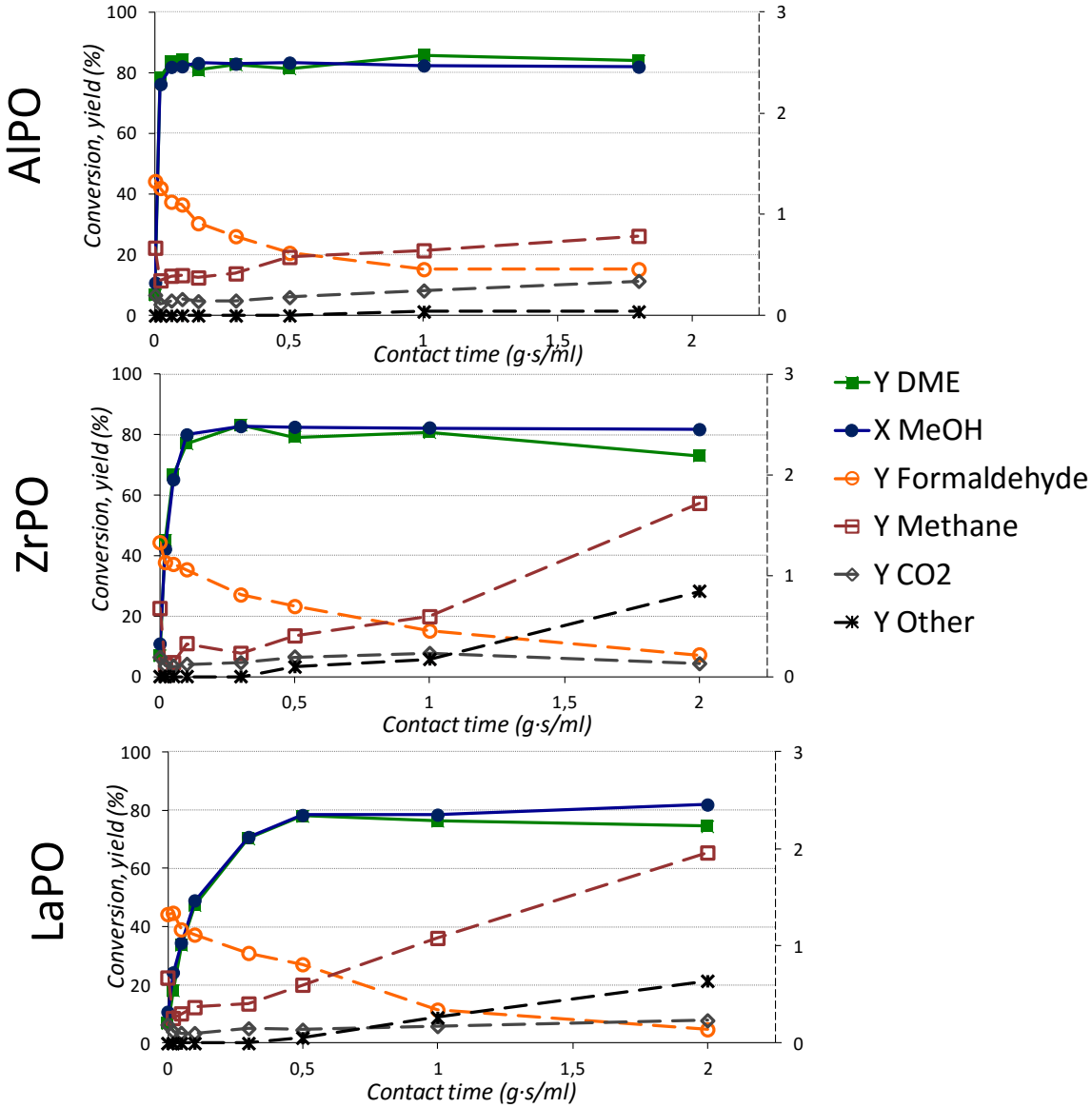

Figure 81: Reactivity of methanol at 400°C and different W/F ratio over AlPO (top), ZrPO (center) and LaPO (bottom). Dashed lines are referred to secondary Y axis. The result at 0.0 g·s/mL was obtained using the empty reactor, with no catalyst.

Going back to results shown in Figure 81, the same phenomena were observed with the three catalysts, specifically:

- Formaldehyde was consumed;
- CO_2 yield was constant throughout the entire range of increasing W/F (it can derive directly from methanol decomposition[126]);
- Both methane and ethylene and propylene (other – black line) yield increased when the W/F ratio was increased.

However, the rate of at which yields varied was different depending on the catalyst type.

The most important products, which can add important information on the mechanism of reaction, were methane, ethylene and propylene.

In fact similar reactions, leading to the formation of olefins from methanol, are known to occur in the case of the MTO process[126, 127, 128]. One of the most accepted hypothesis is that this reaction proceeds through the formation of a carbene species[129], which is a neutral $:CH_2$ with a free electron pair. This species was never isolated in this form, because it is very reactive and acts as a strong electron acceptor in order to reach a stable configuration. Indeed, some authors already hypothesized the formation of iso-C_5 olefins from methanol and isobutene coupling through carbene formation[130, 131].

One key result that confirms the possible formation of a carbene as the highly reactive intermediate is the formation of hydrocarbons observed when methanol alone was fed on the phosphate catalysts. As in the MTO process[127, 128, 126], in fact, we noticed the formation of methane, ethene and propene, that increased along with the W/F ratio. Obviously they formed in very little amount, because these phosphates do not possess the proper acidity requirements needed for a good MTO catalyst, but this was anyway a good proof for the presence of a carbene mechanism. Moreover another strong proof derives from the detection of 1,1-dimethylcyclopropane when methanol and isobutene were co-fed (see paragraph regarding AlPO); in fact, as is possible to see later in the paragraph, cyclopropane derives from the reaction between a carbene species and a C-C double bond.

Carbene formation can provide a good explanation for methanol behavior shown in Figure 81: if we assume that formaldehyde was transformed into heavy compounds because of catalyst acidy (indeed the catalyst appeared greyish at the end of the test), the formation of hydrogen is also likely, which could interact with carbene to form methane. In fact, as seen from Figure 80, the more formaldehyde was consumed, the more methane formed, and this agrees with the previous assumption.

Concluding, the model involving carbene formation can be assumed to be valid also in the case of methanol/DME-isobutene coupling over phosphate catalysts: carbene can be the common active specie that forms from either methanol or DME, and reacts with isobutene to give isoprene or 2-methylbutene, as detailed in Figure 28.

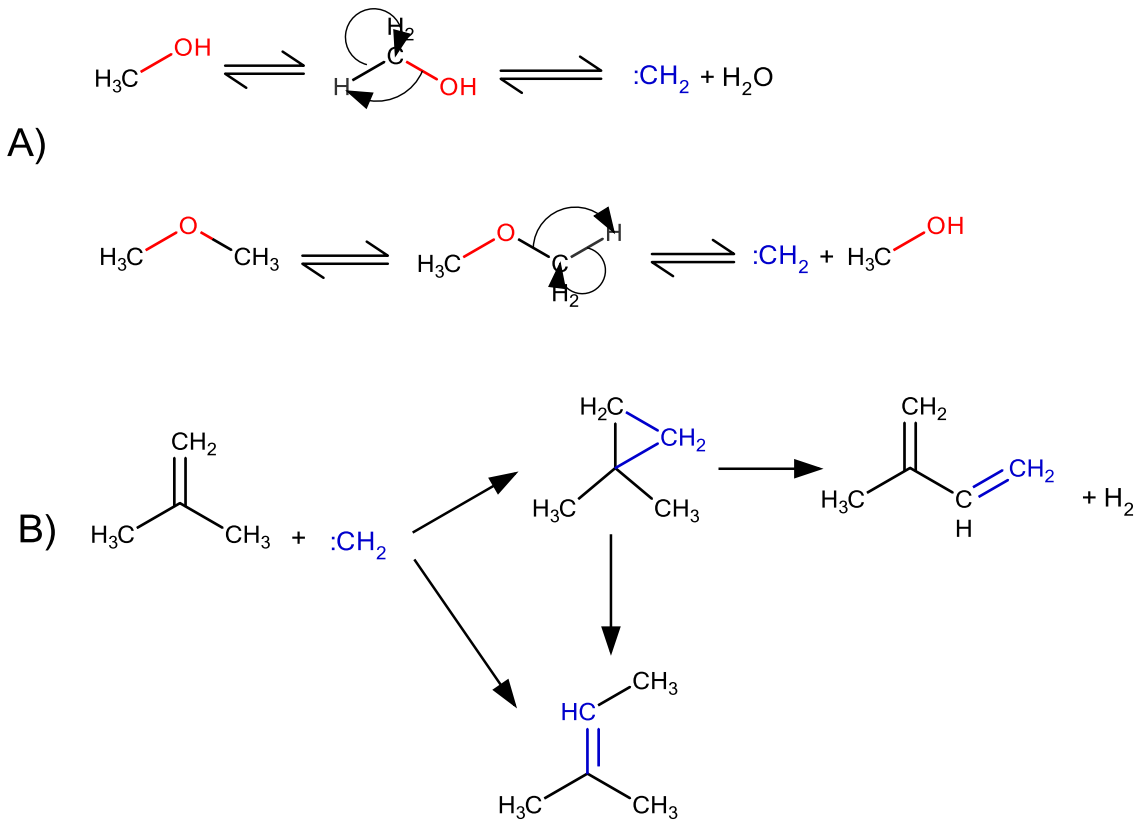

Figure 82: Formation of carbene from methanol or DME (A) and its interaction with isobutene to give 2-methylbutenes and isoprene (B).

As shown in Figure 82, carbene can form from methanol (or DME) dehydration (or de-methanolation)[130]. Carbene is a strong electron acceptor and unstable specie, so it prefers to be transformed back to the reagent, but if an electron donor is present, $:CH_2$ can react and give olefinic products. When only methanol is fed to the catalyst, carbene is formed as well, but it does not find any molecule which can act as an acceptor. In this case, olefin formation is given only by the coupling of two or more carbene species, but this is a rare event because of the dilution of the reagents; therefore the amount of olefins produced is low. Conversely, when methanol (or DME) is co-fed with isobutene, the latter can act as a carbene acceptor and the yield of olefins increases because of this interaction, which shifts the equilibrium towards the formation of more carbene finally generating more C_5 products. As reported in Figure 79 and Figure 82, products deriving from the coupling between isobutene and carbene are 2-methylbutenes and isoprene.

Carbene interaction with isobutene can proceed through C-H or C-C insertion[132]; if C-H insertion occurs, the result is a chain elongation by one C atom; this insertion can occur only on terminal C-H bonds of isobutene because the tertiary carbon atom, sharing the double bond with the terminal C atom, is not bonded to any hydrogen atom. The interaction between carbene and one of the C-H bond leads to the direct formation of 2-methylbutenes.

The other possible reaction between carbene and isobutene can occur on a C-C bond. This event is more probable than C-H bond insertion, because of three main reasons:

- The double C-C bond is more reactive than the single C-H bond;
- The carbene is also an electron acceptor[132] and the electron-richest species present in the reaction environment is the isobutene double bond;
- The carbene shows a sp^2 hybridization with one sp^2 and one p orbital which can be occupied by the lone pair. This configuration can easily overlap the π bond[132] of isobutene.

Insertion of carbene on the C=C bond leads to iso-C_5 olefins through the formation of an intermediate which is 1,1-dimethylcyclopropane. The latter is known to thermally decompose to 2-methylbutenes[133, 134], but in the presence of a suitable catalyst the C-H bond of this molecule[130, 135] can be activated and it can be decomposed to isoprene. So, in our case, once 1,1-dimethylcyclopropane is formed, it can decompose by means of a non-catalytic reaction to form 2-methylbutenes, but on the other hand its decomposition can be also catalyzed through the activation of one C-H bond, and in this case isoprene is formed. These possible mechanisms are schematized in Figure 83.

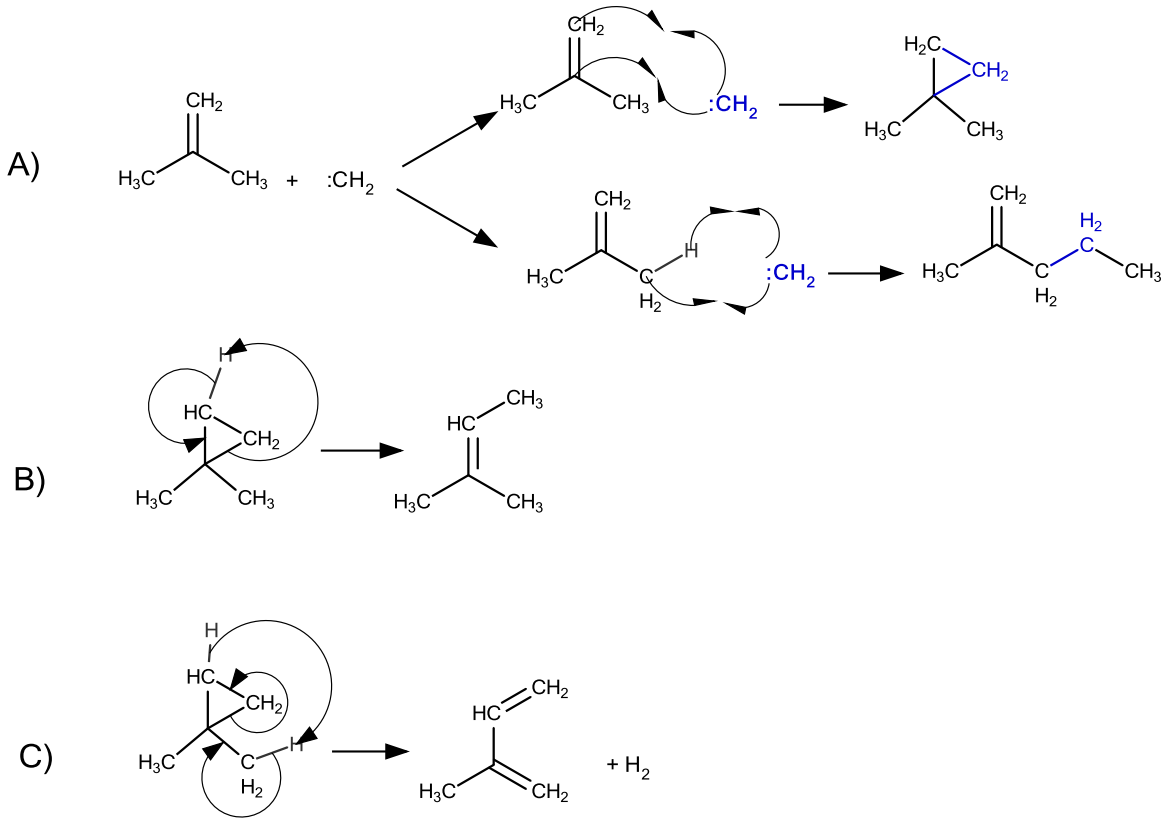

Figure 83: Possible mechanisms of formation of isoprene and 2-methylbutenes by interaction of carbene with isobutene (A) and possible rearrangement of 1,1-dimethylcyclopropane to 2-methylbutenes (B) and to isoprene (C) .

Therefore the formation of iso-C_5 olefins can derive from different reaction pathways:

- 2-methylbutenes can form either from carbene insertion in isobutene C-H terminal bond, or from thermal decomposition of the intermediate formed by carbene insertion on the C-C double bond.
- Isoprene can form from carbene interaction with isobutene C-C double bond and the successive catalyzed decomposition of the intermediate, with co-production of hydrogen.

According to the classic organic chemistry, carbene interacts more easily with the C-C double bond than with C-H, both because of the reactivity of π bonds and because of similar molecular orbital configurations. In our case this can be assumed as being true, but it needs to be confirmed by DFT calculations.

In any case, if the hypothesis put forward is true, the rates of 2-methylbutenes and isoprene formation should depend on the competition between thermal and catalytic decomposition of 1,1-dimethylcyclopropane.

This can explain the different behaviours seen with AlPO, ZrPO and LaPO: with the three catalysts, carbene formation occurs because of catalyst acidity, and carbene then interacts with isobutene to form 1,1-dimethylcyclopropane. In the presence of LaPO, however, it is possible that the intermediate is simply desorbed and then thermally decomposed to 2-methylbutenes, whereas isoprene is produced only in minor amount through catalyzed decomposition.

Conversely, AlPO and ZrPO are more efficient in catalyzing 1,1-dimethylcyclopropane decomposition to isoprene and hydrogen; however this pathway still competes with thermal decomposition, which leads anyway to the formation of 2-methylbutenes.

Differences and similarities in products distribution can be explained by taking into account the nature of active species: all of the three phosphates are acid, probably because of the presence of –OH groups at the surface, and catalyze both the etherification of methanol and the formation of the carbene species. However, differences in 2-methylpentenes and isoprene yields obtained was probably attributable to the different degree of covalency/ionicity of bonds involved in methanol activation.

LaPO is characterized by more ionic bonds because of the scarce overlap between La and phosphate orbitals. In fact, La orbitals have very different energy compared to P and O orbitals.

On the other hand, AlPO and ZrPO can establish bonds having a partial covalent character, in fact they feature respectively p and d orbitals at an energy level that is similar to that one of phosphate. A greater covalent character of the bonds allows the formation of empty antibonding orbitals, which allow an easier interaction between the catalyst and the absorbed molecules, thus developing, for instance, a stronger interaction with 1,1-

dimethylcyclopropane and hence a more facilitated formation of isoprene. This interaction is less strong in case of LaPO because of the more ionic nature of the bonds involved.

Another possibility is that, at the temperature at which the reaction is carried out, carbene insertion in the C-H bond competes with insertion in C=C; in this case it is possible to formulate an alternative hypothesis. As explained above, carbene insertion in C-H bond leads to the formation of 2-methylbutenes, whereas insertion in C=C leads to an intermediate species which can evolve either to isoprene or 2-methylbutenes.

This can explain why over LaPO yield to isoprene was lower than that obtained with the other phosphates.

On the other hand, ZrPO and AlPO are active in facilitating carbene insertion into the C=C bond, with formation of 1,1-dimethylcyclopropane. The latter can desorb and thermally decompose to 2-methylbutenes or can further undergo catalytic decomposition to isoprene and hydrogen. These two pathways are competitive and, over these two catalysts, lead in the end to the formation of both C_5 olefins.

Anyway, it is not possible to discriminate between the different hypothesis formulated on the basis of catalytic tests only; however, even though the formation of main products can be explained in different ways, however all the hypothesis take into account carbene as the key intermediate species. Carbene formation is well supported both by literature data[130] and by catalytic tests carried out over the three phosphates. Some DFT calculation are however needed in order to discriminate between the different hypothesis.

3.3.2.4 Spent catalysts characterization

Despite the catalysts employed did not show any deactivation during time-on-stream (about 4 h for each experimental point), their colour turned from white to grey during the reaction. This indicates the deposition of heavy compounds. Downloaded catalysts were characterized by means of ATR-IR spectroscopy to determine if any change in their structure and composition had taken place during reactivity experiments. We also tried to investigate on the nature of heavy compounds by means of Raman spectroscopy, but because of fluorescence, it was not possible to see any band, just a flat background. So, in order to determine the presence of C over the catalyst, we carried out SEM-EDX mapping of elements.

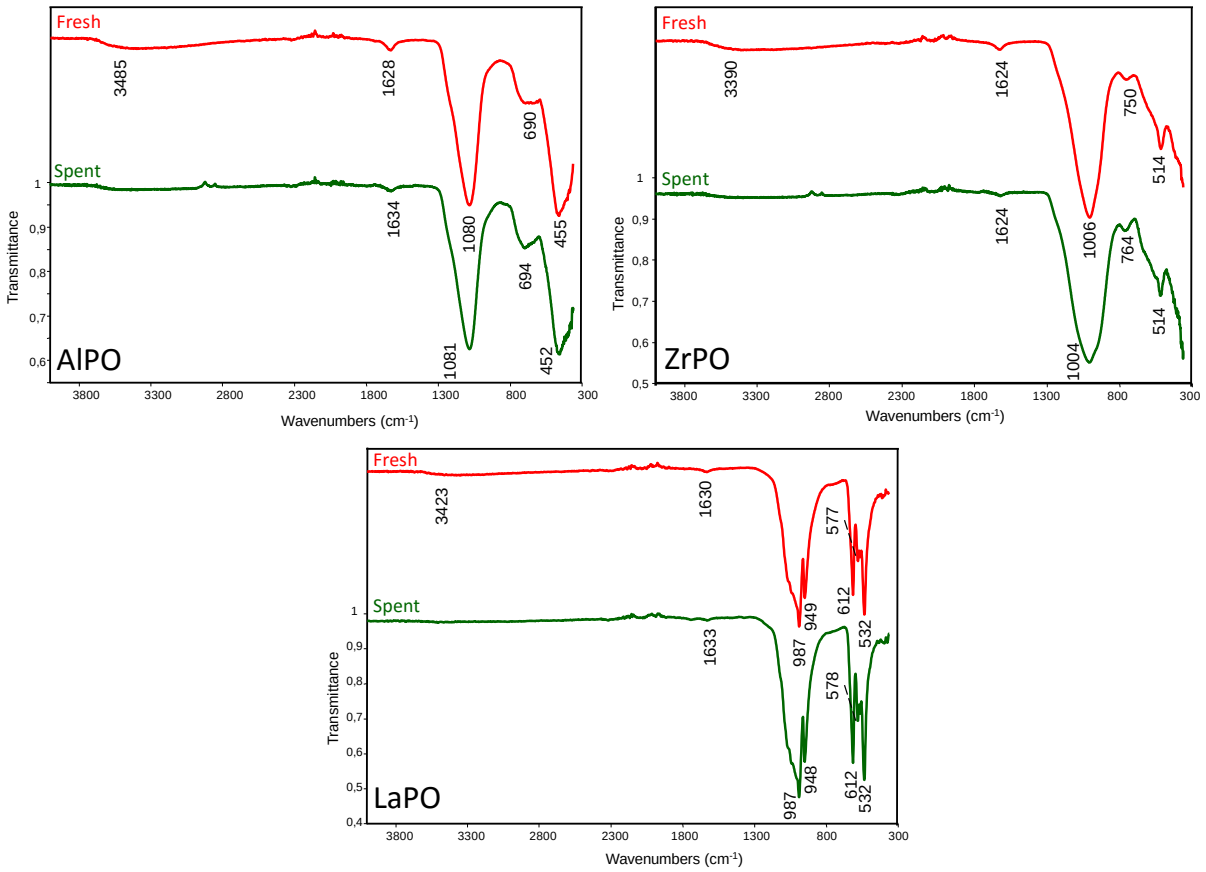

Figure 84: IR-ATR spectra of fresh and used catalyst safter reaction at 400°C and W/F 2.0 g·s/mL.

Comparison of ATR-IR spectra for fresh and used catalysts showed no substantial difference (Figure 30). All absorption bands typical of the starting materials remained unchanged, indicating that the catalysts did not undergo any relevant structural modification. SEM-EDX experiment confirmed the presence of carbon over the used catalyst. This is probably due to heavy compounds deposition on the catalyst surface.

Characterization of used catalysts indicates that all of the three metal phosphates preserved their original structure. Formation of carbonaceous deposits over the catalysts was detected, but apparently this did not influence catalytic performance during the time of the reactivity experiment.

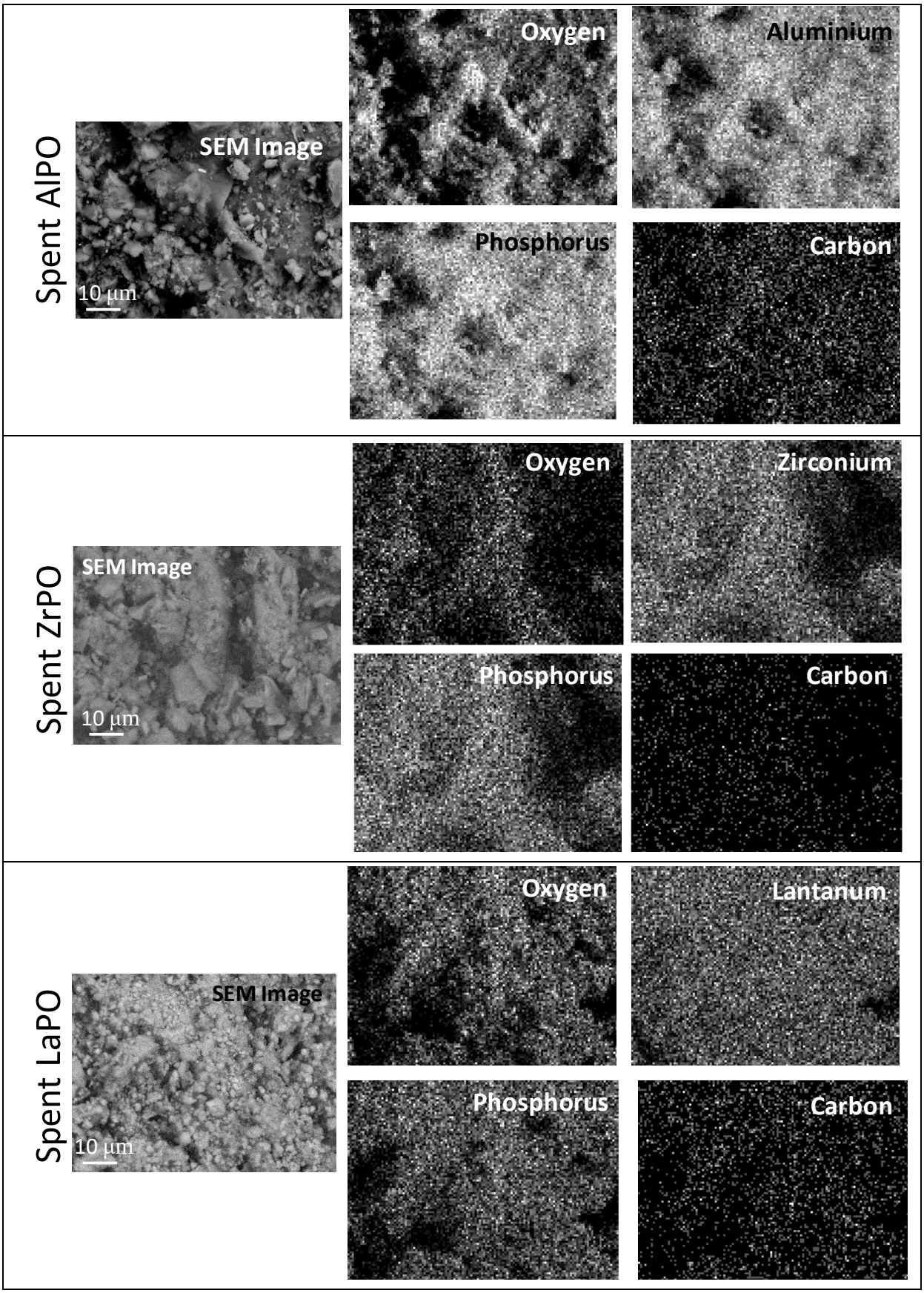

Figure 85: SEM-EDX analysis of catalysts used, after reaction at 400°C and W/F 2.0 g·s/mL. Top: AlPO, middle: ZrPO, bottom: LaPO.

3.3.2.5 *Effect of temperature on products distribution*

In order to evaluate the effect of temperature, we carried out catalytic tests on methanol-isobutene coupling at 300°C also.

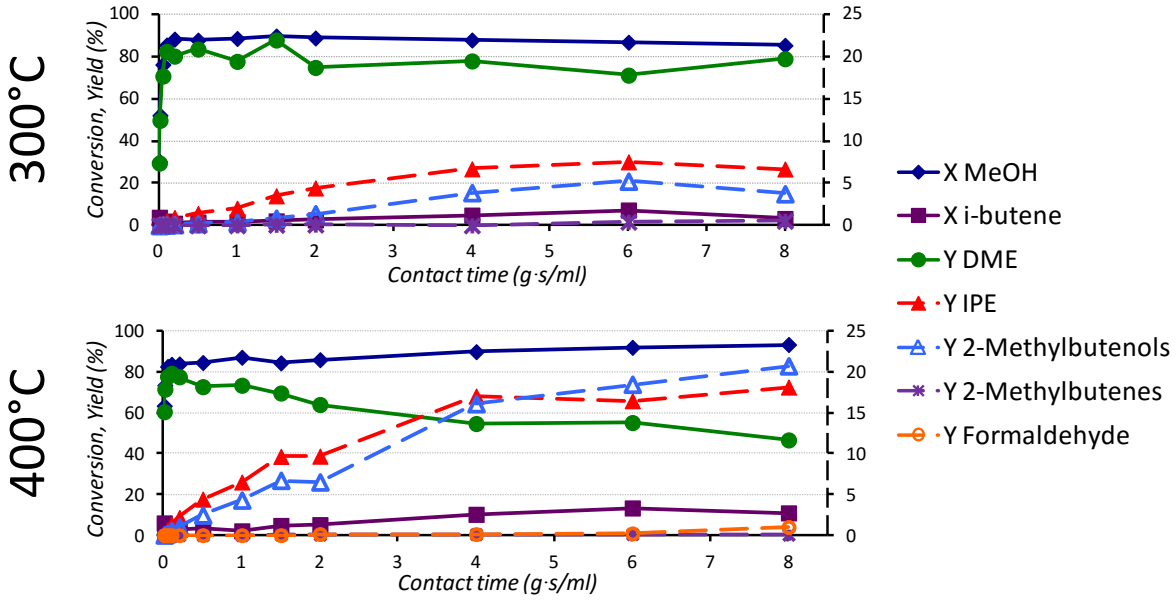

Figure 86: Reaction between 3% methanol and 18% isobutene in N_2 over AlPO at 300°C (top) and 400°C (bottom). Effect of W/F ratio on reagents conversions and products yields. Dashed lines are referred to the secondary Y axis.

Figure 86 shows a comparison for methanol-isobutene coupling over AlPO at 300 and 400°C. It is shown that the trend of yields did not change with temperature. Isoprene, 2-methylbutenes and DME were kinetically primary compounds at both 300 and 400°C. Formaldehyde was not detected at 300°C, but we found 2-methylbutenols; this indicates that isoprene hydration occurred at 300°C also, but this temperature was not high enough to allow occurrence of the retro-Prins reaction and formaldehyde production. The same was found also for LaPO and ZrPO (see Figure 87). Data collected at 300°C were in agreement with the reaction scheme shown in Figure 77; moreover differences among the three phosphates shown at 400°C were observed at 300°C also. However, the lower temperature led to some differences in catalytic behaviour. First, for all catalysts DME yield was higher at 300°C than at 400°C; at the same time, lower yields to iso-C_5 olefins were found. These two aspects are strictly related to each other when the carbene mechanism is taken into account. Both carbene and DME formation derive from acid-catalyzed reactions: carbene from methanol or DME monomolecular dehydration or de-methanolation, DME from methanol etherification. Both reactions are thermodynamically favoured by the increase of temperature because are endothermal, but when temperature was increased from 300 up to 400°C, dehydration became more preferred than etherification, so the reaction was shifted toward the preferred formation of dehydration products. In our case, DME is the product of etherification, whereas carbene is generated by monomolecular dehydration.

Etherification occurred at both 300 and 400°C, but when the temperature was increased up to 400°C, methanol and DME started to give monomolecular dehydration at a greater extent. This led to higher formation of carbene which resulted in an increase of iso-C_5 olefins.

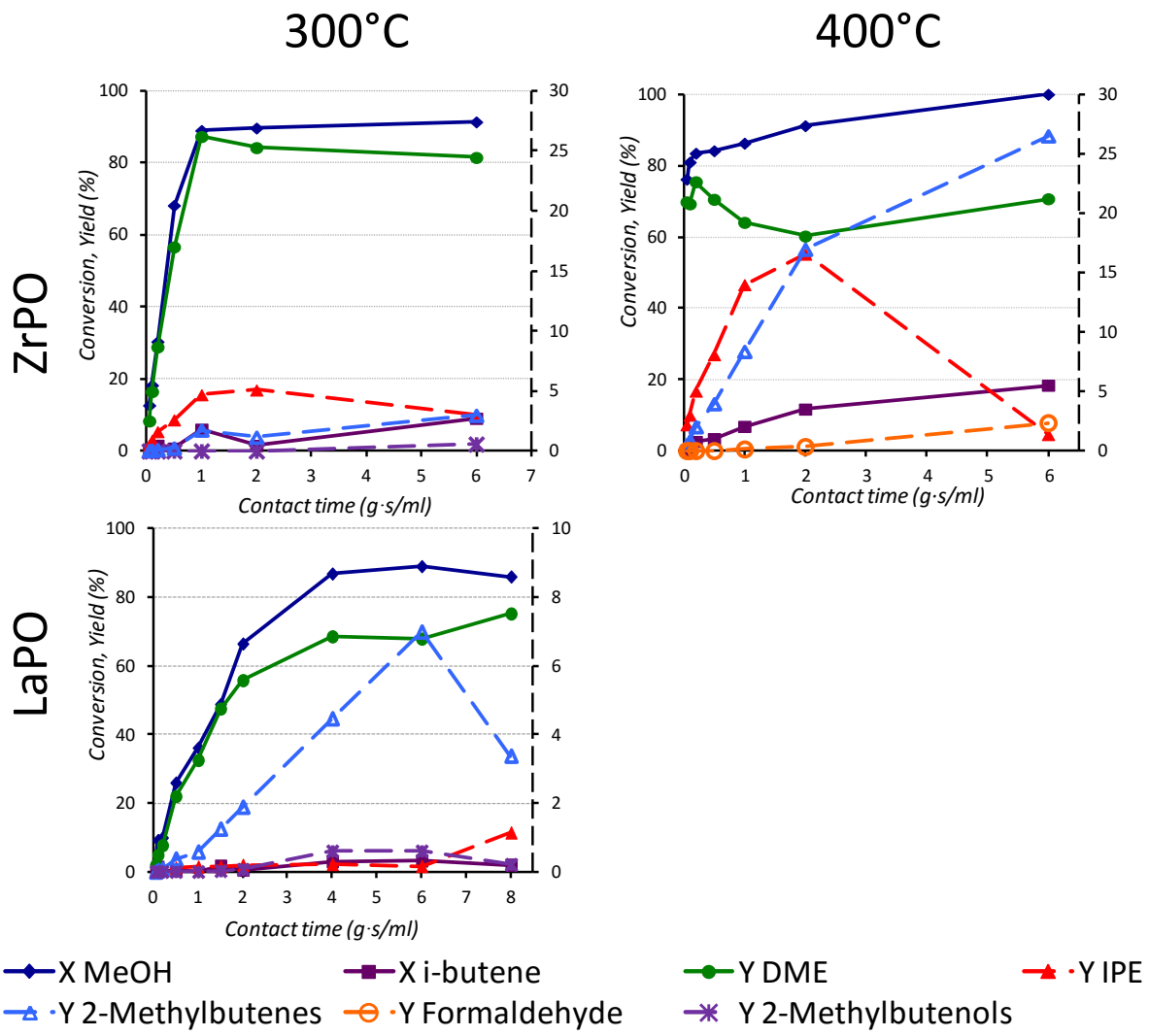

Figure 87: Reaction between 3% methanol and 18% isobutene in N_2, over ZrPO (top) and LaPO (bottom) at 300°C (left) and 400°C (right – only for ZrPO). Effect of W/F ratio on reagents conversions and products yields. Dashed lines are referred to the secondary Y axis.

3.3.2.6 Effect of reagents ratio on products distribution

Besides the elucidation of the reaction scheme, another objective of the research work was to find at which conditions isoprene yield can be increased. As shown by catalytic tests, the main reaction product was DME. Formation of this product occurred through interaction between two molecules of methanol; theoretically, if methanol concentration is decreased, bimolecular reactions should become less facilitated. In this way, formation of DME might less favored and methanol-isobutene coupling might become the more preferred reaction. This principle was applied by carrying out the reaction at different methanol-to-isobutene

feed ratios, while keeping the total amount of organic fraction fed constant. Results of these experiments are shown in Figure 88.

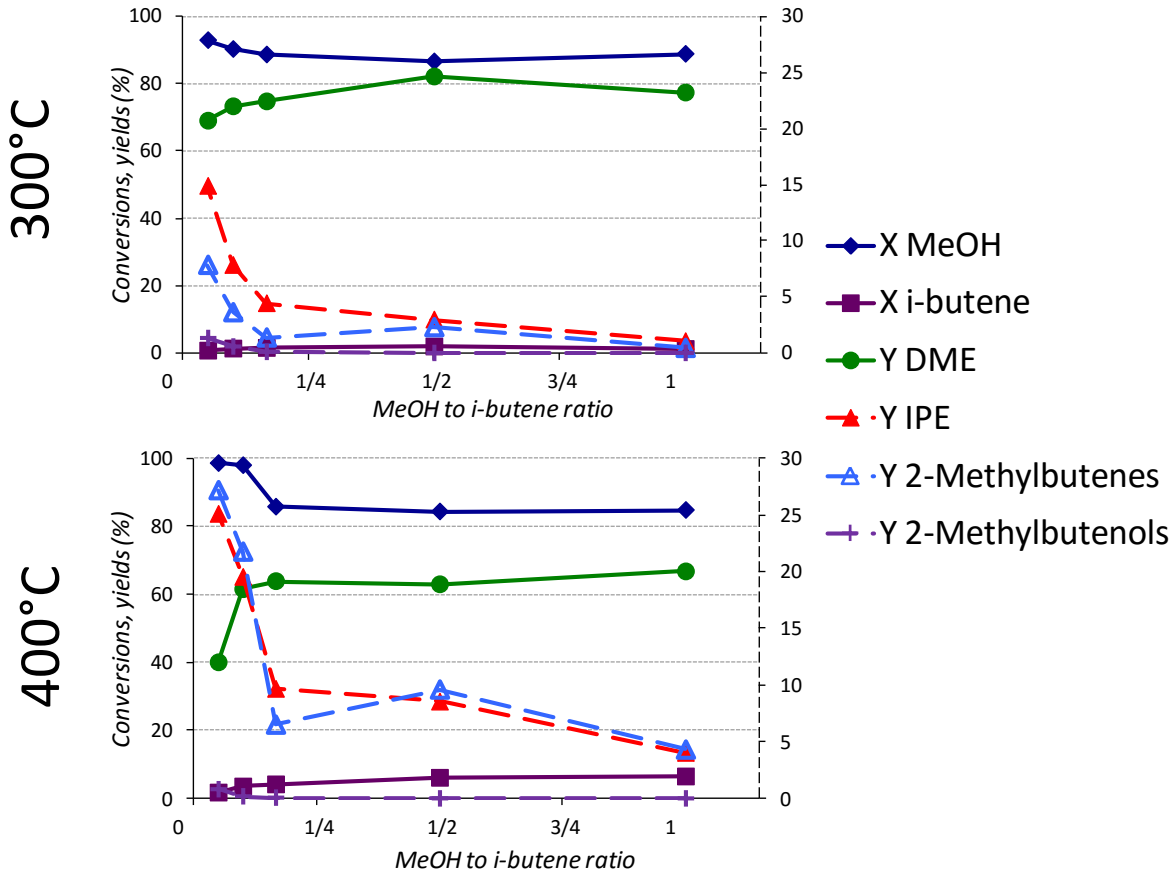

Figure 88: Effect of methanol-to-isobutene feed ratio on products distribution with AlPO at W/F 2.0 g·s/mL and 400°C. Total organic fraction was 21% in N_2. Dashed lines are referred to the secondary Y axis.

The hypothesis formulated was correct; actually, by decreasing the methanol-to-isobutene ratio it was possible to obtain higher yields of iso-C_5 olefins. This occurred at both 300 and 400°C; in line with tests carried out at different temperatures, still higher isoprene yields were obtained at the higher temperature.

A further decrease in methanol percentage was not possible because of technical reasons.

The extrapolation of results shown in Figure 35 might suggest that using a methanol-to-isobutene ratio close to zero, methanol should be totally converted to isoprene. In order to investigate this possibility, we carried out an experiment by replacing the inert gas with isobutene. A mixture made of 3 mol% methanol and 97% isobutene was fed onto the AlPO catalyst; results are shown in Figure 35.

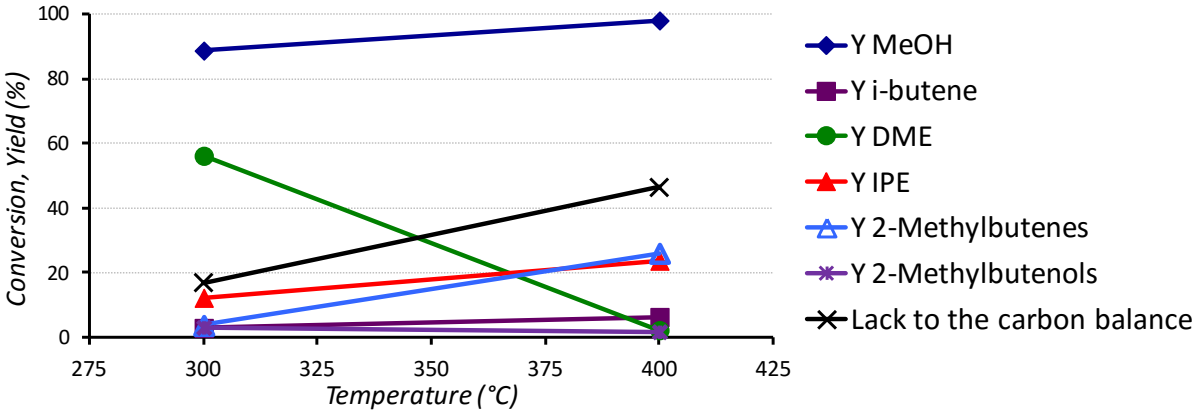

Figure 89: Product distribution obtained by feeding 3% methanol in 97% isobutene with AlPO catalyst, W/F 2.0 g·s/mL, at 300 and 400°C.

Results demonstrate the following:

- Under the conditions used, DME formation was significantly reduced, and at 400°C was almost totally suppressed.
- Isoprene yield was not enhanced with respect to the test at lowest methanol-to-isobutene ratio shown in Figure 88.
- The lack in carbon balance was due to a large quantity of other unidentified products, mainly deriving from the acid-catalyzed oligomerization of isobutene and other reactions involving oligomers and methanol.

Therefore, too high concentrations of isobutene caused the formation of dimers and oligomers, which finally also reacted with methanol. These reactions were in competition with isoprene formation, and its yield finally did not increase further.

3.3.3 The anaerobic-modified-Prins reaction over Cu or Co oxides supported over AlPO

Cu and Co oxides were supported over AlPO in the aim of increasing isoprene yield.

As said before, isoprene formation occurred also over the simple metal phosphate, but the reaction led to the formation of two main undesired by-products, DME and 2-methylbutenes. In the previous paragraph we described how DME formation can be in part decreased in favour of the formation of iso-C_5; anyway still the problem of 2-methylbutenes formation remained unsolved. In this chapter this issue is dealt with using a different approach. Instead of looking for a method to decrease the undesired product yield, we tried to increase isoprene yield by providing an alternative route to isoprene, via intermediate formation of formaldehyde (modified-Prins reaction). In other words, we hoped to accelerate the pathway leading to isoprene by increasing the concentration of the in-situ generated formaldehyde; thus, isoprene would form by both the direct methanol-isobutene coupling and the modified-Prins reaction, in which methanol is first dehydrogenated to

formaldehyde, and the latter is then transformed to isoprene through the Prins reaction with isobutene.

As described at the beginning of the chapter, for this purpose a multifunctional catalyst is needed, able to carry out both methanol dehydrogenation and Prins reaction. As the acid support we chose AlPO, whereas Cu and Co oxides were selected to carry out the first step of methanol dehydrogenation. In fact these two oxides were found to be active in alcohols dehydrogenation at anaerobic conditions[136].

As described in the experimental part, Co and Cu oxides were supported over AlPO at different nominal metal loading. Then they were tested at 400°C at the W/F ratio of 1.5 g·s/mL; methanol and isobutene concentration were respectively 3 and 18%, diluted in N_2. Results are shown in Figure 90.

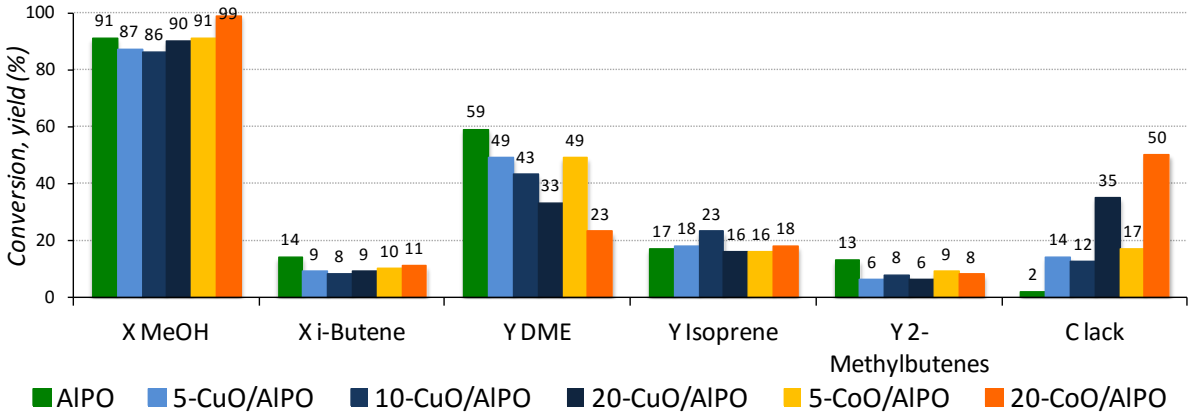

Figure 90: Product yields obtained by feeding 3% methanol and 18% isobutene over Co and Cu oxides supported over AlPO at W/F 1.5 g·s/mL and 400°C. C loss is the lack in carbon balance due to the presence of unidentified peaks in the chromatogram, corresponding to heavy compounds.

With all catalysts, we also detected the formation of methane and CO_2.

Results reported in Figure 90s can be summarized as follows:

- All catalysts showed high methanol conversion;
- DME yield decreased with the increase of metal loading;
- Isoprene yield showed a limited increase compared to AlPO alone; the highest yield was 23%, obtained with 10-CuO/AlPO.
- 2-Methylbutenes yield was higher with AlPO.
- The lack in the carbon balance, indicating the presence of heavy compounds, was the higher in the case of higher metal loading, whereas the lowest carbon loss was obtained with AlPO. Intermediate values were obtained in the other cases. With 20-CoOx/AlPO, the 15% lack in the C balance was mainly due to CO_2 formation.

No one of the catalysts used gave significant improvements in terms of isoprene yield compared to AlPO. However, the products distribution was affected by the metal loading.

A clear example was DME; its yield decreased with the increase of metal loading, for both CuOx/AlPO and CoOx/AlPO. This can be due to the coverage of the AlPO acid sites by the

metal oxides. With fewer acid sites available, methanol was converted to DME at a minor extent. The major effect was shown with Co oxide, and this is in good agreement with SEM-EDX characterization results. In fact, 20-CoOx/AlPO showed an homogeneous distribution of the metal oxide over the AlPO surface, whereas in case of 20-CuO/AlPO the formation of metal oxide aggregates was shown. A more homogeneous distribution of CoOx on AlPO surface led to a greater extent of acid sites coverage, that finally resulted in lower DME yield. Moreover. the increase of metal loading led also to a greater formation of heavy compounds. Probably this occurred to the detriment of isoprene. If we take into account the catalysts made of CuOx supported over AlPO, isoprene maximum yield was achieved with 10% CuO, but when the loading increased up to the 20%, isoprene yield decreased in favor of heavy compounds. This may indicate that at high metal loading, isoprene may react further and form heavy compounds. Moreover, the same effect was also shown with Co oxide. Finally, it is possible to see that yield to 2-methylbutenes always decreased with supported metal oxides catalysts compared to AlPO alone; this effect seemed to be not affected by the metal oxide loading.

As said before, isoprene formation was not significantly increased by supporting Cu or Co oxides over AlPO. In order to understand if this was due to the fact that the metal oxide was not active in methanol dehydrogenation or to some other reactions which consumed the formaldehyde generated, we carried out experiments with 10-CuO/AlPO by decreasing the W/F ratio. Results are shown in Figure 91.

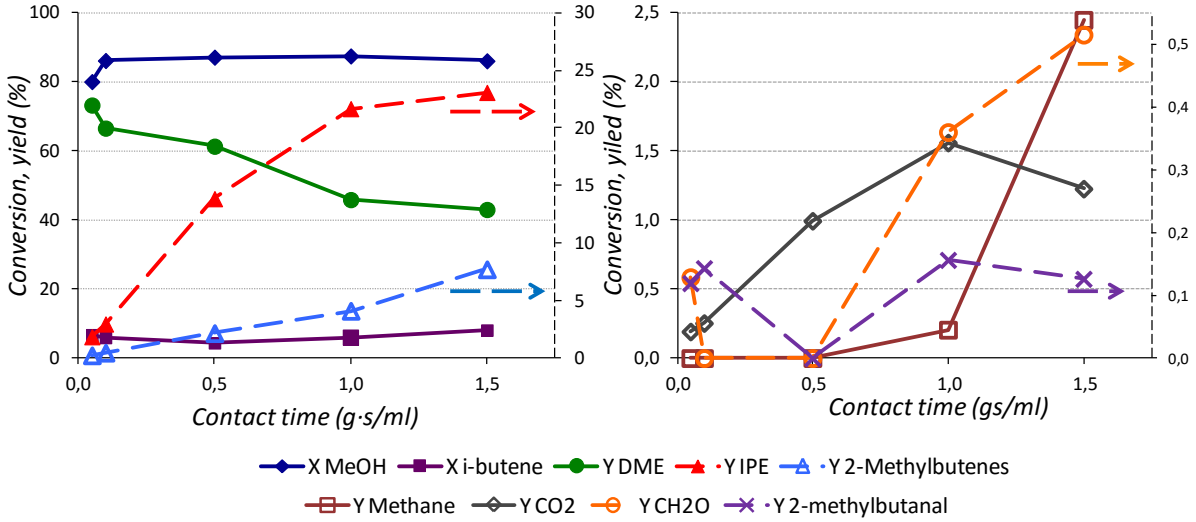

Figure 91:Reaction between 3% methanol and 18% isobutene in N_2, with 10-CuO/AlPO at 400°C. Effect of W/F ratio on reagents conversions and products yields. Dashed lines are referred to the secondary Y axis.

Products obtained in case of 10-CuO/AlPO were the same as with AlPO, with the exception of 2-methylbutanal. As shown in Figure 92, this aldehyde derives from the rearrangement of 2-methybuten-1-ols.

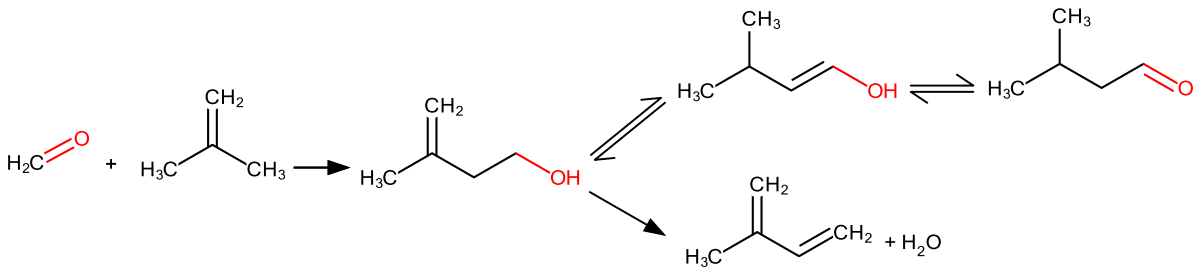

Figure 92: Prins reaction with 2-Methylbuten-1-ol and rearrangement to 2-methylbutanal.

Yields profiles were the same as for AlPO, with the exception of formaldehyde and 2-methylbutanal. These two products showed similar yield profile: they started to be produced at the lowest contact time investigated, then they were consumed, and finally they were produced again. This behaviour can be explained by taking into account the anaerobic-modified-Prins reaction and the methanol-isobutene coupling described in the previous paragraph. At early contact time, formaldehyde was produced by methanol dehydrogenation, while 2-methylbutanal formed as a side product from the intermediates compounds of the Prins reaction (Figure 92). At intermediate contact time, both of them were consumed: formaldehyde by the Prins reaction, and 2-methylbutanal by the shift of the equilibrium to isoprene. When the W/F ratio was further increased, both aldehydes were formed again, because of hydration and subsequent retro-Prins reactions occurring on Isoprene.

These data can demonstrate the existence of both the methanol-isobutene coupling and the Prins reaction on these bifunctional catalysts. However, the contribution of the Prins reaction to isoprene formation was marginal.

To sum up: supporting Cu and Co oxides on AlPO was not an efficient method in the aim of increasing isoprene yield. Even though greater amounts of formaldehyde were generated, which then reacted in-situ with isobutene, finally the rate of this reaction was not high enough to provide a significant increase of isoprene yield.

3.3.4 The aerobic- and anaerobic-modified Prins reaction with a double-layer catalytic bed reactor

As described before, the modified-Prins reaction can be obtained by contacting methanol and isobutene on a double catalytic bed, in which the first bed contains a redox catalyst and the second an acid catalyst. In this way methanol is first transformed to formaldehyde, then the latter reacts on the second catalytic bed with isobutene to give isoprene.

From literature information[137] [138], Iron Vanadate (abbreviated: FeVO) was chosen as the catalyst for the conversion of methanol to formaldehyde, both in aerobic and anaerobic

conditions. AlPO was chosen as the acid catalyst because of its good performance in the Prins reaction[110].

Since the inlet gas passes through the reactor with a downstream flow, the catalysts were loaded inside the reactor in such a way to have AlPO on the bottom and FeVO on the top, as shown in Figure 93.

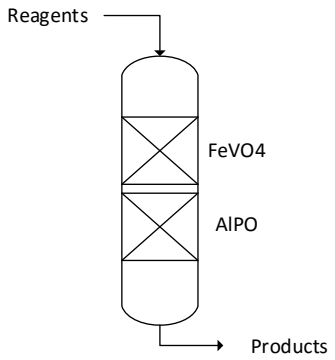

Figure 93: Arrangement of the double-layer catalytic bed.

Reaction conditions are shown in Table 10.

	Anaerobic-modified-Prins reaction	Aerobic-modified-Prins reaction
Inert gas	N_2	N_2
Total gas flow (mL/min)	60	60
Isobutene (%) in inlet flow	18	18
Methanol (%) in inlet flow	3	3
Oxygen (%) in inlet flow	0	2
W/F for $FeVO_4$ (g·s/mL)	0.3	0.3
W/F for AlPO (g·s/mL)	0.9	0.9
Temperature range (°C)	300-400	200-400
Pressure (atm)	1	1

Table 10: reaction conditions used with the double-layer catalytic bed.

The aerobic-modified-Prins reaction was carried out with an oxygen concentration under the minimum oxygen concentration (MOC), needed to avoid the formation of a flammable mixture.

One problem of the Prins reaction is coke and heavy compounds formation, which can deactivate the catalyst[110, 113]; in order to limit this problem, formaldehyde is usually fed in defect with respect to isobutene. Therefore, we decided to feed the methanol/isobutene mixture with a 1/6 molar ratio.

Under both anaerobic and aerobic conditions we found the same products:

- Isoprene, which derives from both the modified-Prins reaction and direct methanol-isobutene coupling, as described in the previous paragraphs.
- Dimethyl ether (DME), formed by methanol acid-catalyzed etherification.

- 2-Methylbutenes, which form by interaction between methanol or DME and isobutene with AlPO (see previous pharagraphs).
- CH_4 and CO_2, which form by formaldehyde and methanol decomposition or, in the case of CO_2, by combustion in the presence of oxygen.

For technical reasons the determination of CO was possible only for a few points during the aerobic-modified-Prins reaction; CO forms by both formaldehyde and methanol decomposition and partial combustion.

Figure 94 shows yields to products and reagents conversions both in anaerobic (A) and aerobic (B) conditions. In the next paragraphs, the results of each test will be discussed, then the two experiments will be compared.

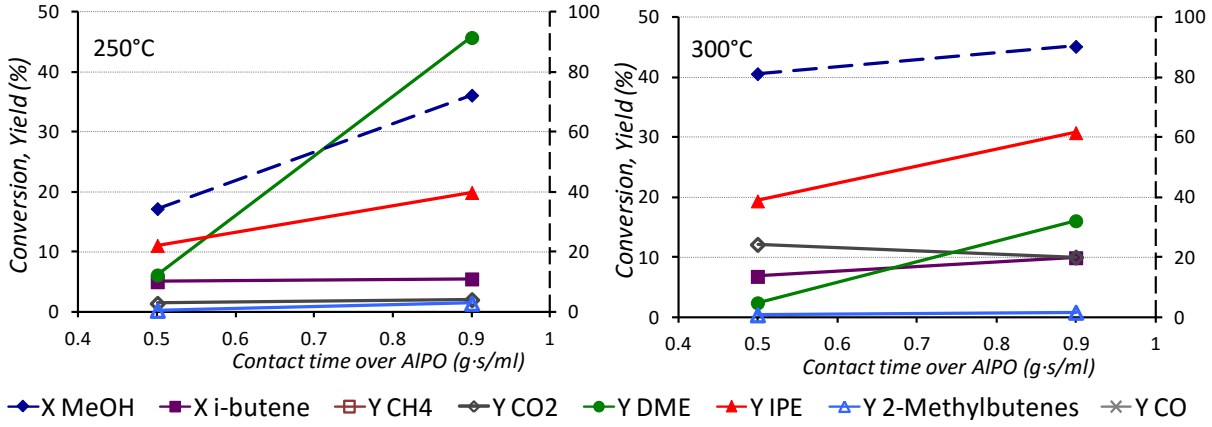

Figure 94: Reagents conversions and products yields obtained with FeVO + AlPO double-layer catalytic bed in the anaerobic (A-left) and anaerobic (B-right) modified-Prins reaction. Dashed lines are referred to the secondary Y axis.

3.3.4.1 ***The anaerobic-modified-Prins reaction with the FeVO-AlPO double-layer catalytic bed***

In order to compare results and investigate on the role of FeVO, we carried out a catalytic test using the anaerobic-modified-Prins conditions, but loading only AlPO in the reactor. Other reaction conditions were the same as those reported in Table 10. Results are given in Table 11.

T (°C)	X MeOH	X i - Butene	Y DME	Y IPE	Y 2-Methylbutenes	Y CH_4	Y CO2
300	88	3	64	7	3	0	0
400	89	10	58	17	10	0	0

Table 11: Results obtained by feeding methanol and isobutene in anaerobic conditions over AlPO at W/F 0.9 g·s/mL.

The comparison of results shown in Table 11 and in Figure 94(left) demonstrates that the presence of FeVO unfortunately did not contribute significantly to isoprene yield. Actually, at higher temperature it had a detrimental effect on the reaction. In fact at 300°C isoprene yield was the same in both cases, while, at 400°C it was 10% lower in the presence of FeVO also. The same effect was also shown, albeit at a lower extent, on 2-methylbutenes yield.

The reason for this behaviour can be found if CH_4 and CO_2 yields are also taken into account. These products derived from methanol or formaldehyde decomposition, and they formed at a much greater extent when also FeVO was present. This means that the detrimental effect of this catalyst was due to its high activity in methanol or formaldehyde decomposition.

Therefore methanol, and probably formaldehyde as well, were decomposed on the first layer of the catalytic bed, and only a limited amount of formaldehyde reached the second bed. This effect was more relevant when the temperature was increased; in fact isoprene yield over the double-layer bed decreased and, on the other hand, CO_2 and CH_4 yields also increased, indicating a faster decomposition of methanol and formaldehyde.

The same effect can explain the lower DME yield observed in the case of the double-layer bed. When only AlPO was used, its acidity contributed to give a high DME yield; however, when FeVO was present as the first layer, a lower amount of methanol reached the downstream AlPO bed, which finally turned to a lower DME yield. This effect was more relevant at 350 and 400°C.

3.3.4.2 The aerobic-modified-Prins reaction with the FeVO-AlPO double-layer catalytic bed

A different effect was obtained when the catalytic test was carried out by co-feeding oxygen. As shown in Figure 94, the presence of oxygen had a positive effect on isoprene yield, while C_1 decomposition to CH_4 and CO_2 was almost suppressed.

Isoprene yield could be increased up to the 30% (300°C), which is about three times as much the yield obtained in the same conditions, but without FeVO.

Moreover, a “blank” test carried out in the same conditions, but in the absence of FeVO, gave the same results as those reported in Table 11. This means that oxygen did not have any effect on the catalytic behavior of AlPO.

Therefore, it is possible to say that in this case almost all of the isoprene produced derived from the modified-Prins reaction, and the methanol-isobutene coupling catalysed by AlPO gave a minor contribution. This can be deduced also from products distribution: while methanol-isoprene coupling over AlPO always gave both isoprene and 2-methylbutenes, in this case 2-methylbutenes were absent until 350°C.

However, at 350 and 400°C a major contribution of isobutene-methanol coupling cannot be excluded, in fact 2-methylbutenes also formed, albeit with low yield. Anyway, at these temperatures a fast decrease of isoprene yield was shown, an effect attributable to C_1 combustion. In fact both CO and CO_2 formation rapidly increased with temperature, while methane was present in small amount only at 400°C.

Other useful information were obtained from a short-lifetime experiment. The double-layer catalytic bed was kept under the reagents stream for 20 hours, then it was regenerated at

450°C for 3 hours in a flow of 40 mL/min of air, and finally reagents were fed again in order to see the effectiveness of regeneration. Results are given in Figure 95. These experiments showed the following:

- Methanol and isobutene conversion, and isoprene yield decreased with time-on-stream;
- DME yield first rapidly increased, but then decreased;
- Formaldehyde was not formed at the beginning of the experiment, but then its yield increased;
- The regeneration treatment did not lead to a complete recovery of the initial catalytic behavior. In fact products distribution was different from that shown by the fresh catalyst. Probably longer regeneration times or at higher oxygen concentrations were needed.

The anomalous behaviour of DME can be explained by taking into account for the discussion rerpoted in chapter 2.3.1 for FeVO. FeVO needs an equilibration time to reach a steady state; during this time its activity in alcohols dehydrogenation to aldehydes decreased. Therefore, the first point in Figure 41 was probably obtained when FeVO was still active in methanol conversion to formaldehyde; however its activity then decreased and DME formation increased, because more unconverted methanol reached the second layer containing AlPO. Later on, also AlPO started to deactivate[110] and DME yield decreases. Therefore, DME behaviour at the beginning of the experiment was due to FeVO equilibration, but after a few hours time-on-stream FeVO showed a more stable behaviour; however, the trend shown after a few hours was instead due to AlPO deactivation.

The trends for methanol conversion, and isoprene and formaldehyde yields can be explained by taking into account AlPO deactivation. In fact, the decrease of isoprene yield was related to the increase of formaldehyde yield. This indicates that isoprene mainly derived from the Prins reaction. Deactivation of the AlPO acid sites caused a decrease of the reaction rate between formaldehyde and isobutene to isoprene, while formaldehyde still was produced on the first FeVO layer. The same effect can explain the decrease of isobutene conversion.

However, it is not possible to exclude a contribution of methanol- or DME-isobutene coupling, catalyzed by AlPO, on isoprene formation. In fact the increase of formaldehyde yield did not exactly match the decrease of isoprene yield. This means that, despite the deactivation of acid sites, still isoprene was produced. Probably, the deactivation of AlPO acid sites had no effect on isoprene production by means of the carbene mechanism. Indeed, it cannot be excluded that an active role in carbene formation is also due to carbonaceous deposits, as it was also recently proposed by Ivanova et al[139] for the Prins reaction over AlPO.

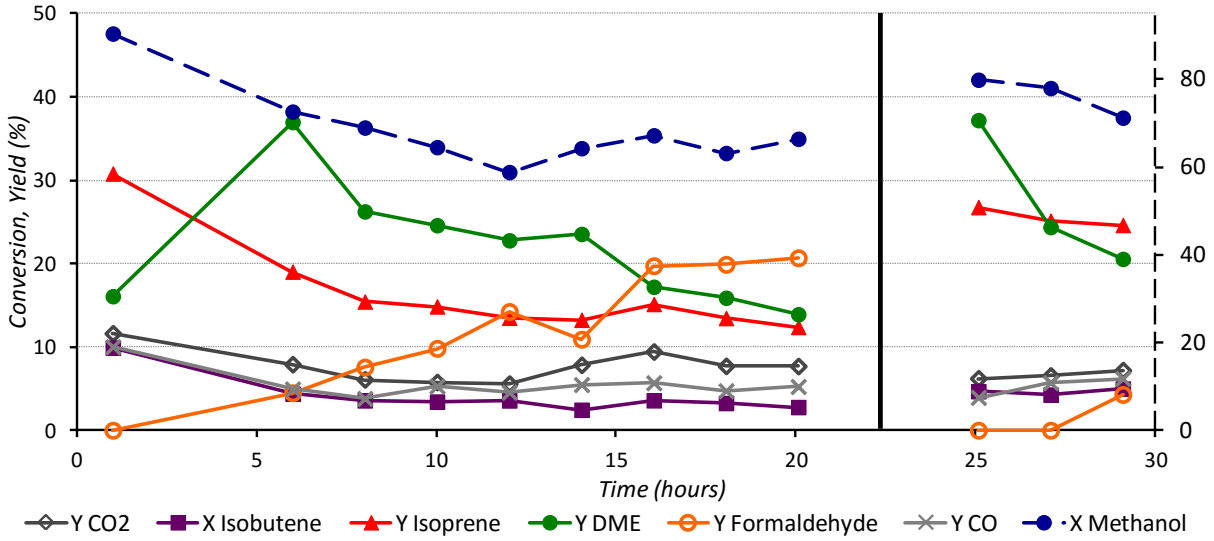

Figure 95: Reagents conversions and products yields during short-lifetime experiment at 300°C conducted on FeVO + AlPO double-layer catalytic bed. Dashed line is referred to the secondary Y axis. Methane was not detected, 2-methylbutenes were present at all times with yield <0,5%. Black vertical line between 20 and 25 hours indicates catalyst regeneration, carried out in 40 mL/min air flow at 450°C for 3 h.

To summarize, in this case it is possible to say that the modified-Prins reaction occurred at a considerable extent in aerobic conditions with the FeVO + AlPO double-layer catalytic bed. Moreover it is possible to identify a range of temperature in which the yield to isoprene was the highest. At temperatures lower than 300°C, catalysts were less active, in fact methanol conversion was low. On the other hand, at 350°C and above, methanol started to be converted also to CO and CO_2. This reaction subtracts the formaldehyde necessary for the Prins reaction, thus causing a decrease of isoprene yield.

A short-lifetime experiment showed that the aerobic-modified-Prins reaction greatly contributed to isoprene formation, as described in Figure 65-C. The behaviour of the double bed derived from a combination of FeVO and AlPO behaviours. FeVO had to reach a steady - state performance; after an initial transient period, its behaviour became constant. On the other hand, AlPO gradually deactivated, probably because of carbonaceous deposits that blocked the acid sites needed for the Prins reaction[110]. Regeneration could partially restore the initial behaviour, but for a complete recovery of the chemical-physical properties of the fresh catalyst, stronger conditions for regeneration were probably necessary.

3.3.4.3 *Conclusions on the anaerobic- and aerobic-modified-Prins reaction over FeVO + AlPO double-layer catalytic bed*

The aim of this reactor configuration was to realize a modified-Prins reaction by feeding isobutene and methanol first on a catalyst able to convert methanol to formaldehyde, and immediately after on a catalyst able to convert formaldehyde and isobutene into isoprene. FeVO and AlPO were chosen as catalysts for this purpose. This double-layer bed was tested under both aerobic and anaerobic conditions.

Results shown in Figure 94 demonstrate that isoprene yield was much higher when oxygen was fed together with the reagents. This can be explained by taking into account results obtained by feeding ethanol over FeVO, both in aerobic and anaerobic conditions, described in paragraph 2.3.1.

The presence of oxygen strongly enhanced the aldehyde formation with a concomitant decrease of decomposition products (e.g., methane in the case of methanol); therefore, in the absence of oxygen, FeVO catalyzed more efficiently methanol decomposition instead of dehydrogenation.

When instead oxygen was co-fed, FeVO catalyzed more efficiently methanol oxidation to formaldehyde, while decomposition occurred at a lower extent.

Concluding, the double-layer catalytic bed made of FeVO + AlPO was not effective in the anaerobic-modified-Prins reaction, because FeVO had a detrimental effect on catalytic performance; in fact, AlPO alone gave higher isoprene yield.

Conversely, the double bed set up was effective in isoprene formation in the aerobic-modified-Prins reaction; an outstanding 30% isoprene yield could be achieved with the fesh catalyst, but a strong deactivation led rapidly to a decline of this value, until a stable value of 12-13% was reached, probably mainly deriving from the contribution of the carbene mechanism.

3.4 Overall conclusions on the modified-Prins reaction and isobutene-methanol coupling

An alternative route to produce isoprene, based on the reaction between isobutene and methanol, has been investigated.

Current processes for isoprene production are mainly based on petrochemical routes, which consist in the extraction and purification of isoprene from C_5 refinery stream, or in iso-C_5 hydrocarbons dehydrogenation. These processes can be carried out only in large scale plants, connected to naphtha steam cracking units. An alternative route is the Prins reaction between formaldehyde and isobutene. The two reagents can react together to form isoprene through an acid-catalyzed reaction. The process is less dependent on petroleum availability, because isobutene might be produced by dehydration of bio-based isobutanol, and formaldehyde might be obtained from biomass gasification to syngas, methanol synthesis and dehydrogenation. However, it presents some drawbacks: it is carried out in two step, each of them combined with a downstream purification process, and formaldehyde is a carcinogenic compound, difficult to handle because of its instability and reactivity. In the past, some attempts to improve this process were carried out, but no one of them was then industrialized. One interesting approach is to avoid the use of formaldehyde by employing a system able to generate it from methanol and consume in-situ through the Prins reaction with isobutene. Some attempts done in this direction use oxygen to oxidize methanol to formaldehyde, even though this may increase the process risk because of the possible formation of flammable mixtures.

A solution to this problem, proposed in the literature[121, 129, 130, 131], might be to synthesize formaldehyde by means of methanol dehydrogenation. Also in this case, however, literature data show low yields.

Our first aim was to develop a catalytic system able to transform methanol to formaldehyde and also catalyse the reaction between formaldehyde and isobutene to form isoprene through the Prins reaction. However, the most important part of the work concerned the investigation of the reaction scheme of the reaction. In fact, the knowledge of the reaction network and mechanism is the basis for the development of a more efficient catalyst.

The theoretical reaction scheme implies first formaldehyde formation from methanol, and then isoprene formation through the reaction between formaldehyde and isobutene. However, we discovered that an unexpected mechanism occurs on metal phosphates. This route, which scheme was determined by catalytic tests carried out over phosphate catalysts, is shown in Figure 77.

The reaction between isobutene and methanol at 400°C, over Al, Zr and La phosphate catalysts gave isoprene, 2-methylbutenes and dimethyl ether as the kinetically primary

products, whereas formaldehyde and other typical intermediates of the Prins reaction were kinetically secondary products.

Dimethyl ether was the main reaction product, formed through methanol acid-catalyzed etherification.

Isoprene and 2-methylbutenes synthesis occurred by means of a carbene mechanism: carbene (neutral :CH_2 with a lone electron pair) formed by monomolecular dehydration of methanol or by de-methanolation of dimethyl ether. In both cases, carbene formed through an acid-catalyzed mechanism. Isoprene and 2-methylbutenes were then formed by means of different mechanisms of interaction between the carbene species and isobutene. Results suggest that isoprene formation was catalysed by the acid sites, whereas 2-methylbutenes seemed to form mainly by thermal reaction.

Moreover, other products formed by different mechanisms; in fact we found that isoprene could undergo consecutive reactions to heavy compounds or to 2-methylbutenes through hydrogenation. Isoprene was also hydrated to give 2-methylbutenols, which rearranged to iso-C_5 carbonyl compound or decompose to formaldehyde and isobutene through a retro-Prins reaction.

To sum up, with metal phosphate catalysts the direct alkylation of isobutene with methanol was the main reaction; this reaction went through a carbene mechanism and led directly to 2-methylbutenes and isoprene. Other reactions occurred either because of catalyst acidity or because occurred on isoprene. Isoprene and 2-methylbutenes formation competed in a parallel reaction scheme.

In order to improve isoprene yield, we tried to develop a multifunctional catalytic system able to provide an alternative route to isoprene. This was done by preparing a catalyst made of both a dehydrogenation and an acid active phase. The acid component was the Al phosphate (AlPO); this allowed us to compare results obtained with the pure phosphate with those obtained with the multifunctional catalyst.

We prepared catalysts made of Co or Cu oxide supported over AlPO, with different metal loading. We found two main effects: (a) a decrease of dimethyl ether yield, due to the coverage of AlPO acid sites by the metal oxide, and (b) a slight improvement of isoprene yield due to methanol dehydrogenation catalysed by the metal oxide. With these systems, isoprene formed from both isobutene-methanol coupling and the modified-Prins reaction, but unfortunately the latter gave a minor contribution only. In fact the best increase of isoprene yield was 5% only, with a catalyst made of 10% CuOx supported on AlPO. However, Co and Cu oxides also catalyzed the formation of heavy compounds from isoprene oligomerisation.

Finally was tested a double-layer catalytic bed made up of Iron vanadate (FeVO) and AlPO. This configuration was not efficient, in fact the yield of isoprene was not better than that

achieved with $AlPO_4$ only. This is because under anaerobic conditions FeVO catalysed methanol and formaldehyde decomposition. Conversely, when also oxygen was co-fed, FeVO catalysed the formation of formaldehyde and the downstream catalytic bed catalysed the Prins reaction. A maximum yield of isoprene of 30% was obtained with the fresh catalyst, a value close to those reported in previous patents.

Results indicate that with the multifunctional catalyst we tested, two routes to isoprene occurred in concomitance: the isobutene-methanol coupling, and the modified-Prins reaction. The first reaction was faster compared to the second one, in fact isoprene yield was not significantly increased when the dehydrogenation catalyst was present, besides AlPO. However, when oxygen was co-fed together with isobutene methanol, the modified-Prins reaction occurred with a higher rate; in this case, isoprene yield was significantly improved.

4. ETHANOL PARTIAL OXIDATION FOR HYDROGEN PRODUCTION CATALYZED BY Pt, Rh and Ru NANOPARTICLES

4.1 Introduction

A project regarding ethanol partial oxidation for hydrogen production over Pt nanoparticles was carried out during the abroad research stay of my PhD programme. During this period I was a guest at Liebniz-Instute für Katalyse (LIKAT) in Rostock (Germany). The work on ethanol partial oxidation was carried out under the supervision of Dr. Habil. Evgenii Kondratenko.

Nowadays the larger part of worldwide energy demand is covered by fossil fuels. Because of increasing environmental issues there is a growing interest regarding cleaner fuels, which can reduce the environmental footprint of energy production[140]. One alternative source for energy storage and production is H_2, which can be used as an energy source in fuel cells. A fuel cell is an electrochemical device able to transform the chemical energy contained in H_2 into electrical energy. Moreover a fuel cell shows high efficiency (40-50% against 20-30% of internal combustion engines), with negligible emissions[141].

Around 90% of H_2 are currently produced from steam reforming, partial oxidation and autothermal reforming of methane or light hydrocarbons[142, 143].

These processes lead to the co-production of CO in different quantities with H_2, the resulting mixture is called syngas. The latter can be used as a reagent for some chemical processes, such as methanol synthesis or Fischer-Tropsch reaction. But for some purposes, such as ammonia synthesis or fuel cell applications, CO is an undesired product because it can reduce the efficiency of both fuel cells and ammonia catalyst[143, 144]. So, for these applications, high purity H_2 is required.

This purpose can be achieved by pushing the reaction toward the production of H_2 and CO_2.

A typical steam reforming process, aimed to obtain high purity H_2 is made of three main parts: in the first part CO and H_2, the so-called syngas, are produced. The second step is aimed at maximizing H_2 yield by transforming CO and water into CO_2 and H_2 through the water gas shift reaction. Last step is methanation of residual CO with H_2[145]. Then CO_2 can be easily removed with a basic scrubber.

This process is nowadays fully optimized for the production of high purity H_2, but it presents some drawbacks:

- Three passages are economically disadvantageous.
- Steam reforming reaction requires heating because it is endothermic.
- Further heating is required to generate water steam.

An alternative route for H_2 production can be partial oxidation reaction. It consists of H_2 production by oxidation of organic reagents in presence of a quantity of oxygen that is sub-stoichiometric with respect to the amount required for total combustion reaction. Co-

products of partial oxidation are CO_2 and CO with the latter being formed in lower amounts. Anyway this reaction presents some advantages if compared with steam reforming:

- It requires a lower amount of heat than steam reforming, because it is exothermic.
- If enough O_2 is employed, formation of CO can be minimized and the resulting mixture is already rich in CO_2 and H_2, without the needing of further steps.

The main drawback of the reaction regards the hazard connected to the formation of flammable mixtures due to the presence of O_2 with flammable substances. Moreover a further cost is represented by oxygen separation and purification from air. Since CO is a poison for fuel cells, and it is produced in lower amount in partial oxidation than in steam reforming, catalytic partial oxidation can represent an alternative source of high purity hydrogen for energy storage and production.

Nowadays, partial oxidation of light hydrocarbons is used for hydrogen production[143]143, however a cleaner, more reliable and sustainable source is required to replace hydrocarbons. One of the more promising substances available for this purpose is ethanol[146]. Ethanol is a renewable source, produced from the fermentation of biomass and easily available all over the world.

Formation of hydrogen through catalytic partial oxidation of ethanol has been studied over catalysts based on transition metals loaded over different supports. Both the metal and the support seem to play a key role in the overall reaction. In fact partial oxidation process comprises a complex network of reactions, which have influence on each other[147, 148]. A typical catalyst for ethanol partial oxidation comprises an active phase often made of a noble metal such as Pt or Pd, but also Ir, Co, Ni, Zn or Ru can be used. Typical supports are ZrO_2, Al_2O_2 or SiO_2;[149, 150, 151, 159, 160, 161, 162, 163]. CeO_2 is also often applied for this purpose because of its oxygen storage properties, which can enhance catalytic activity of the active phase[152]. Indeed catalytic activity in partial oxidation reaction is governed by the interaction between the support and the active phase[153].

One of the most studied catalytic system for ethanol partial oxidation is made of Pt or Rh supported on ceria or alumina[158, 159, 161, 162]. These catalytic systems show a hydrogen yield from 20 to 80%. Best yields were obtained with a catalyst based on Rh-Ce supported on a ceramic foam[159], whereas for alumina supported catalysts it was found that the yield of hydrogen was between 50 and 60%, and it follows the order Rh-Ru>Rh>Pt[159]. However this performance can be further enhanced, for example employing metal nanoparticles[154]. The principal feature of nanoparticles is a high surface to volume ratio, because it determines their unique properties; as a consequence, metal nanoparticles show higher activity when compared to conventional catalysts. Therefore, if the activity of the active phase is increased, in principle the same results can be achieved with lower metal loading. Literature data concerning synthesis of H_2 from hydrocarbons, show that noble metal nanoparticles are

more active and selective than their conventional counterparts. Moreover, such results were obtained with a nanoparticles metal loading 100 times inferior than that one used with conventional catalysts[155, 154, 155].

Starting from these assumptions, the present work initially dealt with ethanol partial oxidation over Pt nanoparticles-based catalysts. Pt nanoparticles were supported at 0.1 and 0.01% metal loading over Si/Al/O supports having different SiO_2 to Al_2O_3 ratio. The investigation on the effect of contact time on product distribution enabled us to determine a simplified reaction scheme. The catalysts were then tested to determine the effect of the metal loading, of the support and of the temperature on product formation. At the best conditions found, catalysts based on Rh and Ru nanoparticles loaded over the same supports were then tested. These data were useful in order to determine the effect of different metals and to better investigate the role of the support in partial oxidation of ethanol.

This work presents only catalyst activity data, characterization is on-going, in order to better understand the interaction between metal nanoparticles and supports.

4.2 Experimental

Since the work about Ethanol POX was carried out at LIKAT, different methods were employed with respect to those described in first chapter0. This chapter briefly introduces methods and techniques employed to carry out this research work.

4.2.1 Catalyst preparation

Catalysts were synthesized according to literature methods[156, 157], which proved to be reliable in the aim of obtaining narrow distribution of nanoparticles dimension between 1 and 1.5 nm[154, 155, 156].

Briefly, Pt nanoparticles were prepared by reduction of a Pt salt in basic environment. $H_2PtCl_6 \cdot 6H_2O$ was dissolved in ethylene glycol in order to obtain a metal concentration around 0.04 mol/l. This solution was added dropwise to a 0.5 mol/l solution of NaOH in ethylene glycol heated at 120°C. In these conditions Pt^{4+} is reduced to Pt^0 by ethylene glycol.

Pt nanoparticles, prepared with this method were supported over different commercial supports: SiO_2, Siral40, Siral10, Siral1 and Al_2O_3. "Siral® (Sasol)" indicates a material made of SiO_2 and Al_2O_3 in different proportions, the number after "Siral" indicates the mass percentage of SiO_2; the remaining part is Al_2O_3

Prior to the deposition on the support, Pt nanoparticles were separated from ethylene glycol by means of the following procedure.

A precise volume of nanoparticles solution, necessary to obtain 0.1% or 0.01% metal loading over the support was taken apart. 5 ml of acetone were then added to this aliquot and the solution was thoroughly mixed for 10 seconds. This solution was quickly added to 10 ml of toluene and was mixed thoroughly again for 10 seconds. When two phases were separated, the toluene phase containing Pt nanoparticles was collected. This procedure was repeated 5-6 times, until a viscous nanoparticles solution was obtained. Then nanoparticles solution was diluted with 25 ml of ethanol, 10 g of the support was added to the solution and stirred for 18 h. The suspension was then dried at ambient temperature, under a fume hood.

Prior to the catalytic tests the powders were pressed into tablets and crashed into fraction between 250 and 450 μm.

The same procedure was followed for Rh and Ru nanoparticles. Metal precursors were respectively $RhCl_3$ and $RuCl_3$. In order to obtain surface areas similar to 0.1% supported Pt nanoparticles, Rh and Ru were supported at 0.05% m/m[155, 158].

4.2.2 Catalytic tests

Catalytic tests were carried out in a setup equipped with tubular PFR quartz reactor heated by a ventilated furnace. N_2, O_2 and ethanol were fed to the reactor in a precise ratio by

controlling their flows with three mass-flow meters. Ethanol was vaporized in a heated chamber in which it was then mixed with N_2 and O_2.

The setup was equipped with a by-pass line, for the precise determination of feeding mixture composition. Feed components and reaction products were quantified by means of on-line GC. GC was equipped with four sampling valves, connected with four capillary columns: HP-FFAP, HP-PlotQ, Molesieve 5A and HP-Alumina. HP-FFAP and HP-PlotQ columns were connected to a FID, while the other two columns were connected to a TCD. This configuration allows to analyze ethanol and light hydrocarbons from C_1 to C_3 at the FID, while CO, CO_2 and H_2 are analyzed at the TCD.

In a typical experiment 0.05g of catalyst were loaded into the quartz reactor between two thin layers of glass wool. A layer of SiC was added to ensure good heating of the incoming reagent mixture. Ethanol and oxygen were fed to the catalyst diluted in N_2. Their respective concentrations were 2.50 and 3.75%. They correspond to the exact molar ratio of the reagents of ethanol partial oxidation. The reaction is carried out at 700°C and atmospheric pressure.

Reagents conversions and products selectivity were calculated as follows:

- Reagent conversion: $X = \frac{n_r^{in} - n_r^{out}}{n^{in}}$
- Product yield: $Y = \frac{n_p^{out}}{n_r^{in}} \cdot \frac{c_r}{c_p}$

Where:

- “n” indicates a number of moles
- “c” indicates the number of carbon atoms of the molecule. It indicates number of hydrogen atoms when the formula is referred to H_2 yield
- subscript “p” indicates a product
- subscript “r” indicates a reagent
- superscript “in” indicates the parameter quantified before the reaction (for instance the moles of reagent fed to the reactor)
- superscript “out” indicates the parameter quantified after the reaction (e.g. moles of unconverted reagent or moles of product)
- Yields are referred to ethanol

Some experiments were carried out with different amount of catalyst in order to determine the effect of the contact time on product distribution.

Table 12 shows results of blank experiments, carried out at 700°C with a quartz reactor filled with SiC and glass wool, but without catalyst. Results are compared with the same experiment, carried out in an empty quartz reactor.

Data indicates that ethanol is totally consumed also without catalyst. Main products derive from decomposition to hydrocarbons or from combustion to CO_x. Just a minor amount of it is converted to H_2. Results obtained from the blank experiment are practically the same as

those obtained with empty reactor. The only difference is an higher amount of CO_2 yield and O_2 conversion given by the presence of SiC and glass wool.

Blank experiment, demonstrate that ethanol totally undergoes thermal decomposition.

	X(Ethanol)	Y(Methane)	Y(Ethane)	Y(Ethene)	Y(CO_2)	Y(CO)	Y(H_2)	X (O_2)
Empty	100%	14%	2%	14%	3%	54%	9%	60%
Blank	100%	11%	1%	11%	9%	58%	9%	72%

Table 12: Products yields and reagents conversions obtained with an empty quartz reactor and with the reactor filled with SiC and glass wool (Blank). Reaction conditions: 2.50% ethanol and 3.75% O_2 in N_2, reaction temperature 700°C, atmospheric pressure. All the dashed lines are referred to the secondary axis, on the right.

4.3 Results and discussion

Ethanol partial oxidation was carried out under different conditions in order to investigate the parameters affecting product yield distribution and in order to get some information on the reaction mechanism through analysing the effect of contact time of product formation. Then the effects of metal loading, kind of support and temperature on products yields were also investigated.

4.3.1.1 Investigation about the reaction scheme of ethanol partial oxidation.

Reaction scheme of ethanol partial oxidation was determined through the investigation of the effect of contact time on reagent conversion and products yields. These experiments lead us to identify primary, intermediate, and final products. With this set of information it was then possible to draw a plausible reaction scheme.

Figure 96 shows the effect of contact time on product distribution at 700°C, when ethanol and oxygen are fed to Pt nanoparticles supported over different supports. Carbon balance was always over 90%. Because of technical reasons water is not represented in terms of yield, but in terms of arbitrary units, which are proportional to its quantity, calculated on the base of oxygen balance. This expedient was useful to detect the trend of water production with contact time. Zero contact time was determined by carry out measurements on a reactor loaded with SiC and glass wool, but without catalyst.

Some of the used catalysts appeared to have turned colour from grey to black because of heavy compound deposition. Anyway, any loss of activity or catalyst deactivation was detected, in fact, conversion of feed components and product selectivity were constant along 5 hours of reaction time.

In all cases ethanol conversion was complete, while oxygen conversion was not complete only when the reaction was carried out without catalyst. Products yield distribution was similar in the case of Pt nanoparticles supported over Siral1 or Al_2O_3, but for Pt supported over SiO_2 the situation was slightly different.

With Siral1 and Al_2O_3 supports we observed what follows:

- Ethane, ethene and methane yields declined with the increase of contact time.
- H_2 and CO_2 yields increased.
- CO yield was constant.
- Water trend decreased.

These data indicate that light hydrocarbons are intermediate products yielding CO_2 and H_2. So ethanol is first thermally decomposed to light hydrocarbons with the co-production of water. Then light hydrocarbons react with oxygen to give partial oxidation to H_2 and CO_2, or with water to give steam reforming to CO and H_2. Reactions can be summarized as follow:

$CH_3CH_2OH \rightarrow (C_2H_6 + C_2H_4 + CH_4) + H_2O$

$(C_2H_6 + C_2H_4 + CH_4) + O_2 \rightarrow H_2 + CO_2$

$(C_2H_6 + C_2H_4 + CH_4) + H_2O \rightarrow H_2 + CO$

Anyway is possible that part of the reagent is burnt to CO_2 and H_2O.

CO yield was quite constant probably because its formation was balanced by reactions that consumed it. For example, at low contact time CO can be produced by incomplete combustion or as a co-product of ethanol decomposition to methane. On the other side, at higher contact time, CO can be consumed by oxygen to form CO_2, but at the same time, it can be formed as co-product of steam reforming.

It is also possible that CO is consumed by water gas shift reaction, which transforms water and CO into CO_2 and H_2. This is in line with results obtained, but water gas shift reaction is slightly exothermic, so it is unfavoured at the reaction conditions at which partial oxidation was carried out[159].

With 0,1% Pt/SiO_2 the same trends were shown, but with some differences:

- H_2 yield decreased when catalyst was added to the reactor, then it increased slightly with contact time.
- Methane yield did not decrease.
- Water quantity was higher than in the other two cases.

This behaviour is compatible with the purposed reaction scheme, but in this case the catalyst behaves in a different way. Probably 0,1% Pt/SiO_2 is more efficient to catalyze complete oxidation instead of partial oxidation. This can explain why with this catalyst an higher amount of CO_2 and water is formed, while H_2 yield is lower.

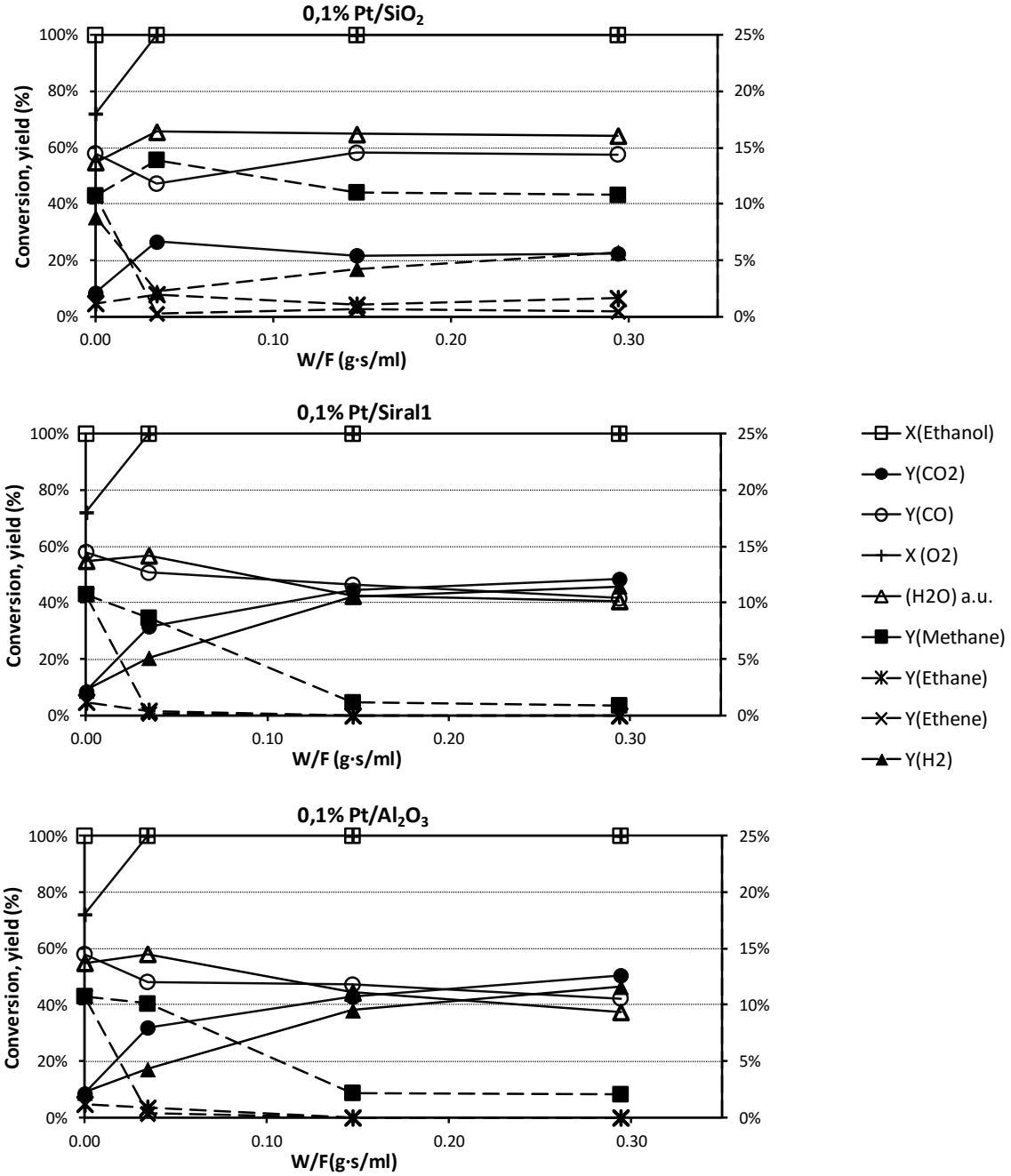

Figure 96: Effect of contact time on product distribution and ethanol conversion in presence of Pt nanoparticles at 0,1% metal loading, supported over SiO_2 (top), Siral1 (centre), C) Al_2O_3 (bottom). Reaction conditions: 2.50% ethanol and 3.75% O_2 in N_2, reaction temperature 700°C, atmospheric pressure. All the dashed lines are referred to the secondary axis, on the right.

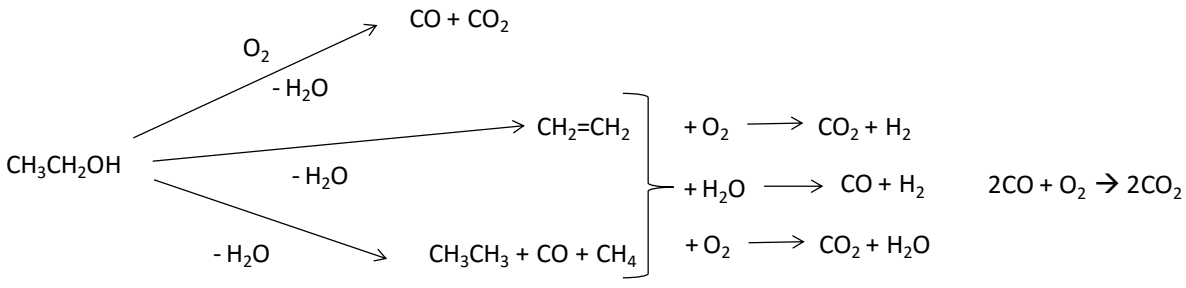

Figure 97: Simplified reaction scheme of ethanol partial oxidation over Pt NPs-based catalysts

4.3.1.2 Effect of the type of support

Product distribution was evaluated at 700°C and 0,29 g·s/ml over different commercial supports with different Si-to-Al ratio, with or without the presence of Pt nanoparticles. Results are shown in Figure 98 and Figure 99. Ethanol conversion was always total; oxygen conversion was total in all cases, except in the blank experiment and in the experiment with bare Al_2O_3. In these two cases conversion was 72 and 76%, Respectively. Carbon balance was always higher than 90%.

All the experiments carried out with bare supports or with empty reactor show the formation of the same products in similar amounts. Methane and ethane were formed with yields around 10% and 1%, respectively. Ethene yield are around 10%, the highest (14%) being shown with SiO_2 and the lowest one (6%) with Siral10. Also CO and H_2 yields were similar in all cases. CO yield was between 50 and 60%, whereas H_2 yield was between 11 and 6%.

In the case of CO_2, differences were more relevant; Siral10 showed the highest yield (24%), whereas the lowest was obtained with the blank reactor (9%). Other CO_2 yields were between 10 and 17%.

Strong differences were shown when Pt nanoparticles were supported over the supports. First, hydrocarbons yields were significantly lower, close to zero in most cases. Moreover, it is possible to detect two main cases:

1. Yield to H_2 and CO_2 were enhanced. This indicates that the catalyst is efficient to catalyze intermediates transformation by means of partial oxidation.
2. CO_x yields were enhanced, with little or nil increment of H_2 yield. This indicates that catalyst is more efficient in intermediates combustion.

Al_2O_3, Siral1 and Siral40 behaved as in case 1, an intermediate behaviour was shown by SIral10, whereas SiO_2 behaviour was more similar to case 2.

Therefore, supports were shown to have a negligible influence on ethanol and intermediate products transformation, in fact product distributions obtained with bare supports were similar to the one obtained with blank reactor. Moreover, in those cases, main reaction seemed to be combustion to CO_x, in fact H_2 formed only in low amount.

On the other hand, partial oxidation to H_2 occurred at a greater extent in the presence of Pt nanoparticles. In this case, differences between catalysts were more marked. In fact the highest H_2 yield was obtained over Pt-Siral10, while the lowest one over Pt-SiO_2.

These results lead to two main conclusions:

- H_2 formation occurs mainly in presence of Pt nanoparticles, while bare supports are inefficient catalysts.
- The main influence of the support on the catalytic behaviour is not given by the interaction between gas-phase molecules and support, but by interaction between Pt nanoparticles and support. In some cases this interaction leads to a strong

enhancement of H_2 and CO_2 yields, while in other cases this enhancement effect is less pronounced or even absent.

It is possible to analyse the influence of SiO_2 and Al_2O_3 content in supports on catalytic performance by comparing H_2 yields and CO_2/CO ratio with support composition. Results of this comparison (Table 13) indicate that the presence of SiO_2 had a detrimental effect on catalytic performance. In fact, the higher was SiO_2 content, the lower were H_2 yield and CO_2/CO ratio. In these cases, the main effect of Pt nanoparticles was that of increasing light hydrocarbons combustion to CO_x.

Best results were obtained with supports containing the greater amount of Al_2O_3. Al_2O_3 and Siral1 showed the best values of both H_2 yield and CO_2/CO ratio, Siral10 showed a slight improvement of H_2 yield, but CO_2/CO ratio slightly decreased.

Therefore, it is possible to conclude that best performance was obtained when Pt nanoparticles were supported over Al_2O_3-rich supports, whereas when they were supported over SiO_2-rich supports they catalyzed more efficiently combustion than partial oxidation to H_2.

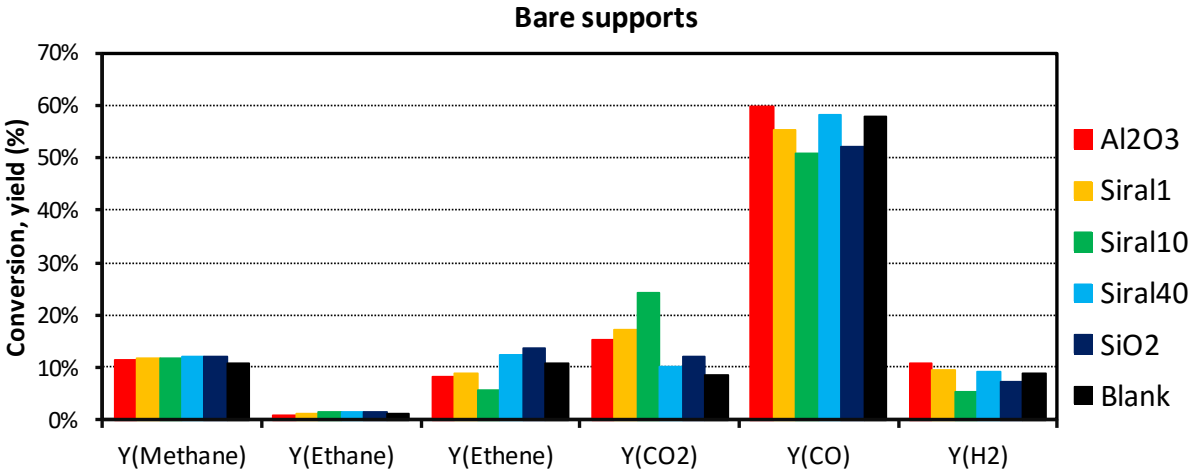

Figure 98: Effect of different bare supports based on SiO_2 and Al_2O_3 on product distribution. Blank experiment was carried out in a reactor filled with SiC and glass wool. Reaction conditions: 2.50% ethanol and 3.75% O_2 in N_2, contact time 0.29 g·s/ml, atmospheric pressure, 700°C. Ethanol conversion was total in all cases.

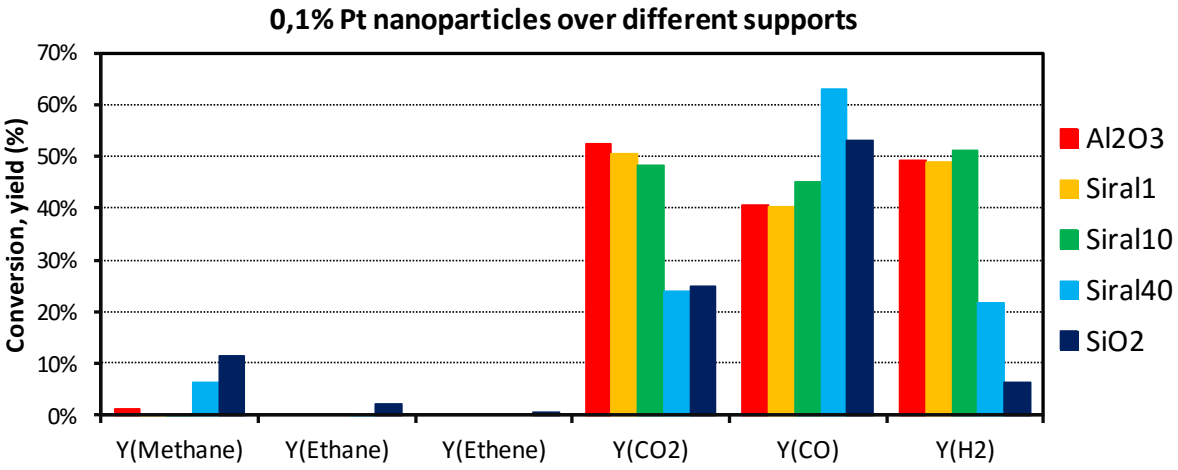

Figure 99: Effect on product distribution of loading 0,1% Pt nanoparticles on different supports. Reaction conditions: 2.50% ethanol and 3.75% O_2 in N_2, contact time 0.29 g·s/ml, atmospheric pressure, 700°C. Ethanol conversion was total in all cases.

SiO_2 content (% m/m)	H_2 Yield	CO_2/CO
100 (SiO_2)	6%	0.47
40	22%	0.38
10	51%	1.07
1	49%	1.25
0 (Al_2O_3)	49%	1.29

Table 13 (referred to Figure 99): Effect of SiO_2 content of the support toward H_2 yields and CO_2/CO yields ratio.

4.3.1.3 Effect of metal loading

As said before, one of the most important advantages given by the nanoparticles is that, because of their high activity, a lower metal loading is needed. This implies a lower catalyst cost. However, one of the risks that may occur working with nanoparticles is to obtain a lower intrinsic activity when a higher metal loading is used. This happens because nanoparticles tend to aggregate into larger particles. Therefore an investigation on the effect of metal loading can provide useful information on the range at which metal nanoparticles show higher activity. Moreover, the comparison between product distribution at different metal loading also allows to better discriminate on which reactions are catalyzed by the nanoparticles and which by the support.

Figure 100 shows the effect of metal loading on product distribution at 700°C and 0.29 g·s/ml contact time.

In all cases carbon balance was higher than 89%. As in the previous paragraph, water is indicated in terms of arbitrary units.

Some general trends can be observed in all cases with the increase of metal loading:

- Methane yield decreased. The strongest decrease was shown between 0.01 and 0.1% metal loading, while yields between 0 and 0.01% were similar.

- Ethene formed in absence of Pt nanoparticles, then it was immediately consumed, also at the lowest metal loading, and its yield decreased significantly.
- Ethane yield was around 1% in all cases. It was consumed with the increase of metal loading.
- CO yield was between 60 and 80% with the bare support, at 0.01% Pt content it was produced with similar yield in most cases. Finally, its yield decreased significantly between 0.01 and 0.1%Pt loading. This last effect was not shown by SiO_2 and Siral40. In these latter cases, in fact, CO yield was stable around 60%.
- CO_2 and H_2 yields grew, with the exception of Pt/SiO_2.
- Water formation declined.

Differences of product yields between the various catalysts were in line with those discussed in the previous chapter.

These data indicates that the metal plays a key role in the transformation of intermediates to H_2. With the bare support, ethanol is mainly decomposed into methane, ethane and ethene or burnt to CO and CO_2, and just a little amount of it is transformed to H_2.

When 0.01% Pt nanoparticles are added, steam reforming and partial oxidation start to take place, which lead to an improvement of H_2 yield. The latter undergoes further increase at the highest metal loading; moreover at 0.01% Pt loading, CO yield declines in favour of CO_2. Best results were obtained with 0.1% Pt loading; in fact, the highest H_2 yields were found, and CO yield was the lowest, in favour of CO_2.

The increase of metal loading led to a general improvement of desired products yields without any loss of activity; this indicates that, in these conditions, Pt nanoparticles did not undergo aggregation effects, which should have led to loss of activity and selectivity.

As described at the beginning of the chapter, metal nanoparticles are more active than particles of bigger size. So, theoretically a lower metal loading is required to carry out the reaction. Table 14 shows a brief comparison with some literature data regarding ethanol partial oxidation carried out over Pt-based catalysts. Experiments reported in literature were carried out at different reaction conditions. Therefore an unambiguous comparison is difficult; anyway, it is possible to make some observations. In examples taken from literature, Pt-based catalysts contained either 1.5 or 5% metal loading, an showed 48% maximum selectivity to H_2[160]. This result is comparable with the one obtained in this work, but in our case it was obtained with a metal loading fifty time lower. Moreover all non-nanometric Pt-based catalysts need a preactivation in H_2 flow, which is not necessary with our Pt nanoparticles. These data confirm that nanoparticles show a greater activity. Sometimes, greater activity means lower selectivity, but, in our case, Pt nanoparticles, not only were more active, but also maintained a high selectivity to H_2. Finally, it is possible to comment that results obtained with 0,1% Pt nanoparticles supported over Al_2O_3 gave the best performance compared to catalysts from literature, shown in Table 14.

So, because of their higher activity and selectivity, Pt nanoparticles represent a good alternative as catalysts for ethanol partial oxidation. In fact, it is possible to prepare catalysts with lower metal loading and with an higher efficiency for partial oxidation. This makes it possible to obtain best results using lower quantity of noble metal. Moreover Pt nanoparticles do not need any preactivation procedure. The only drawback of nanoparticles is that the synthesis procedure is more complex than for conventional supported catalysts.

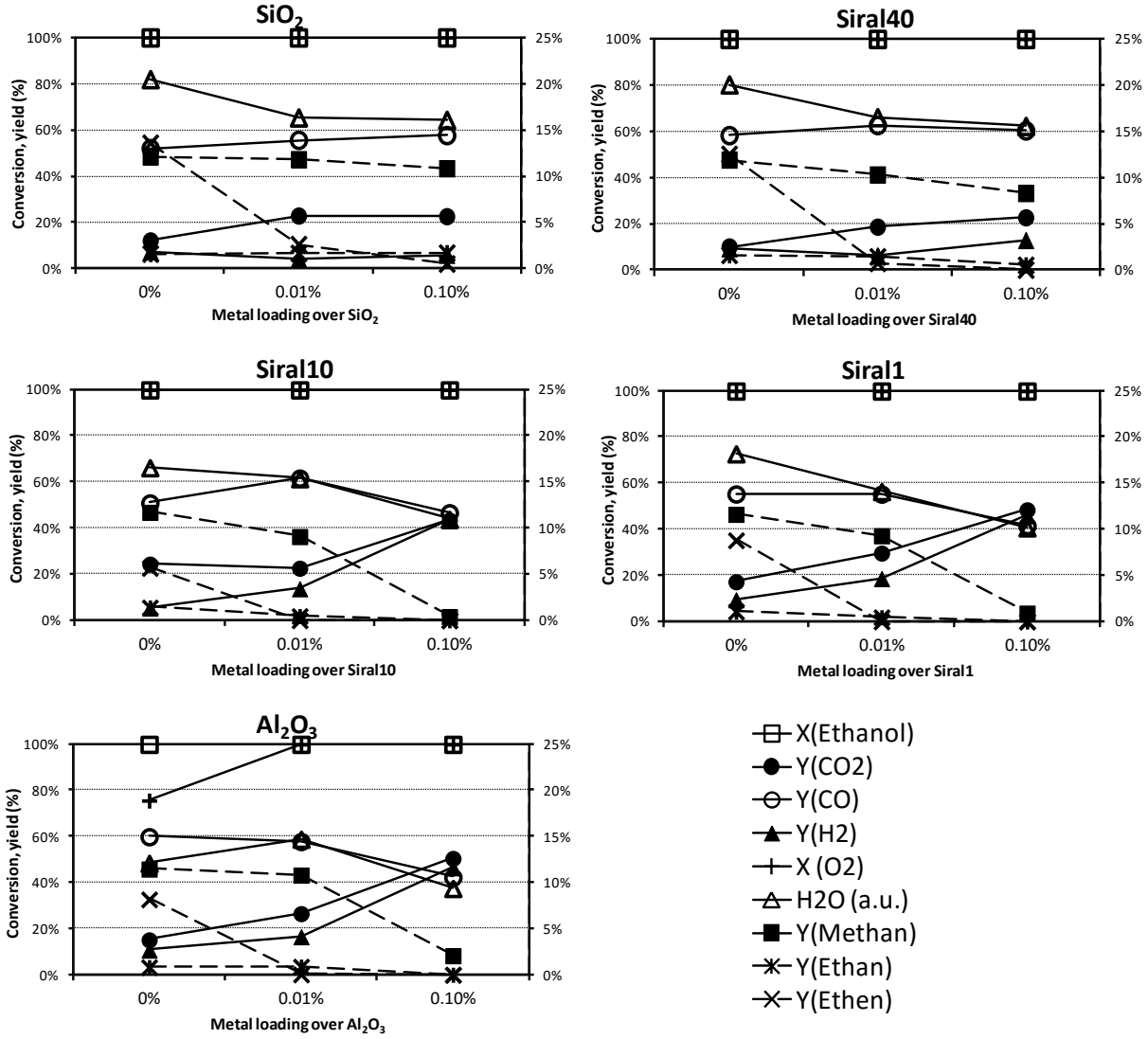

Figure 100: Effect of metal loading on product distribution and ethanol conversion in presence of Pt nanoparticles supported over different supports. 0% metal loading indicates that the reaction was carried out over the bare support. Reaction conditions: 2.50% ethanol and 3.75% O_2 in N_2, contact time 0.29 g·s/ml, atmospheric pressure, 700°C. All the dashed lines are referred to the secondary axis, on the right.

Catalyst	Reaction conditions: T (°C) – Ethanol/O_2	Y H_2 (X Ethanol) (%)	Metal loading (%)	Reference
Pt/γ-Al_2O_3	700 – 1.5	41 (85)	5	160
Pt/ZrO_2	900 (adiabatic) – 1.5	21 (70)	2	161
Pt/Al_2O_3	300 – 2	0 (80)	1.5	162
Pt/ZrO_2	300 – 2	20 (80)	1.5	162
Pt/$CeZrO_2$	300 – 2	20 (80)	1.5	162
Pt/CeO_2	400 – 2.5	30 (100)	1.5	163
Pt/Al_2O_3	700 – 0.67	49 (100)	0.1	This work

Table 14: Partial oxidation of ethanol with Pt-based catalyst. Comparison with literature data. H_2 Yields are re-calculated with the formula used in this work.

4.3.1.4 Effect of temperature

Some experiments were carried out in order to evaluate Pt nanoparticles activity at different temperatures.

Figure 101 shows the effect of temperature on product distribution with different catalysts.

In all cases both ethanol and oxygen conversion were total (the latter is not shown in the graph).

Carbon balance was around 70% at 500°C, but it increased with temperature, up to values higher than 90% at 700°C. Low carbon balances at lower temperatures may indicate formation of carbonaceous deposits or other unidentified compounds deriving from ethanol decomposition. With the increase of temperature heavy compounds formations was probably prevented by combustion or partial oxidation of coke precursors[164].

Both H_2 and CO yields grew with rising temperature; other products behaved differently depending on the catalyst used. The yield of light hydrocarbons was higher at 500°C and it declined with the raise of temperature, mainly in favour of CO and H_2. In all cases, except for 0.1% Pt/SiO_2, the yield of methane showed a maximum at 600°C, then it decreased. This behaviour indicates that ethanol decomposition to methane increased from 500 to 700°C. At 700°C, temperature is high enough to oxidize methane to H_2 and CO_x, whereas at 600°C this reaction probably occurs at a lower extent, and methane yield is higher. 0.1% Pt/SiO_2 is an exception because methane yield increased with temperature and did not show a maximum value. This happens because, as shown before, 0.1% Pt/SiO_2 seems to be a poorly efficient catalyst for the production of H_2 by partial oxidation, and part of methane remains unconverted.

The best temperature to obtain the highest H_2 yield was 700°C, but one of the objectives of partial oxidation is to limit CO formation, in order to obtain a mixture composed mainly of H_2 and CO_2. Figure 102 shows the effect of temperature on CO_2/CO ratio with the different catalysts. For all catalysts, this ratio decreased with temperature. Despite the best H_2 yields

were obtained at the highest temperature, an increment of the latter has a detrimental effect if our purpose is to limit CO formation.

CO formation can derive from partial combustion, ethanol decomposition or steam reforming. It is possible to state that the increase of CO yield mainly derives from steam reforming because of the following reasons:

- Steam reforming is the only reaction that leads to the formation of both CO and H_2.
- Data show that the amount of water decreases with an increase of temperature.
- Steam reforming is endothermic and is favoured at high temperature.

To summarize: the general effect of temperature is to increase hydrogen yield, probably by favouring the transformation of light hydrocarbons and coke precursors. This probably occurs mainly by steam reforming. In fact, the decline of light hydrocarbons yield with the increase of temperature, correspond to an increase of CO and H_2, whereas CO_2 yield remains constant or, in some cases, even decreases. Anyway, data obtained are not sufficient to exclude that the increase of H_2 yield with temperature is given at a certain extent by partial oxidation also.

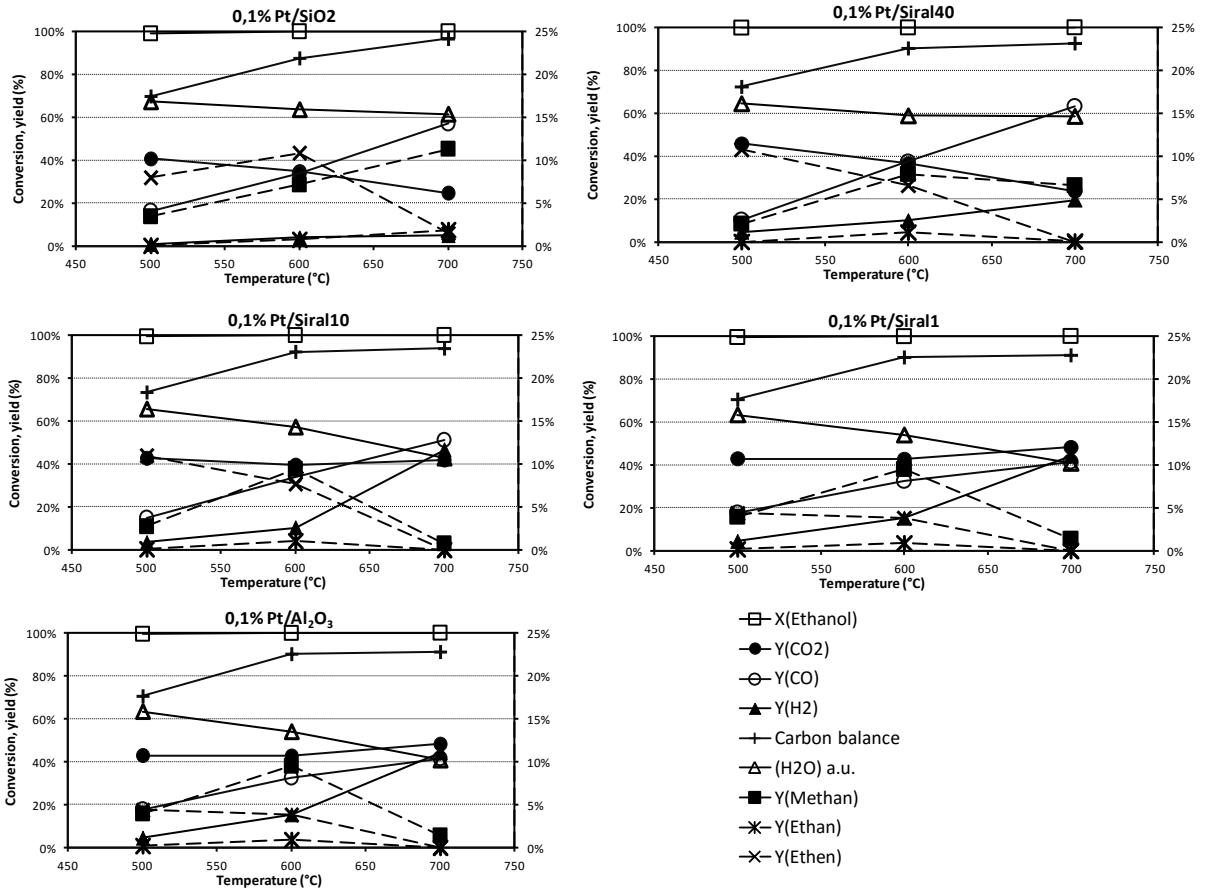

Figure 101: Effect of temperature on product distribution and ethanol conversion in presence of Pt nanoparticles at 0,1% metal loading, supported over different supports. Reaction conditions: 2.50% ethanol and 3.75% O_2 in N_2, contact time 0.29 g·s/ml, atmospheric pressure. All the dashed lines are referred to the secondary axis, on the right.

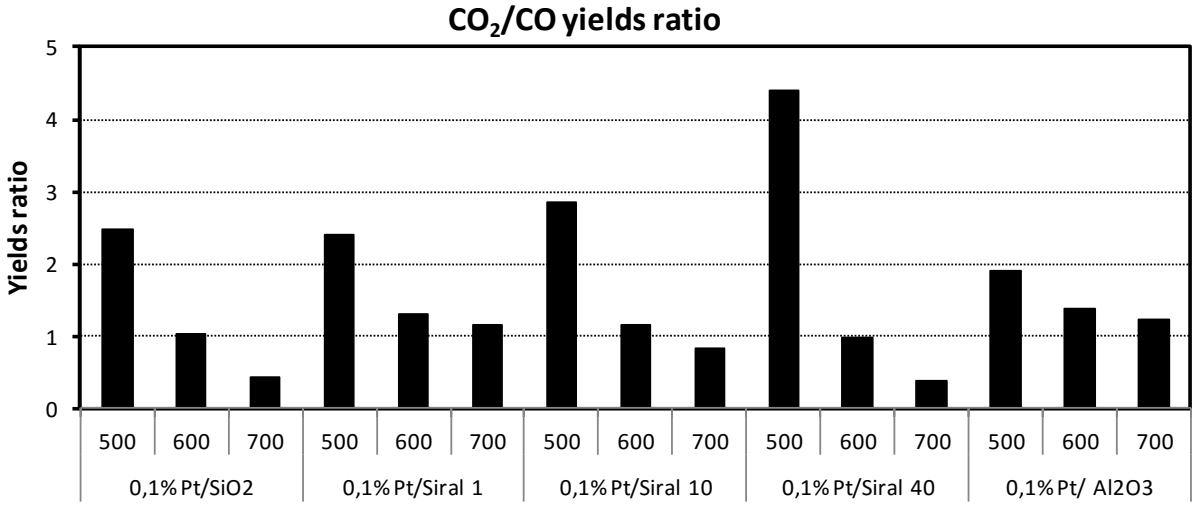

Figure 102: Effect of temperature on CO_2/CO yields ratio over different catalysts.

4.3.1.5 Comparison among Pt, Rh and Ru nanoparticles activity over different supports.

The catalytic activity of Pt, Rh and Ru nanoparticles was compared over different supports, at 700°C and 0.29 g·s/ml; results are shown in Figure 8.

Pt, Ru and Rh nanoparticles were shown to be active in ethanol partial oxidation, and their catalytic activity is strongly influenced by the kind of support.

Good results (with H_2 and CO_2 yields over 40%) were obtained when metal nanoparticles were supported over Siral10 and Siral1. Low H_2 and CO_2 yields were obtained over SiO_2 and SIral40. 0.05% Rh and 0.05% Ru over Al_2O_3 showed good CO_2 but poor H_2 yield, whereas, over the same support, Pt showed H_2 yield close to 50%.

Therefore, it is possible to generalize that Pt, Rh and Ru nanoparticles can be active and selective catalysts for ethanol partial oxidation, but their catalytic properties strictly depend on the support type. When they are supported over Siral1 and Siral10, it is possible to obtain high selectivity in partial oxidation, while the opposite occurs with SiO_2.

Anyway, the most curious behaviour is obtained with Al_2O_3; in fact, when Pt, Ru or Rh are supported on alumina, significantly different results are observed; with Pt, is possible to obtain 49% H_2 yield, which decreases down to 30% with Rh and to 18% with Ru.

Some further information can be obtained by comparing the behaviour of bare alumina with that one of supported catalysts (Figure 104).

A remarkable difference is observed for methane yield: it is close to zero with Pt/Al_2O_3, while it is around 10% in the other two cases. If we compare results shown in Figure 104, we can see that the yield shown by Rh and Ru nanoparticles supported over Al_2O_3 is the same as that one obtained with bare Al_2O_3. Moreover these two catalysts appear not to be able to convert ethane, whereas ethene was converted in all of the three cases. This means that these two catalysts are not able to convert methane and ethane to CO_x and H_2. This result is in contrast with what reported in literature for methane partial oxidation. In fact, literature

data show the opposite behaviour: with Pt nanoparticles supported over Al_2O_3 , methane transformation to H_2 is less efficient than with the catalysts based on Rh nanoparticles[154.] However, in the case of ethanol partial oxidation we need to take into account that not only methane reaches the catalytic surface. As explained before, ethanol thermally decomposes to yield a mixture of products, which are then transformed further. Methane is only one component of this mixture, and it is possible that the other components have a negative influence on the catalytic behaviour. An explanation for this behaviour can be given by taking into account competitive absorption phenomena. For example, it is possible to observe that oxygen is totally converted only when metal nanoparticles are present, otherwise, with bare alumina, it reaches 76% conversion only.

This means that the three types of metal nanoparticles investigated are able to activate oxygen, but the latter will react with the chemical species with the higher concentration over the catalyst surface. The latter will depend on the affinity of the different catalysts toward each one of the compounds present in the gas-phase.

So, 0.1% Pt/Al_2O_3 converts both CO and hydrocarbons, the first to CO_2 and the latter to H_2 and CO_x. This probably means that 0.1% Pt/Al_2O_3 shows similar affinity for hydrocarbons and CO. On the other hand, 0.05% Rh/ Al_2O_3 and 0.05% Ru/ Al_2O_3 do not convert hydrocarbons efficiently, but they are efficient in the conversion of CO to CO_2. This means that, in this case, Rh and Ru over alumina show stronger affinity for CO than for the other intermediates, and this results in a lower hydrogen yield.

Indeed, these arguments are fully speculative. The real situation is evidently much more complex. As explained before, partial oxidation involves a complex network of reaction, in which any reaction can have influence on the others. Therefore, Rh and Ru have probably more affinity toward CO, but, as shown in the figure, they can convert also ethylene, and the latter can be converted in part by means of partial oxidation, in part by steam reforming and in part by combustion. The final amount of hydrogen, CO and CO_2 will be given by the relative contribution of these three reactions.

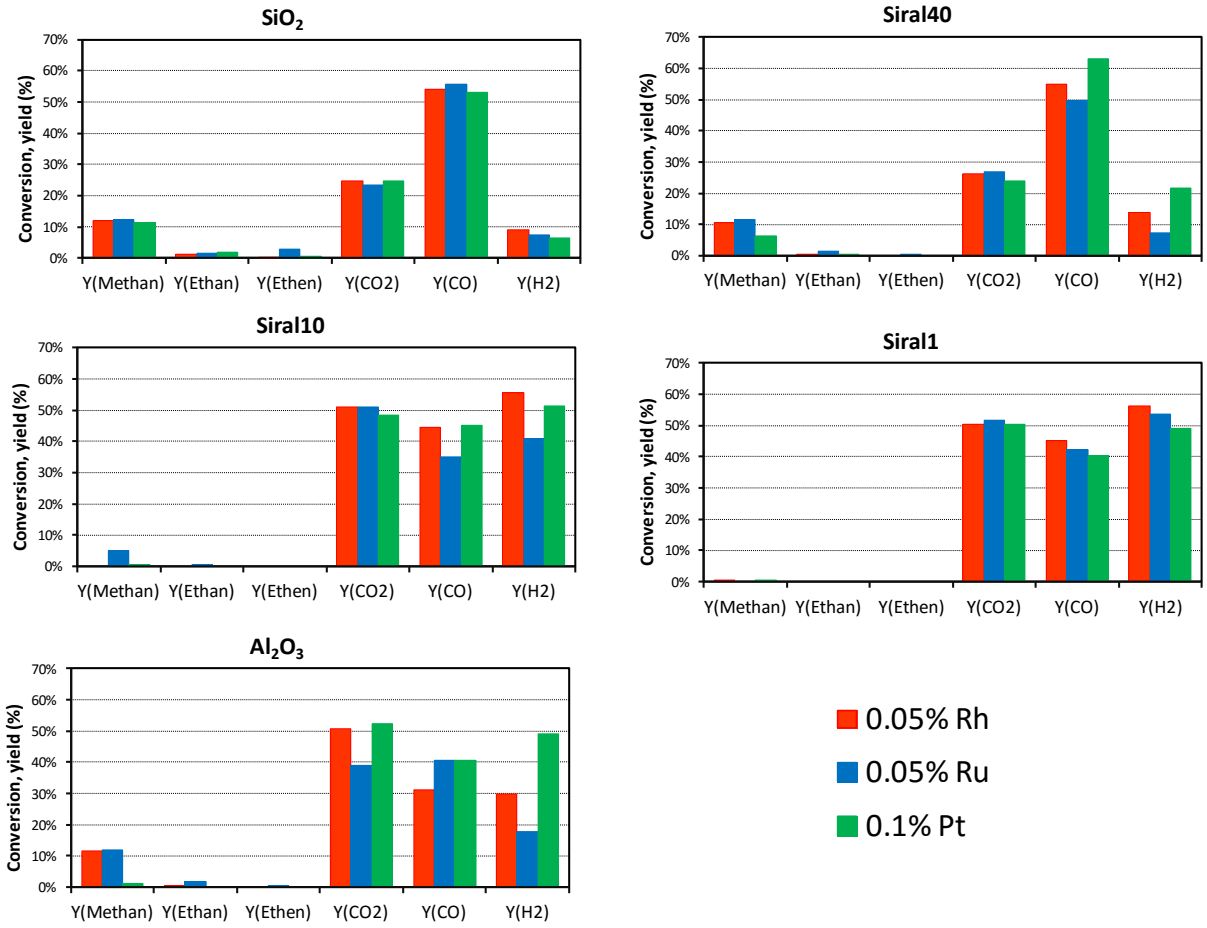

Figure 103: Comparison between results obtained with 0.1% Pt, 0.05% Rh and 0.05% Ru nanoparticles loaded over different supports. Reaction conditions: 700°C, 2.50% ethanol and 3.75% O_2 in N_2, contact time 0.29 g·s/ml, atmospheric pressure.

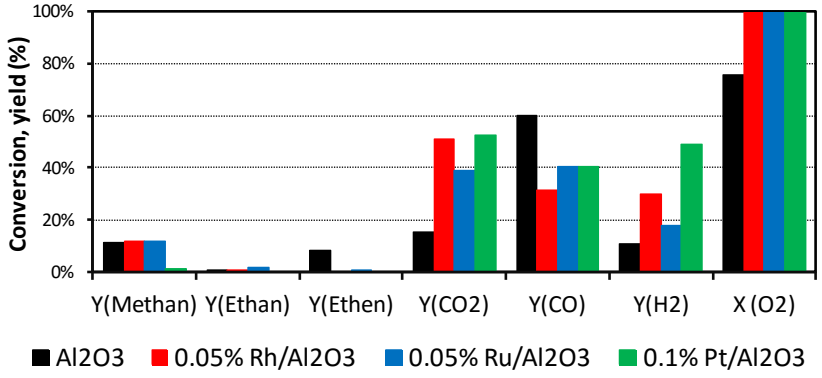

Figure 104: Comparison between the catalytic behaviour of Al_2O_3 and Rh, Ru and Pt nanoparticles supported over Al_2O_3. Reaction conditions: 700°C, 2.50% ethanol and 3.75% O_2 in N_2, contact time 0.29 g·s/ml, atmospheric pressure. Ethanol conversion was total in all cases.

4.4 Summary

It was demonstrated that deposition of colloidally prepared well-defined noble Rh, Ru or Pt nanoparticles results in active and selective catalysts for ethanol partial oxidation to H_2 and CO_2. In fact, with a metal loading from 10 to 100 times lower than conventional catalysts (see Table 14), it is possible to obtain H_2 yield around 50%.

On the basis on the effect of contact time on product distribution at 700°C, it can be concluded that the first step of ethanol partial oxidation is its conversion into C_1-C_2 hydrocarbons, CO_x, water and a small amount of H_2. Then, the hydrocarbons are transformed to CO, H_2 and CO_2 by partial oxidation and steam reforming. Finally, CO can be further oxidized to CO_2 to a minor extent. The increase in temperature from 500 to 700°C contribute to convert more efficiently the intermediates into H_2 and CO_x. But, on the other side, it has a detrimental effect, because it causes a decrease of CO_2/CO ratio. This may happen because higher temperatures favour steam reforming, a reaction which consumes water and hydrocarbons intermediates to produce CO and H_2.

It was confirmed that Pt, Rh and Ru nanoparticles are the active species, which enhance the transformation of intermediates to H_2 and CO_x. Indeed, bare supports (SiO_2, Siral1, Siral10, Siral40 and Al_2O_3) have a negligible influence on products distribution, and improvement in H_2 yield are detected only in presence of supported Pt, Rh or Ru nanoparticles. However, the supports plays a key role in the overall catalytic performances, best results were obtained when Pt, Rh or Ru nanoparticles are loaded over Al_2O_3, Siral1 and Siral10. With these catalysts, both H_2 and CO_2 yields were between 40% and 55% at 700°C, which are the best results obtained in this work.

Since it was determined that bare supports have a negligible influence on products distribution, the reason of different behaviour should be investigated in the effects connected with different interactions between nanoparticles and supports. For example different oxygen mobility of the support can affect the redox properties of the nanoparticles[162]. Another possibility is that nanoparticles catalytic activity is affected by the way in which the intermediates are absorbed over supports. Some spectroscopic studies, such as in-situ DRIFT experiments, combined with catalyst characterization, such as TPROR, can better elucidate the reasons of such different behaviours.

Versalis SpA is gratefully acknowledged for sponsoring part of the research activity described in this thesis.

Prof. Dr. Fabrizio Cavani is heartily acknowledged to give me the magnificent opportunity to attend this PhD course at the research group of "Catalytic processes development" of the University of Bologna, under its supervision.

5. BIBLIOGRAPHY

[1] F. Cavani, G. Centi "Sustainable Development and Chemistry" *Kirk Othmer Encyclopedia of Chemical Technologies*.

[2] De Jong, E.; Higson, A.; Walsh, P.; Wellisch, M. *Bio-based Chemicals*, **2012** IEA Bioenergy – Task 42 Biorefinery.

[3] J. H. Clark *Green Chemistry* **1999**, *1*, 1, 1

[4] F. Sandun, S. Adhikari, C. Chauda, M. Naveen *Energy and Fuels,* **2006**, *20*, 1727

[5] B. G. Hermann, K. Blok, M. K. Patel *Environmental Science and Technologies,* **2007**, *41*, 7915

[6] B. Kamm, P. R. Gruber, M. Kamm "Biorefineries – Industrial Processes and Products" *Ullmann's Encyclopedia of Industrial Chemistry*

[7] E. de Jong, A. Higson, P. Walsh, M. Wellisch *Biofuels, Bioproducts and Biorefining*, **2012**, *6*,606

[8] E. de Jong, M. A. Dam, L. Sipos, G.-J. M. Gruter *ACS Symposium Series*, **2012**, *1105*, 1

[9] V. Benessere, M. E. Cucciolito, A. De Santis, M. Di Serio, R. Esposito, F. Ruffo, R. Turco *Journal of American Oil Society,* **2015**, *92*, 1701

[10] A. Godard, P. De Caro, S. Thiebaud-Roux, E. Verdenne, Z. Mouloungui *Journal of American Oil Society,* **2013**, *90*, 133

[11] P. T. Anastas, J. B. Zimmerman *Environonmental Sicence and Technologies,* **2003**, *37*, 94A

[12] S. Tang, R. Bourne, R. Smith, M. Poliakoff, *Green Chemistry*, **2008**, *10*, 268.

[13] E. V. Makshina, M. Dusselier, W. Janssens, J. Degrève, P. A. Jacobs, B. Sels *Chem. Soc. Rev.* **2014**, *43*, 7917

[14] C. Angelici, B. M. Weckhuysen, P. C. A. Bruijnincx *ChemSusChem* **2013**, *6*, 1

[15] R. Arjona Antolin, J. L. Sanz Yague, A. Corma Canos, M. E. Domine WO 2014/001595 A1 (03 January 2014) assigned to "Albengoa Bioenergia Nuevas Tecnologias S.A."

[16] B. Jorgensen, S. E. Christiansen, M. L. Dahl Thomsen, C. H. Cristiensen *Journal of Catalysis*, **2007**, *251*, 332

[17]P. C. Zonetti, J. Celnik, S. Letichevsky, A. B. Gaspar, L. G. Appel, *Journal of Molecular Catalysis A: Chemical*, **2011**, *334*, 29

[18] H. Idriss, E. G. Seebauer *Journal of Molecular Catalysis A: Chemical,* **2000**, *152*, 201

[19] Posada, J. A.; Patel, A. D.; Roes, A.; Blok, K.; Faaij, A. P. C.; Patel, M. K. *Bioresour. Technol.*, **2013**, *135*, 490.

[20] Rass-Hansen, J.; Falsig, H.; Jørgensen, B.; Christensen, *C. H. J. Chem. Technol. Biotechnol.*, **2007**, 82, 329.

[21] Kilos, B.; Bell, A. T.; Iglesia, E. *J. Phys. Chem. C*, **2009**, *113*, 2830.

[22] Miller, J. M.; Lakshmi, L. J.; Ihasz, N. J.; Miller, J. M. *J. Mol. Catal. A Chem.,* **2001**, *165*, 199.

[23] Jørgensen, B.; Kristensen, S. B.; Kunov-Kruse, A. J.; Fehrmann, R.; Christensen, C. H.; Riisager, A. *Top. Catal.,* **2009**, *52*, 253.

[24] Feng, T.; Vohs, J. *J. Phys. Chem. B,* **2005**, *109*, 2120.

[25] Oyama, S. T.; Somorjai, G. a. *J. Phys. Chem.* **2009**, *94*, 5022.

[26] Wang, C.; Cai, Y.; Wachs, I. E. *Langmuir,* **1999**, *15*, 1223.

[27] Sobolev, V. I.; Danilevich, E. V.; Koltunov, K. Y. *Kinet. Catal.,* **2013**, *54*, 730.

[28] Santacesaria, E.; Sorrentino, A.; Tesser, R.; Di Serio, M.; Ruggiero, a. *J. Mol. Catal. A Chem.* **2003**, *204-205*, 617.

[29] Yun, D.; Zhao, Y.; Abdullahi, I.; Herrera, J. E. *J. Mol. Catal. A Chem.,* **2014**, *390*, 169.

[30] Lin, H. M.; Kao, S. T.; Lin, K. M.; Chang, J. R.; Shyu, S. G. *J. Catal.*, **2004**, *224*, 156.

[31] Chimentão, R. J.; Herrera, J. E.; Kwak, J. H.; Medina, F.; Wang, Y.; Peden, C. H. F.: *Appl. Catal. A Gen.*, **2007**, *332*, 263.

[32] Herrera, J. E.; Isimjan, T. T.; Abdullahi, I.; Ray, A.; Rohani, S.: *Appl. Catal. A Gen.*, (2012), *417-418*, 13.

[33] Kwak, J. H.; Herrera, J. E.; Hu, J. Z.; Wang, Y.; Peden, C. H. F.: *Appl. Catal. A Gen.* **2006**, *300*, 109.

[34] Li, X.; Iglesia, E. *Chemistry,* **2007**, *13*, 9324.

[35] Kim, D. W.; Kim, H.; Jung, Y. S.; Kyu Song, I.; Baeck, S. H.: *J. Phys. Chem. Solids,* **2008**, *69*, 1513.

[36] Mehlomakulu, B.; Nguyen, T. T. N.; Delichre, P.; Van Steen, E.; Millet, J. M. M.: *J. Catal.*, **2012**, *289*, 1.

[37] Gomez, M. F.; Arrua, L. a; Abello, M. C. *Ind. Eng. Chem. Res*., **1997**, 36, 3468.

[38] Koltunov, K. Y.; Sobolev, V. I. *Catal. Ind.*, **2012**, *4*, 247

[39] Feng, T.; Vohs, J. M.: *J. Phys. Chem. B,* **2004**, 108, 5647.

[40] Beck, B.; Harth, M.; Hamilton, N. G.; Carrero, C.; Uhlrich, J. J.; Trunschke, A.; Shaikhutdinov, S.; Schubert, H.; Freund, H. J.; Schlögl, R.; Sauer, J.; Schomäcker, R. *Journal of Catalysis*, **2012**, 296, 120.

[41] Tesser, R.; Maradei, V.; Di Serio, M.; Santacesaria, E. *Ind. Eng. Chem. Res.* **2004**, 43, 1623.

[42] Lin, Y. C.; Chang, C. H.; Chen, C. C.; Jehng, J. M.; Shyu, S. G. *Catal. Commun.* **2008**, 9, 675.

[43] Quaranta, N. E.; Soria, J.; Cortés Corberán, V.; Fierro, J. L. G. *J. Catal.* **1997**, 171, 1.

[44] Massa, M.; Häggblad, R.; Andersson, A. *Top. Catal.,* **2011**, *54*, 685.

[45] Häggblad, R.; Wagner, J. B.; Hansen, S.; Andersson, A. *J. Catal.,* **2008**, *258*, 345.

[46] Häggblad, R.; Massa, M.; Andersson, A. *J. Catal,.* **2009**, *266*, 218.

[47] Häggblad, R.; Hansen, S.; Wallenberg, L. R.; Andersson, A. J. Catal., **2010**, 276, 24.

[48] Wang, F.; Xu, J.; Dubois, J.-L.; Ueda, W. *ChemSusChem,* **2010**, *3*, 1383.

[49] Massa, M.; Häggblad, R.; Hansen, S.; Andersson, A. *Appl. Catal. A Gen.,* **2011**, *408*, 63.

[50] Routray, K.; Zhou, W.; Kiely, C. J.; Wachs, I. E. ACS Catal., **2011**, 1, 54.

[51] Liu, F.; He, H.; Lian, Z.; Shan, W.; Xie, L.; Asakura, K.; Yang, W.; Deng, H., *J. Catal.,* **2013**, 307, 340.

[52] Hikazudani, S.; Kikutani, K.; Nagaoka, K.; Inoue, T.; Takita, Y. *Applied Catalysis A: General* **2008**, *345*, 65

[53] Owen, O. S.; Kung, M. C.; Kung, H. H. *Catalysis Letters* **1992**, *12*, 45

[54] Resini, C.; Milella, F.; Busca, G. *Phys. Chem. Chem. Phys.* **2000**, *2*, 2039

[55] Briand, L. E.; Jehng, J.-M.; Cornaglia, L.; Hut, A. M.; Wachs, I. E. *Catalysis Today* **2008**, *78*, 257

[56] Wachs, I. E.; Birand, L. WO 03/053556 A2, Assigned to Leigh University.

[57] Nivoix, V.; Gillot, B. *Mater. Chem. Phys.* **2000**, *63*, 24.

[58] Nivoix, V.; Gillot, B. *Chem. Mater.* **2000**, *12*, 2971.

[59] Nivoix, V.; Bernard, F.; Gaffet, E.; Perriat, P.; Gillot, B. *Powder Technol.* **1999**, *105*, 155.

[60] Nivoix, V.; Gillot, B. *Solid State Ionics* **1998**, *111*, 17.

[61] Science, E. **2000**, *34*, 1735.

[62] Nakamura, Y.; Murayama, T.; Ueda, W. *ChemCatChem* **2014**, 6, 741

[63] Morton, C. D.; Slipper, I. J.; Thomas, M. J. K.; Alexander, B. D., *J. Photochem. Photobiol. A Chem.* **2010**, *216*, 209.

[64] Mandal, S.; Hazra, S.; Das, D.; Ghosh, A. *J. Non. Cryst. Solids* **1995**, *183*, 315.

[65] Tian, H.; Wachs, I. E.; Briand, L. E. *J. Phys. Chem. B*, **2005**, *109*, 23491.

[66] Gillot, B.; Nohair, M. *Phys. Status Solid Appl. Res.,* **1995**, *148*, 239.

[67] Nohair, M.; Aymes, D.; Perriat, P.; Gillot, B. *Vib. Spectrosc.* **1995**, *9*, 181.

[68] Klissurski, D.; Iordanova, R.; Radev, D.; Kassabov, S.; Milanova, M.; Chakarova, K. *J. Mater. Sci.* **2004**, *39*, 5375.

[69] Gillot, B.; Nivoix, V. *Mater. Res. Bull.,* **1999**, *34*, 1735.

[70] Nivoix, V.; Gillot, B. *Solid State Ionics,* **1998**, *111*, 17.

[71] Nivoix, V.; Gillot, B. *Chem. Mater.,* **2000**, *12*, 2971.

[72] Šurca Vuk, A.; Orel, B.; Dražič, G. *J. Solid State Electrochem.,* **2001**, *5*, 437.

[73] Šurca Vuk, A.; Orel, B.; Dražič, G.; Colomban, P. *Monatshefte fur Chemie / Chem. Mon.* ***2002***, *133*, 889.

[74] Trevisanut, C.; Bosselet, F.; Cavani, F.; Millet, J. M. M. *Catal. Sci. Technol.* **2015**, *5*, 1280.

[75] Cocchi, S.; Mari, M.; Cavani, F.; Millet, J. M. M. *Appl. Catal. B Environ.* **2014**, *152-153*, 250.

[76] Trevisanut, C.; Mari, M.; Millet, J.-M. M.; Cavani, F. *Int. J. Hydrogen Energy* **2015**, *40*, 5264.

[77] Ochoa, J. V.; Trevisanut, C.; Millet, J.-M. M.; Busca, G.; Cavani, F. *J. Phys. Chem. C* **2013**, *117*, 23908.

[78] Kodama, T.; Gokon, N. *Chem. Rev.* **2007**, *107*, 4048.

[79] Chieregato, A.; Velasquez Ochoa, J.; Bandinelli, C.; Fornasari, G.; Cavani, F.; Mella, M. *ChemSusChem* **2015**, *8*, 377.

[80] C. Badini, G. Saracco, V. Serra *Appl. Catal. B. Environ.* **1997**, *11*, 307

[81] Nyquist, R.A.; Kaegel R. O. *Infrared Spectra of Inorganic Compounds*, Academic Press INC, **1971**

[82] Resini, C.; Milella, F.; Busca G. *Phys. Chem. Chem. Phys.* **2000**, *2,* 2039

[83] De Waal, D.; Hutter, C. *Material Research Bulletin* **1994**, *29*, 8, 843

[84] Wei, Y. J.; Nam, K. W.; Chen G.; Ryu, C. W.; Kim, B. K. *Solid State Ionics* **2005**, *176*, 2243

[85] Volkov, V. L.; Kadyrova, N. I.; Zakharova, G. S.; Kuznetsov, M. V.; Podval'naya, N. V.; Mikhalev, K. N.; Zainulin, Yu. G. *Russian Journal of Inorganic Chemistry* **2007**, *52*, 3, 329

[86] Owen, O. S.; Kung, H. H. *Jour. Mol. Cat.* **1993**, *79*, 265

[87] Texier, F.; Servant, L.; Bruneel, J. L.; Argoul, F. *Jour. Electroanal. Chem.* **1998**, *446*, 189.

[88] Zonetti, P. C.; Celnik, J.; Letichevsky, S.; Gaspar, A. B.; Appel, L. G. *Jour. Mol. Cat. A: Chemical* **2011**, *334*, 29.

[89] Inui, K.; Kurabayashi T.; Sato, S. *App. Cat. A: General* **2002**, *237*, 53

[90] Botto, I. L.; Vassallo, M. B.; Baran, E. J.; Minelli, G. *Materials Chemistry and Physics* **1997**, *50*, 267.

[91] Safety Data Sheet – Isoprene. Provided by Sigma Aldrich Co.

[92] Chemsystems Perp programs – Isoprene/Bioisoprene, PERP 2012S2, report abstract, April 2013.

[93] M. Guaita, F. Ciardelli, F. La Mantia, E. Pedemonte, *Fondamenti di scienza dei polimeri,* Edizioni nuova cultura.

[94] M. Morton, *Elastomers, synthetic, survey*, Kirk Othmer encyclopaedia of chemical technologies.

[95] H. M. Weitz, E. Loser, *Isoprene*, Ullmann's encyclopaedia of industrial chemistry, Vol. 20.

[96] H. M. Lybarger, *Isoprene,* Kirk Othmer encyclopaedia of chemical technologies.

[97] A. Chauvel, G. Lefebvre, *Petrochemical processes – 1,* IFP publications, Gulf publishing company 1989, pages 227 – 232 and pages 341 – 345.

[98] G. L. O'Connor, S. W. Kaiser, J. H. Mc Cain, EP 0272663 (21 December 1987), assigned to Union Carbide Co.

[99] T. Reis, *Chem. Process Eng.,* 53 (1), Jan 1972, pp. 34 – 36.

[100] T. Chikatsu, S. Shimokawa, Y. Yoshida, M. Imamura, I Nishiwaki, T. Akimoto, T. Fujiwara, GB 1325932 (8 August 1973), assigned to Japan Synthetic Rubber Co. Ltd.

[101] V. K. Ramanujam, B. B. Slim, C. Nelson, M. Maccaulley, WO 2014/204670 (24 December 2014), assigned to GTG Technology US LLC.

[102] T. Reis, *Chem. Process Eng.,* 53 (3), Mar 1972, pp. 66 – 78.

[103] R. A. Buyanov, N. A. Pakhomov, *Kinetics and Catalysis,* **2001**, *42*, (1), 72.

[104] http://yarsintez.ru/index_e.php?it=2

[105] K. K. Gil'manov, R. G. Romanova, A. A. Lamberov, R. R. Gill'mullin, *Petroleum Chemistry,* **2010**, *50,* (5)**.**

[106] K. K. Gil'manov, A. A. Lamberov, R. R. Gill'mullin, E. A. Pavlova, *Petroleum Chemistry,* Col. 2011, *51*, (3).

[107] E. Dimitriu, V. Hulea, I. Fechete, C. Caterniescu, A. Aurox, J. Lacaze, C. Guimon, *Applied Catalysis A: General,* **1999**, *181*, 15

[108] T. Reis, *Chem. Process Eng.,* 53 (2), Feb 1972, pp. 68 – 71.

[109] O. S. Pavlov, S. A. Karaskov, S. Y. Pavlov, *Theoretical foundations of chemical engineering,* **2011**, *45*, (4).

[110] V. L. Shushkevich, V. V. Ordomsky, I. I. Ivanova, *Applied Catalysis A: General,* **2012** 441 – 442, 21

[111] GB 1312192 (7 July 1970) assigned to Takeda Chemical Industries Ltd.

[112] Y. Ninagawa, O. Yamada, T. Renge, S. Kyo, T. Osaki, K. Kushida, US 4511751 (16 April 1985) assigned to Kuraray Company Ltd.

[113] E. Dimitriu, D. Trong On, S. Kaliaguine, *Journal of Catalysis,* **1997**, *170*, 150.

[114] Safety data sheet: 2-methyl-1-butene. Provided by Sigma-Aldrich Co.

[115] http://biosciences.dupont.com/media/news-archive/news/2009/the-worlds-first-goodyear-concept-tires-made-with-bioisoprenetm-technology-arrive-in-copnhagen-in-time-for-united-nations-climate-change-conference/

[116] David W. Lehyson, Thomas S. Zak, US 0043144 (12 February 2009) assigned to LyondellBasell Industries

[117] Robert J. Gartside, Shane R. Kleindienst, WO 016842 (11 February 2011) assigned to Lummus Technology Inc.

[118] T. Matsumoto, H. Miyake, K. Miyoshi, H. Kamiyama, Y. Tachibana, *Journal of Japan Petroleum Institute,* 1979, *22* (3), 142.

[119] Y. Watanabe, J. Kobayashi, Y. Toyoshima, T. Tokumaru, M. Saito, US 3621072 (23 December 1971), assigned to Sumitomo Chemical Company Ltd.

[120] Y. Watanabe, J. Kobayashi, Y. Toyoshima, T. Tokumaru, M. Saito, US 3574780 (13 April 1971), assigned to Sumitomo Chemical Company Ltd.

[121] P. Y. Gokhberg, B. N. Gorbunov, A. P. Khardin, V. R. Rudkovsky, V. M. Belayev, A. I. Lukashov, L. V. Shpantseva, V. V. Orlyansky, US 4147736 (3 April 1979)

[122] V. Siva Kumar, A. H. Padmasri, C. V. V. Satyanarayana, I. Ajit Kumar Reddy, B. David Raju, K. S. Rama Rao, *Catalysis Communications,* 2006, *7*, 745.

[123] S. Lucas, E. Champions, D. Bregiroux, D. Bernache-Assollant, F. Audubert, *Journal of Solid State Chemistry*, 2004, *177*, 1302.

[124] J. E. Hueey, E.A Keiter, R. L. Keiter, *Chimica Inorganica,* Piccin editore.

[125] A. Clearfield, J. A. Stynes, *Journal of Inorganic and Nuclear Chemistry,* **1964,** *26*, 117.

[126] I. M. Dahl, S. Kolboe, *Catalysis Letter,* 20, (2006), 329-336

[127] M. Bjorgen, S. Svelle, F. JOensen, J. Nerlov, S. Kolboe, F. Bonino, L. Palumbo, S. Bordiga, U. Olsbye, *Journal of Catalysis,* 249, (2007), pp 195-207.

[128] S. Svelle, F. Joensen, J. Nerlov, U. Olsbye, K.P. Lillerud, S. Kolboe, M. Bjorgen, *Journal of American Chemical Society – Communications,* 128, (2006), pp 14770-14771

[129] S. N. Khadzhiev, M. V. Magomedova, E. G. Peresypkina, *Petroleum Chemistry,* 54, (2014), pp 245-269.

[130] P. Ya. Gokhberg, A. P. Khardin, V. Z. Sharf, V. V. Akat'ev, *Neftekhimiya*, 24, (1984), pp 636-642.

[131] V. V. Akat'ev, P. Ya. Gokhberg, V. Z. Sharf, *Neftekhimiya*, 27, (1987), pp 83-86.

[132] J. Clayden, N. Greeves, S. Warren, *Organic Chemistry,* pp 1055 – 1066, 2012 Oxford University Press.

[133] J. Nisar, A. Mukhtiar, I. A. Awan, *Reaction Kinetics and Catalysis Letters*, 95, (2008), pp 399-406.

[134] J. E. Baldwin, R. Shukla, *Journal of Physical Chemistry*, 103, (1999), pp 7821-7825.

[135] J. T. Kiss, I. Palinko, A. Molnar, *Spectrocimica Acta Part A*, 52, (1996), pp 185 - 189

[136] F. Cavani, F. Folco, L. Ott, J. Riegler, L. Schmid, M. Janssen, WO 2014/147161, (25 September 2014), assigned to Lonza Ltd.

[137] L. E. Briand, J. M. Jehng, L. Cornaglia, A. M. Hirt, I. E. Wachs, *Catalysis today,* **2000**, *78*, 257.

[138] M. Massa, R. Haggblad, A. Andersson, *Top Catal,* **2011**, *54*, 685.

[139] I. Ivanova, V. L. Sushkevich, Y. G. Kolyagin, V. V. Ordomsky *Angewandte Chemie International Edition,* **2013**, *52*, 12961

[140] Armaroli, N.; Balzani V. *Angewandte Chemie International Edition,* **2007**, *46*, 52

[141] Song, C. *Catalysis Today*, **2002,** *77*, 17

[142] Das, D.; Veziroglu, T. *International Journal of Hydrogen Energy,* **2001**, *26*, 13.

[143] Haüssinger, P.; Lohmüller, R.; Watson, A. M.: Hydrogen, 2.Production, *Ullmann's Encyclopedia of industrial chemistry*. Vol. 18

[144] Haüssinger, P.; Lohmüller, R.; Watson, A. M.: Hydrogen, 6. Uses, *Ullmann's Encyclopedia of industrial chemistry*. Vol. 18

[145] Haryanto, A.; Sandun, F.; Murali, N.; Adhikari, S. *Energy and Fuels*, **2005**, *19*, 2098

[146] De Jong, E.; Higson, A.; Walsh, P.; Wellisch, M. *Bio-based Chemicals*, IEA Bioenergy – Task 42 Biorefinery.

[147] Sheng, P. Y.; Yee, A.; Bowmaker, G. A.; Idriss, H. *Journal of Catalysis,* **2002**, *208*, 393.

[148] Wang, W.; Wang, Y.; *Internation Journal of Hydrogen Energy*, **2008**, *33*, 5035

[149] Hebben, N.; Dihem, C.; Detuschmann, O. *Applied Catalysis A: General,* **2010**, *388*, 255

[150] Cai, W.; Wang, F.; Zhan, E.; Van Veen, A. C., Mirodatos, C.; Shen, W. *Journal of Catalysis,* **2008**, *257*, 96

[151] Wanat, E. C., Suman, B.; Schmidt, L. D. *Journal of Catalysis*, **2005**, *235*, 18

[152] Costa, L. O. O.; Silva, A. M.; Borges, L. E. P.; Mattos, L. V.; Noronha, F. B. *Catalysis Today,* **2008**, 138, 147.

[153] Kraleva, E.; Sokolov, S.; Schneider, M.; Ehrich, H. *International Journal of Hydrogen Energy*, **2013**, *38*, 4380

[154] Kondratenko, V. A., Berger-Karin, C.; Kondratenko, E. V. *ACS Catalysis,* **2014**, *4*, 3136

[155] Berger-Karin, C.; Sebek, M.; Pohl M.-M.; Bentrup, U.; Kondratenko, V. A.; Steinfeldt, N.; Kondratenko, E. V. *ChemCatChem*, **2012**, *4*, 1368

[156] Otroshchenko, T.; Sokolov, S., Stoyanova, M.; Kondratenko, V. A.; Rodemerck, U.; Linke, D.; Kondratenko, E. V. *Angew. Chem. Int. Ed.* **2015,** *54*, 15880-15883

[157] Wang, Y.; Ren, J.; Deng, K.; Gui, L.; Tang, Y. *Chem. Mater.* **2000**, *12*, 1622

[158] Abe, T.; Tanizawa, M.; Watanabe, K.; Taguchi, A. *Energy and Environmental Science*, **2009**, *2*, 315

[159] Hohn, K. L.; Lin, Y.-C. *ChemSusChem* **2009**, *2*, 927

[160] Salge, J. R.; Deluga, G. A., Schmidt, L. D. *Journal of Catalysis* **2005**, *235*, 69

[161] Loganathan, K., Leclerec, C. A. *Fuel* **2012**, *96*, 434

[162] Mattos, L. V., Noronha, F. B. *Journal of Power Soueces* **2005**, *145*, 10

[163] Mattos, L. V., Noronha, F. B. *Journal of Catalysis* **2005**, *233*, 45

[164] Salazar-Villalpando, M. D.; Miller, A. C. *Chem. Eng. Jour.* **2011**, *166*, 738